AD-A141 793 STATOR BLADE ROW GEOMETRY MODIFICATION INFLUENCE ON 1/3
TWO-STAGE AXIAL-FLOW..(U) IOWA STATE UNIV AMES
ENGINEERING RESEARCH INST D L TWEEDT ET AL. DEC 83
UNCLASSIFIED ISU-ERI-AMES-84179 AFOSR-TR-84-0418 F/G 21/5 NL

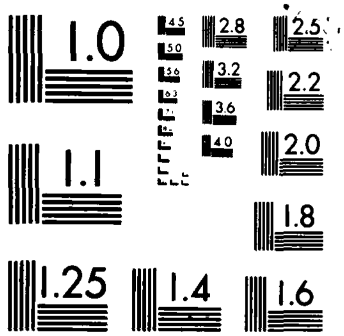

MICROCOPY RESOLUTION TEST CHART
NATIONAL BUREAU OF STANDARDS 1963-A

AFOSR-TR- 84-0418

AD-A141 793

DTIC FILE COPY

D. L. TWEEDT
T. H. OKIISHI

DECEMBER 1983

STATOR BLADE ROW GEOMETRY MODIFICATION INFLUENCE ON TWO-STAGE, AXIAL-FLOW COMPRESSOR AERODYNAMIC PERFORMANCE

TURBOMACHINERY
COMPONENTS RESEARCH PROGRAM

ISU-ERI-Ames-84179
TCRL-25
ERI Projects 1394, 1490, 1645

ENGINEERING RESEARCH INSTITUTE
IOWA STATE UNIVERSITY
AMES IOWA USA

84 05 30 056

ENGINEERING
RESEARCH

ENGINEERING
RESEARCH

ENGINEERING
RESEARCH

ENGINEERING
RESEARCH

ENGINEERING
RESEARCH

TECHNICAL REPORT

STATOR BLADE ROW GEOMETRY MODIFICATION INFLUENCE ON TWO-STAGE, AXIAL-FLOW COMPRESSOR AERODYNAMIC PERFORMANCE

Daniel L. Tweedt
Theodore H. Okiishi
December 1983

ISU-ERI-Ames-84179
TCRL-25
ERI Projects 1394, 1490, 1645

DEPARTMENT OF MECHANICAL ENGINEERING
ENGINEERING RESEARCH INSTITUTE
IOWA STATE UNIVERSITY, AMES

REPORT DOCUMENTATION PAGE		READ INSTRUCTIONS BEFORE COMPLETING FORM
1. REPORT NUMBER AFOSR-TR- 84-0418	2. GOVT ACCESSION NO. AD-A141 793	3. RECIPIENT'S CATALOG NUMBER
4. TITLE (and Subtitle) Stator Blade Row Geometry Modification Influence on Two-Stage, Axial-Flow Compressor Aerodynamic Performance		5. TYPE OF REPORT & PERIOD COVERED Technical Report 1 October 1978 - 30 April 1983
		6. PERFORMING ORG. REPORT NUMBER TCRL-25
7. AUTHOR(s) Daniel L. Tweedt and Theodore H. Okiishi		8. CONTRACT OR GRANT NUMBER(s) F49620-83-K-0023
9. PERFORMING ORGANIZATION NAME AND ADDRESS Engineering Research Institute/Mechanical Engineering Department Turbomachinery Components Research Laboratory, Iowa State University, Ames, Iowa 50011		10. PROGRAM ELEMENT, PROJECT, TASK AREA & WORK UNIT NUMBERS 61102F 2307/A4
11. CONTROLLING OFFICE NAME AND ADDRESS Air Force Office of Scientific Research Directorate of Aerospace Sciences (AFOSR/NA) Bldg. 410, Bolling AFB, D.C.		12. REPORT DATE December 1983
		13. NUMBER OF PAGES 243
14. MONITORING AGENCY NAME & ADDRESS (if different from Controlling Office)		15. SECURITY CLASS. (of this report) Unclassified
		15a. DECLASSIFICATION/DOWNGRADING SCHEDULE

16. DISTRIBUTION STATEMENT (of this Report)

Approved for Public Release; Distribution Unlimited

17. DISTRIBUTION STATEMENT (of the abstract entered in Block 20, if different from Report)

18. SUPPLEMENTARY NOTES

19. KEY WORDS (Continue on reverse side if necessary and identify by block number)

axial-flow turbomachinery
axial-flow compressor
stator

20. ABSTRACT (Continue on reverse side if necessary and identify by block number)

The influence of stator row geometry modification on the aerodynamic performance of a two-stage, low-speed, axial-flow research compressor was assessed in the experiments described in this project.

Stator geometry modifications tested included stator leading edge forward symmetrical sweep, large-radius blade/annulus wall corner fillets, and stator hub gap sealing (shrouding).

(continued)

20. Abstract. (continued)

Comparisons were made between detailed aerodynamic data associated with baseline and modified configurations. Substantial stator exit flow-field changes attributable to symmetrical sweeping of stator leading edges and to hub clearance sealing were observed with some evidence of corresponding near end wall loss reduction. The effects of large radii filleting were less clear.

Interesting conclusions about the off-design flow rate performance of the compressor also resulted from consideration of experimental data.

TABLE OF CONTENTS

SYMBOLS AND NOTATION

A	compressor flow passage annulus area, m^2
A_v	venturi flow passage area, m^2
c	blade chord length, m
FCC	comparison of integrated and venturi flow coefficients (Eq. 10.34), percent
g	local acceleration of gravity, m/s^2
H	total head with respect to barometric pressure (Eq. 10.5) N-m/kg
h	static head with respect to barometric pressure, N-m/kg
h_{hg}	barometric pressure, m of Hg
h_w	casing static head with respect to barometric pressure (Eq. 10.9), N-m/kg
i	incidence angle (Fig. 10.1), degrees
P_{atm}	barometric pressure (Eq. 10.1), N/m^2
P_t	total pressure with respect to barometric pressure, m of water
P_v	venturi static pressure with respect to barometric pressure, m of water
P_w	casing static pressure with respect to barometric pressure, m of water
PHH	percent passage height from hub (Eq. 10.4), percent
Q_a	integrated volumetric flow rate at probe-traversing measurement stations (Eq. 10.32), m^3/s
Q_v	venturi volumetric flow rate (Eq. 10.30), m^3/s
R	gas constant, N-m/(kg-°K)
r	radius from compressor axis, m
RPM	rotor rotational speed, rpm
S	circumferential space between blade camber lines, degrees

T	compressor drive-shaft torque, N-m
t	temperature, °K
t_{baro}	barometer ambient temperature, °K
t_{max}	blade section maximum thickness, m
U	rotor blade velocity (Eq. 10.14), m/s
V	absolute fluid velocity (Fig. 10.1; Eq. 10.12), m/s
V'	relative fluid velocity (Eq. 10.21), m/s
V_y	tangential component of absolute fluid velocity (Eq. 10.17), m/s
V'_y	tangential component of relative fluid velocity (Eq. 10.19), m/s
V_z	axial component of fluid velocity (Eq. 10.15), m/s
Y	circumferential traversing position, degrees
β_y	absolute flow angle with respect to axial direction (Fig. 10.1), degrees
β'_y	relative flow angle with respect to axial direction (Fig. 10.1; Eq. 8.23), degrees
γ_{H_2O}	specific weight of water manometer fluid (Eq. 10.3), N/m^3
γ_{hg}	specific weight of mercury, N/m^3
ΔP_v	pressure differential across venturi, m of water
ΔY_{fs}	freestream region in the circumferential space between blades, degrees
δ	deviation angle (Fig. 10.1), degrees
η	hydraulic efficiency (Eqs. 10.42, 10.43, and 10.44)
η_m	mechanical efficiency (Eq. 10.54)
κ	blade angle, angle between tangent to blade camber line and axial direction (Fig. 10.1), degrees
ρ	density of air (Eq. 10.2), kg/m^3

σ	blade row solidity
ϕ	venturi flow coefficient (Eq. 10.31)
$\bar{\phi}$	circumferential-mean flow coefficient (Eq. 10.29)
ϕ_a	integrated flow coefficient at probe-traversing measurement stations (Eq. 8.33)
ψ	head-rise coefficient (Eqs. 10.36 through 10.41 and 10.51, 10.52, 10.53)
ω	total-head loss coefficient (Eqs. 10.45 and 10.46)

Subscripts

h	annulus inner surface, hub
i	ideal
m	mechanical
overall	overall compressor
R	rotor
S	stator
stage	stage
t	annulus outer surface, tip
v	venturi
1	blade-row inlet
2	blade-row outlet
1R	first rotor
2R	second rotor
1S	first stator
2S	second stator

Superscripts

$'$	relative to rotor
$\bar{}$	average; blade-to-blade circumferential-average
$\dot{\bar{}}$	radial mass-average
$=$	cross-section average

LIST OF FIGURES

LIST OF TABLES

1. INTRODUCTION

The fluid flow viscous losses occurring in production axial-flow turbomachines continue to challenge designers. Even seemingly small gains in aerodynamic efficiency are vigorously sought by manufacturers to remain competitive. Better management of the complicated flows in end wall regions of the blade rows of a turbomachine is one example of a specific improvement goal.

A low speed research compressor can be a useful tool in this quest for improved performance. In particular, viscous phenomena may be ascertained in considerable detail, and a variety of builds designed to result in improved flows can be tried somewhat economically.

This report is about research initiated to provide a clearer understanding of the potential for better managing the end-wall flows in an axial-flow compressor. More specifically, the use of stator geometry modification (blade shape and end-wall fillets and/or sealing) to improve stage performance was explored.

Two kinds of stator blades were used. A baseline stator, conventional in geometry, provided baseline data against which to compare data for other stator geometries. A modified stator featuring forward symmetrical sweep of the leading edge from mid-span to the inner and outer annulus walls was also utilized.

Both large and small blade/end-wall corner fillets were tested in the second stage stator row of the compressor with the modified stator blades. This investigation into the influence of large

corner-fillets on end-wall flows also supplied data on the effects of sealing a stator/stationary end-wall clearance gap. These sealing effects were further investigated with the baseline stators.

2. RESEARCH COMPRESSOR EXPERIMENTAL FACILITY

The axial-flow research compressor and data acquisition system of the Iowa State University Engineering Research Institute/Mechanical Engineering Department Turbomachinery Components Research Laboratory that were used to accomplish the experimental research outlined in this report are briefly described in this section. More comprehensive and detailed information about this equipment is provided by Hathaway and Okiishi [1].

2.1. Axial-Flow Research Compressor

The two-stage axial-flow research compressor rig (see Figure 2.1) of the Turbomachinery Components Research Laboratory was used in the aerodynamic performance testing of four different compressor builds. These builds consisted of the same rotor blade rows and two kinds of stator blade rows, namely, baseline and modified. The rotor and baseline stator blades were designed to be representative of typical transonic compressor blades in terms of high reaction stages, axially discharging stators, and the absence of inlet guide vanes. A uniform spanwise distribution of total pressure was prescribed for each rotor exit. The blade section profiles used for all blades were double circular arc, and were considered conventional and appropriate for the low-speed testing involved. The two-stage compressor design data are summarized in Table 2.1.

The modified stator blades, as already mentioned, featured forward symmetrical sweep of each stator leading edge from mid-span

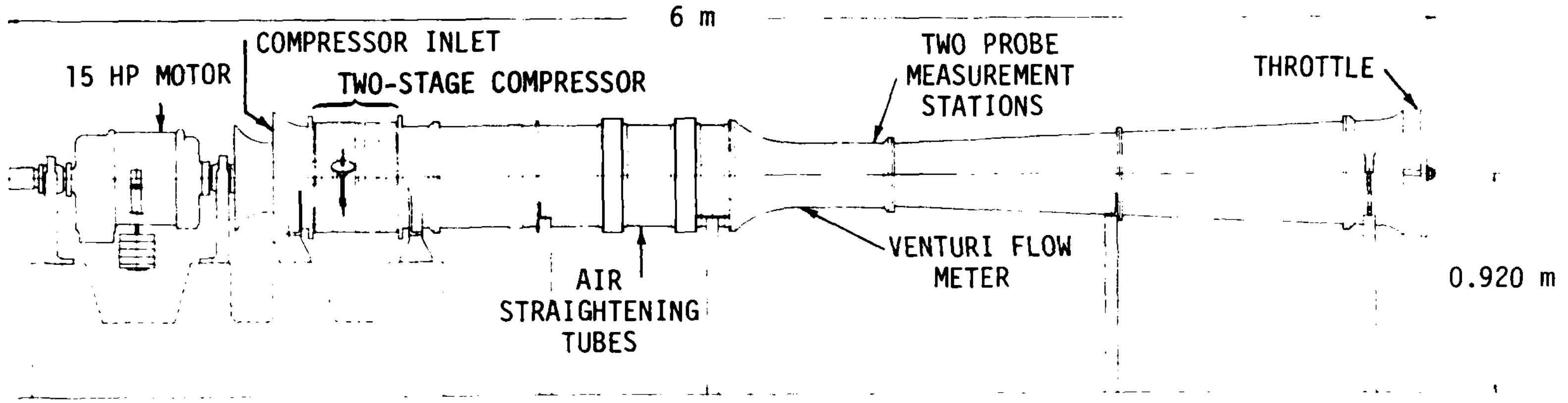

Figure 2.1 Schematic of research compressor.

Table 2.1. Summary of two-stage compressor design data.

Rotor speed	2400 rpm
Flow rate	5.25 lb_m/s (2/38 kg/s)
Pressure ratio	1.019
Number of blades	
Rotor	21
Stator	30
Blade material	fiberglass with steel trunnion and spine
Blade aerodynamic chord	2.30 in. (6.07 cm) constant for rotor and baseline stator
	2.38 in. to 3.03 in. (6.04 to 7.70 cm) for modified stator
Blade section profile	double circular arc
Blade stacking axis location	radial line through center of gravity of blade sections for rotor and baseline stator blades
	radial line through blade section trailing edge circle centers for modified stator blade
Leading and trailing edge radius to aerodynamic chord ratio	0.01 constant
Maximum thickness to aerodynamic chord ratio	0.10 to 0.06 linear variation from blade root to other end of blade span
Annulus flow path	
Hub radius	5.60 in. (14.22 cm) constant
Tip radius	8.00 in. (20.32 cm) constant

to the inner and outer annulus walls. The baseline and modified stator blade geometries are compared in Table 2.2, and some representative blade section profiles for the baseline and modified rotor and stator blades are shown in Figures 2.2, 2.3, and 2.4, respectively. The baseline rotor and stator blade designs are discussed in more detail by Hathaway and Okiishi [1]. The modified stator blade design details are summarized in Appendices A and B. All blades were manufactured as described by Hathaway and Okiishi [1], with clearances between blade extremities and the casing (for rotor blades) and hub (for stator blades) kept constant at 0.034 inches (0.864 mm) (1.4 percent span) by precision grinding of blade tips to appropriate radii with the blades mounted in place.

The four different compressor builds consisted of two baseline stator builds, namely, baseline 1 and baseline 2, and two modified stator builds, modified 1 and modified 2. The two builds with each kind of stator blade geometry (baseline and modified) differed only in the second stage stator row, as indicated in Table 2.3. A meridional plane view of the compressor blading with build features summarized in note form is provided in Figure 2.5. The large corner fillets used in the second stage stator row of the modified 2 build involved a radius of 0.25 inches. All small corner fillets were made as small as was practical.

Table 2.2. Comparison of stator blade geometries.

Similarities between Baseline and Modified Stator Blades

- Number of blades per row
- Blade surface finish
- Mid-span chord length
- Spanwise distribution of maximum thickness to chord ratios

Differences between Baseline and Modified Stator Blades

Baseline	Modified
Stacking point at center of gravity	Stacking point at trailing edge circle center
No leading edge sweep	Symmetrical leading edge forward sweep
Constant spanwise distribution of chord length	Varying spanwise distribution of chord length

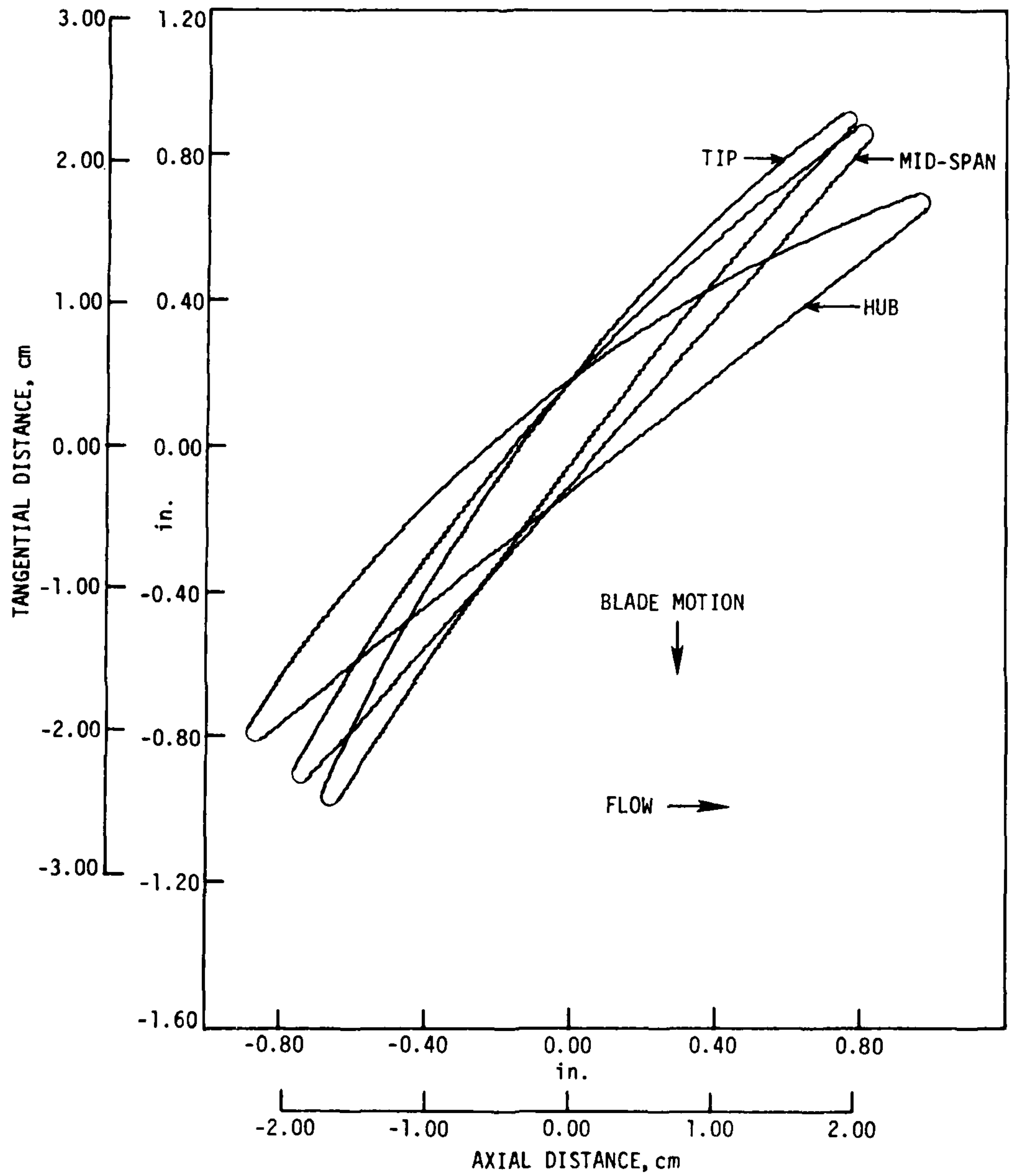

Figure 2.2. Representative compressor rotor blade sections (same for baseline and modified builds).

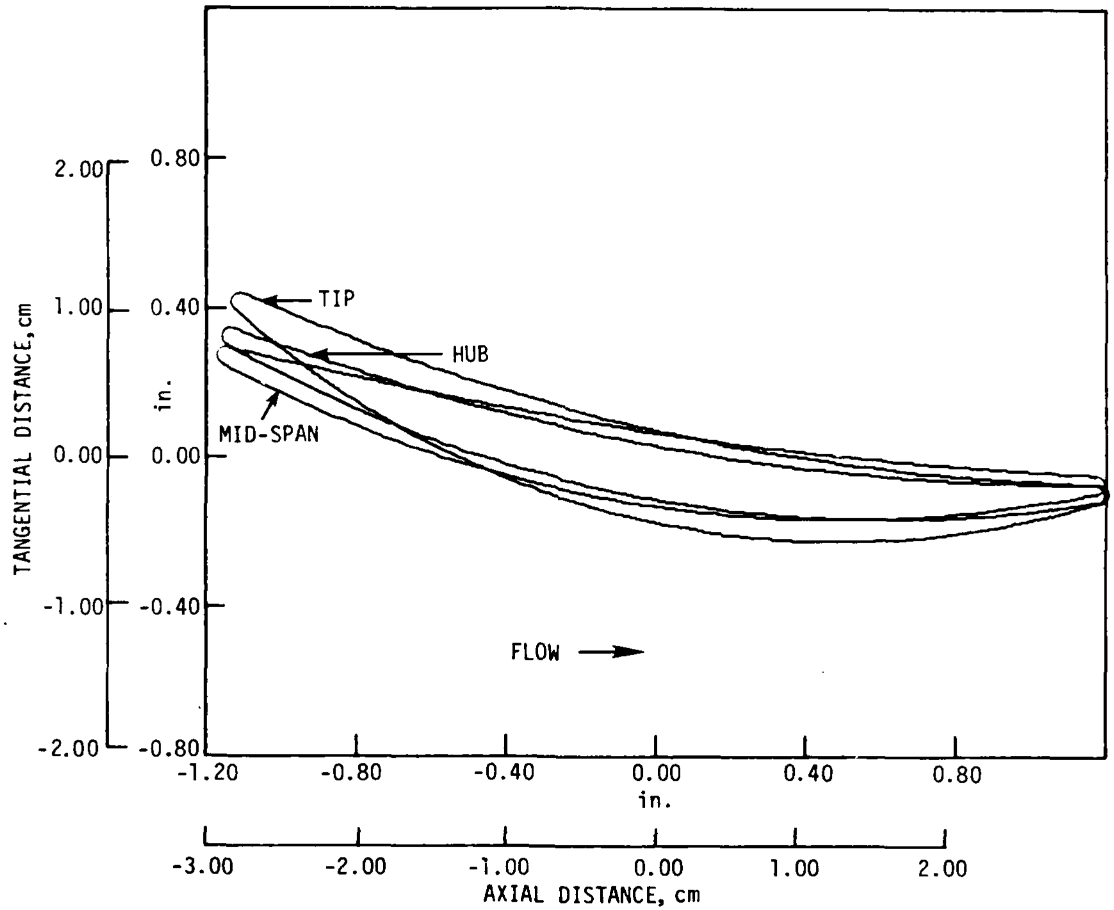

Figure 2.3 Representative baseline stator blade sections.

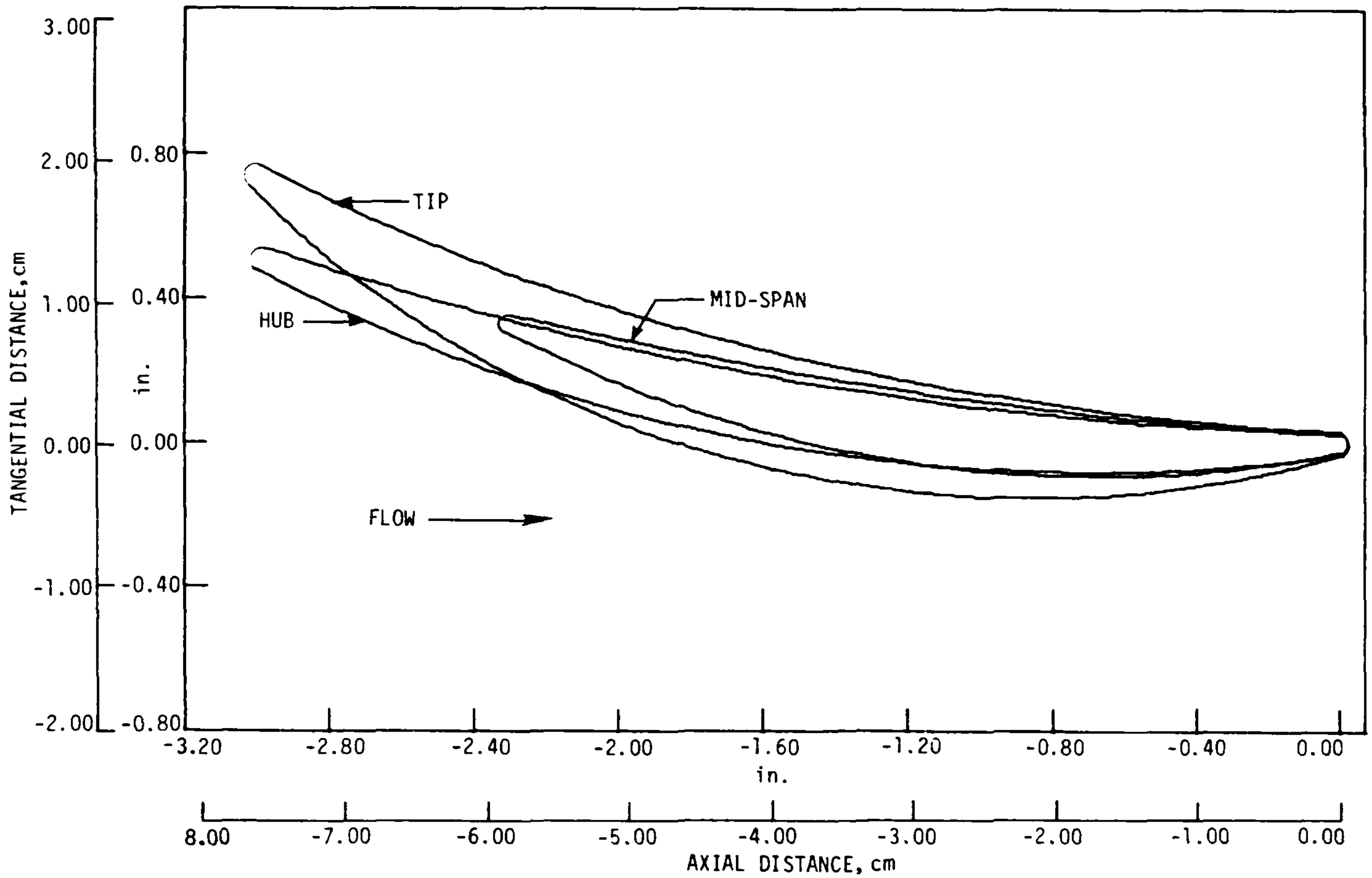

Figure 2.4 Representative modified stator blade sections.

Table 2.3. Comparison of compressor builds.

Baseline 1	Baseline 2	Modified 1	Modified 2
baseline rotor blade rows	baseline rotor blade rows	baseline rotor blade rows	baseline rotor blade rows
small corner fillets at inner endwall for first and second stage rotor blade rows	small corner fillets at inner endwall for first and second stage rotor blade rows	small corner fillets at inner endwall for first and second stage rotor blade rows	small corner fillets at inner endwall for first and second stage rotor blade rows
clearance between first stage stator blade tips and rotating inner endwall	clearance between first stage stator blade tips and rotating inner endwall	clearance between first stage stator blade tips and rotating inner endwall	clearance between first stage stator blade tips and rotating inner endwall
clearance between second stage stator blade tips and stationary inner endwall	shrouded second stage stator--small corner fillets at inner endwall	clearance between second stage stator blade tips and stationary inner endwall	shrouded second stage stator--large corner fillets at inner endwall

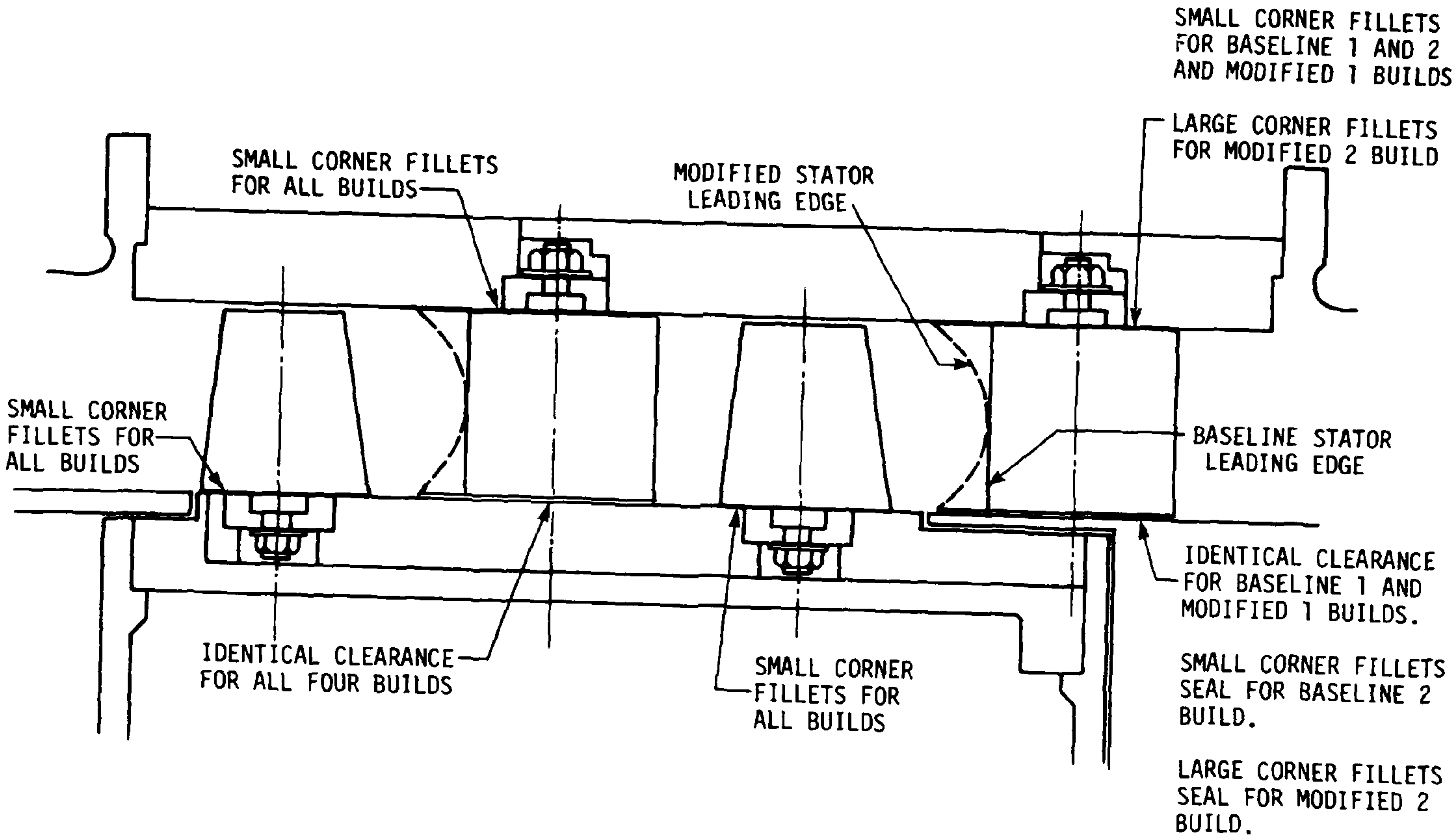

Figure 2.5 Meridional plane view of compressor blading.

2.2. Data Acquisition System

The data acquisition system included the following basic items:

- Slow-response pressure instrumentation
- Probe and stator blade row actuators
- Scanivalve system
- Venturi flow meter
- Temperature instrumentation
- Compressor drive-shaft torque measurement device
- Computer control system
- Oscilloscope (Tektronix type R546B with type 3A7 Differential Comparator and type 3A1 Dual-Trace Amplifier)

The slow-response pressure instrumentation included a cobra probe (United Sensor type CA-120-24-F-18-CD), a Kiel probe (United Sensor type KBC-24-L-22-W), casing static pressure taps, and a mercury-in-glass barometer (Princo Instruments model B-222). The probes were immersed and yawed with a probe actuator (L. C. Smith Company model BBS-3180) controlled by a control indicator (L. C. Smith Company model DI-3R) and switchbox (L. C. Smith Company model DI-3R-SB4). The measurement station locations are shown in Figure 2.6.

A scanivalve pressure-port selector system (Scanivalve Company model 48D3-1016) including a strain-gauge pressure transducer (Scanivalve Company model PDCR22), solenoid drive (Scanivalve Company model DS3-48) and control (Scanivalve Company model CTLR2/S2-S6), a signal conditioner (Endevco model 4470), and an amplified bridge

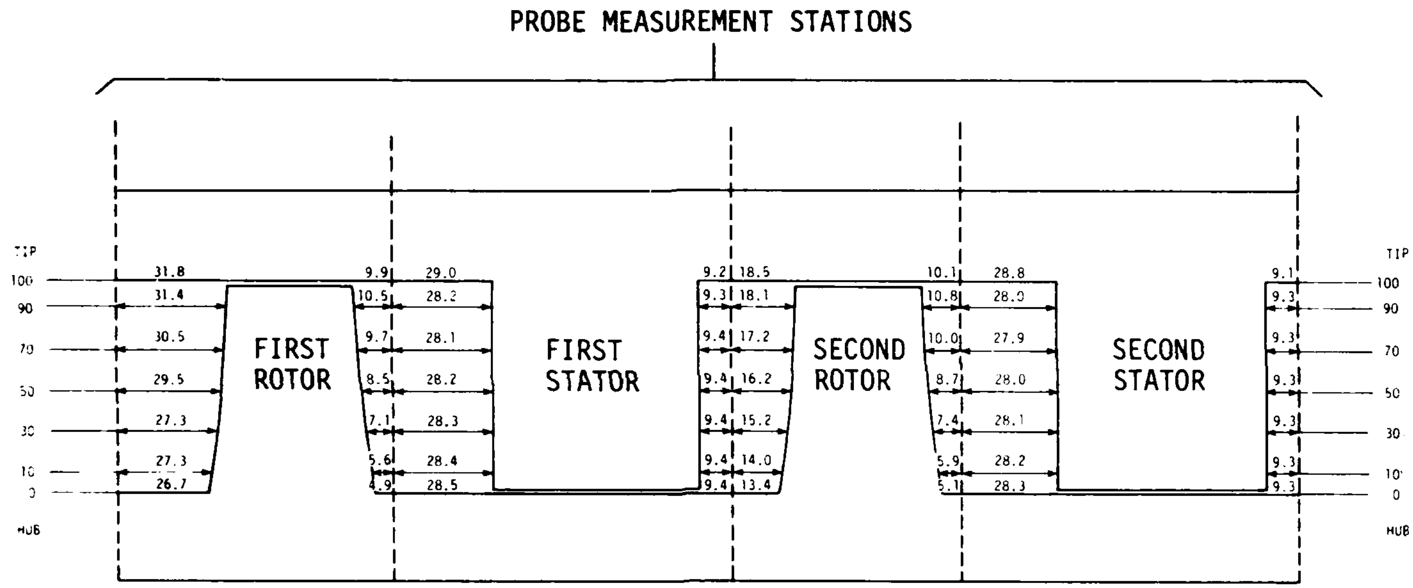

Figure 2.6 Schematic showing axial location of probe measurement stations relative to adjacent blade rows (dimensions in mm).

circuit conditioner (Endevco model 4476.2A) were used to acquire all pressure measurements.

Temperature measurements were acquired using a solid-state thermocouple reference junction (Pace Engineering Company model LRJ49-8TT) with copper-constantan thermocouples.

A desk top computer (Commodore PET model 2001-32) and digital voltmeter (Hewlett Packard model 3455A) were used in combination with a multiple channel voltage scanner (Hewlett Packard model 3495A) to control the data acquisition process.

A schematic illustrating how these components interacted with each other appears in Figure 2.7.

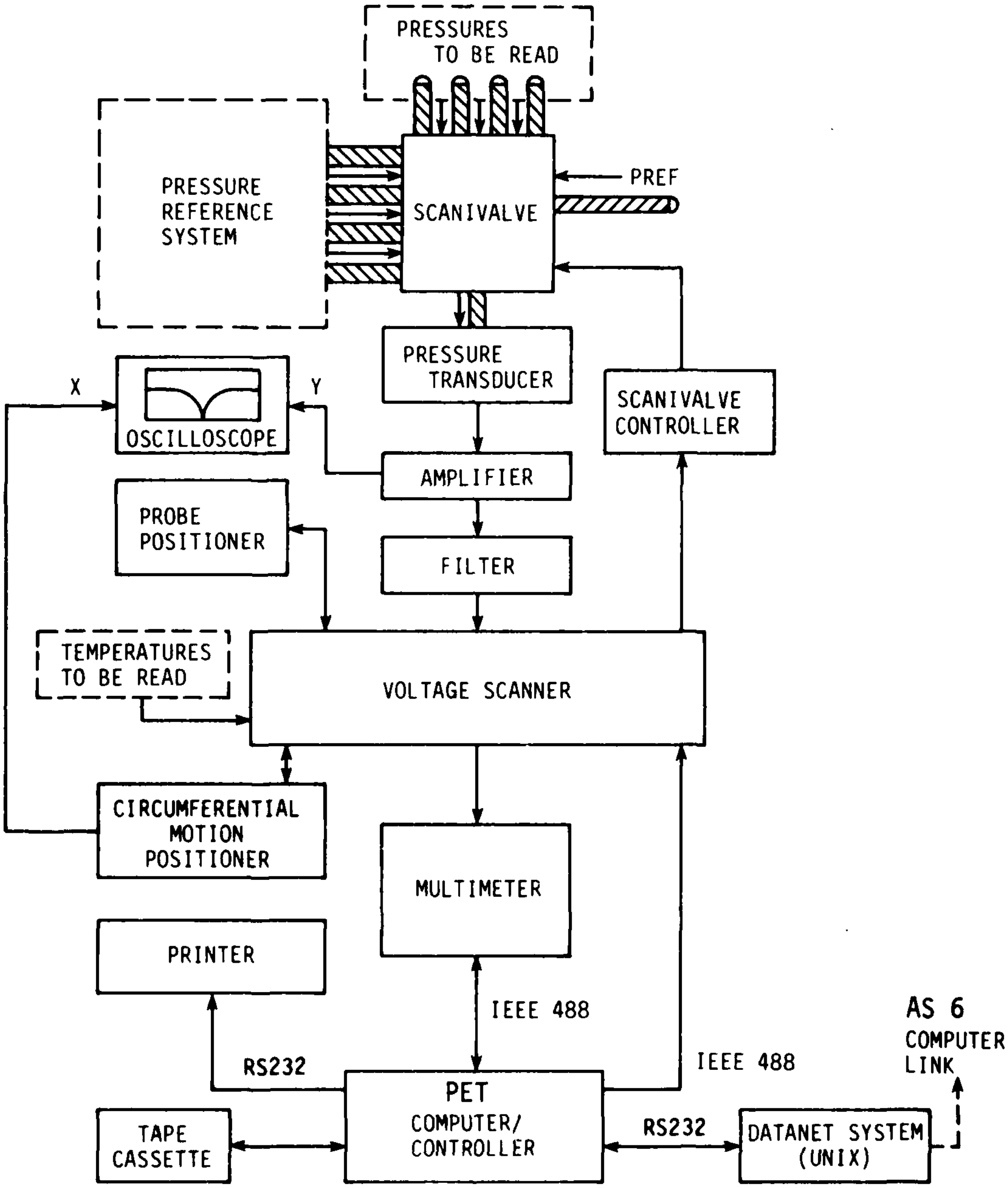

Figure 2.7 Schematic of data acquisition system.

3. EXPERIMENTAL PROCEDURE AND DATA REDUCTION

Involved with the present experiment were the following specific goals:

- Construct overall performance maps for the baseline 1 and modified 1 compressor builds
- Establish from these performance maps a flow rate at which to obtain detailed flow-field data for the four different compressor builds
- Test the four compressor builds at the selected flow rate (operating point) in order to obtain detailed time-average total-pressure and flow angle data at each blade row inlet and exit station
- Track the first stage stator wake flow through the second stage rotor

Details involved in attaining these goals are summarized below. More complete information about the calibration procedures involved is provided in Reference 1.

3.1. Calibration

The equipment calibrations necessary before and during data acquisition were as follows:

- Probe and stator blade row actuator position/potentiometer voltage calibrations (probe yaw angle and immersion position and stator blade row circumferential position)

- Pressure-transducer calibrations (on-line using the pressure reference system described in Reference 2)
- Shaft torque measurement device (torque meter) calibrations
- Thermocouple calibrations using a mercury-in-glass thermometer

The Kiel and cobra probes were positioned immersion-wise relative to their respective actuators with a depth micrometer. The cobra probe zero yaw angle position was ascertained by "nulling" the probe side port pressures with the probe immersed in a stream of air from a flow nozzle, with the actuator mounted at right angles to the nozzle flow direction. The Kiel probe was also tested in the nozzle flow where it could accurately measure total pressure within an angular range of as much as ±45 degrees from the actual flow direction. After these probes were adjusted and calibrated, appropriate constants were entered into the data acquisition computer programs [1].

On-line pressure-transducer calibration was accomplished using a pressure reference system [2] consisting of several water columns of differing heights and triple-beam balances. This system provided four reference pressures against which the pressure transducer could be calibrated. Calibration of the pressure transducer consisted of a linear least-squares correlation of transducer output voltage versus the known reference column pressures. The reference column pressures were determined with a resolution of 0.003 inches (0.076 mm) of water or better from linear least-squares correlation equations which were determined from a periodic (about three month intervals) calibration of column pressure versus column weight. Therefore, it was necessary to only weigh each column prior to testing in order to determine the

reference column pressures. Each column pressure and transducer voltage recorded was referenced to one of the columns, the same column each time. This was done to reduce errors due to thermal drift and other transient errors between successive readings, as well as to insure that the linear transducer correlation went through zero as it should. The above procedure consistently provided a transducer linear correlation coefficient of transducer voltage versus column pressure of 0.99999 or better. The calibration was repeated if this correlation criterion was not met. The pressure trnsducer was repeatedly checked in this manner prior to making any pressure measurements.

An additional water column was used to provide a base pressure to one side of the scanivalve transducer in order to insure that the pressure transducer was always displaced from zero. This eliminated errors from having the transducer pressure fluctuate around zero.

Thermocouples were calibrated against a precise mercury-in-glass thermometer. Since the flow was virtually incompressible, this procedure was sufficiently accurate for the situation involved.

Torque measurements were obtained by floating the drive motor on air bearings and applying a torque counter to the drive-motor torque. The balancing torque was applied by adding discrete weights to a torque arm, with a so-called torque meter being used to resolve the torque arm loads. This meter, employing a load transducer (strain gauge on a cantilevered beam) and accompanying circuitry, was subject to considerable transient drifting, and as such needed periodic recalibration during any measurement sequence. A built-in calibration

circuit was used to accomplish this, allowing adjustment to the correct 0 to 1 kg full-scale meter deflection.

3.2. Data Acquisition

All measurements were made with slow-response (time-averaging) instrumentation. Testing was done at the design rotor speed of 2400 rpm only, which was maintained with a feed-back electronic control system to within ±1 rpm. Four general measurement procedures were used. The first involved acquisition of overall performance data from which overall performance maps were constructed. With these overall performance data, a single operating point could be selected at which to obtain detailed aerodynamic performance data for the different compressor builds. This detailed performance testing required another two measurement procedures, one associated with the Kiel probe (total pressure) another with the cobra probe (flow angle). The fourth procedure was associated with the first stage stator wake tracking experiment.

As mentioned earlier, the data acquisition system was controlled by a desk-top computer. A separate "data acquisition program" was constructed for each of the first three general measurement procedures mentioned above. Logic diagrams (Figure 3.1) for these are included with the following discussion.

3.2.1. Overall Performance Data Acquisition

Three basic types of measurement were involved in this procedure; namely, casing static-pressure, fluid temperature, and drive-shaft

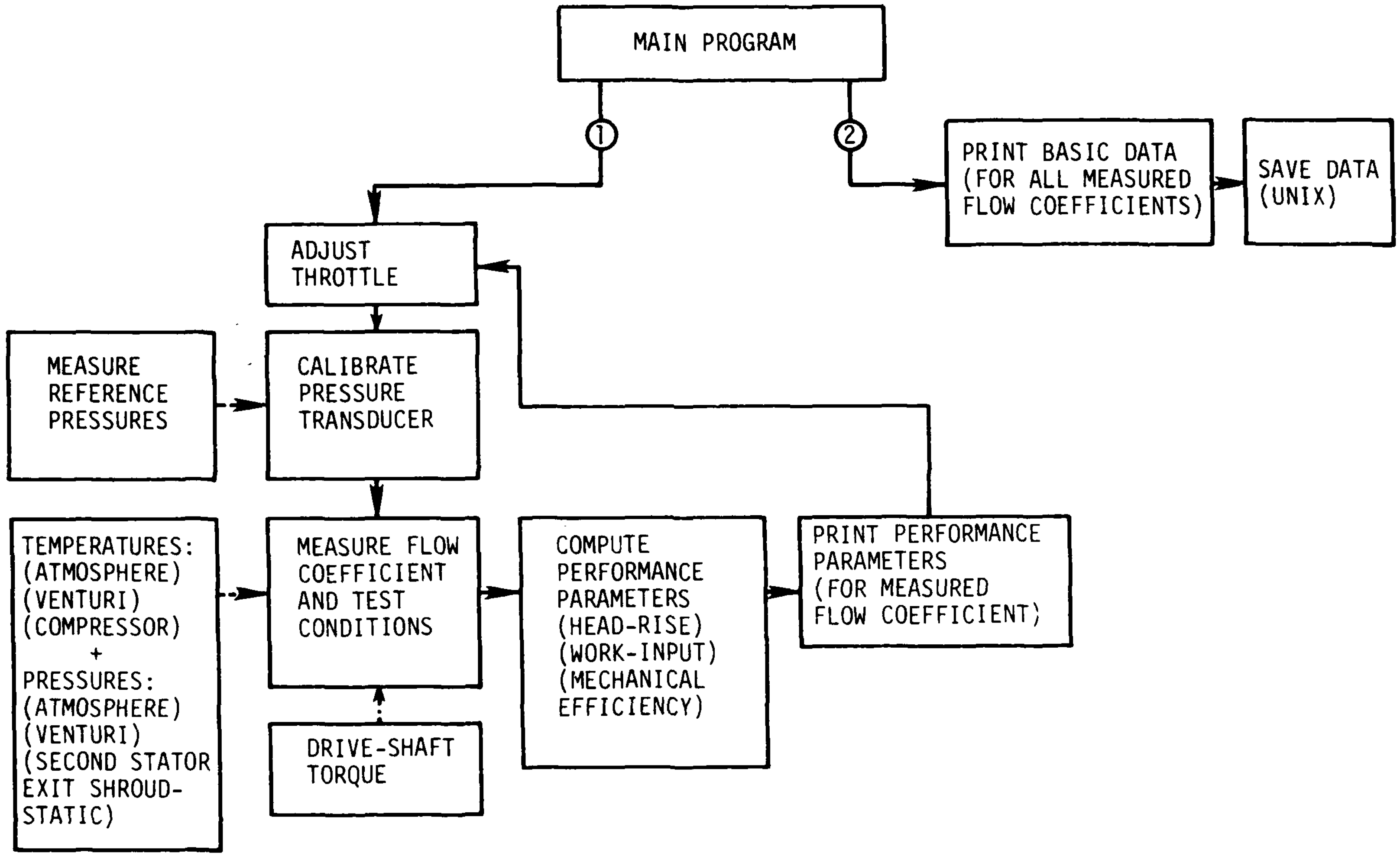

(a) OVERALL PERFORMANCE MEASUREMENT

Figure 3.1 Logic diagrams for data acquisition.

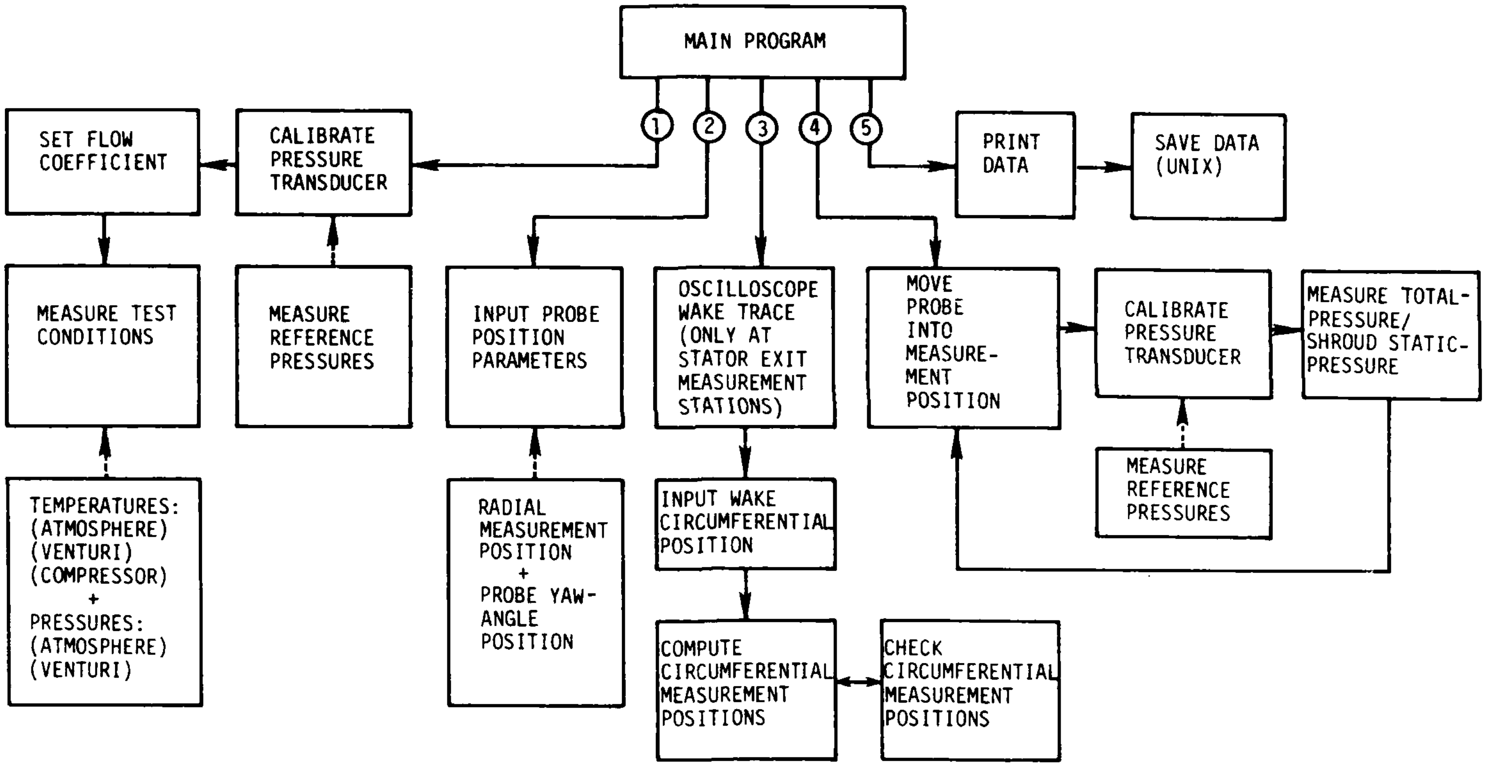

(b) KIEL PROBE (TOTAL PRESSURE) MEASUREMENT

Figure 3.1 continued.

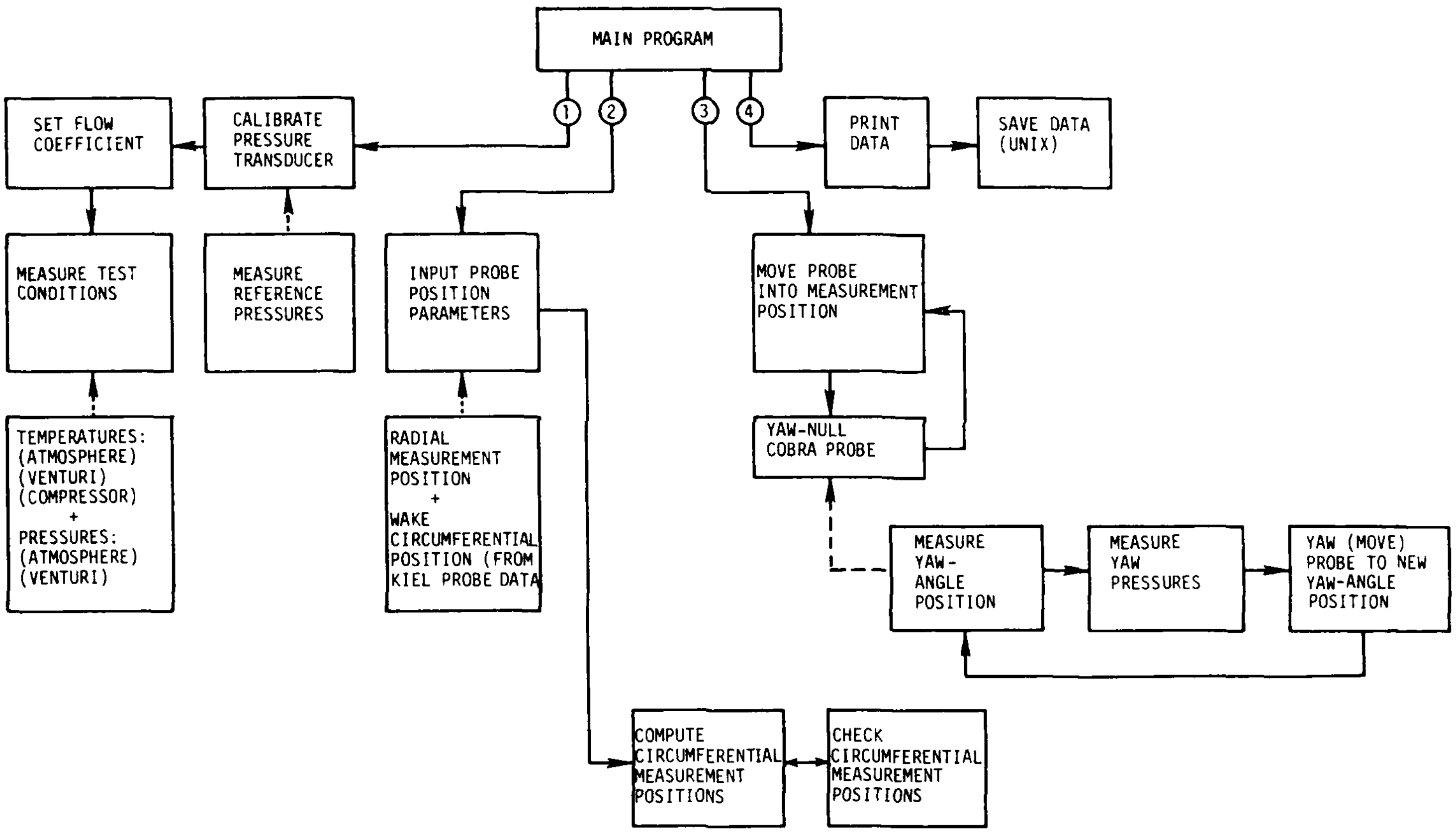

(c) COBRA PROBE (ABSOLUTE FLOW ANGLE) MEASUREMENT

Figure 3.1 concluded.

torque. Casing static pressures were obtained both at the venturi meter throat and the second stator exit station. Fluid temperature was measured in the lab, near the compressor inlet and at the venturi throat. The logic diagram for the data acquisition program used to automate this procedure is presented in Figure 3.1(a).

3.2.2. Detailed Data Acquisition

Sets of detailed data were acquired at a fixed operating point of the compressor (shaft speed = 2400 rpm and flow coefficient = 0.500). The measurements involved in obtaining these data were total pressure, casing static pressure, and absolute flow angle. Total pressure was measured with a Kiel probe, and absolute flow angle was measured with a cobra probe.

The Kiel probe was set at a fixed yaw angle for any given axial measurement station. This angular setting was not critical since the Kiel probe was capable of measuring total pressure accurately to within ±45 degrees of the actual flow angle. At the compressor inlet and stator exit stations, this setting was approximately 0 degrees while at the rotor exit stations a setting of 25 degrees was used. Qualitative oscilloscope traces of the circumferential variation of total pressure at various span locations were made at the stator exit stations to reveal the stator wake location. This information was used to pack total-pressure data within the stator wake for better wake definition.

At each stator exit measurement station, absolute flow angles could be measured only in the free-stream regions. This was because flow angles could not be measured accurately with a cobra probe in

the stator wake because of the large total-pressure gradients there. The logic diagrams for the total-pressure and absolute flow angle data acquisitions programs are presented in Figure 3.1(b) and (c), respectively.

Figure 3.2 depicts, to scale, a cascade representation of the compressor blade rows showing locations of the five axial measurement stations and the circumferential extent of the measurement window at each station. Data were acquired at all five axial stations for a complete set of measurements. Circumferential surveys were made by moving the stator rows circumferentially past the stationary probe. It should be noted that the stator blades of both stator rows were "in line" when viewed along the compressor axis for all measurements.

At all axial stations, data were generally obtained at eight annulus passage height (spanwise) locations, specifically, at 5%, 10%, 30%, 50%, 70%, 80%, 90%, and 95% span from the hub. Circumferential surveys were made over one stator pitch at each spanwise location, with the number of circumferential data points depending on the measurement type (total pressure or flow angle) and the axial station involved. Also, a casing static-pressure data point was taken with each total-pressure data set. The number of circumferential data points per stator pitch were as follows:

- STATION 1: 10 total pressure / 6 flow angle
- STATION 2: 10 total pressure / 6 flow angle
- STATION 3: 25 total pressure / 10 flow angle (free-stream only)
- STATION 4: 20 total pressure / 10 flow angle

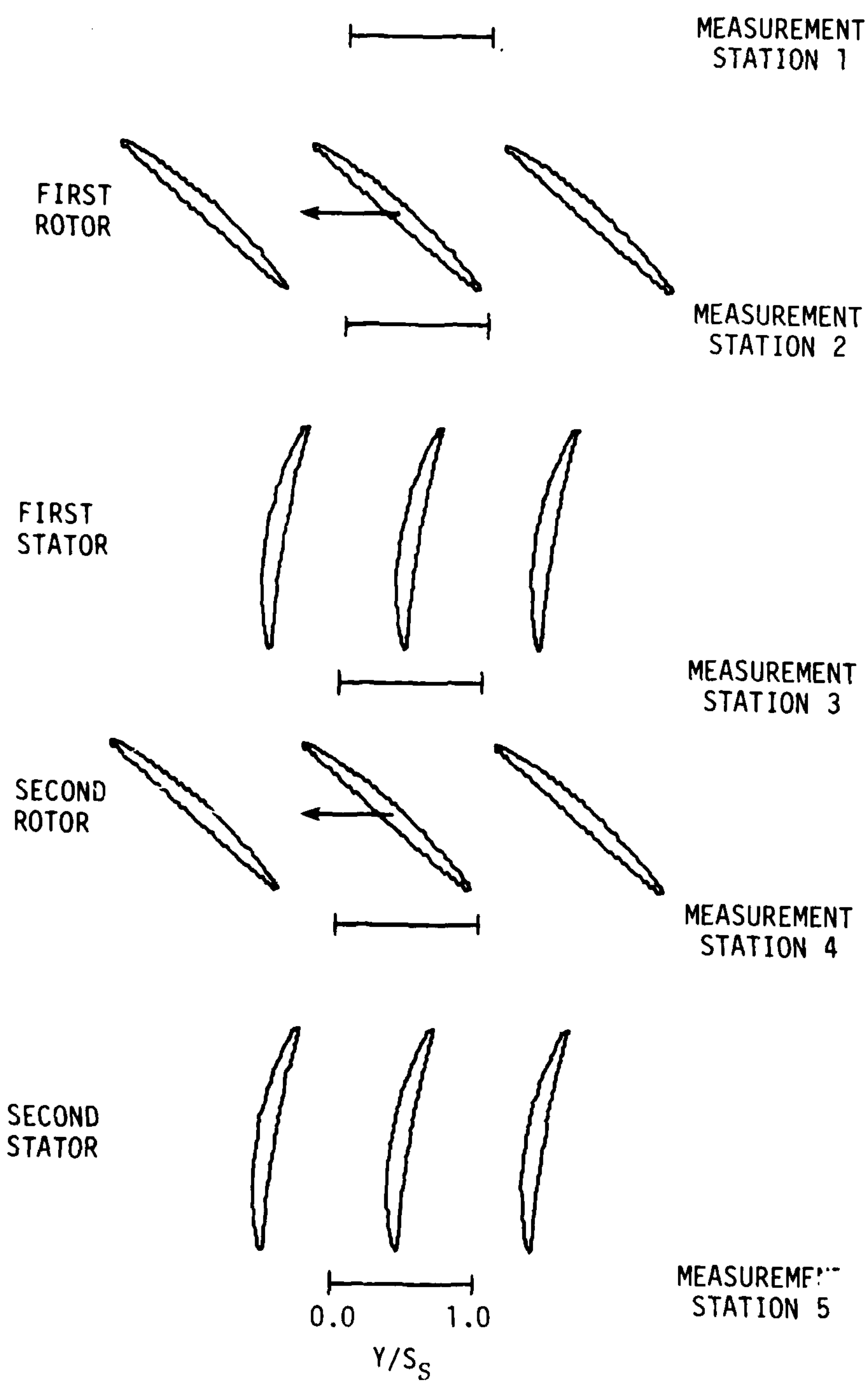

Figure 3.2 Blade cascade showing circumferential measurement window.

- STATION 5: 25 total pressure / 10 flow angle (free-stream only)

Complete sets of data were obtained for the baseline 1 and modified 1 compressor builds. For the baseline 2 and modified 2 builds, total-pressure data were acquired only at axial stations 3, 4, and 5, with flow angle data also acquired at these three stations for the modified 2 build only.

3.2.3. First Stator Wake Tracking Through the Second Rotor

A special series of tests was conducted on the modified 2 compressor build to determine first stator wake movement and dispersion through the second rotor blade row. These tests involved a specially constructed first stator blade with a heating wire wound to form a hot coil over the span of the blade near the trailing edge. In Figure 3.3 is a sketch of this heated stator blade and its location with respect to the circumferential measurement window. Data were obtained with the blade mounted in two different locations, referred to as position I and position II.

The stator wake tracking procedure consisted of activating the heating coil with a 3 amp current using a 120 volt variable transformer, and measuring air flow temperature at the second rotor exit with a thermocouple. This procedure was partially automated by modifying the Kiel probe data acquisition program discussed earlier. For two flow rates (flow coefficient = 0.575 and flow coefficient = 0.500), circumferential temperature surveys (position II) were made at five spanwise locations, specifically, at 10%, 30%, 50%, 70%, and 90% span from the hub. Circumferential temperature surveys at these

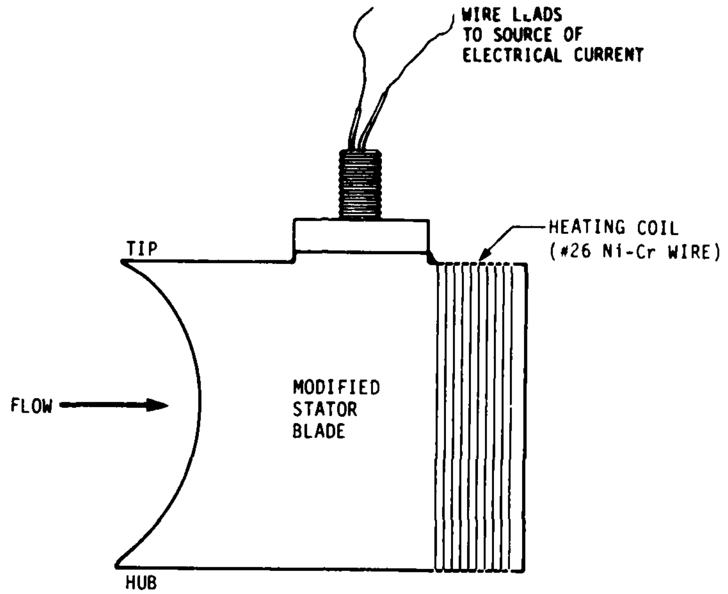

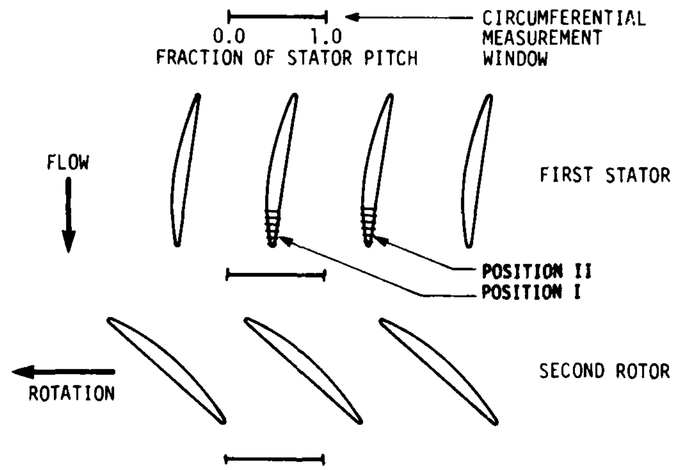

Figure 3.3 Meridional plane view of the modified stator blade equipped with heating coil, and blade cascade view illustrating the position I and position II heated blade locations.

radii were also made for the position I heating coil location at the flow coefficient of 0.575 only. A single circumferential temperature survey (position II) was made at mid-span for the flow coefficient of 0.425. The number of temperature data points for all circumferential surveys was 25 per stator pitch.

The stator wake tracking temperature data were supplemented with a few second rotor exit circumferential surveys of total pressure. The surveys of 20 data points each per stator pitch were made at mid-span only and were used to assess wake avenue distortion caused by the heating coil.

3.3. Data Reduction

Preliminary reduction of the data was performed during acquisition and consisted of determining a primary quantity values of total head, static head, and absolute flow angle. These primary values were subsequently stored on magnetic disk (UNIX). Completion of data reduction generally occurred on the mainframe computer (NAS AS6). For all calculations, the flow was assumed incompressible since velocities involved Mach number levels less than 0.2. Integrals were evaluated using a spline-fit integration scheme [3]. A complete list of all quantities and equations used in reducing the data is presented in Appendix C.

3.3.1. Overall Performance Parameters

All overall performance parameters were computed during acquisition and then transferred to the mainframe computer for plotting (performance

maps). The equations used to compute these parameters (see list below) are presented in Appendix C.

- Overall head-rise coefficient (venturi based, Eq. 10.52)
- Overall head-rise coefficient (second stator exit shroud static-pressure based, Eq. 10.51)
- Mechanical work-input coefficient (shaft torque based, Eq. 10.53)
- Mechanical efficiency (second stator exit shroud static-pressure/shaft torque based, Eq. 10.54)

3.3.2. Flow-Field and Performance Parameters (Detailed Data)

The total head was determined at each flow-field measurement point from the Kiel probe measured total pressure. Circumferential-mean values of total head and absolute flow angle were determined for each spanwise position at every axial measurement station. All circumferential averages, except for flow angle averages at the stator blade row exits, were determined by integrating over one stator blade pitch. Circumferential-mean absolute flow angles at the stator blade row exits were obtained by integrating over the free-stream portion of the flow only.

The static head was assumed to be circumferentially constant, and the spanwise distribution of static head was determined for each spanwise location at every axial measurement station by solving the radial equilibrium equation (Eq. 10.11) using the Runge-Kutta numerical technique [4]. The circumferential-mean casing static head was used as a boundary value. The pressure distribution was obtained by marching radially toward the hub at increments of 5% of passage height. The

circumferential-mean values of total head and absolute flow angle required at each step of the Runge-Kutta solution were obtained with a second-order Lagrange interpolation of their measured spanwise distributions.

From the radial distributions of total head, absolute flow angle, and static head, the circumferential-mean absolute velocities were determined for each spanwise location of every axial measurement station. With the circumferential-mean absolute velocities and flow angles determined, the following circumferential-mean flow values were computed for each spanwise location of every axial measurement station.

- Axial velocity, m/s (Eq. 10.16)
- Absolute tangential velocity, m/s (Eq. 10.18)
- Relative tangential velocity, m/s (Eq. 10.20)
- Relative velocity, m/s (Eq. 10.22)
- Relative flow angle, degrees (Eq. 10.24)
- Blade incidence angle, degrees (Eqs. 10.25 and 10.27)
- Blade deviation angle, degrees (Eqs. 10.26 and 10.28)
- Flow coefficient (Eq. 10.29)

In addition, for each axial measurement station an annulus cross-section integrated flow coefficient was calculated and compared with the flow coefficient determined from the venturi flow meter. In determining the annulus cross-section flow rate and corresponding flow coefficient, the axial velocities at the hub and casing end walls were assumed equal to zero.

The performance parameters were computed using the above circumferential-mean data. The actual and ideal (Euler turbine equation

based) head-rise coefficients and hydraulic efficiency were determined for each of the eight spanwise locations for both rotor rows, stages, and the entire compressor. Total-head loss coefficients were also determined for each rotor and stator blade row. Also, radially mass-averaged values of each of the above performance parameters were determined for both rotor rows, stages, and the entire compressor (see Appendix C).

3.3.3. First Stator Wake Tracking Data

All heat stator wake temperature data obtained at the second rotor exit were normalized before plotting as described below. The so-called relative temperatures were computed by subtracting the venturi meter throat fluid temperature from all temperature values. These relative temperature data were then graphed by the mainframe computer.

3.3.4. General Graph Types

Most reduced data were graphed by the mainframe computer to aid in analysis. Four general types of graphs were used:

- Performance maps--for point data (versus flow coefficient)
- Graphs with circumferential extent--for point data
- Contour maps--for point data
- Spanwise graphs--for circumferential-mean data

It should be noted that for contour mapping, the data acquired over a single stator blade pitch were repeated circumferentially over two stator blade pitches in order to provide better visualization of the flow pattern.

4. RESULTS AND DISCUSSION

Experimental results obtained from aerodynamic performance testing of the two-stage axial-flow compressor are presented and discussed in this section. The sequence of presentation is as follows:

4.1. Uncertainty Analysis

4.2. Overall Compressor Performance

4.3. Baseline 1 Compressor Build--Different Flow Rates

4.4. Comparison of Compressor Builds

A detailed comparison of design code predictions with experimental results for the baseline 1 compressor build at design flow is provided in Reference 1.

4.1. Uncertainty Analysis

Uncertainty estimates associated with the experimental results are presented in this section and the methods used to obtain these estimates are discussed. Primary measurement uncertainty intervals are provided first, followed by a discussion and presentation of the uncertainty intervals in calculated quantities.

Estimated uncertainty intervals for the primary measurement quantities are listed in Table 4.1. Also included in Table 4.1 are typical quantity values. The estimates for transducer pressure and absolute flow angle uncertainty were statistically determined from several sets of repeatability tests. Some actual test data

Table 4.1. Estimated uncertainty intervals for primary measurement quantities.

Quantity	Symbol	Typical Value	Uncertainty Interval (20:1 odds)	
Barometric pressure	h_{hg}	735.0 mm Hg	±0.3	(0.04%)
Transducer pressure	P	60.00 mm H_2O	±0.58	(0.97%)
Temperature	t	300.0 deg. K	±0.5	(0.17%)
Shaft torque	T	11.000 N·m	±0.125	(1.14%)
Absolute flow angle	β_y			
Station 1		0.0 deg.	±1.25	
Station 2		30.0 deg.	±0.90	
Station 3		0.0 deg.	±0.70	
Station 4		30.0 deg.	±0.65	
Station 5		0.0 deg.	±0.70	

sets were also replicated to provide repeatability information. An attempt was made to assess fixed errors in these results.

The estimated uncertainty intervals for so-called "primary computed quantities" are presented in Table 4.2. Primary computed quantities are those data closely associated with primary measurement data and from which the flow-field and performance parameters are directly calculated. Several points should be noted about the information in Table 4.2:

- Most of the uncertainty intervals are for circumferetial-mean quantities.
- The uncertainty intervals for a given quantity depend on the measurement station.
- The uncertainty intervals for circumferential-mean total-head data are smaller than those for individual total-head data.
- The uncertainty intervals for circumferential-mean/radial equilibrium static-head data at stations 3 and 5 are relatively large (compared with the intervals for total-head data).
- Two sets of uncertainty intervals are listed for circumferential-mean absolute flow angle data, one includes a suspected fixed-error uncertainty and the other excludes it.

Some of these observations are discussed further.

The uncertainty intervals for circumferential-mean quantities are smaller than those for the individual quantities used to calculate them, as pointed out above for total head. Similarly, radially mass-averaged quantities have smaller uncertainty intervals than the circumferential-mean quantities from which they are computed. This

Table 4.2. Estimated uncertainty intervals for primary computed quantities.

ESTIMATED UNCERTAINTY INTERVALS (20:1 ODDS)

Station	Total Head H(N-m/kg)	Circumferential-Mean Total Head $\bar{H}$(N-m/kg)	Circumferential-Mean/Radial Equilibrium Static Head $\bar{h}$(N-m/kg)	Circumferential Mean Absolute Flow Angle β_y (deg.)	Circumferential-Mean Absolute Flow Angle (No Fixed Error) $\bar{\beta}_y$ (deg.
1	±5.0	±2.0	±5.0	±0.85	±0.50
2	±5.0	±3.0	±5.0	±0.65	±0.30
3	±5.0	±3.0	±15.0	±0.70	±0.35
4	±5.0	±3.0	±5.0	±0.50	±0.15
5	±5.0	±3.0	±25.0	±0.70	±0.35

is reasonable since an average (mean) datum has less random error uncertainty associated with it than the individual data (normally distributed) from which it is calculated.

The absolute flow angle data have two sets of uncertainty intervals associated with them because the suspected fixed-error uncertainty need not be included when estimating the uncertainty intervals of many calculated results. Most calculated results are practically unaffected by a small systematic error in measured angles because they involve angle difference, e.g., ideal head rise, hydraulic efficiency, and rotor loss. Only the uncertainty intervals for incidence and deviation angles include this fixed-error uncertainty.

Some additional uncertainty in stator exit circumferential-mean absolute flow angle data exists. This uncertainty is due to the fact that different estimates of free-stream extent (flow angles cannot be measured in the wake with a cobra probe) result in different circumferential-mean angles.

The uncertainty intervals for circumferential-mean/radial equilibrium static-head data are relatively large at the stator exits because the predicted values of static head over the blade span (by radial equilibrium using casing static head) are evidently inaccurate. This can be seen from the comparisons of venturi and station integrated flow coefficients presented in Table 4.3. The relatively large error in the stator exit integrated flow coefficients can be traced to static head, since the total-head data are considered accurate. Further, the uncertainty intervals for the static-head data

Table 4.3. Comparison of venturi and axial measurement station integrated flow coefficients for the different compressor builds (ϕ = 0.500).

Station	Venturi Flow Coefficient ϕ	Integrated Flow Coefficient ϕ_a	Flow Coefficient Comparison (Percent) FCC
Baseline 1			
1	0.5001	0.5051	1.0112
2	0.5001	0 4980	-0.4274
3	0.5001	0.4964	-0.7409
4	0.5001	0.5016	0.2989
5	0.5000	0.4876	-2.4900
Baseline 2			
1	0.5001	0.5051	1.0112
2	0.5001	0.4980	-0.4274
3	0.5001	0.4960	-0.8260
4	0.5000	0.5034	0.6778
5	0.5002	0.4910	-1.8412
Modified 1			
1	0.5001	0.5038	0.7433
2	0.5001	0.4961	-0.8002
3	0.5001	0.4911	-1.7991
4	0.5001	0.4981	-0.3997
5	0.5002	0.4863	-2.7780
Modified 2			
1	0.5001	0.5038	0.7433
2	0.5001	0.4961	-0.8002
3	0.5000	0.4918	-1.6527
4	0.4999	0.5021	0.4272
5	0.5000	0.4869	-2.6118

were estimated by using the flow rate comparison values and assuming that, the stator exit flow rate discrepancies were due solely to static-head error.

The uncertainty intervals for flow-field quantities and performance parameters were estimated from those of the "primary computed quantities" using the uncertainty propagation methods of Kline and McClintock [5]. The second-power equation was solved analytically to estimate the uncertainty intervals for overall performance parameters. These are listed in Table 4.4. Uncertainty intervals for circumferential-mean quantities were estimated by solving the second-power equation numerically. To this end, a so-called "Jitter Program" discussed by Moffat [6] was employed. The uncertainty intervals estimated for circumferential-mean flow-field quantities are listed in Tables 4.5 and 4.6. The uncertainty intervals estimated for circumferential-mean performance parameters are presented in Table 4.7. Some of these uncertainty intervals are graphed in Figure 4.1.

4.2. Overall Compressor Performance

Results for overall compressor aerodynamic performance are presented and discussed in this section. Performance curves for the baseline 1 and modified 2 compressor builds are contained in Figure 4.2. Figure 4.2(a) and (b) involve overall head-rise variation with flow coefficient, while in Figure 4.2(c) overall work-input (shaft torque based) is presented. Lastly, an overall efficiency map of the compressor is shown in Figure 4.2(d). Each

Table 4.4. Estimated uncertainty intervals for overall performance parameters.

ESTIMATED UNCERTAINTY INTERVALS (20:1 ODDS).

		Overall Head-Rise Coefficient			
Venturi Flow Coefficient (Value) ϕ	Venturi Flow Coefficient (Uncertainty) ϕ	(Based on Second Stator Exit Shroud Static-Pressure) $\psi_{overall,2,2S}$	(Based on Venturi Static-Pressure) $\psi_{overall,v}$	Overall Work-Input Coefficient (Based on Shaft Torque) $\psi_{i,overall,m}$	Overall Efficiency $\eta_{m,overall,2,2S}$
0.400	±0.0042 (1.1%)	±0.0097 (2.0%)	±0.0034 (0.7%)	±0.0108 (1.5%)	±0.018 (2.5%)
0.500	±0.0034 (0.7%)	±0.0097 (2.4%)	±0.0034 (0.9%)	±0.0072 (1.3%)	±0.021 (2.7%)
0.600	±0.0028 (0.5%)	±0.0097 (3.5%)	±0.0034 (1.5%)	±0.0055 (1.4%)	±0.026 (3.7%)

Table 4.5 Uncertainty estimates (20:1 odds) for circumferential-mean flow-field quantities (ϕ = 0.500).

STATION 1 : ROTOR 1 INLET

PHH	HT N*M/KG	HS N*M/KG	BETA Y DEG.	V M/S	VZ M/S	VY M/S	BETA R DEG.	VR M/S	VYR M/S	FC
5.00	2.0000	5.0000	0.5000	0.1976	0.1977	0.2376	0.2701	0.2250	0.2376	0.0039
10.00	2.0000	5.0000	0.5000	0.1976	0.1976	0.2379	0.2664	0.2254	0.2379	0.0039
30.00	2.0000	5.0000	0.5000	0.1975	0.1975	0.2380	0.2502	0.2266	0.2380	0.0039
50.00	2.0000	5.0000	0.5000	0.1973	0.1973	0.2381	0.2359	0.2278	0.2381	0.0039
70.00	2.0000	5.0000	0.5000	0.1974	0.1974	0.2380	0.2229	0.2287	0.2381	0.0039
80.00	2.0000	5.0000	0.5000	0.1974	0.1974	0.2380	0.2154	0.2285	0.2380	0.0039
90.00	2.0000	5.0000	0.5000	0.1981	0.1981	0.2373	0.2102	0.2286	0.2373	0.0039
95.00	2.0000	5.0000	0.5000	0.1994	0.1993	0.2357	0.2081	0.2279	0.2357	0.0039

STATION 2 : ROTOR 1 EXIT / STATOR 1 INLET

PHH	HT N*M/KG	HS N*M/KG	BETA Y DEG.	V M/S	VZ M/S	VY M/S	BETA R DEG.	VR M/S	VYR M/S	FC
5.00	3.0000	5.0000	0.3000	0.1813	0.1774	0.1727	0.3187	0.1703	0.1727	0.0035
10.00	3.0000	5.0000	0.3000	0.1842	0.1789	0.1715	0.3147	0.1679	0.1715	0.0035
30.00	3.0000	5.0000	0.3000	0.1867	0.1805	0.1703	0.2969	0.1653	0.1703	0.0035
50.00	3.0000	5.0000	0.3000	0.1872	0.1815	0.1695	0.2750	0.1648	0.1695	0.0036
70.00	3.0000	5.0000	0.3000	0.1857	0.1813	0.1693	0.2505	0.1655	0.1694	0.0036
80.00	3.0000	5.0000	0.3000	0.1828	0.1798	0.1704	0.2352	0.1682	0.1703	0.0035
90.00	3.0000	5.0000	0.3000	0.1865	0.1809	0.1699	0.2477	0.1642	0.1700	0.0035
95.00	3.0000	5.0000	0.3000	0.2109	0.1896	0.1718	0.3002	0.1450	0.1718	0.0037

STATION 3 : STATOR 1 EXIT / ROTOR 2 INLET

PHH	HT N*M/KG	HS N*M/KG	BETA Y DEG.	V M/S	VZ M/S	VY M/S	BETA R DEG.	VR M/S	VYR M/S	FC
5.00	3.0000	15.0000	0.3500	0.6353	0.6336	0.1541	0.7506	0.3454	0.1541	0.0124
10.00	3.0000	15.0000	0.3500	0.5824	0.5824	0.1606	0.6033	0.3633	0.1606	0.0114
30.00	3.0000	15.0000	0.3500	0.5734	0.5734	0.1630	0.5739	0.3457	0.1629	0.0112
50.00	3.0000	15.0000	0.3500	0.5630	0.5629	0.1660	0.5474	0.3273	0.1660	0.0110
70.00	3.0000	15.0000	0.3500	0.5536	0.5532	0.1699	0.5285	0.3073	0.1699	0.0108
80.00	3.0000	15.0000	0.3500	0.5494	0.5482	0.1740	0.5276	0.2926	0.1739	0.0107
90.00	3.0000	15.0000	0.3500	0.5922	0.5907	0.1634	0.5760	0.2821	0.1634	0.0116
95.00	3.0000	15.0000	0.3500	0.6515	0.6514	0.1435	0.6148	0.3024	0.1435	0.0128

Table 4.5 concluded.

STATION 4 : ROTOR 2 EXIT / STATOR 2 INLET

PHH	HT N*M/KG	HS N*M/KG	BETA Y DEG.	V M/S	VZ M/S	VY M/S	BETA R DEG.	VR M/S	VYR M/S	FC
5.00	3.0000	5.0000	0.1500	0.1835	0.1442	0.1407	0.3798	0.0918	0.1407	0.0028
10.00	3.0000	5.0000	0.1500	0.1881	0.1641	0.1226	0.3105	0.0983	0.1226	0.0032
30.00	3.0000	5.0000	0.1500	0.1874	0.1677	0.1169	0.2817	0.0960	0.1169	0.0033
50.00	3.0000	5.0000	0.1500	0.1859	0.1685	0.1136	0.2590	0.0939	0.1136	0.0033
70.00	3.0000	5.0000	0.1500	0.1828	0.1658	0.1135	0.2432	0.0919	0.1135	0.0032
80.00	3.0000	5.0000	0.1500	0.1793	0.1615	0.1154	0.2368	0.0912	0.1154	0.0032
90.00	3.0000	5.0000	0.1500	0.1888	0.1661	0.1207	0.2534	0.0832	0.1207	0.0033
95.00	3.0000	5.0000	0.1500	0.2133	0.1759	0.1403	0.3023	0.0731	0.1403	0.0034

STATION 5 : STATOR 2 EXIT

PHH	HT N*M/KG	HS N*M/KG	BETA Y DEG.	V M/S	VZ M/S	VY M/S	BETA R DEG.	VR M/S	VYR M/S	FC
5.00	3.0000	25.0000	0.3500	1.1860	1.1839	0.1472	1.4660	0.5618	0.1473	0.0232
10.00	3.0000	25.0000	0.3500	1.0593	1.0587	0.1497	1.1988	0.5609	0.1498	0.0207
30.00	3.0000	25.0000	0.3500	0.9775	0.9773	0.1586	0.9732	0.5539	0.1586	0.0191
50.00	3.0000	25.0000	0.3500	0.9269	0.9269	0.1660	0.8848	0.5113	0.1659	0.0181
70.00	3.0000	25.0000	0.3500	0.9059	0.9048	0.1750	0.8623	0.4620	0.1750	0.0177
80.00	3.0000	25.0000	0.3500	0.9063	0.9038	0.1827	0.8687	0.4353	0.1827	0.0177
90.00	3.0000	25.0000	0.3500	0.9676	0.9661	0.1676	0.9204	0.4362	0.1677	0.0189
95.00	3.0000	25.0000	0.3500	1.0432	1.0432	0.1474	0.9673	0.4711	0.1475	0.0204

Table 4.6 Uncertainty estimates (20:1 odds) for circumferential-mean incidence and deviation angles (ϕ = 0.500).

INCIDENCE ANGLES (DEG.)

PHH	STATION 1 (ROTOR 1)	STATION 2 (STATOR 1)	STATION 3 (ROTOR 2)	STATION 4 (STATOR 2)
5.00	0.3635	0.6500	0.7708	0.5000
10.00	0.3564	0.6500	0.6362	0.5000
30.00	0.3285	0.6500	0.6030	0.5000
50.00	0.3041	0.6500	0.5730	0.5000
70.00	0.2830	0.6500	0.5503	0.5000
80.00	0.2735	0.6500	0.5466	0.5000
90.00	0.2643	0.6500	0.5881	0.5000
95.00	0.2595	0.6500	0.6241	0.5000

DEVIATION ANGLES (DEG.)

PHH	STATION 2 (ROTOR 1)	STATION 3 (STATOR 1)	STATION 4 (ROTOR 2)	STATION 5 (STATOR 2)
5.00	0.3795	0.7000	0.4024	0.7000
10.00	0.3659	0.7000	0.3429	0.7000
30.00	0.3285	0.7000	0.3068	0.7000
50.00	0.2972	0.7000	0.2788	0.7000
70.00	0.2691	0.7000	0.2576	0.7000
80.00	0.2554	0.7000	0.2484	0.7000
90.00	0.2545	0.7000	0.2565	0.7000
95.00	0.3014	0.7000	0.3032	0.7000

Table 4.7 Uncertainty estimates (20:1 odds) for circumferential-mean performance parameters (ϕ = 0.500).

*** FIRST STAGE ***

PHH	HEAD RISE COEFFICIENT ROTOR	HEAD RISE COEFFICIENT IDEAL	LOSS COEFFICIENT ROTOR	LOSS COEFFICIENT STATOR	EFFICIENCY ROTOR	EFFICIENCY STAGE
5.00	0.0014	0.0041	0.0104	0.0077	0.0159	0.0144
10.00	0.0014	0.0042	0.0104	0.0082	0.0170	0.0169
30.00	0.0014	0.0045	0.0099	0.0085	0.0173	0.0173
50.00	0.0014	0.0049	0.0096	0.0085	0.0182	0.0180
70.00	0.0014	0.0052	0.0093	0.0083	0.0196	0.0190
80.00	0.0014	0.0054	0.0091	0.0079	0.0196	0.0185
90.00	0.0014	0.0055	0.0084	0.0081	0.0148	0.0133
95.00	0.0014	0.0056	0.0077	0.0105	0.0111	0.0109

*** SECOND STAGE ***

PHH	HEAD RISE COEFFICIENT ROTOR	HEAD RISE COEFFICIENT IDEAL	LOSS COEFFICIENT ROTOR	LOSS COEFFICIENT STATOR	EFFICIENCY ROTOR	EFFICIENCY STAGE
5.00	0.0016	0.0029	0.0087	0.0078	0.0092	0.0087
10.00	0.0016	0.0029	0.0072	0.0083	0.0113	0.0112
30.00	0.0016	0.0031	0.0070	0.0084	0.0125	0.0126
50.00	0.0016	0.0033	0.0068	0.0083	0.0135	0.0137
70.00	0.0016	0.0036	0.0067	0.0080	0.0138	0.0137
80.00	0.0016	0.0038	0.0069	0.0076	0.0138	0.0133
90.00	0.0016	0.0039	0.0068	0.0084	0.0128	0.0124
95.00	0.0016	0.0039	0.0061	0.0109	0.0092	0.0098

*** OVERALL ***

PHH	HEAD RISE COEFFICIENT	EFFICIENCY
5.00	0.0014	0.0073
10.00	0.0014	0.0092
30.00	0.0014	0.0100
50.00	0.0014	0.0109
70.00	0.0014	0.0112
80.00	0.0014	0.0109
90.00	0.0014	0.0089
95.00	0.0014	0.0071

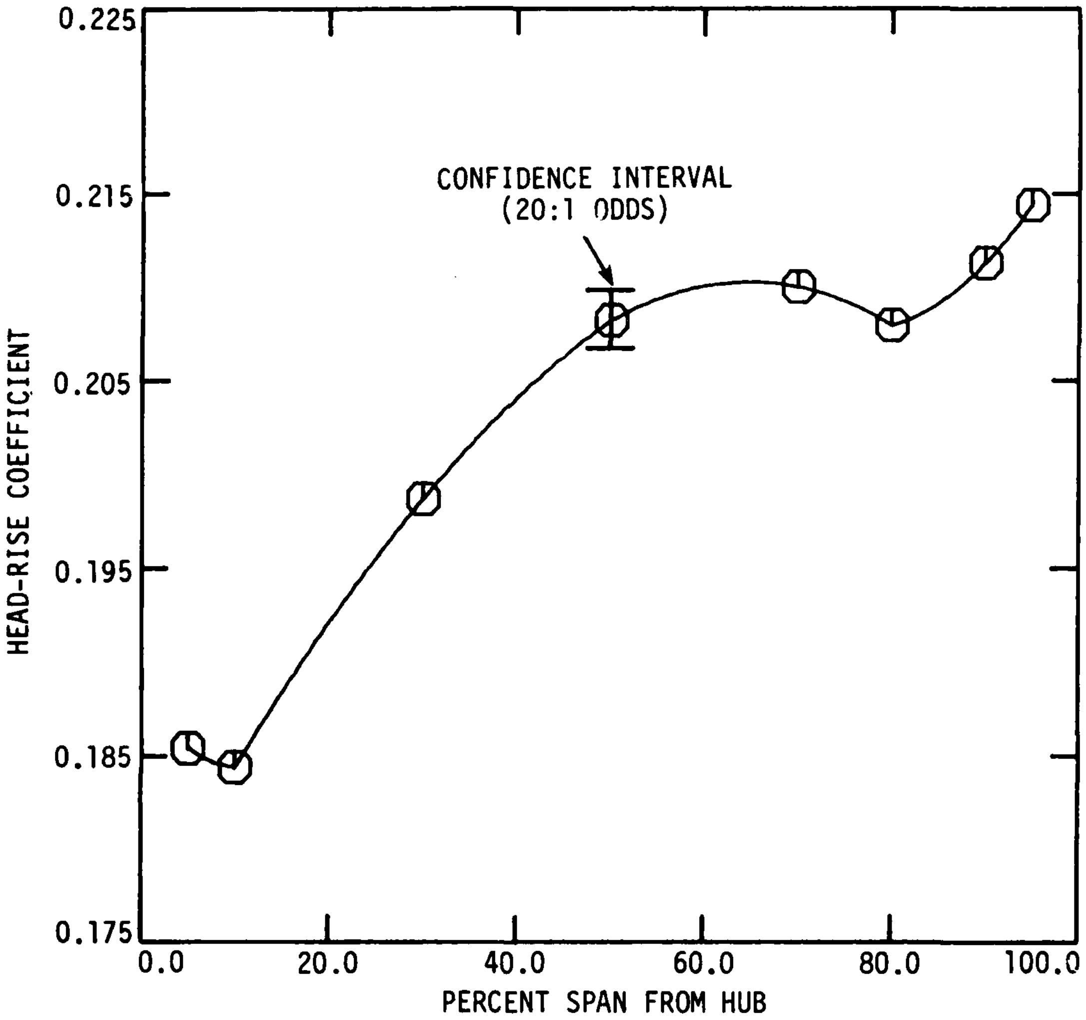

(a) HEAD-RISE

Figure 4.1 Confidence intervals (20:1 odds) for circumferential-mean performance parameters (ϕ = 0.500).

Note: The curves drawn through the data in this and other Figures were generated by a computer plotting routine based on a second order fit. As such, these curves should be interpreted with caution.

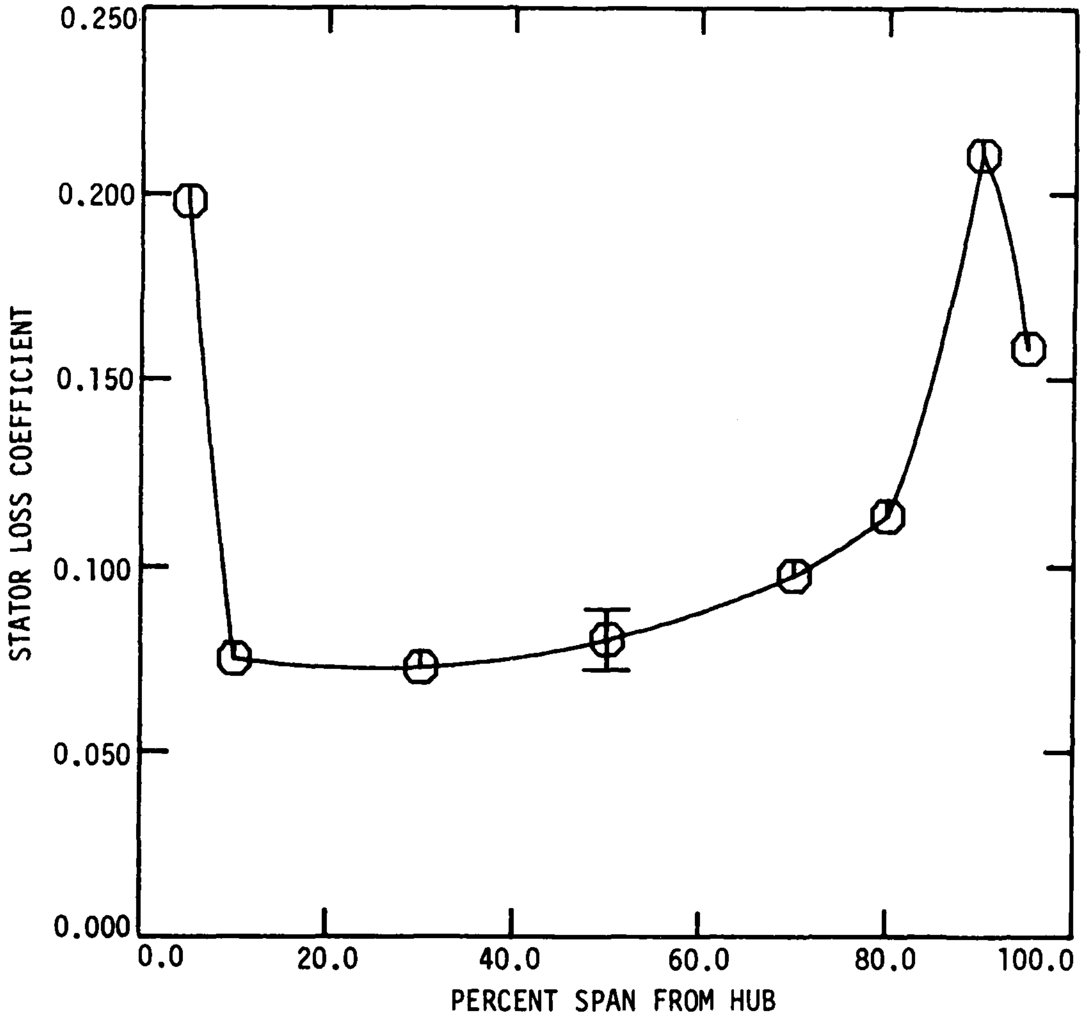

(b) STATOR LOSS

Figure 4.1 continued.

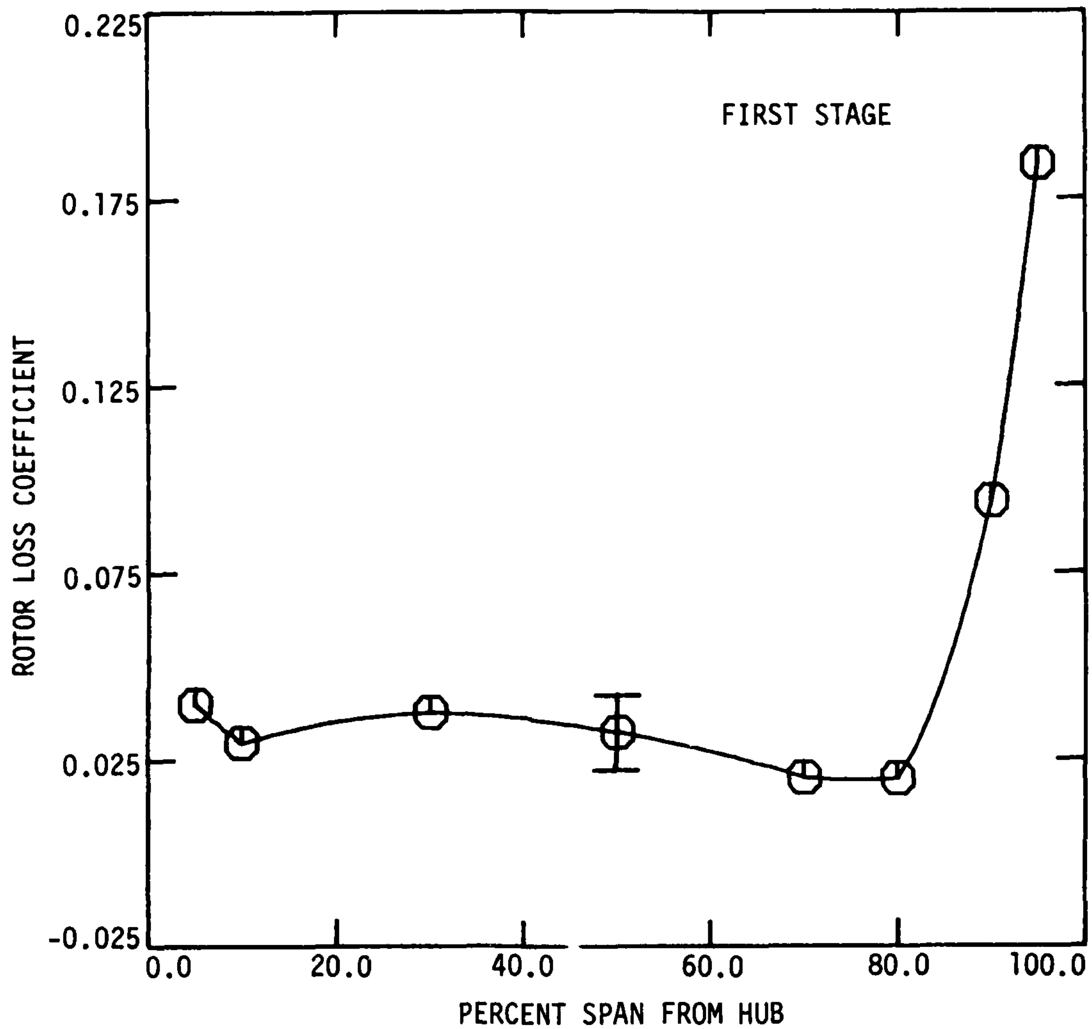

(c) FIRST STAGE ROTOR LOSS

Figure 4.1 continued.

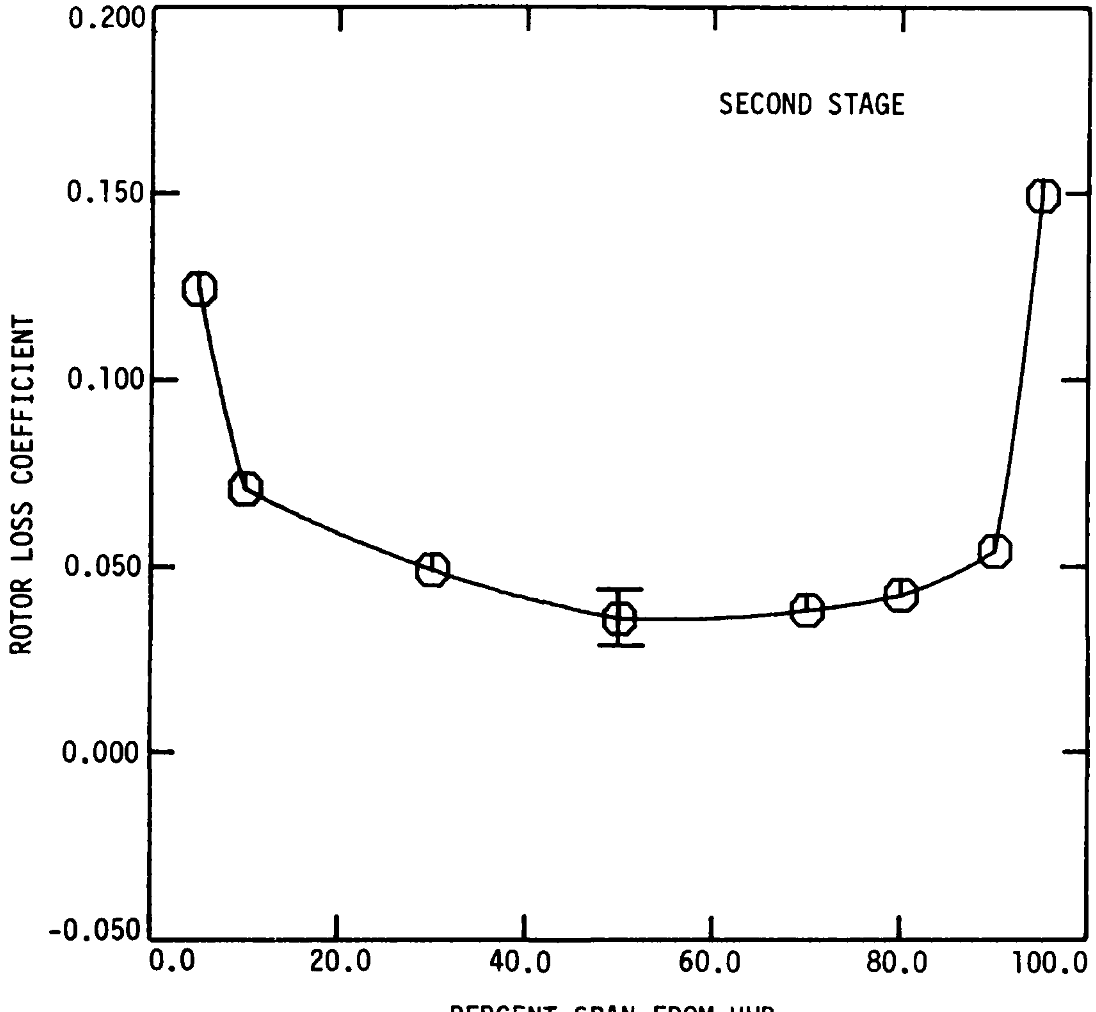

(d) SECOND STAGE ROTOR LOSS

Figure 4.1 continued.

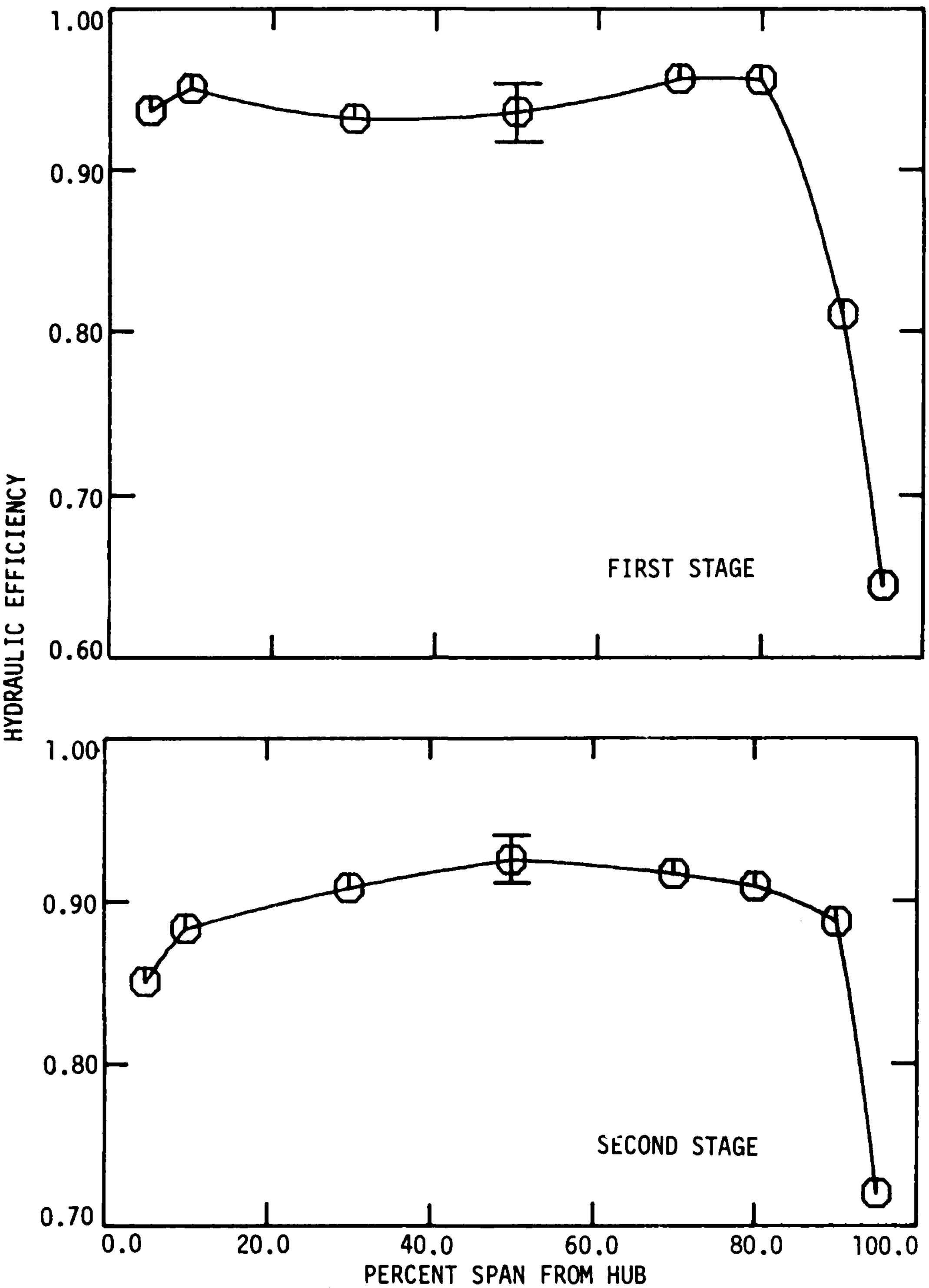

(e) ROTOR AND STAGE EFFICIENCY

Figure 4.1 continued.

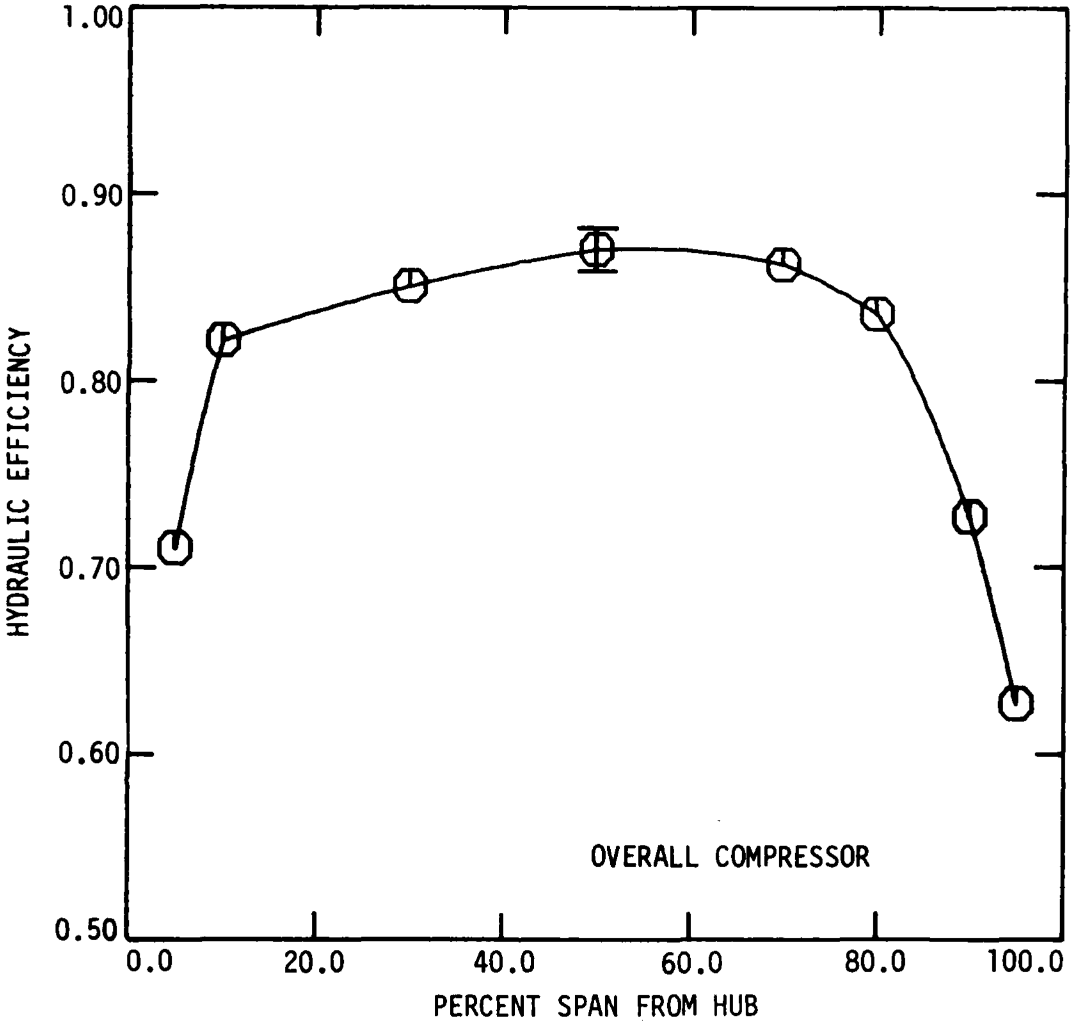

(f) EFFICIENCY FOR OVERALL COMPRESSOR

Figure 4.1 continued.

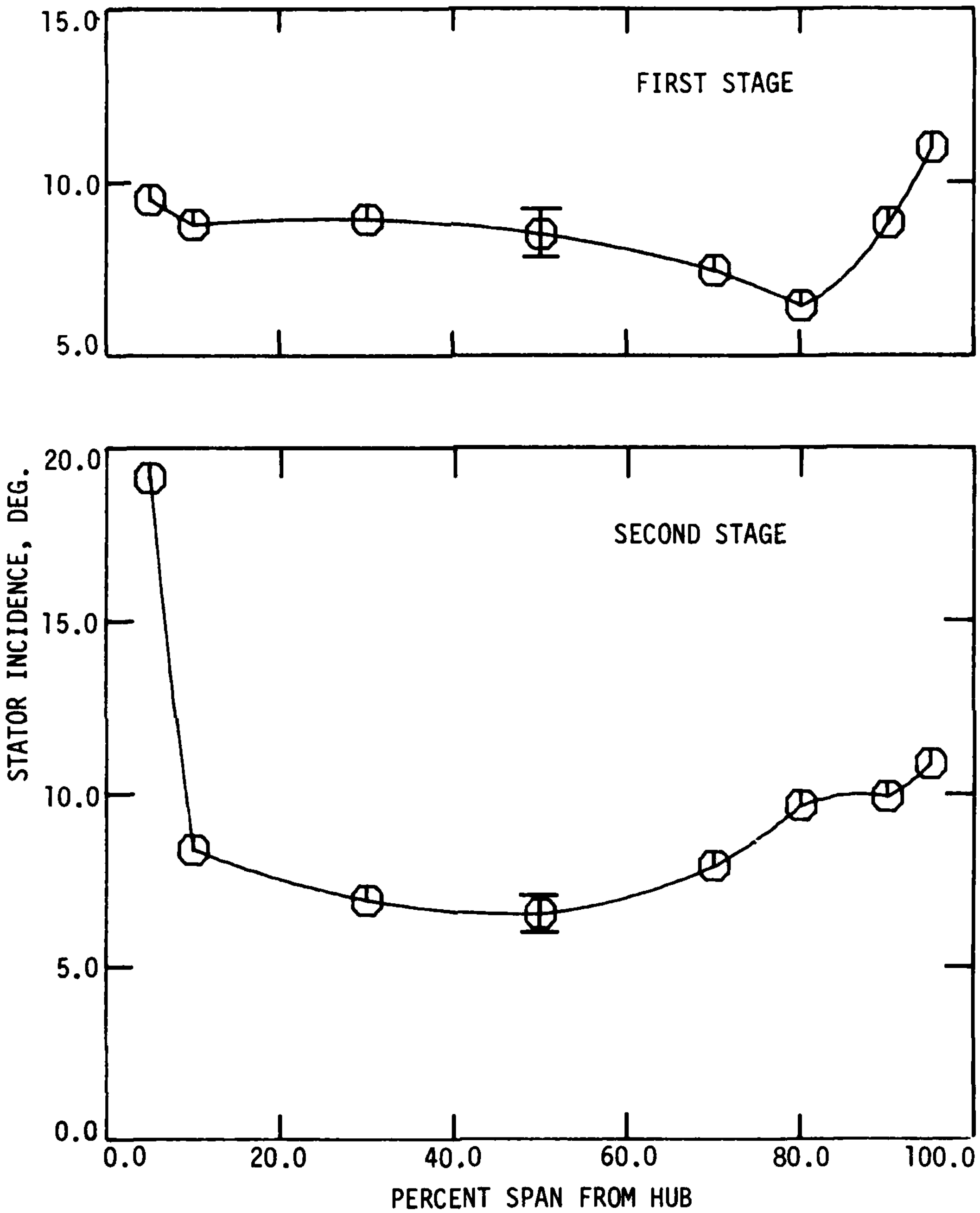

(g) STATOR INCIDENCE

Figure 4.1 continued.

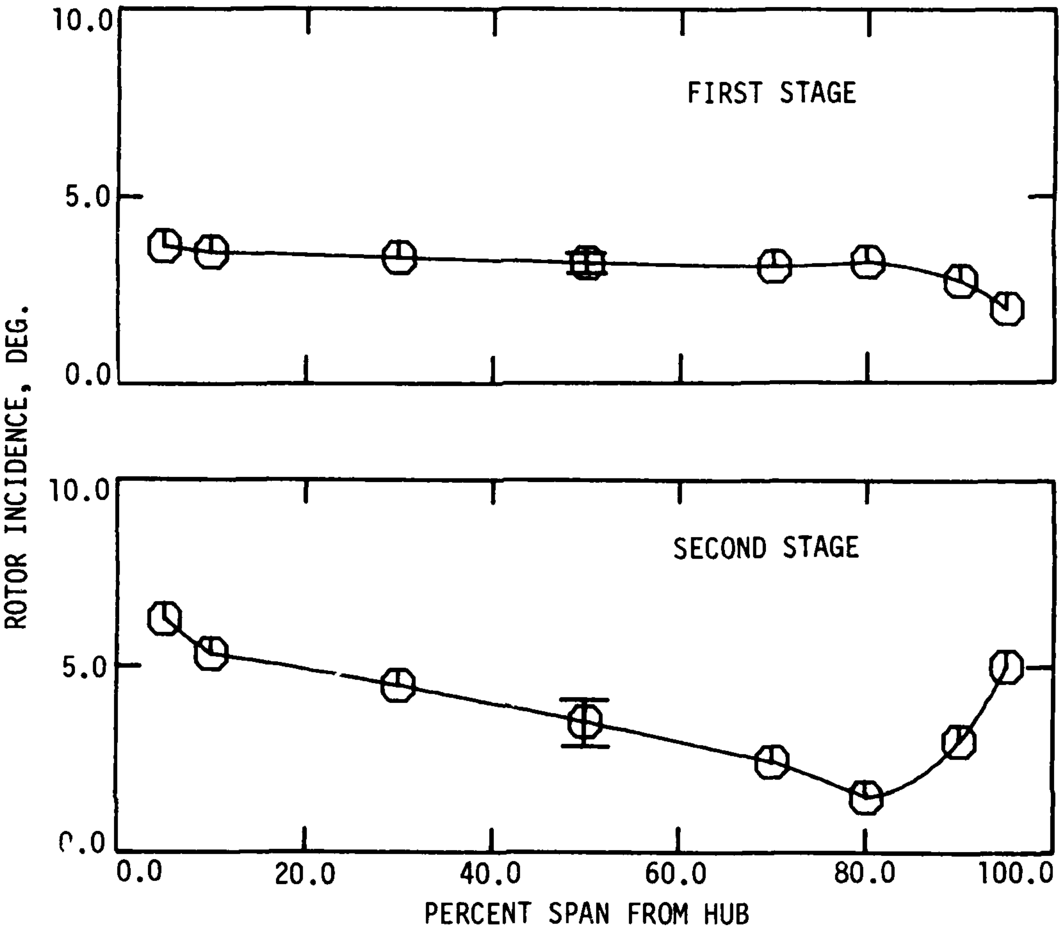

(h) ROTOR INCIDENCE

Figure 4.1 continued.

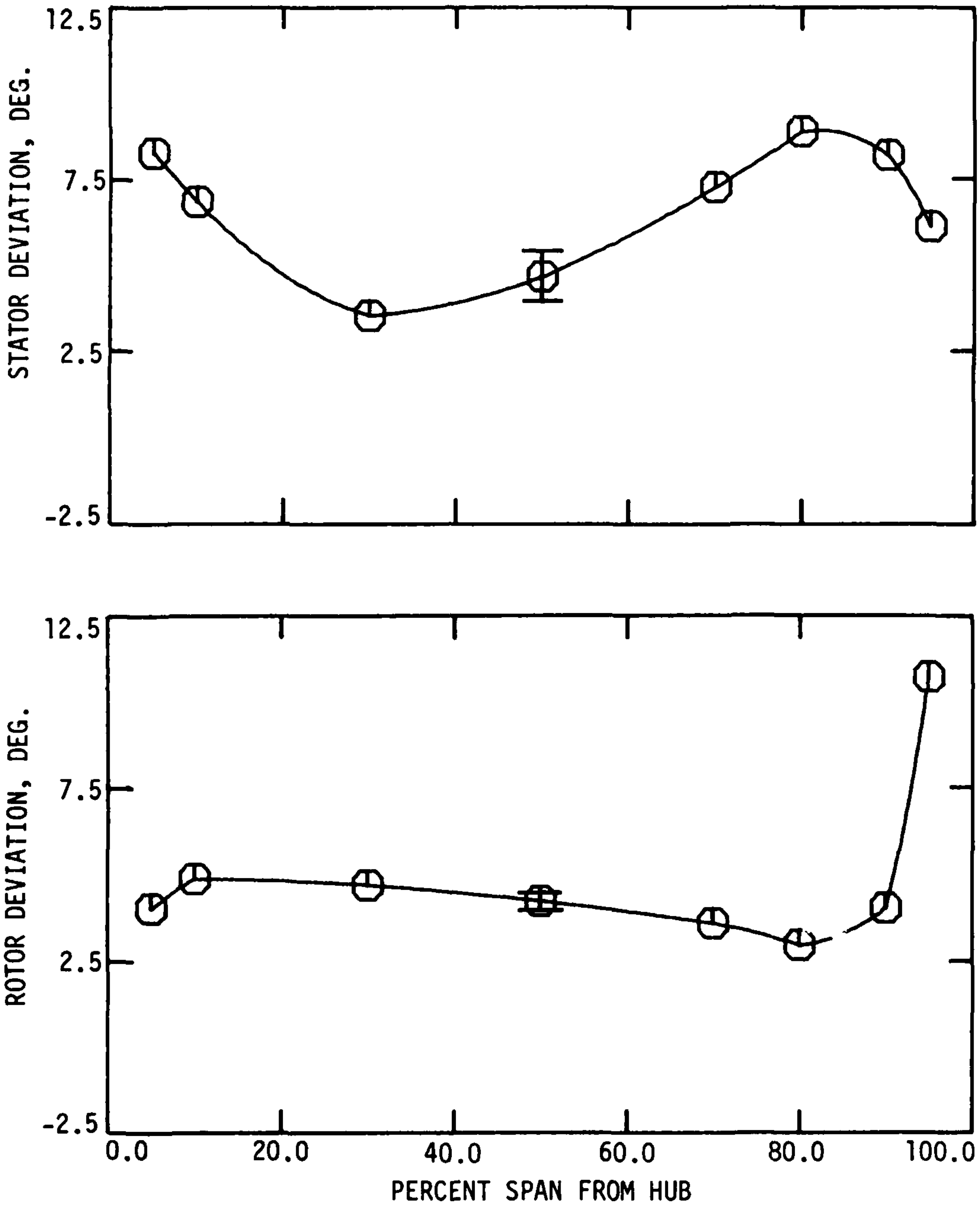

(i) STATOR AND ROTOR DEVIATION

Figure 4.1 concluded.

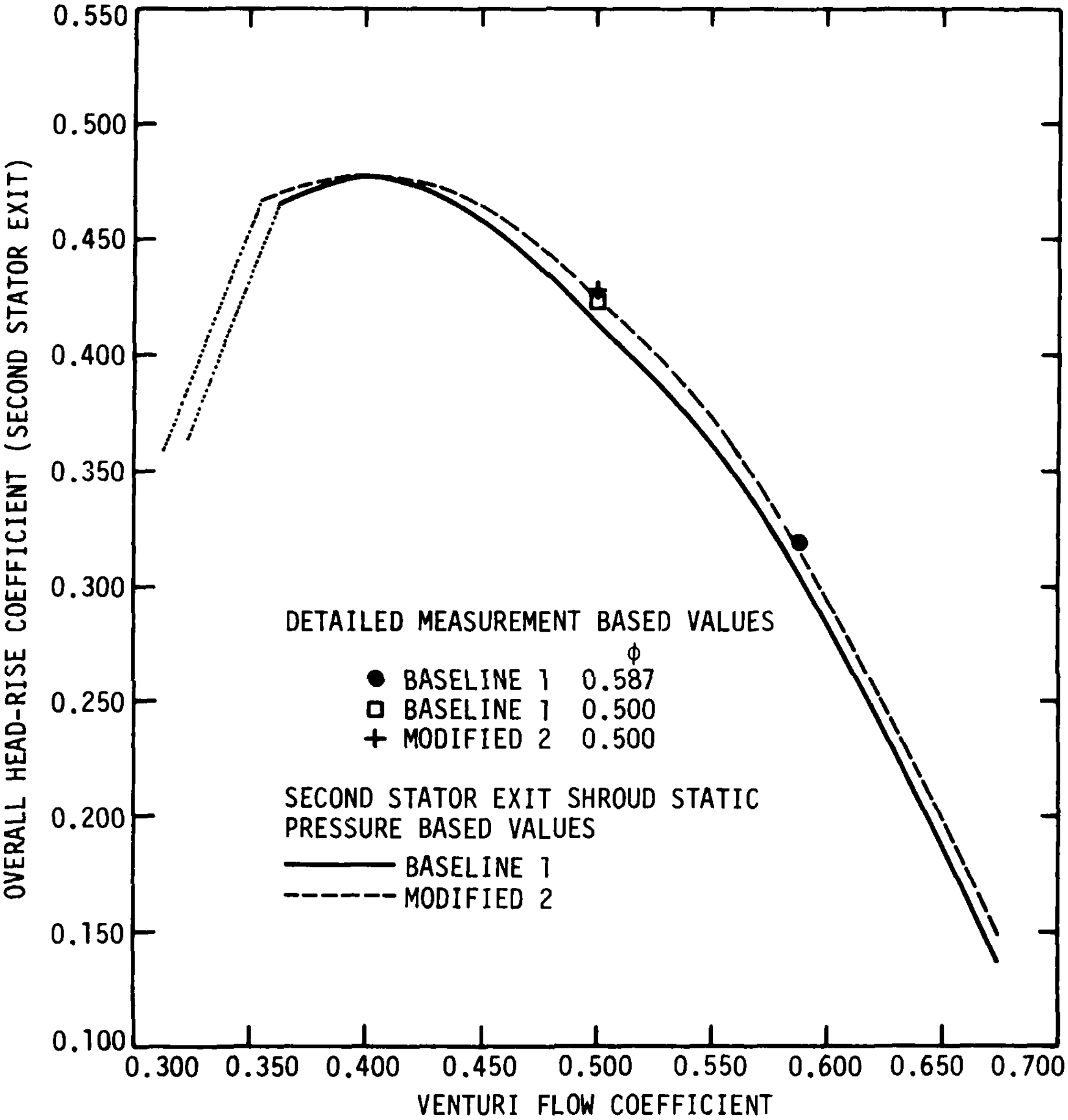

(a) OVERALL HEAD-RISE (SECOND STATOR EXIT)

Figure 4.2 Overall performance parameter variation with flow coefficient.

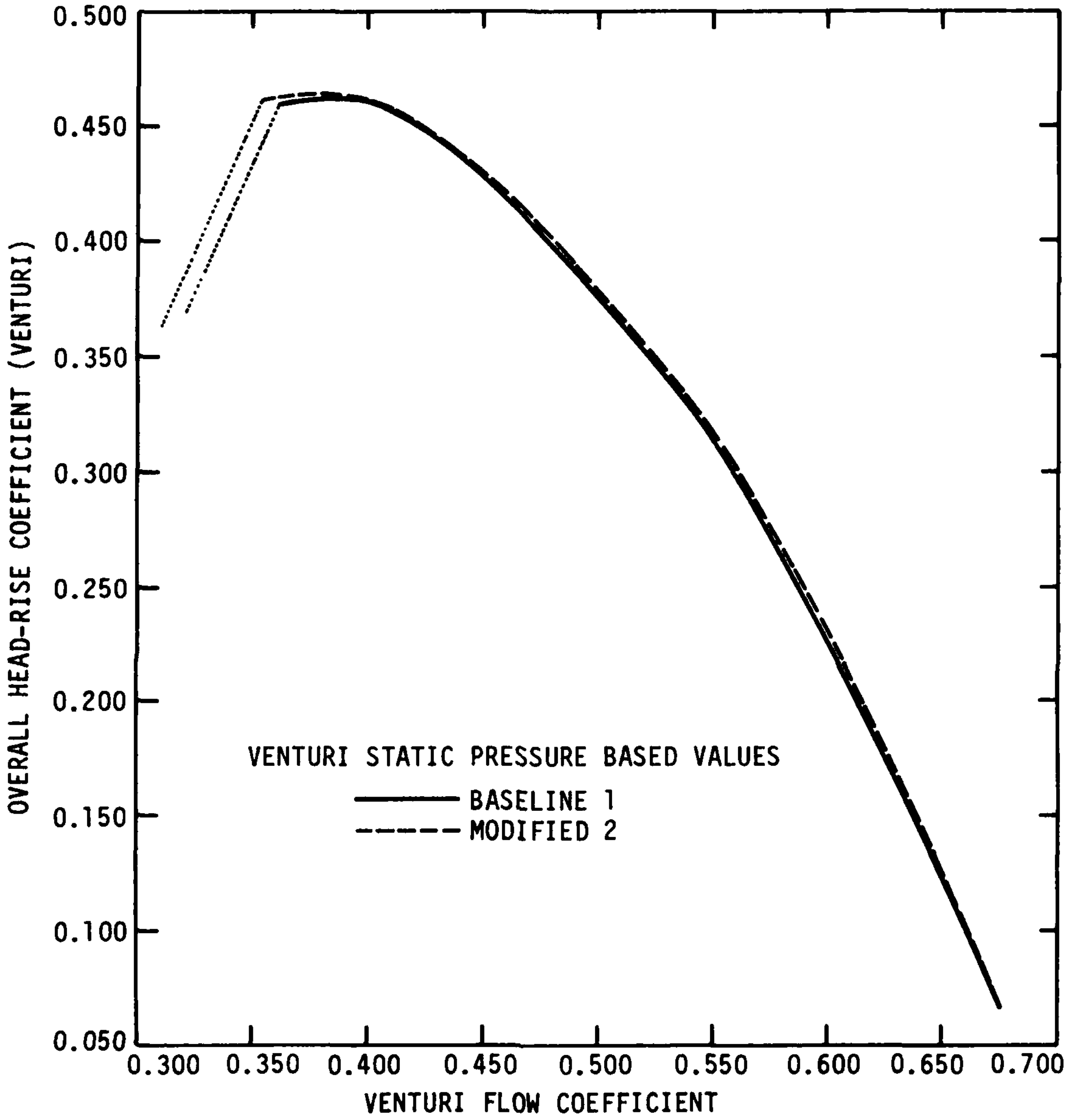

(b) OVERALL HEAD-RISE (VENTURI)

Figure 4.2 continued.

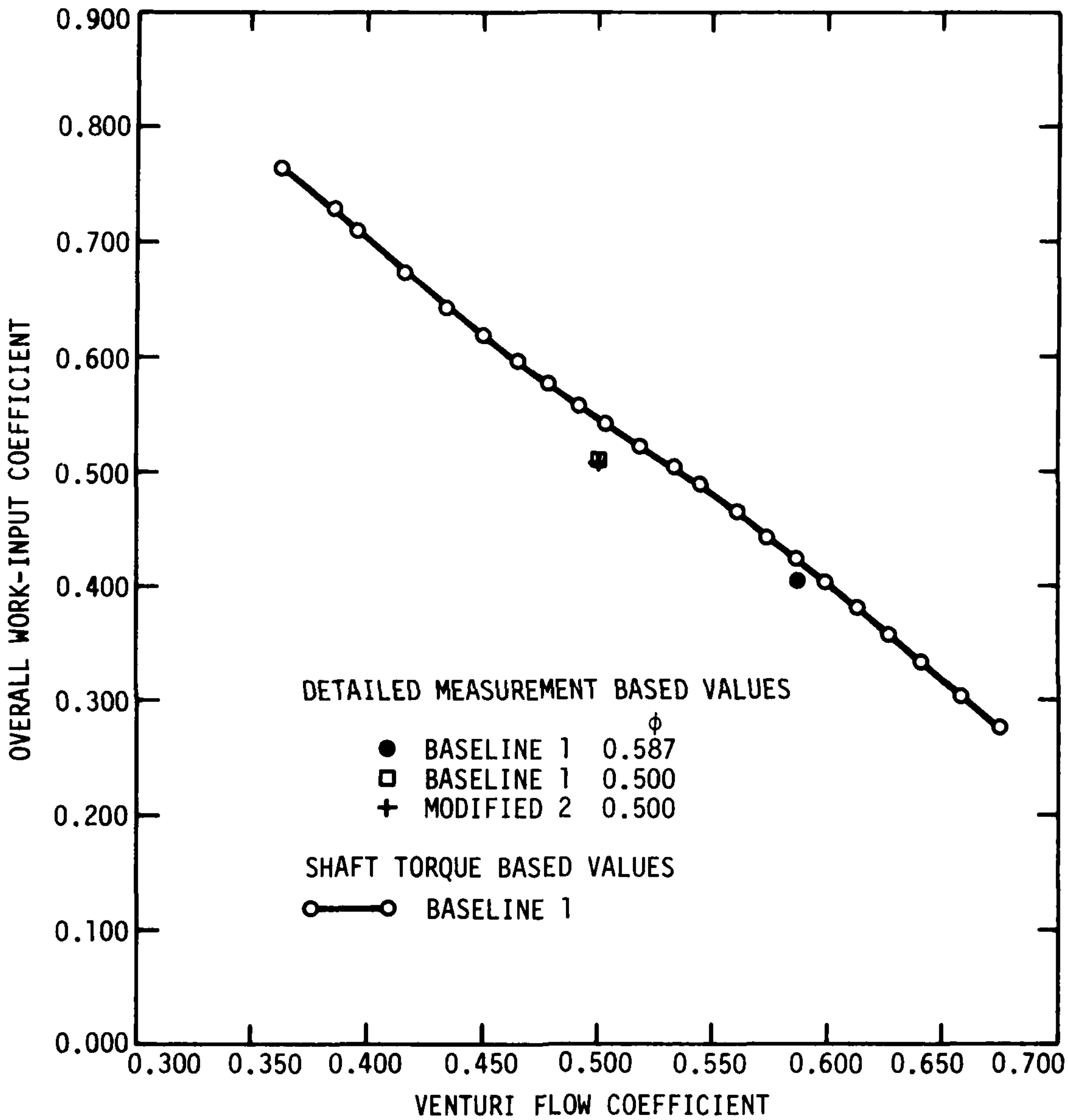

(c) OVERALL WORK-INPUT

Figure 4.2 continued.

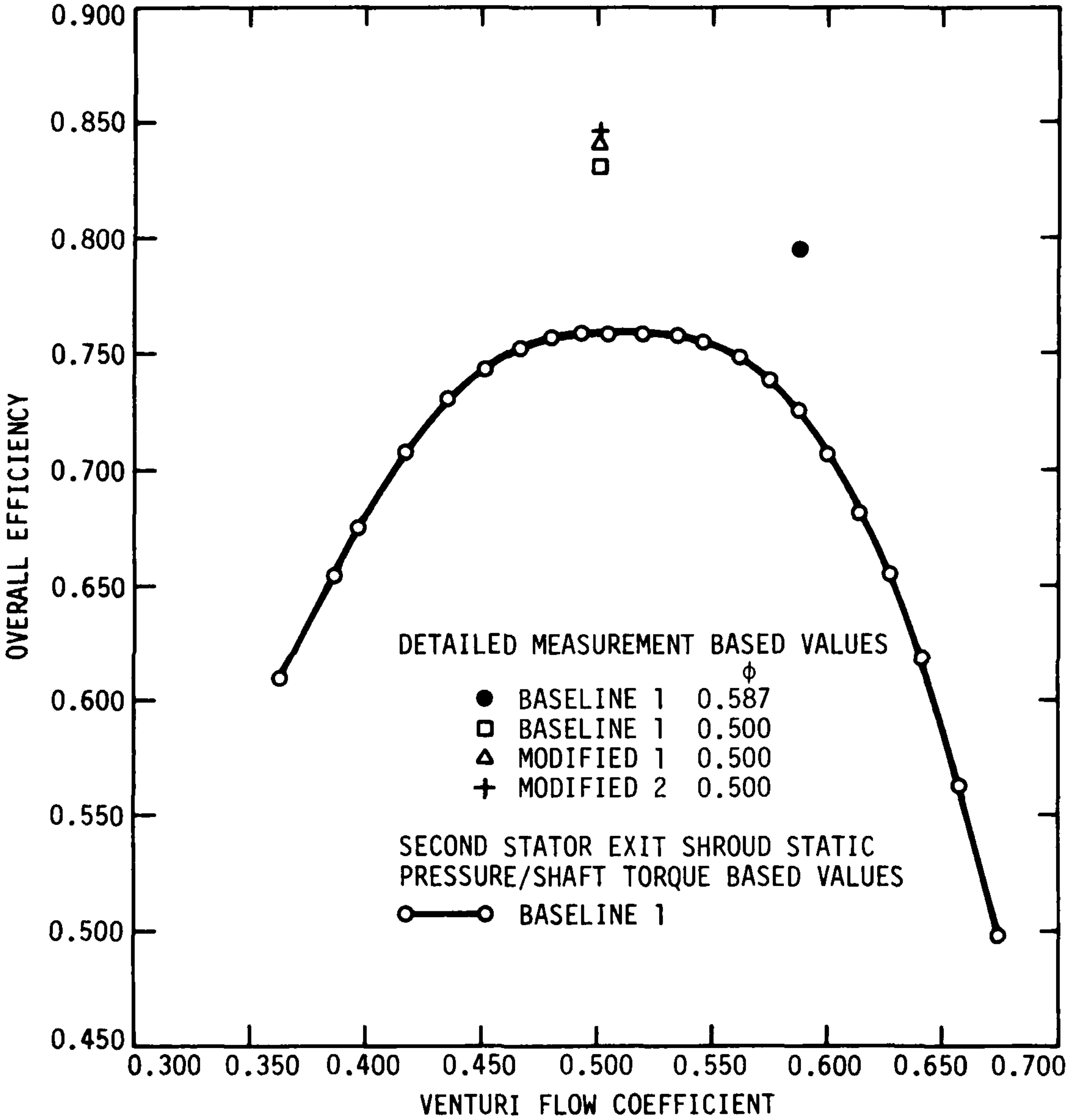

(d) OVERALL EFFICIENCY

Figure 4.2 concluded.

figure also includes data based on detailed measurements. Detailed measurement-based values are those radially mass-averaged overall performance quantities computed from the more extensive Kiel/cobra probe data acquired at selected flow rates.

The overall head-rise curves (Figure 4.2(a) and (b)) are based on data which could be rapidly measured over the entire operating range of the compressor (shaft speed = 2400 rpm). In particular, casing static-pressure measurements were obtained at the second stator exit and at the venturi meter throat for various flow rates and from these data the second stator-exit and venturi overall head-rise coefficients were calculated (Eqs. 8.51 and 8.52, respectively).

The second stator exit shroud static-pressure based head-rise curves in Figure 4.2(a) are only fair approximations to "actual" overall head-rise curves; the detailed measurement-based values included on the map are not coincident with any of the curves. The main reason for the discrepancy is that the measured shroud static-pressure is not sufficiently representative of the actual passage static pressure. These curves must, thus, be used with caution when comparing head-rise performance between different compressor builds. The curves in Figure 4.2(a) indicate differences in head-rise performance between the baseline 1 and modified 2 builds which are similar in magnitude to the discrepancy between the curves and their respective detailed measurement-based values at flow coefficient = 0.500. Further, the detailed measurement values show that the accepted difference in head-rise performance

between the baseline 1 and modified 2 builds is smaller than the two curves might imply.

The venturi throat static-pressure based head-rise curves in Figure 4.2(b) seem to provide a better comparison of head-rise performance of the different compressor builds. The venturi flow is well "mixed out," with the measured throat wall static pressure being representative of the passage static pressure. However, since these curves include losses between the compressor exit and the venturi meter throat, they involve substantially lower head-rise values.

Several conclusions regarding the head-rise performance maps in Figure 4.2(a) and (b) follow:

- The second stator exit shroud static-pressure based head-rise curves (Figure 4.2(a)) are approximate indicators of overall head-rise performance for the compressor. These curves should be used with great caution only for comparing the different compressor builds.
- The venturi static-pressure based head-rise curves (Figure 4.2(b)) provide a better comparison of overall head-rise performance for the different compressor builds. The observed differences, however, are small. The curves for all four compressor builds are not shown because they would be difficult to sort out at the graph scale used.
- The overall and detailed performance data indicate a head-rise benefit associated with the modified stator configuration.

- The stall-limit flow coefficient is significantly different between the baseline 1 and the modified 2 builds. (The baseline 2, modified 1, and modified 2 builds have a similar stall-limit flow coefficient). This difference, although significant, should not be used to establish definite conclusions presently since other unaccounted factors might be involved.

The overall work-input performance map (Figure 4.2(c)) provides a comparison of two types of data. The single curve is based on compressor drive-shaft torque data, and thus shows the overall work-input requirement of the baseline 1 compressor build with mechanical losses included. The detailed measurement-based data show the aerodynamic overall work-input (conventional "ideal" head-rise) of two different compressor builds at fixed operating points. These data indicate that the aerodynamic overall work-input is considerably less than the shaft overall work-input. This is, of course, the expected qualitative result. Quantitatively, the aerodynamic overall work-input is approximately 90% to 95% of the shaft overall work-input. About 5% to 10% of the shaft overall work-input is due to mechanical losses, i.e., bearing friction. Because bearing friction is substantial, the shaft overall work-input curves were unacceptable for comparison of compressor builds. The day-to-day shifts in the shaft overall work-input curves for a single build were as large as the differences between builds. The curve trends for each specific build are, however, very similar. This consistency in curve trend is useful for establishing a representative overall efficiency curve for the compressor.

The shaft overall efficiency curve for the baseline 1 compressor build is presented in Figure 4.2(d). This curve is based on second stator-exit shroud static pressure and shaft torque measurements, and like the shaft overall work-input curve, is not useful for comparing builds. The curve is fairly accurate in trend, however, and therefore, indicates the approximate operating range for peak overall efficiency. Because they involve aerodynamic performance only, the detailed measurement-based efficiencies (aerodynamic overall efficiencies) are suitable for build comparisons. The apparent large gain in aerodynamic overall efficiency associated with using the modified stator configuration will be discussed later.

In Figure 4.3 is shown the variation of first rotor and first stator incidence with flow coefficient at mid-span. These data can be useful in combination with the overall efficiency data (Figure 4.2(d)) for estimating the peak aerodynamic efficiency operating point for the baseline 1 compressor build. In this case, peak aerodynamic efficiency is expected at a flow coefficient between 0.5 and 0.587. The shaft overall efficiency begins to drop slightly at flow coefficient = 0.55. However, this shaft overall efficiency curve is distorted relative to that of the anticipated aerodynamic overall efficiency curve, which would have had its peak shifted somewhat to the right of that shown in Figure 4.2(d) because mechanical losses become proportionately larger relative to the overall work-input as flow coefficient increases. Considering the above, an estimated flow coefficient of 0.550 (rotor incidence = 1 deg and stator incidence = 3 deg) is probably close to the peak aerodynamic efficiency operating point of the baseline 1 build.

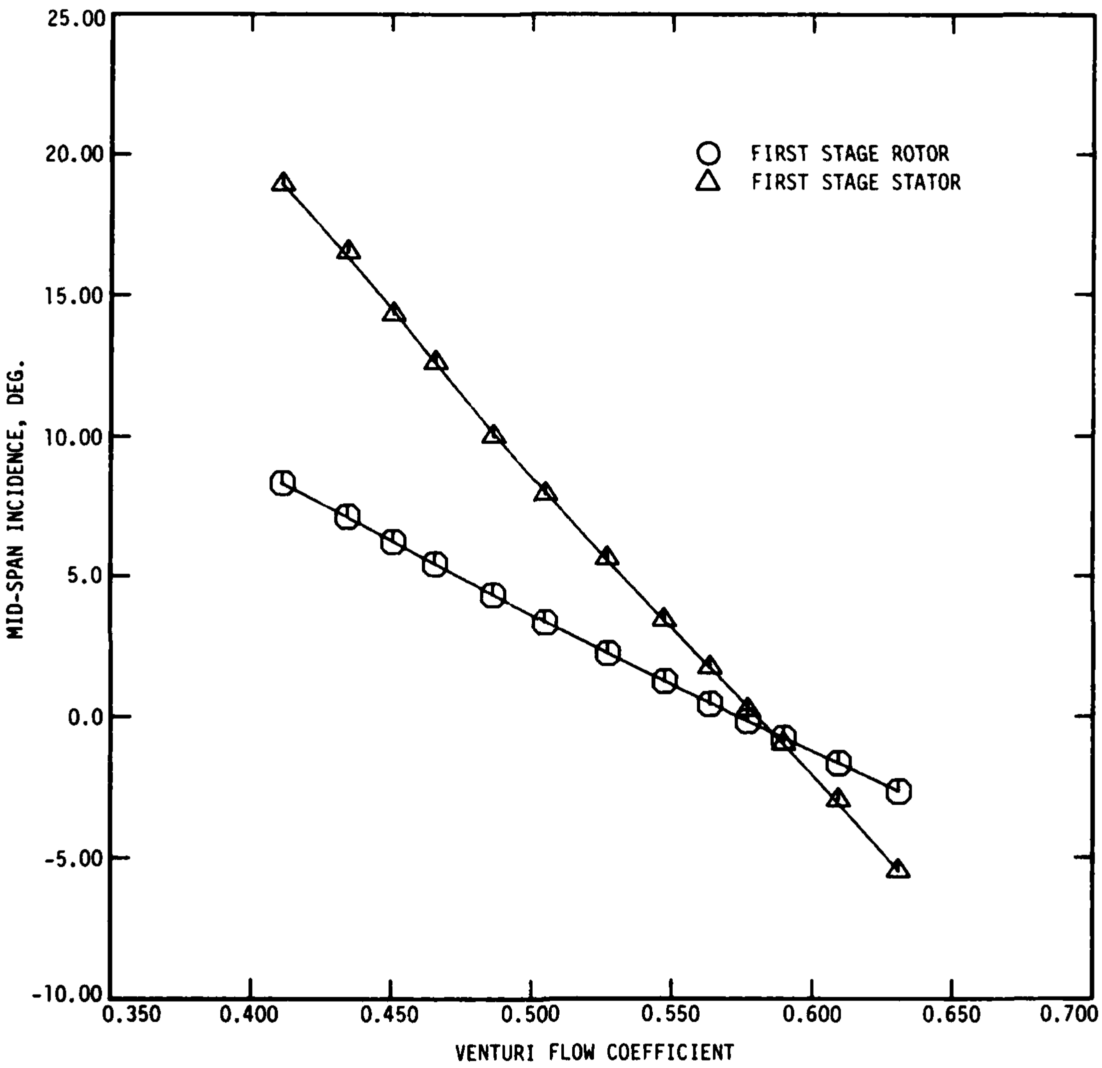

Figure 4.3 First stage incidence angle variation with flow coefficient at mid-span.

Some remarks concerning the decision to test the different compressor builds at a flow coefficient of 0.500 rather than 0.550 seem appropriate at this time. The primary consideration in selecting this flow coefficient was to test at a flow rate which would result in distinct and observable variation in the performance (head-rise) of the different builds while at a reasonably high (near peak) aerodynamic efficiency. Preliminary overall head-rise performance data for the baseline 1 and the modified 1 compressor builds available at the time the flow coefficient selection was made indicated that 0.5 was a good choice. At this flow coefficient the approximate overall head-rise curves indicated a significant head-rise difference associated with the two kinds of stator blades and overall efficiency values within the "flat" peak efficiency ranges involved.

4.3. Baseline 1 Compressor Build--Different Flow Rates

4.3.1. Design/Off-Design Performance Comparison

Results obtained for two operating points of the baseline 1 compressor build, design (venturi flow coefficient = 0.587) and off-design (venturi flow coefficient = 0.500), are presented and compared in this section. The sequence of presentation is as follows:

- rotor, stage, and overall head-rise
- stator loss
- stator incidence and deviation

- ideal head-rise, rotor loss, and rotor incidence and deviation
- rotor, stage, and overall hydraulic efficiencies
- mass-averaged performance

4.3.1.1. Head Rise

Spanwise variations of circumferential-mean head-rise performance are presented in Figure 4.4. Conventional rotor, stage, and overall head-rise curves are shown in Figure 4.4(a), (b), and (c), respectively. In Figure 4.5 are shown rotor exit total-head values, normalized by a single mass-averaged total-head value at the rotor inlet. Figure 4.5 thus provides a comparison of the first and second rotor exit total-head distributions on a common (constant inlet total-head) basis.

The rotor head-rise data are discussed first. The following trends can be noted:

- At design flow, the first and second rotors have different spanwise trends in head rise.
- At off-design flow, both rotors have similar spanwise trends in head rise.
- At both flow rates, the first rotor involves more head rise than the second rotor over most of the span.
- The spanwise trends in first rotor head rise are different for the two flow rates.
- The spanwise trends in second rotor head rise are similar for the two flow rates.
- Near the hub and tip, head-rise values can change abruptly.

The dissimilarity in spanwise trends in head rise for the first and second rotors at design flow is in contrast to the similarity in

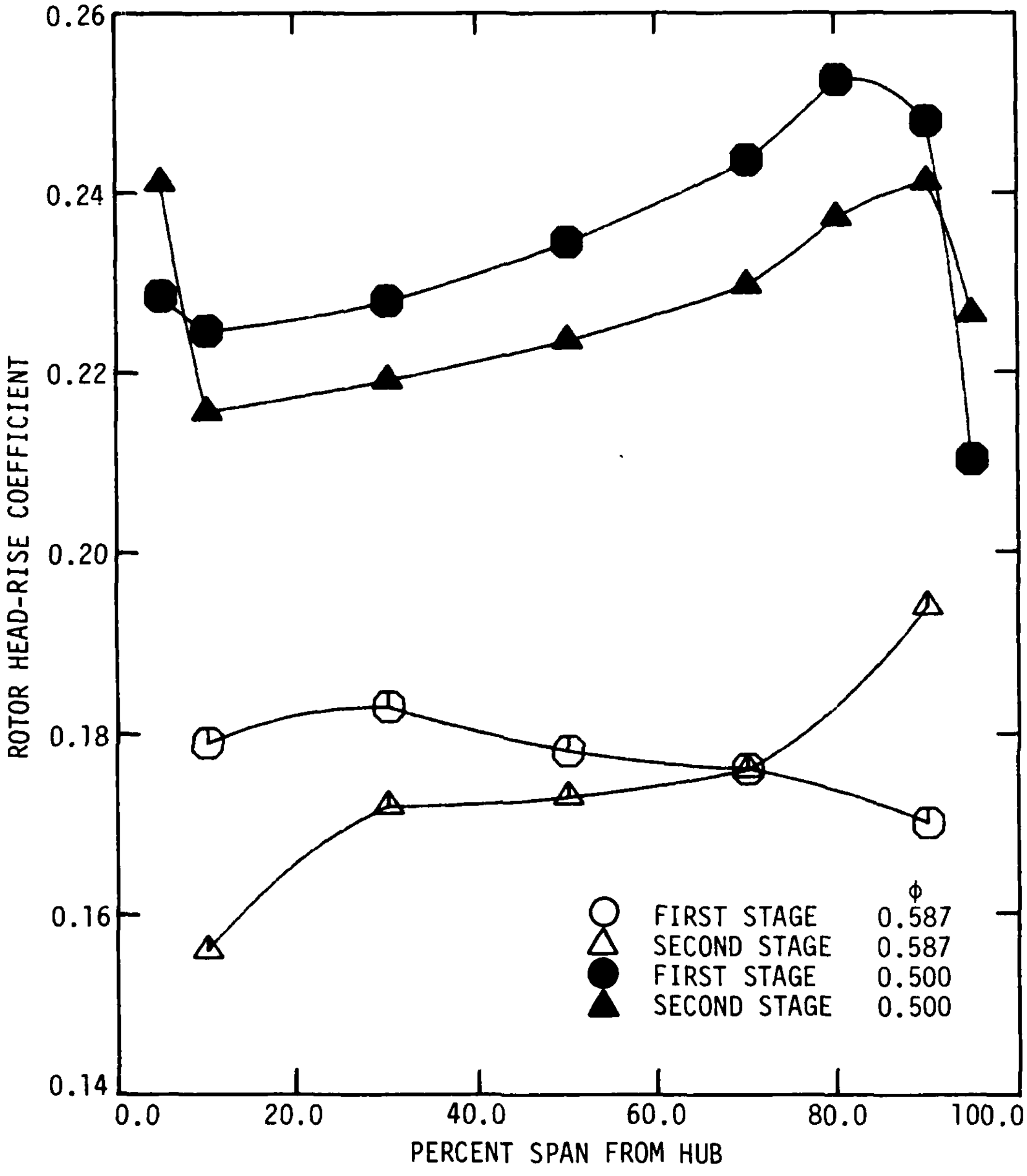

(a) ROTOR

Figure 4.4 Spanwise distribution of circumferential-mean head-rise coefficients for the baseline 1 compressor build at the design (ϕ = 0.587) and the off-design (ϕ = 0.500) operating points.

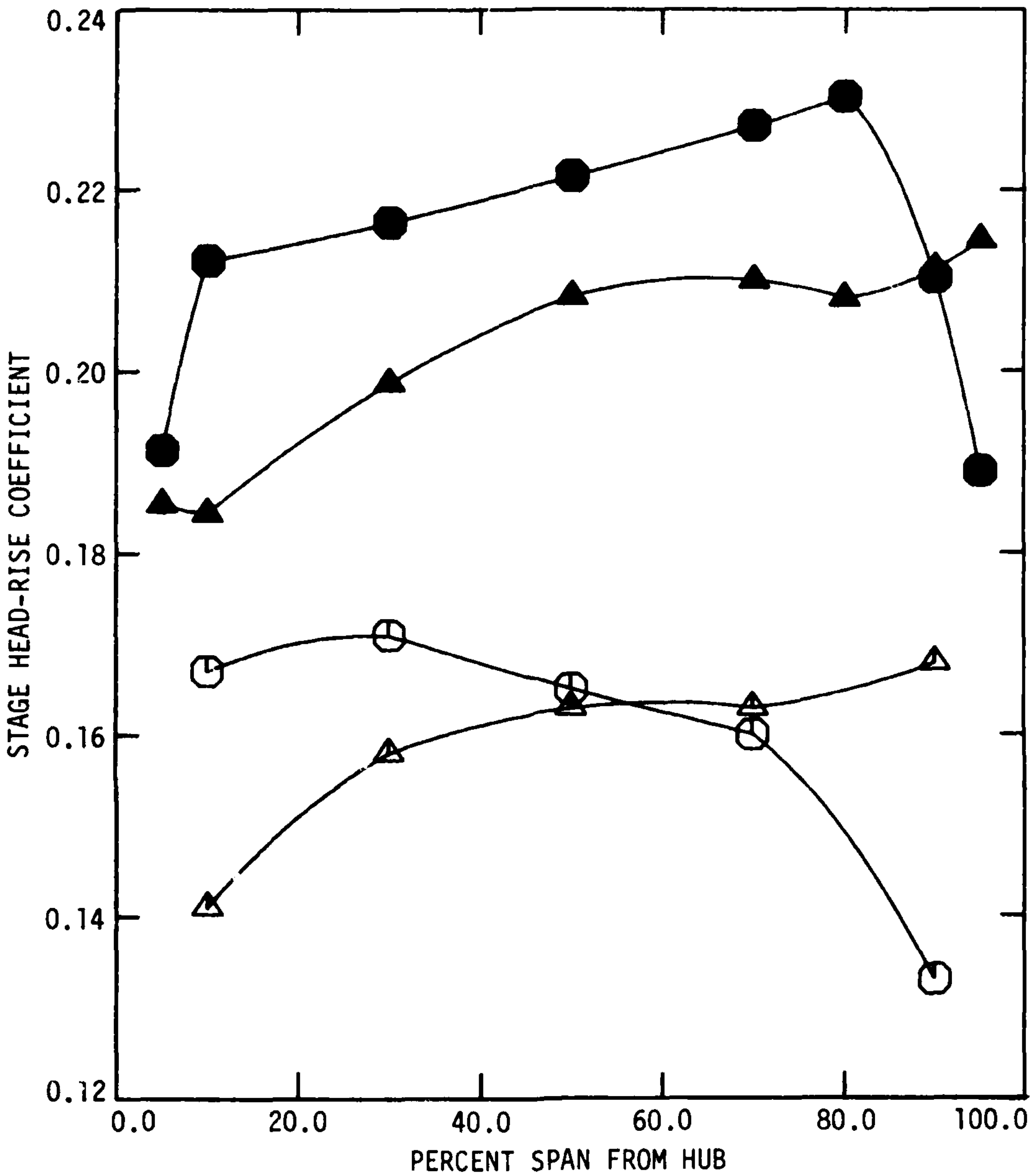

(b) STAGE

Figure 4.4 continued.

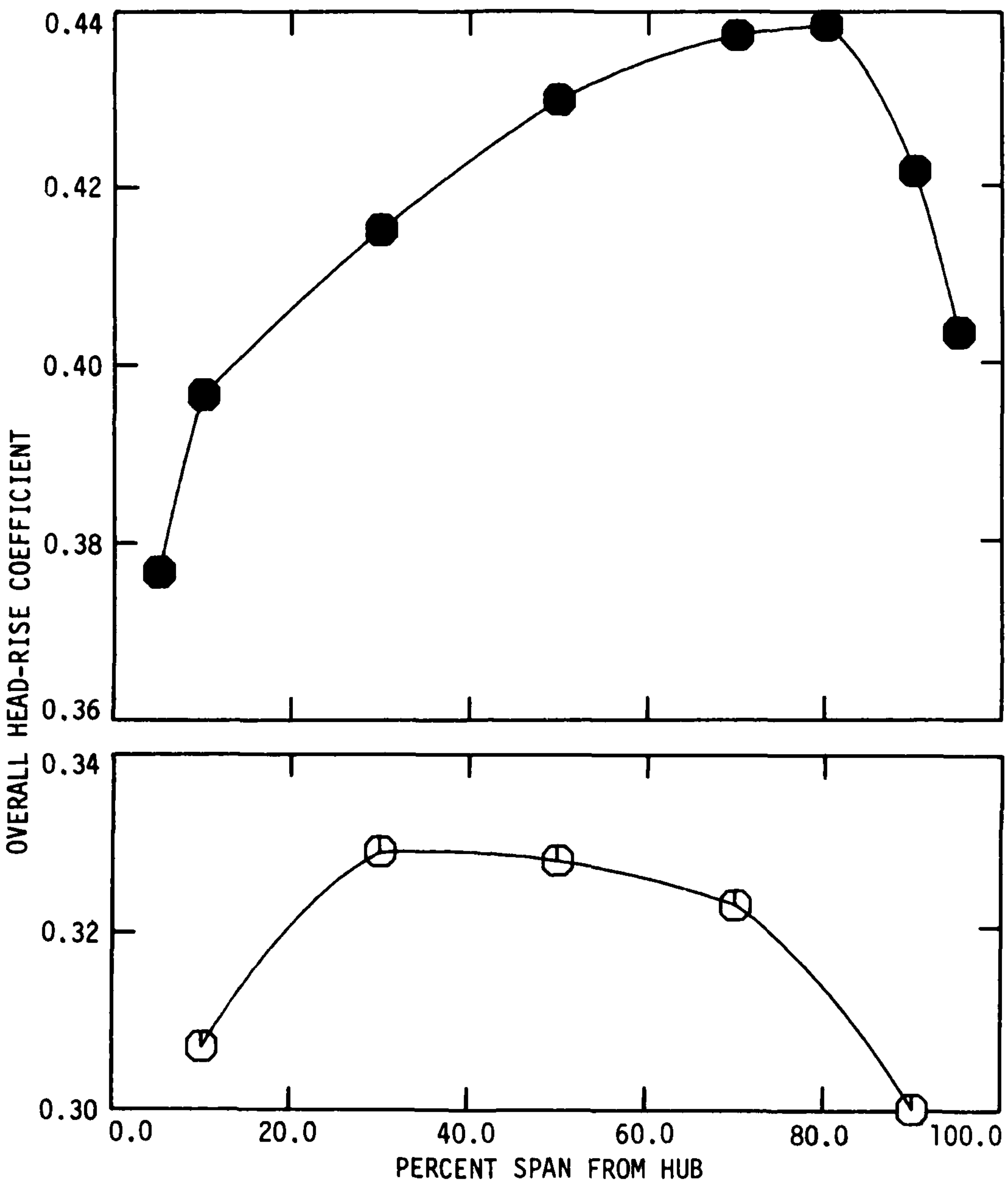

(c) OVERALL

Figure 4.4 concluded.

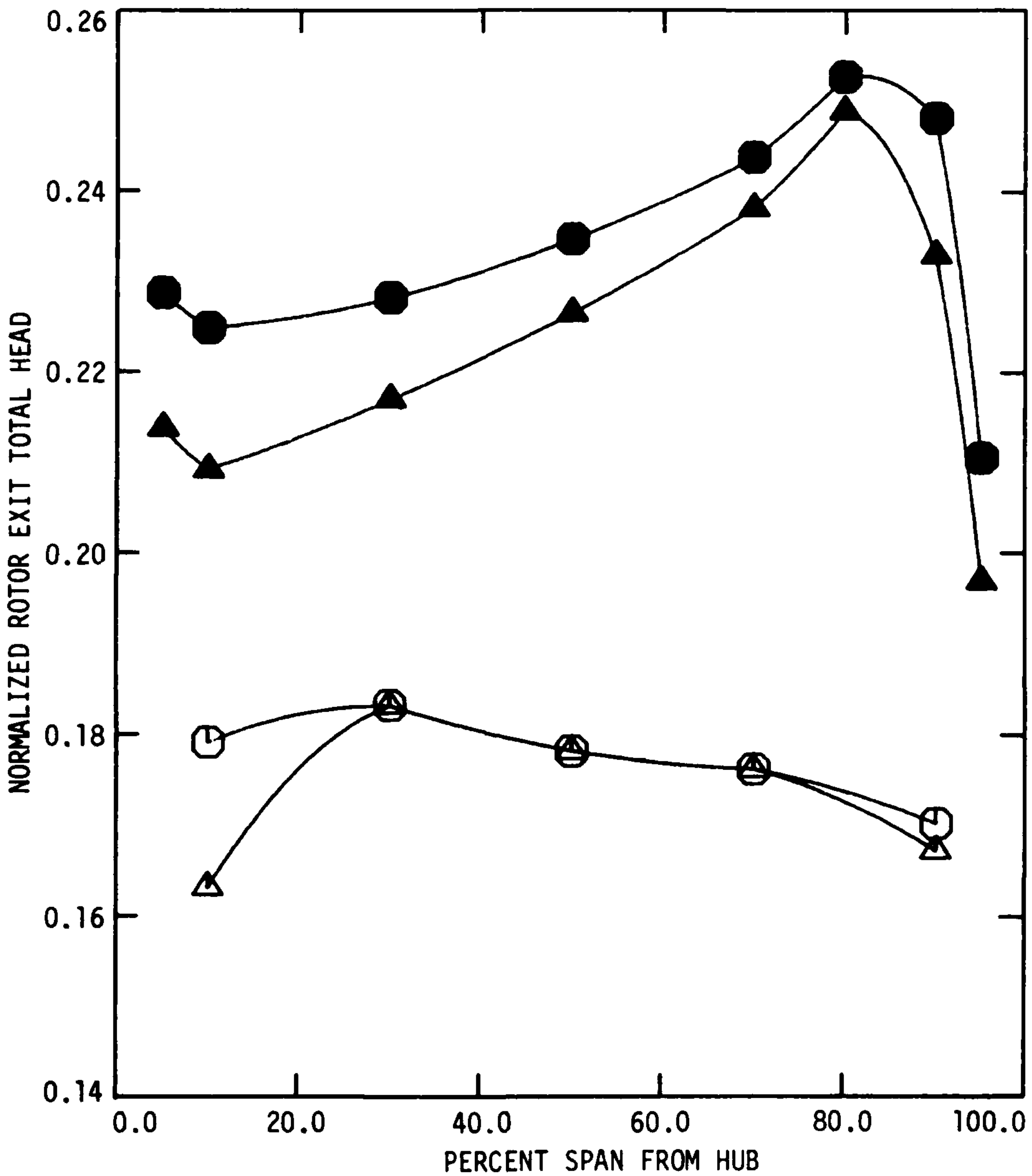

Figure 4.5 Spanwise distribution of normalized circumferential-mean rotor exit total-head values for the baseline 1 compressor build at the design ($\phi = 0.587$) and the off-design ($\phi = 0.500$) operating points.

these trends at off-design flow. This deserves further comment. Figure 4.5 demonstrates how the first and second rotor exit total-head distributions over the span of the blades are similar even though the head-rise distributions may not be. Thus, the spanwise trends in second rotor conventional head-rise (Figure 4.4(a)) are appproximately similar to the spanwise trends in first stator loss. This conclusion is best demonstrated in equation form using the definitions of the rotor head-rise and the stator loss coefficients. The second rotor head-rise coefficient can be written as follows:

$$\psi_{2R} = \frac{\omega_{1S}\bar{V}^2_{1,1S}}{2U_t^2} + \frac{\left(\bar{H}_{2,2R} - \bar{H}_{2,1R}\right)}{U_t^2} \qquad 4.1$$

For similar trends in the distributions of first and second rotor exit total-head values, the second term on the right-hand side of this equation is approximately constant over the blade span. This being the case, the second rotor head-rise will vary spanwise as the first stator loss does. Exact proportionality does not exist because the first stator inlet velocity varies over the blade span, especially near the hub and tip where the second rotor head-rise and first stator loss trends become most dissimilar.

These observations on rotor performance can be summarized:

- The spanwise trends in rotor exit total-head are similar between stages for a given operating point.
- These trends differ with flow rate variation.

- The rotor tends to compensate for variations in the spanwise distribution of total head at its inlet. That is, the rotor exit-flow similarity between stages exists despite the differences between the first and second rotor inlet conditions.
- There is an approximate relationship between the spanwise trend in second rotor head-rise and the spanwise trend in first stator loss, except near the hub and tip.

Some of these results lend support to the so-called "repeating stage" concept as discussed, for example, by Smith [7]. Further, the relationship between the spanwise distributions of second rotor head-rise and first stator loss is not unreasonable. The spanwise distribution of stator loss is related to the stator blade wake distribution. Larger stator losses are associated with larger blade wakes. Thus, larger head rise through the second rotor is relatable to larger stator wakes, the implication being that larger stator wakes can experience more energy addition within the rotor since wake fluid resides longer in the rotor than does free-stream fluid. More data supporting this line of reasoning is presented in section 4.4 of this report.

The stage and overall head-rise performance data (Figure 4.4(b) and (c)) are discussed next. The stage head-rise distributions are similar to their corresponding rotor head-rise distributions, but also reflect the spanwise distribution of stator loss as expected.

The overall head-rise distributions also have a rotor basis for comparing spanwise trend. The spanwise trends in second rotor exit total-head (Figure 4.5) are similar to the spanwise trends of

overall head rise. Each represent the exit conditions for the second rotor and the second stator, respectively. Any difference in shape of the second rotor exit total-head distributions and the overall head-rise distributions represents the influence of second stator losses.

Some general conclusions regarding the head-rise performance of the baseline 1 compressor operating at two different flow rates are now apparent:

- The spanwise trend in total head, as set up by the first rotor, does not change significantly for the fluid as it moves axially through the compressor.
- At design flow this trend is generally decreasing from hub to tip with a peak at 30% span from the hub.
- At off-design flow this trend is generally increasing from hub to tip with a peak at 80% span from the hub.

These general conclusions can also be drawn from the total-head contour maps for each blade row exit of the baseline 1 compressor as presented in Figures 4.6 and 4.7 for the design and off-design flows, respectively. A peculiar result can be noted at this time. In Figure 4.6 (design flow), the second rotor exit total-head contour map indicates two regions of lower total-head within one stator pitch over most of the span. This is surprising because only one lower total-head region was expected. This behavior was further investigated and the results are presented and discussed in section 4.3.2.

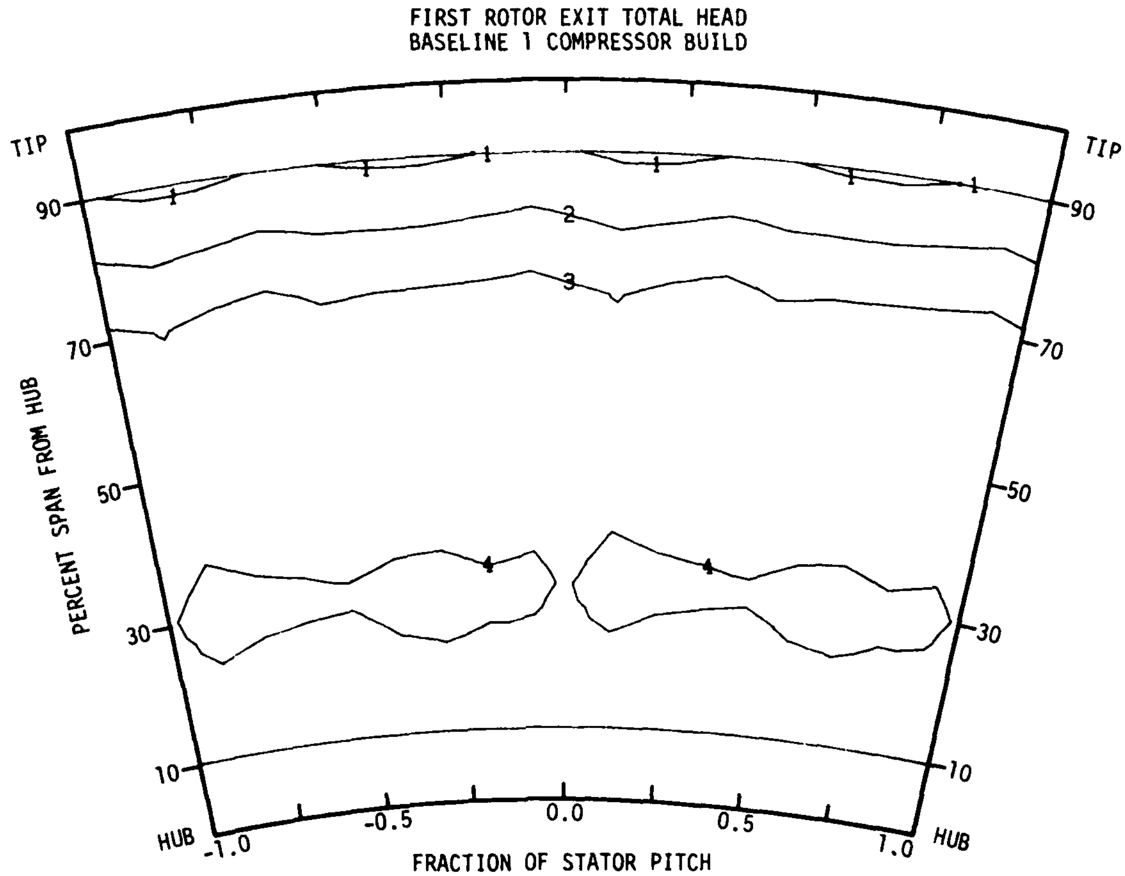

CURVE LABEL	CURVE VALUE (N-M/KG)
1	415
2	435
3	455
4	475

Figure 4.6 Total-head contour maps for each blade row exit of the baseline 1 compressor build at the design operating point (ϕ = 0.587).

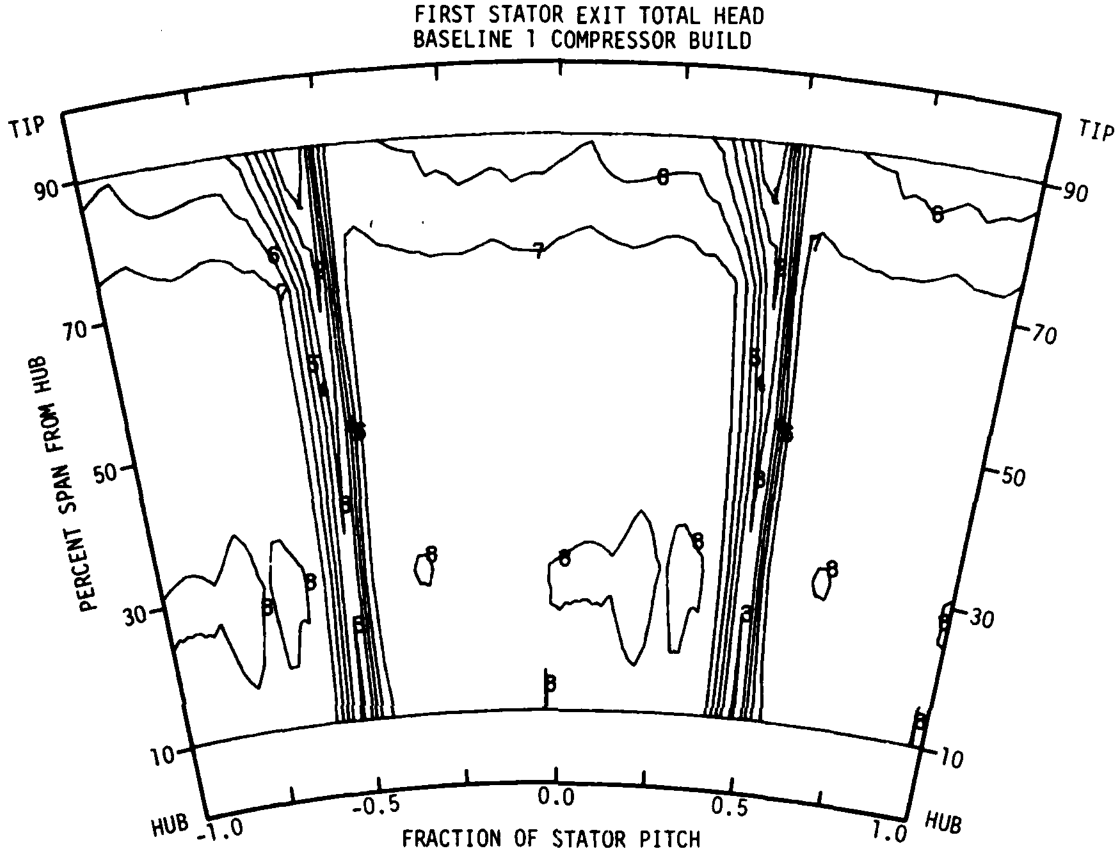

CURVE LABEL	CURVE VALUE (N-M/KG)
1	115
2	165
3	215
4	265
5	315
6	365
7	415
8	465

Figure 4.6 continued.

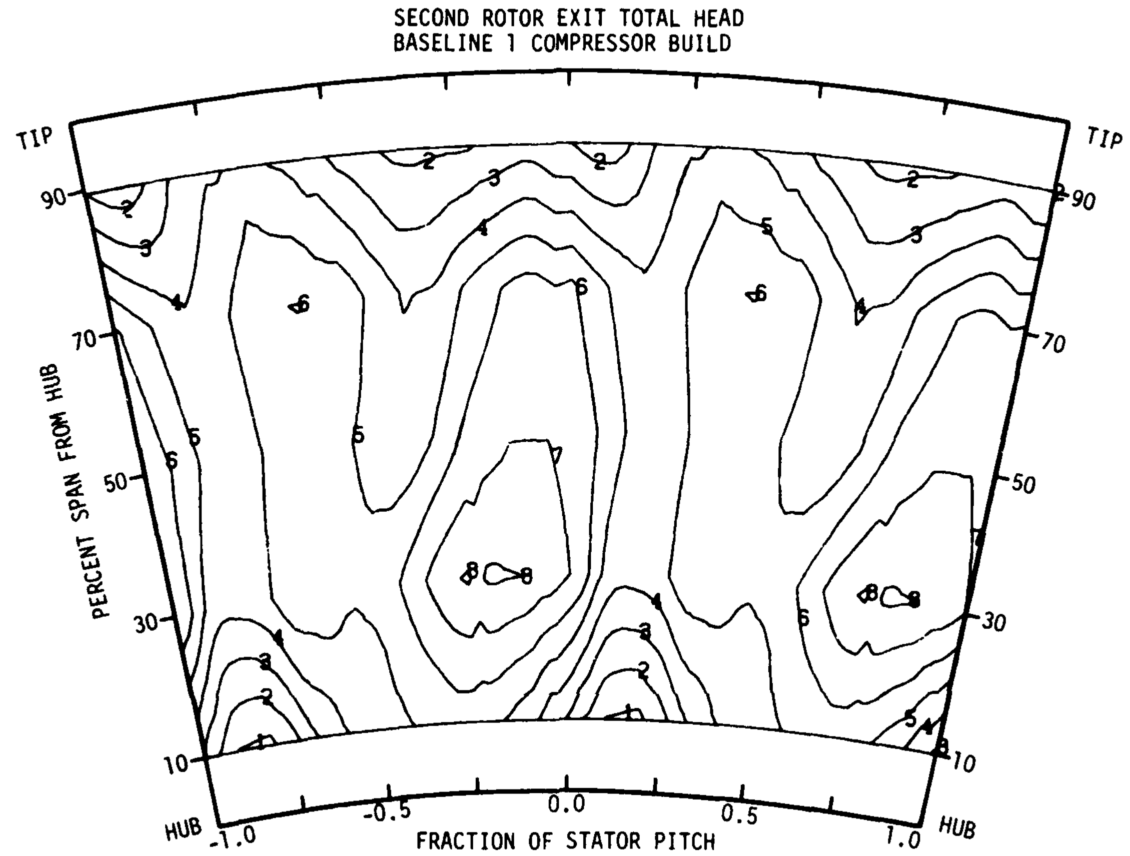

CURVE LABEL	CURVE VALUE (N-M/KG)
1	790
2	810
3	830
4	850
5	870
6	890
7	910
8	930

Figure 4.6 continued.

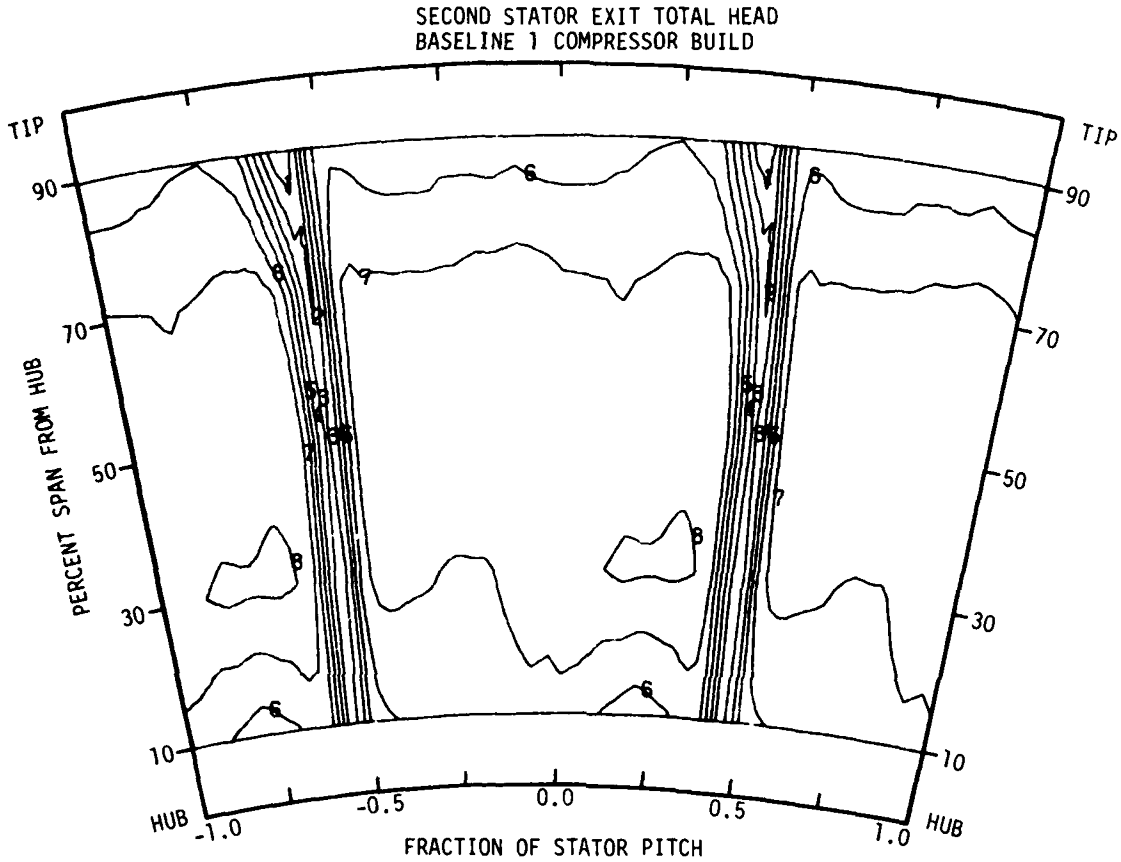

CURVE LABEL	CURVE VALUE (N-M/KG)
1	550
2	600
3	650
4	700
5	750
6	800
7	850
8	900

Figure 4.6 concluded.

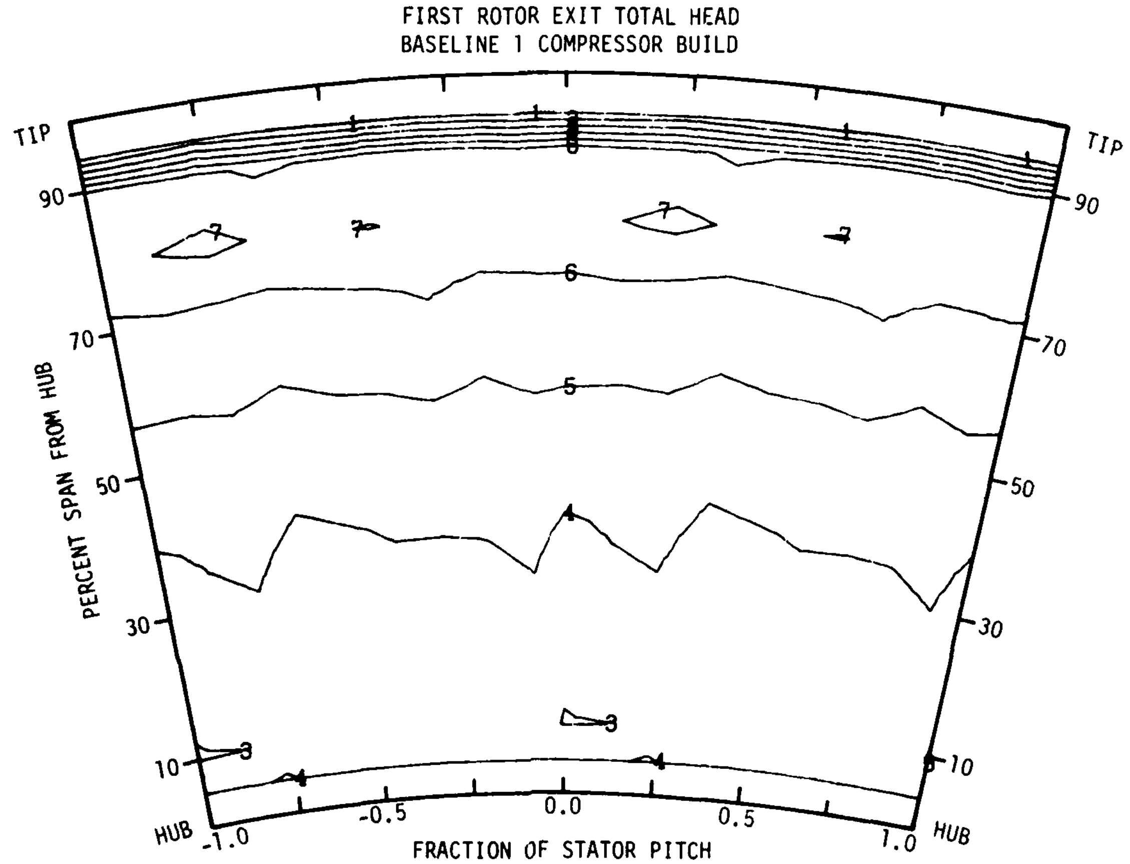

CURVE LABEL	CURVE VALUE (N-M/KG)
1	540
2	560
3	580
4	600
5	620
6	640
7	660

Figure 4.7 Total-head contour maps for each blade row exit of the baseline 1 compressor build at the off-design operating point ($\phi = 0.500$).

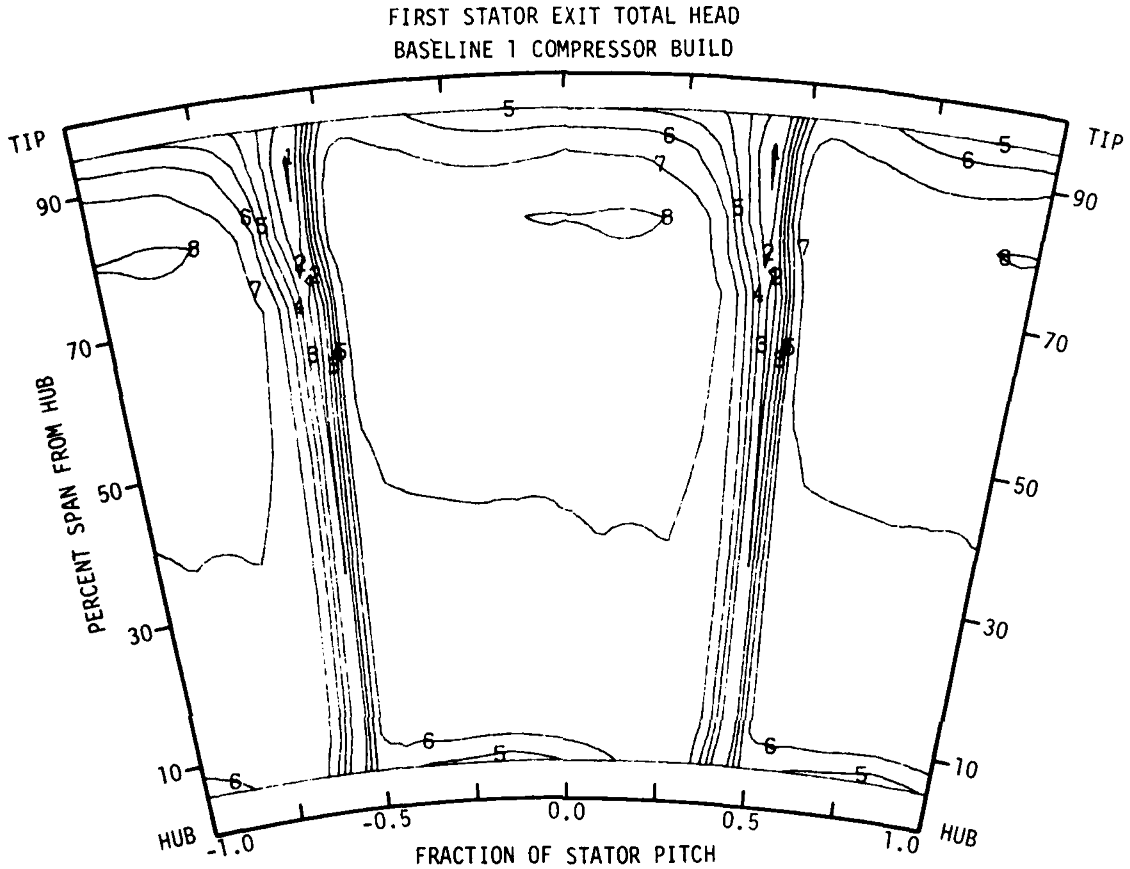

CURVE LABEL	CURVE VALUE (N-M/KG)
1	290
2	340
3	390
4	440
5	490
6	540
7	590
8	640

Figure 4.7 continued.

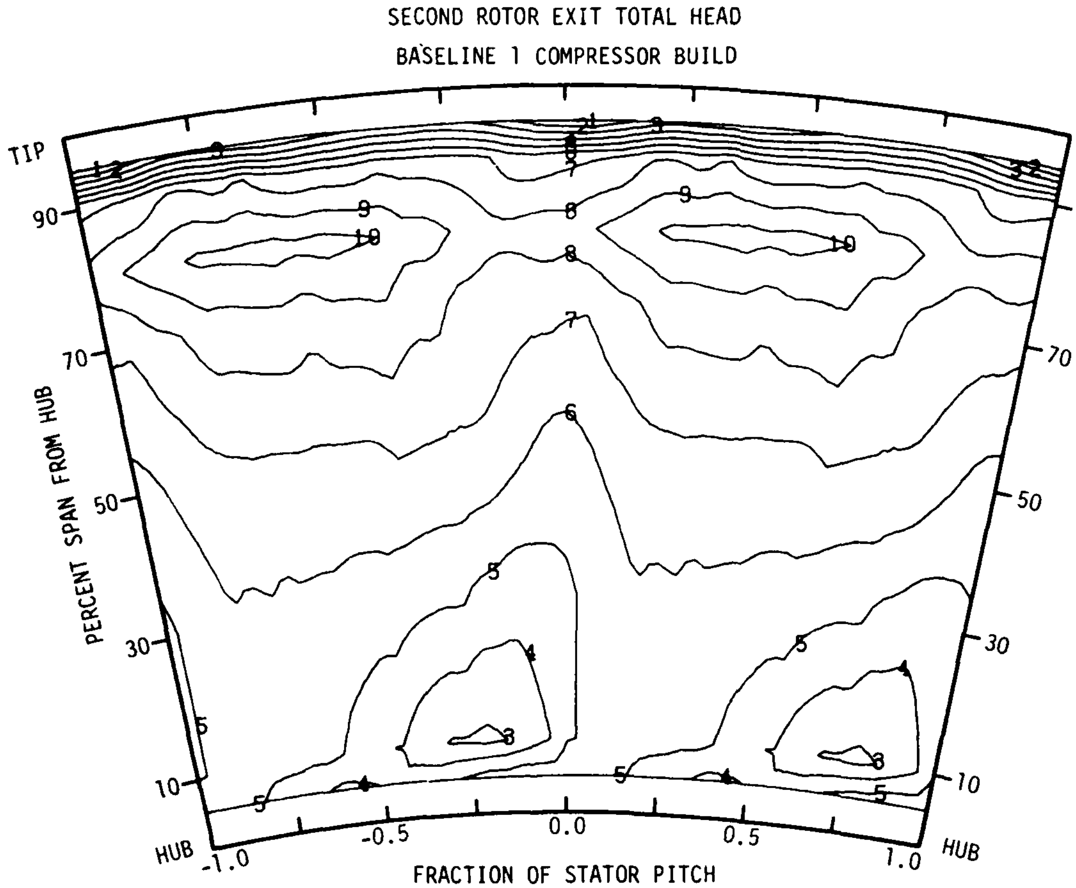

CURVE LABEL	CURVE VALUE (N-M/KG)
1	1050
2	1070
3	1090
4	1110
5	1130
6	1150
7	1170
8	1190
9	1210
10	1230

Figure 4.7 continued.

SECOND STATOR EXIT TOTAL HEAD
BASELINE 1 COMPRESSOR BUILD

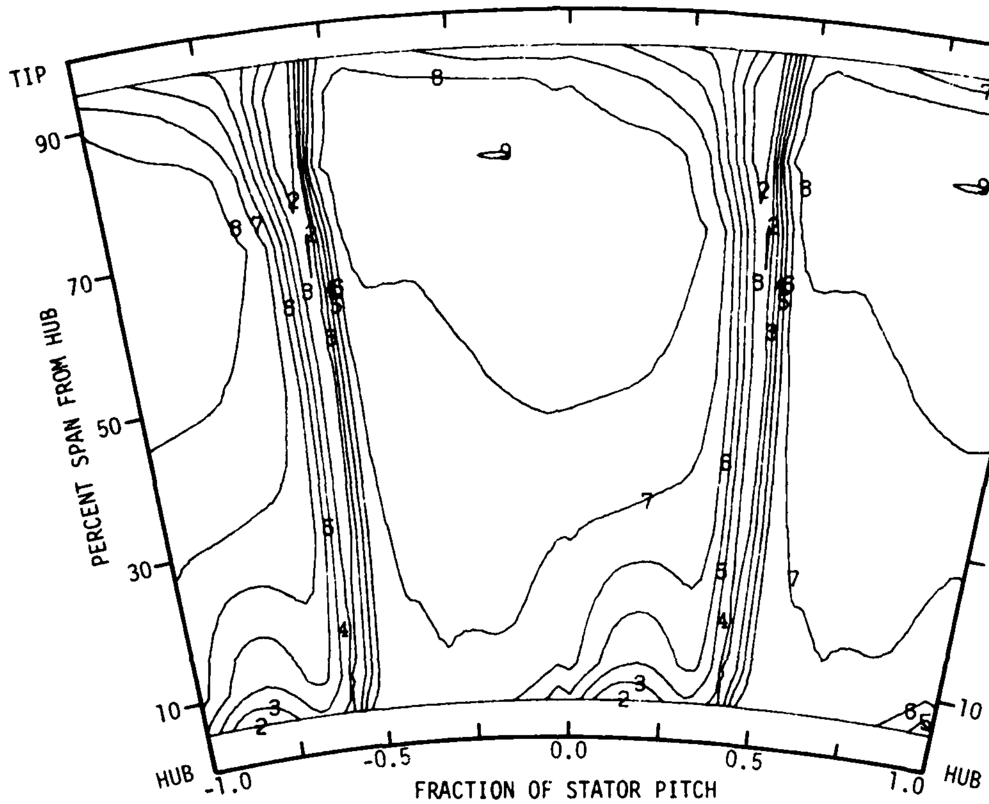

CURVE LABEL	CURVE VALUE (N-M/KG)
2	850
3	900
4	950
5	1000
6	1050
7	1100
8	1150
9	1200

Figure 4.7 concluded.

AD-A141 793 STATOR BLADE ROW GEOMETRY MODIFICATION INFLUENCE ON TWO-STAGE AXIAL-FLOW..(U) IOWA STATE UNIV AMES ENGINEERING RESEARCH INST D L TWEEDT ET AL. DEC 83 2/3

UNCLASSIFIED ISU-ERI-AMES-84179 AFOSR-TR-84-0418 F/G 21/5 NL

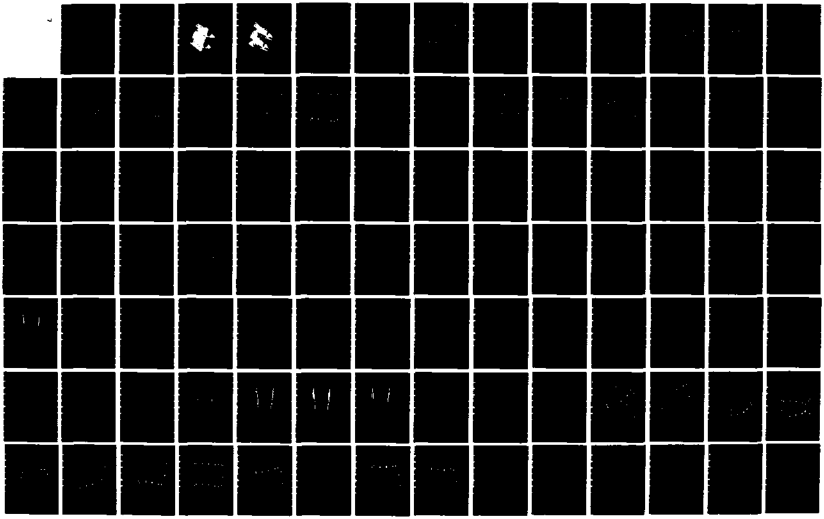

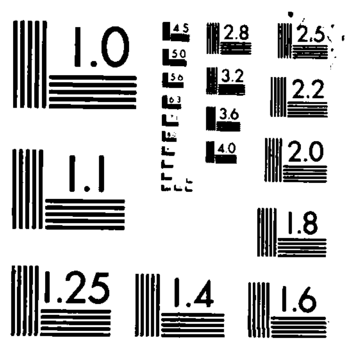

MICROCOPY RESOLUTION TEST CHART
NATIONAL BUREAU OF STANDARDS 1963 A

In Figure 4.8, immediately following the contour maps, are shown two total-head topographic (3-D) maps for the first and second stator exits at off-design flow. These maps may serve to help the reader better visualize the stator exit contour maps.

4.3.1.2. Stator Loss

Spanwise variations of circumferential-mean stator loss coefficients are presented in Figure 4.9. The first and second stator loss data are presented separately in Figure 4.9(a) and (b), respectively. In Figure 4.9(c), data for both stages are presented together for stage-to-stage comparison purposes.

An analysis of these graphs reveals several aspects of the baseline 1 build stator loss performance:

- For each stage, the spanwise trends in stator loss are similar for design and off-design flows.
- For each stage, the off-design flow stator losses are greater than the design flow stator losses.
- In all cases, the stator loss increases from mid-span to near-tip (90% span from the hub).
- The second stator loss increases from mid-span to the hub at both flow rates, but more so for the off-design flow rate. This is in contrast to the first stator loss behavior.
- Near the hub and tip, stator loss can change abruptly, increasing near the hub and decreasing near the tip.
- At design flow, the first stator loss is greater than the second stator loss over most of the span, except near the hub.

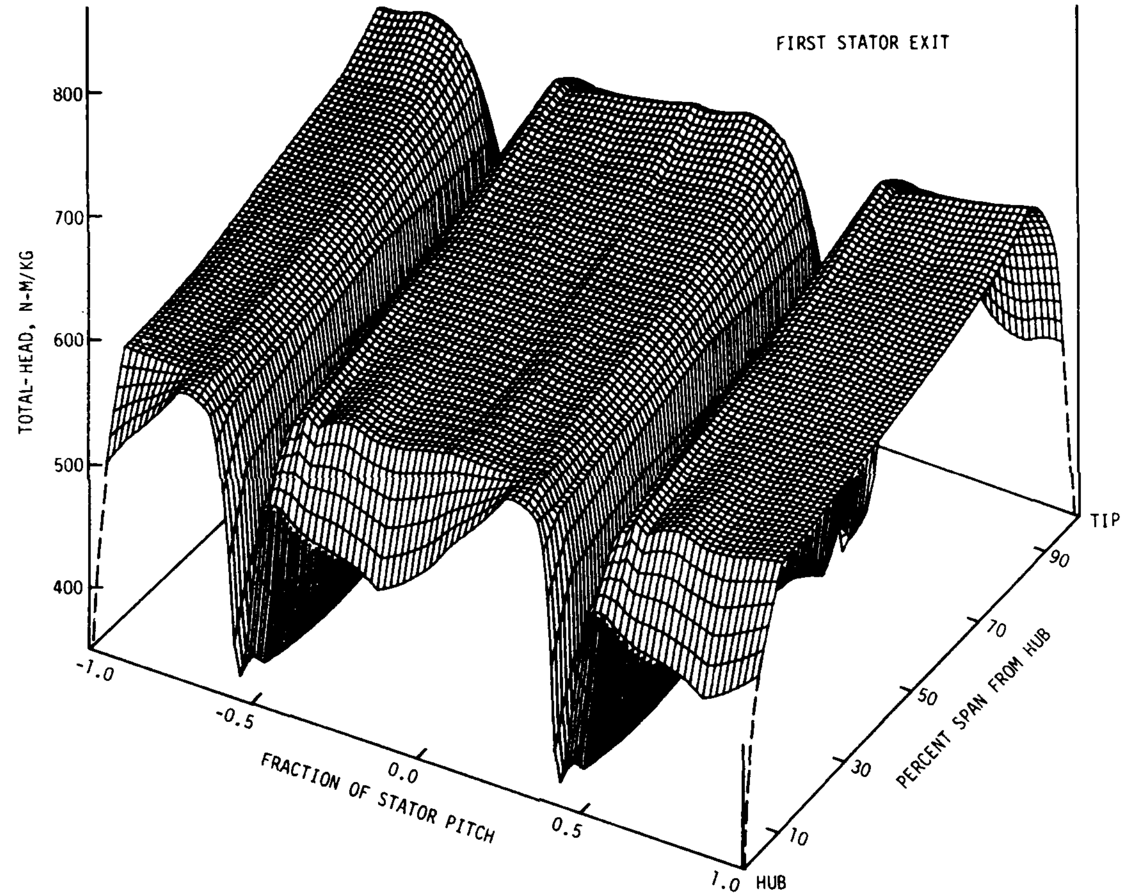

Figure 4.8 Total-head topographic maps for each stator row exit of the baseline 1 compressor build at the off-design operating point (ϕ = 0.500).

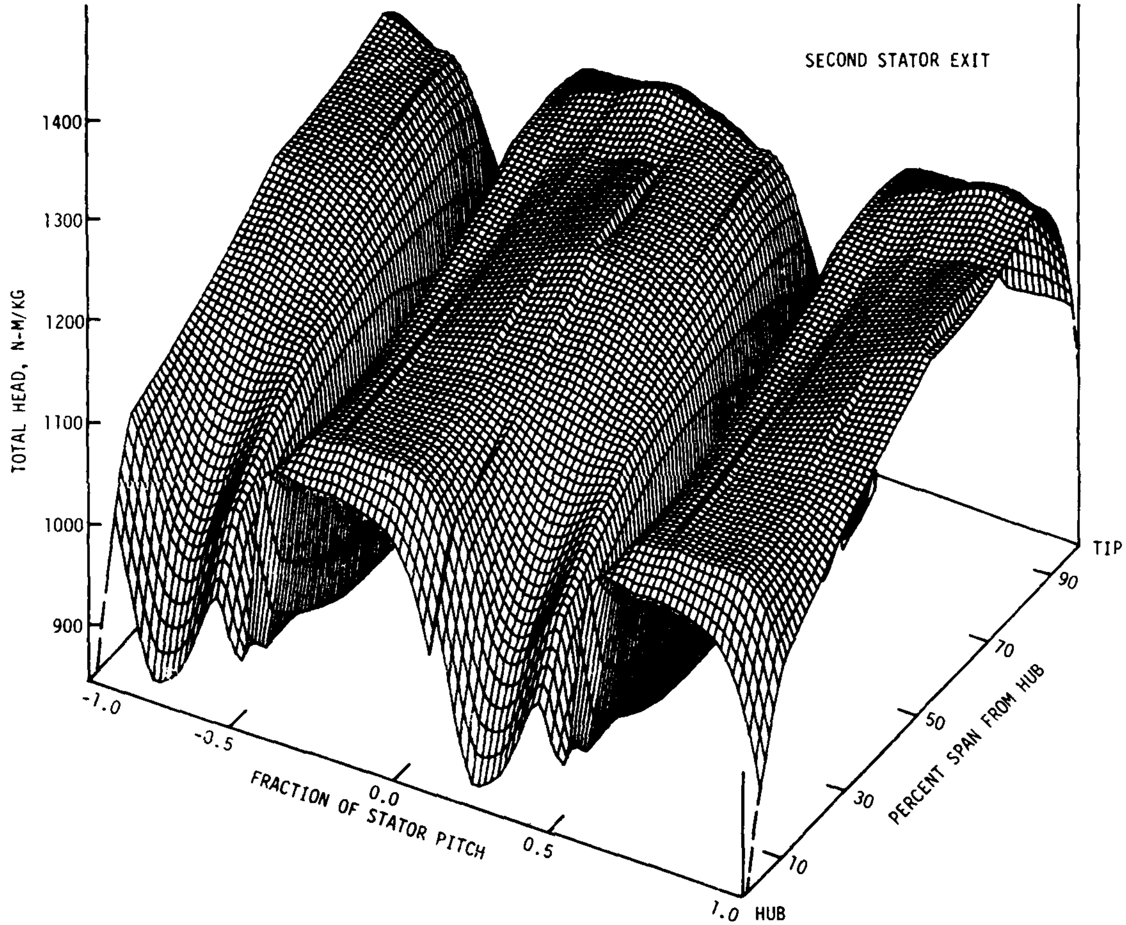

Figure 4.8 concluded.

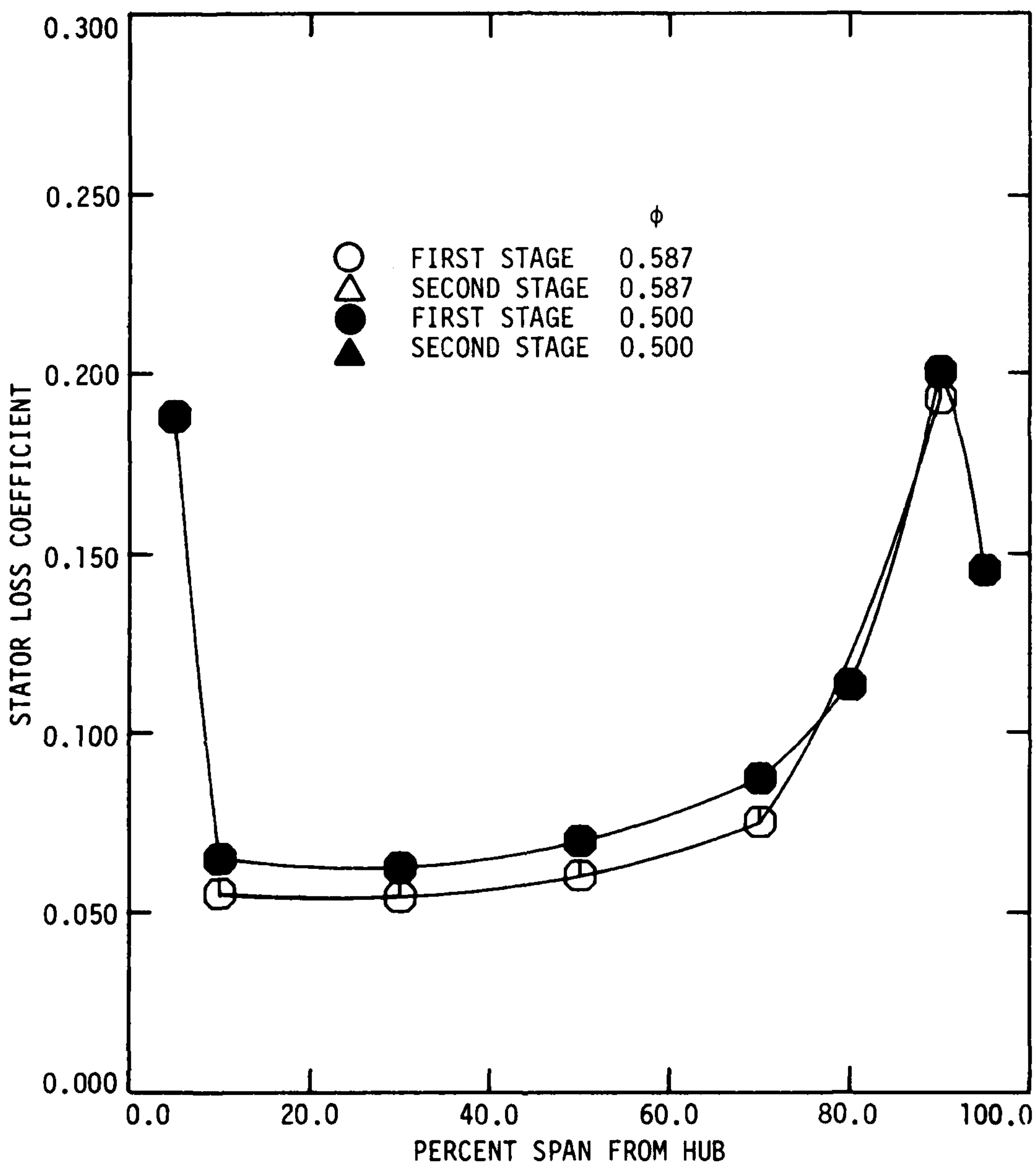

(a) FIRST STAGE STATOR

Figure 4.9 Spanwise distribution of circumferential-mean stator loss coefficients for the baseline 1 compressor build at the design ($\phi = 0.587$) and the off-design ($\phi = 0.500$) operating points.

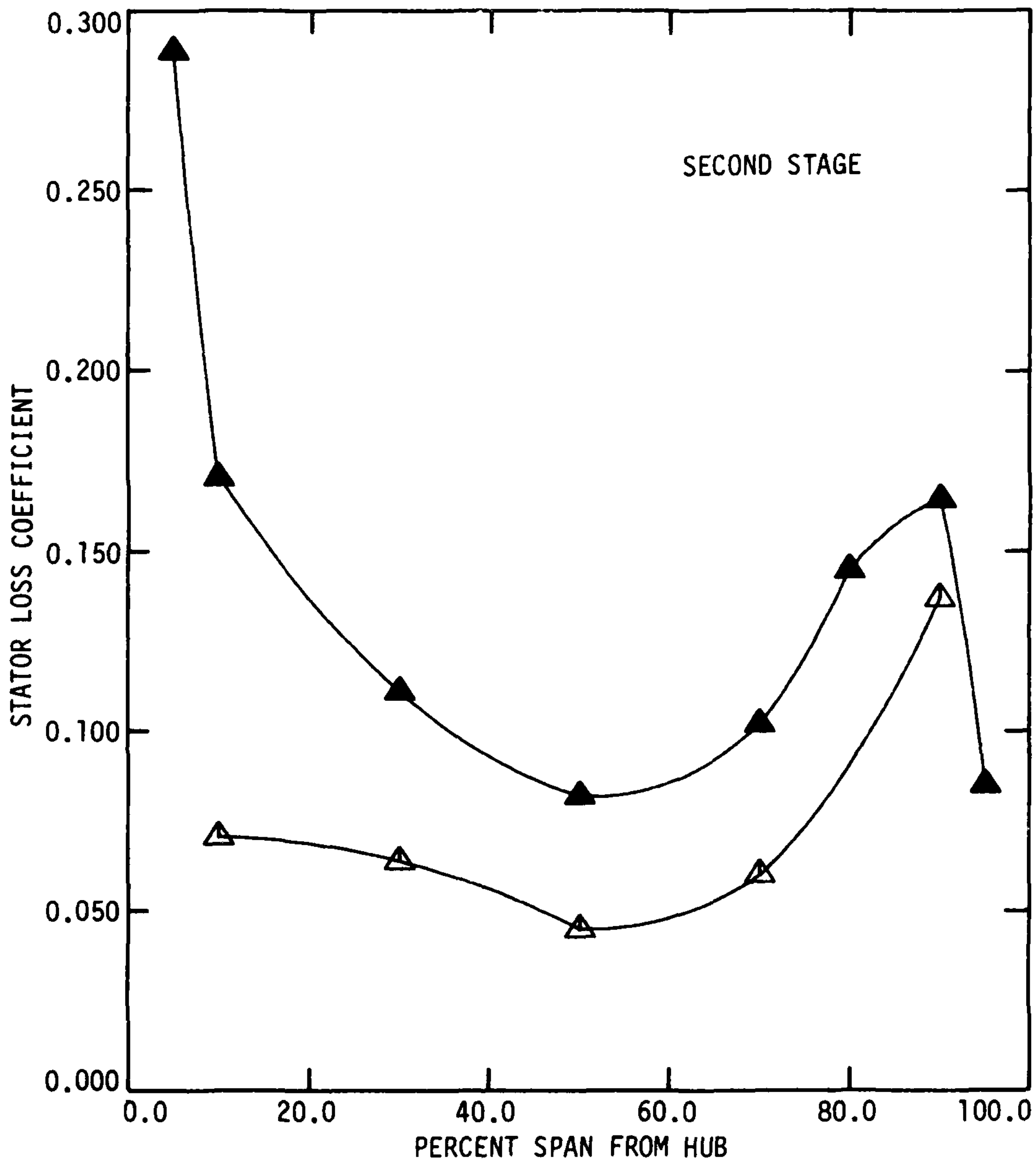

(b) SECOND STAGE STATOR

Figure 4.9 continued.

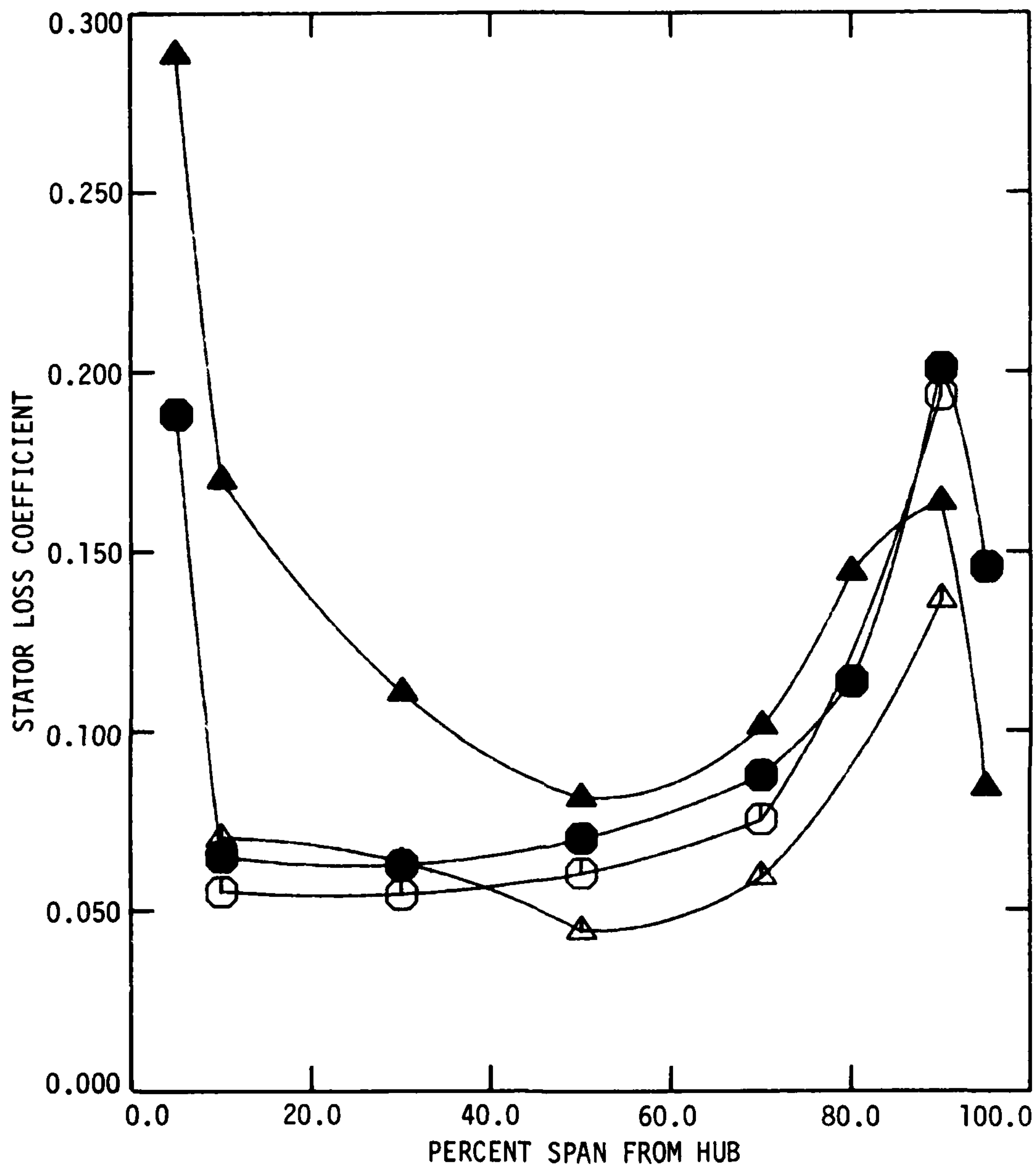

(c) BOTH STAGES

Figure 4.9 concluded.

- At off-design flow, the first stator loss is less than the second stator loss over most of the span, except near the tip.

In the following discussion, much reference is made to the total-head contour maps presented in Figures 4.6 and 4.7, particularly those for the stator exits. The stator exit maps are useful for analyzing the spanwise trends in stator loss. As will become evident, the spanwise graphs of circumferential-mean stator loss summarize much of the wake and end-wall flow behavior apparent from these contour maps. It should be noted regarding the maps, however, that only the gradients in total head are important. Also, only the spanwise trends in stator loss, not the magnitudes of stator loss, are reflected in the spanwise wake behavior.

Several observations about first stage stator performance can be pointed out. First, for both flow rates the stator wake has a fairly uniform width, and a slight increase in depth, from 10% to 70% span from the hub. This slight increase in wake depth shows up in the stator loss graphs as a gradual increase in loss. The wakes flare out into a combined wake/end-wall flow from 70% span to the tip. This results in a corresponding increase in stator loss. The abrupt increase in stator loss very near the hub (data at 5% span for off-design flow only) is associated with a "piling-up" of lower-momentum fluid on the pressure side of the stator blade. Excess lower-momentum fluid is expected in this region from the hub boundary layer. The "piling-up" is caused by hub rotation, where the hub is moving to the left as viewed on the stator exit contour maps.

The abrupt decrease in stator loss very near the tip (data at 95% span for off-design flow only) is somewhat difficult to interpret. Actually, a continued increase in stator loss is expected as the tip is approached. This unexpected behavior is probably due mainly to radial mixing of the flow near the tip. The first rotor head-rise curves in Figure 4.4(a) show a rapid decrease in rotor head-rise near the tip (95% span). The first stage head-rise curves, however, indicate that this lower head-rise region has expanded towards the "core" flow to include 90% span at the stator exit. This implies a mixing of the lower- and higher-momentum fluids at 95% and 90% span, respectively, as the fluid moves through the stator. Since the stator loss coefficient parameter does not take into account this radial mixing, the loss computed at the tip is too low, while that near the tip (90% span) is too high.

The second stator loss performance is qualitatively similar to that of the first stator for the outer half of the span. However, from mid-span to hub the loss performance is considerably different between the stages, especially for the off-design flow. This difference between stages is attributed to the second stator hub being stationary, whereas the first stator hub, as mentioned before, is rotating.

The second stator exit total-head contour maps (Figures 4.6 and 4.7) show a substantial region of lower-momentum fluid adjacent to that stator suction surface near the hub, particularly for the off-design flow. On the maps the region appears as a group of concentric half-circles with the center located somewhere very near the hub.

This region is evidence of a "leakage vortex," the likes of which have also been observed by others in conjunction with a stationary-blade/ stationary-hub gap (for example, see Leboeuf et al. [8]). A leakage vortex, with its large static-pressure gradient, pulls local lower-momentum fluid toward its center, resulting in the so-called "solid body" image on the total-head contour maps [8]. This region of lower-momentum fluid is, as expected, associated with an increase in the second stator loss near the hub. The off-design losses are considerably greater than those at design, and this is consistent with the size and strength of the lower-momentum regions on the contour maps. That is, the leakage vortex at off-design is larger in size and involves a steeper total-head gradient than the one at design.

The "vortex" size comparison between the design and off-design flows tends to support the contention that the lower-momentum region is indeed a leakage vortex. The off-design flow--being lower than the design flow--produces a higher loading on the stator blades. Thus, one expects a stronger leakage at the hub since the flow through the clearance is driven by the static pressure differences (loading) between hub blade-section pressure and suction surfaces.

4.3.1.3. Stator Incidence and Deviation

Spanwise variations of circumferential-mean stator incidence and deviation angles are presented in Figure 4.10(a) and (b), respectively. These results are discussed primarily as they relate to corresponding stator loss performance. The main points are as follows:

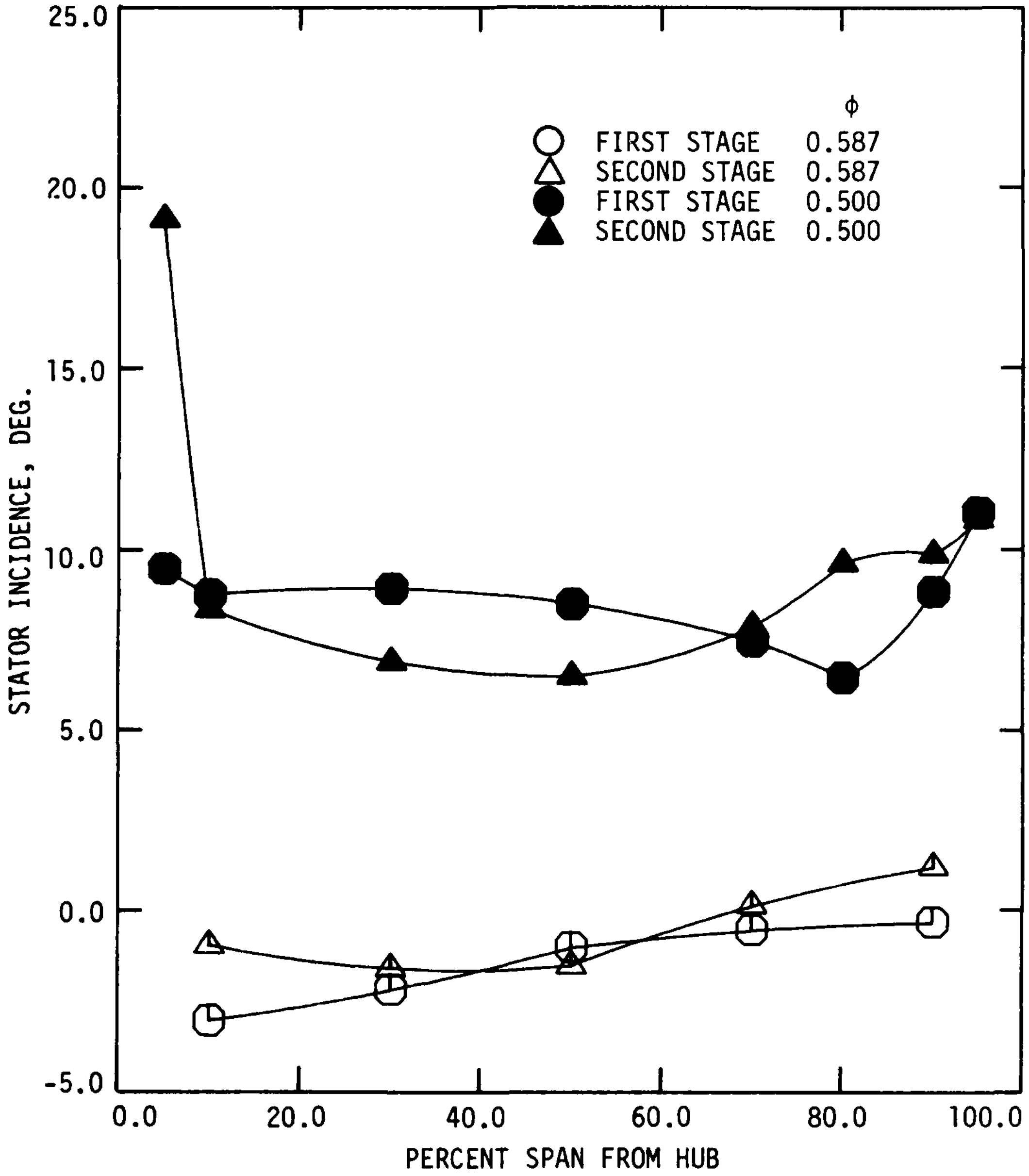

(a) STATOR INCIDENCE

Figure 4.10 Spanwise distribution of circumferential-mean stator incidence and deviation angles for the baseline 1 compressor build at the design (ϕ = 0.587) and the off-design (ϕ = 0.500) operating points.

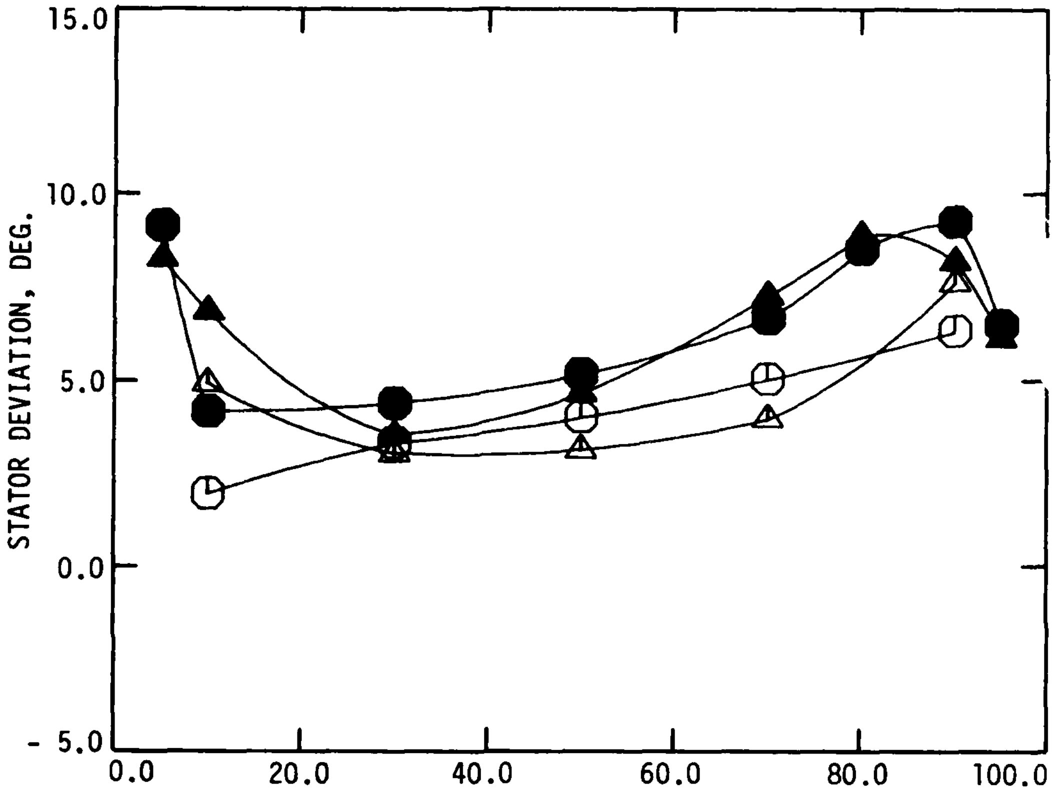

(b) STATOR DEVIATION

Figure 4.10 concluded.

- The stator incidence angle at off-design flow (approximately 8 deg) is much larger than the incidence angle at design flow (approximately -1 deg).
- There is no definite relationship between the spanwise trends in stator incidence angle and those in stator loss.
- Higher stator loss levels can be associated with larger positive incidence angle values.
- There is an approximate correlation between the spanwise trends in stator deviation angle and those in stator loss.

The stator incidence angle at off-design flow is expected to be larger than the incidence angle at design flow because the off-design flow rate is lower than the design value. The larger stator incidence angle at off-design flow is also expected to result in a higher stator loss level (Figure 4.9), since, for the kind of blading design involved [1,9], an 8 degree incidence angle would tend to produce a higher loss than would a -1 degree incidence angle.

4.3.1.4. Rotor Performance

Spanwise variations of circumferential-mean rotor performance data are presented in this subsection. Rotor head-rise is not included here since it has already been discussed. Conventional ideal head-rise (Euler turbine equation based) and rotor loss curves are shown in Figures 4.11 and 4.12, respectively. Rotor incidence and deviation angles are presented in Figure 4.13. These data are only briefly discussed and are included for completeness and possible future reference.

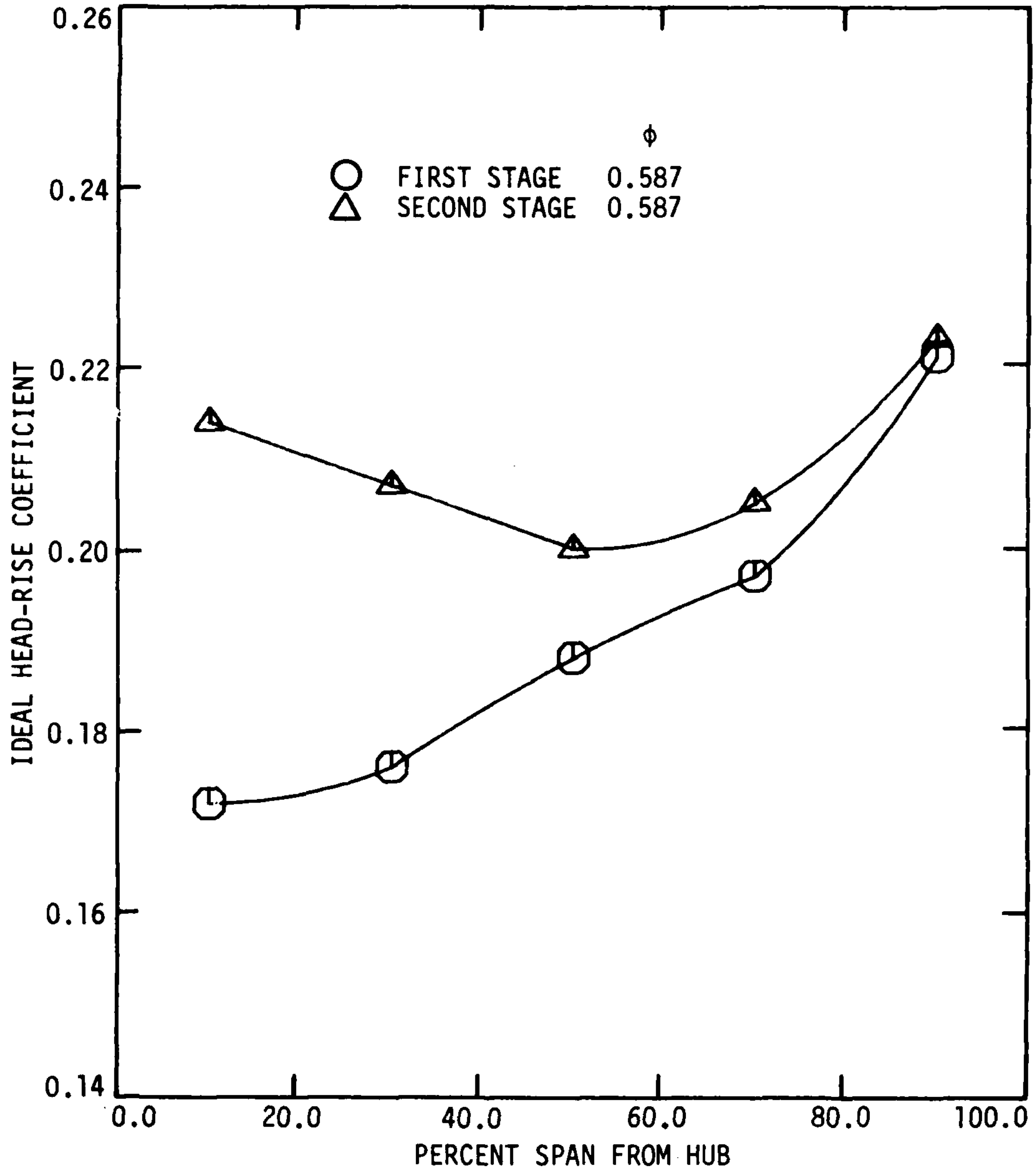

(a) DESIGN (ϕ = 0.587)

Figure 4.11 Spanwise distribution of circumferential-mean ideal head-rise coefficients for the baseline 1 compressor build at the design (ϕ = 0.587) and the off-design (ϕ = 0.500) operating points.

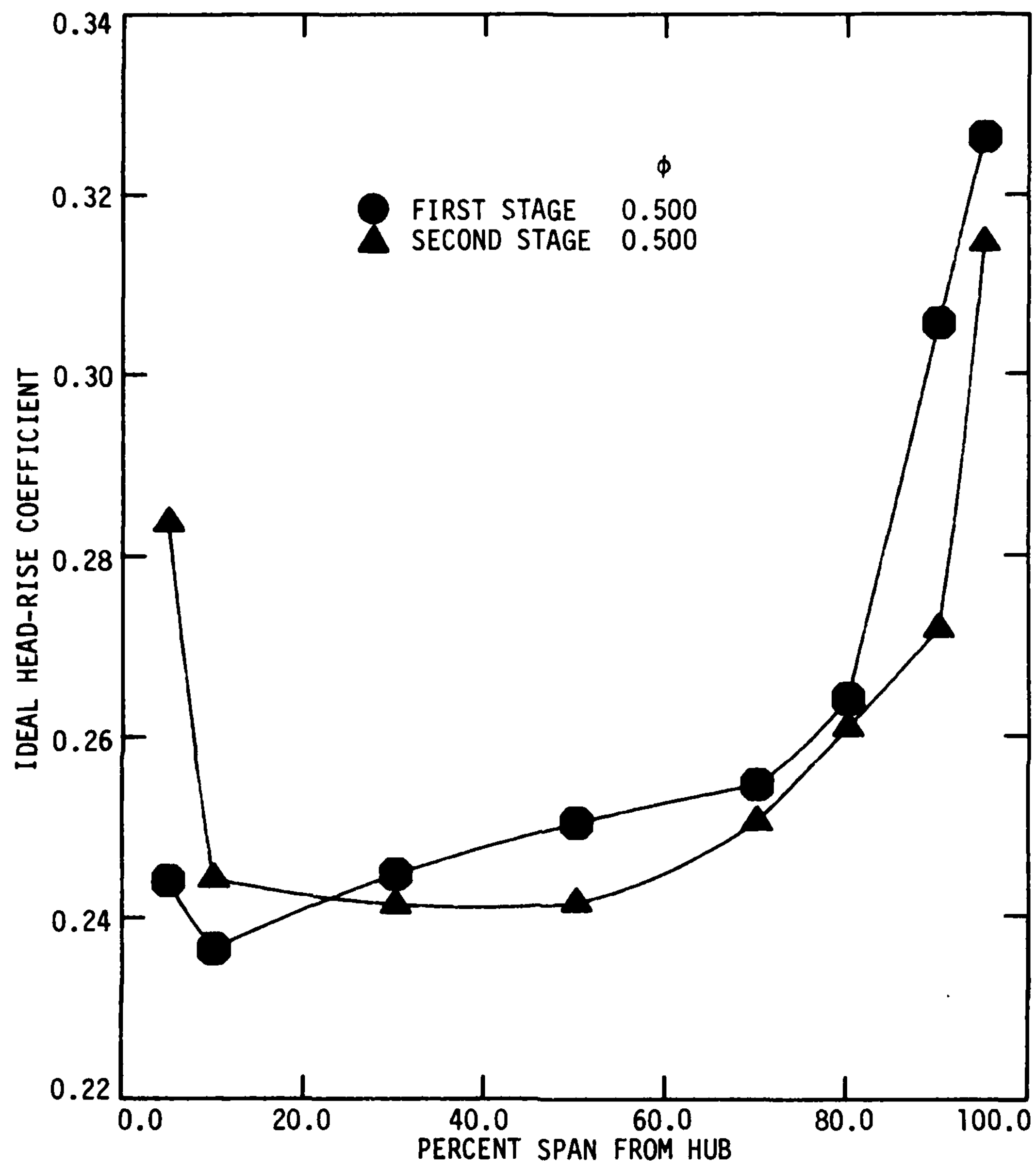

(b) OFF-DESIGN (ϕ = 0.500)

Figure 4.11 concluded.

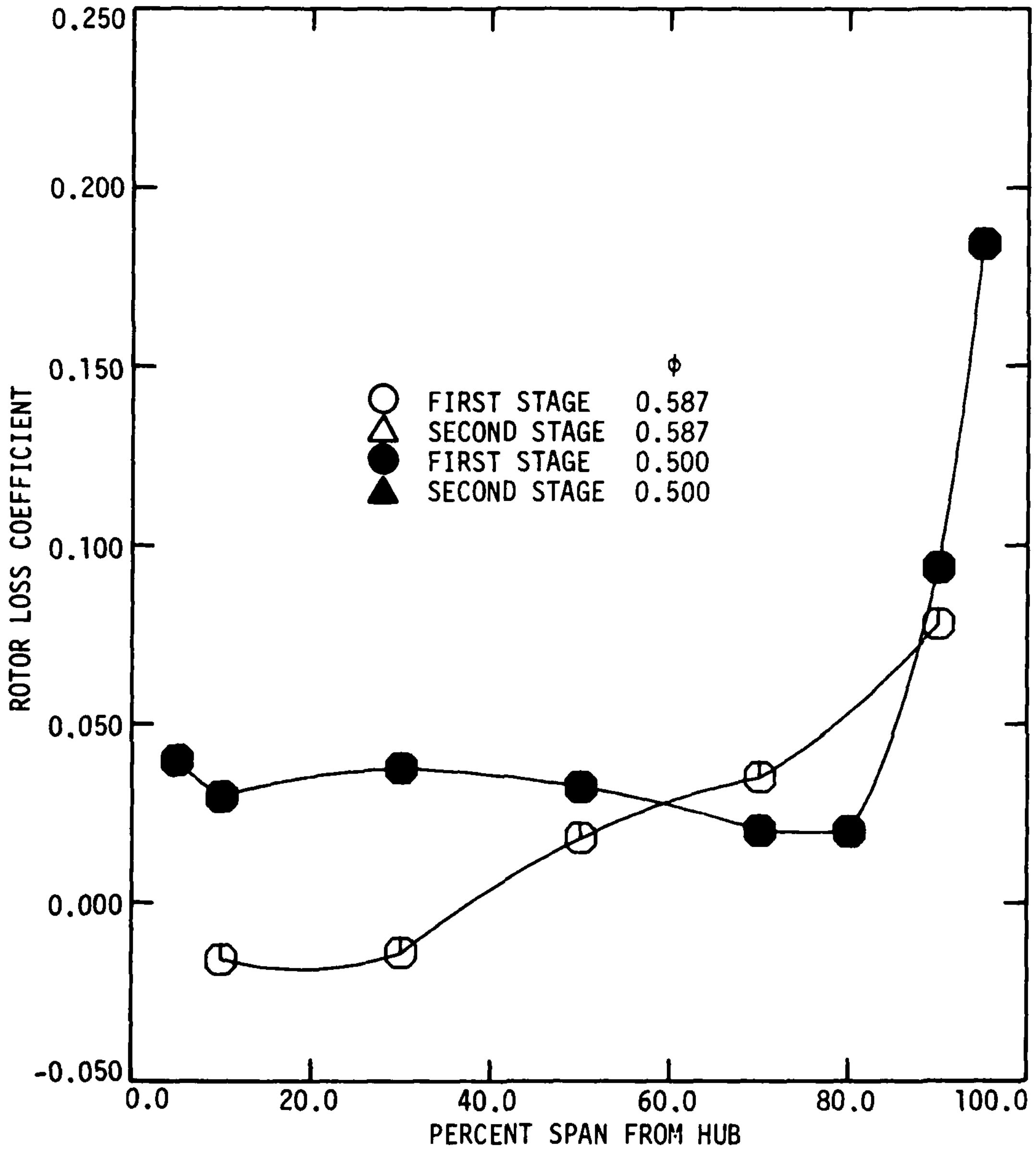

(a) FIRST STAGE ROTOR

Figure 4.12 Spanwise distribution of circumferential-mean rotor loss coefficients for the baseline 1 compressor build at the design (ϕ = 0.587) and the off-design (ϕ = 0.500) operating points.

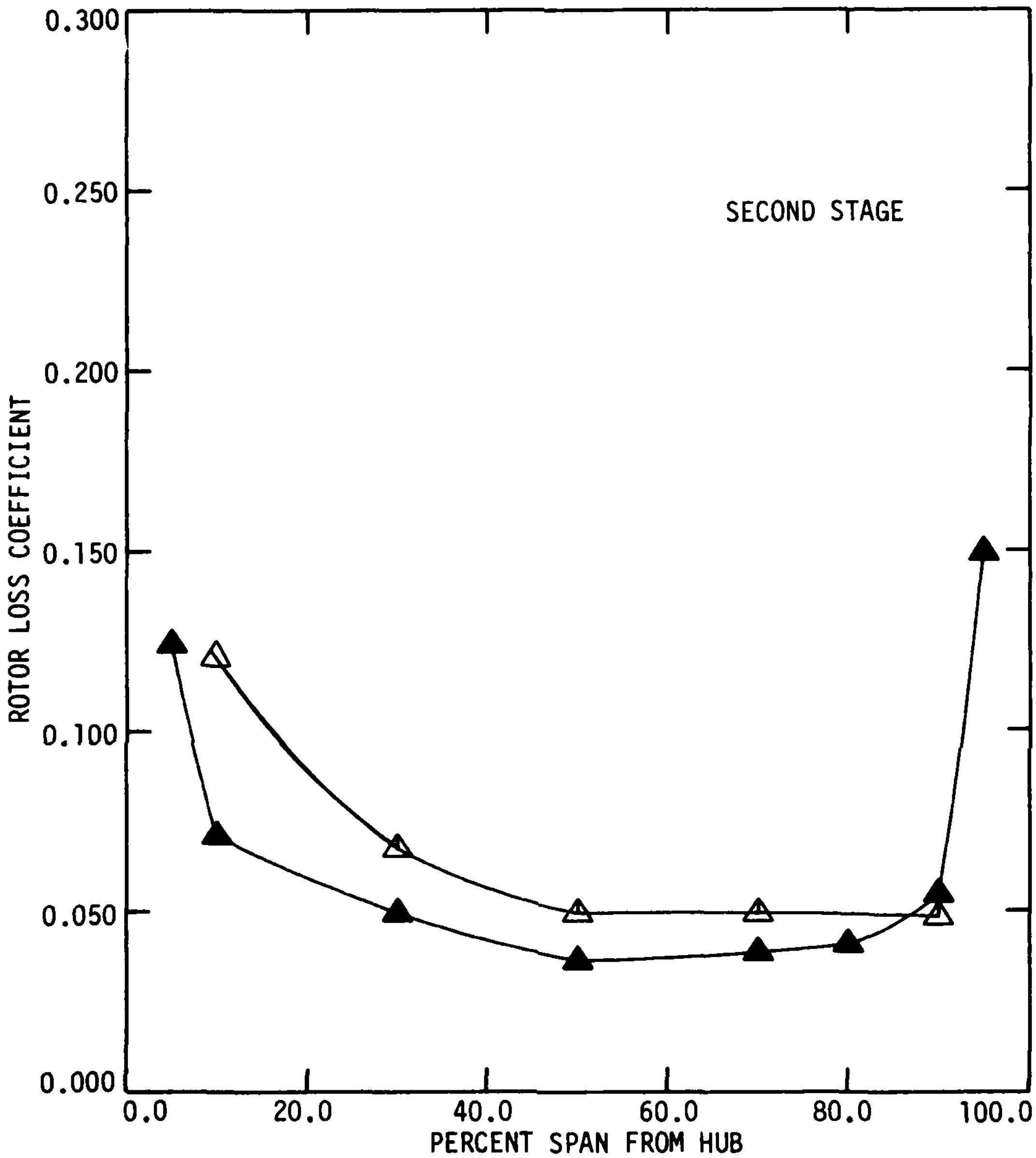

(b) SECOND STAGE ROTOR

Figure 4.12 continued.

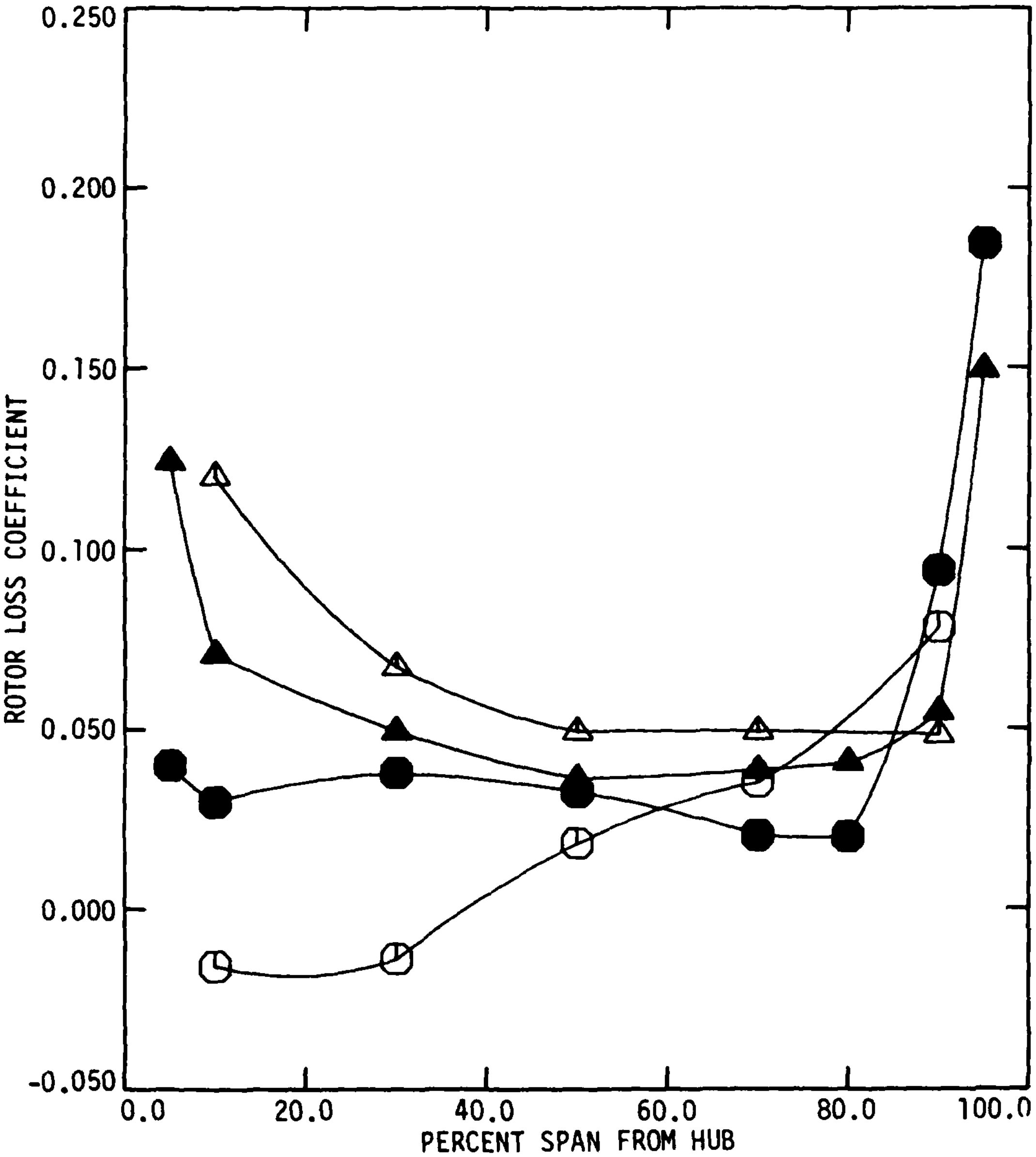

(c) BOTH STAGES

Figure 4.12 concluded.

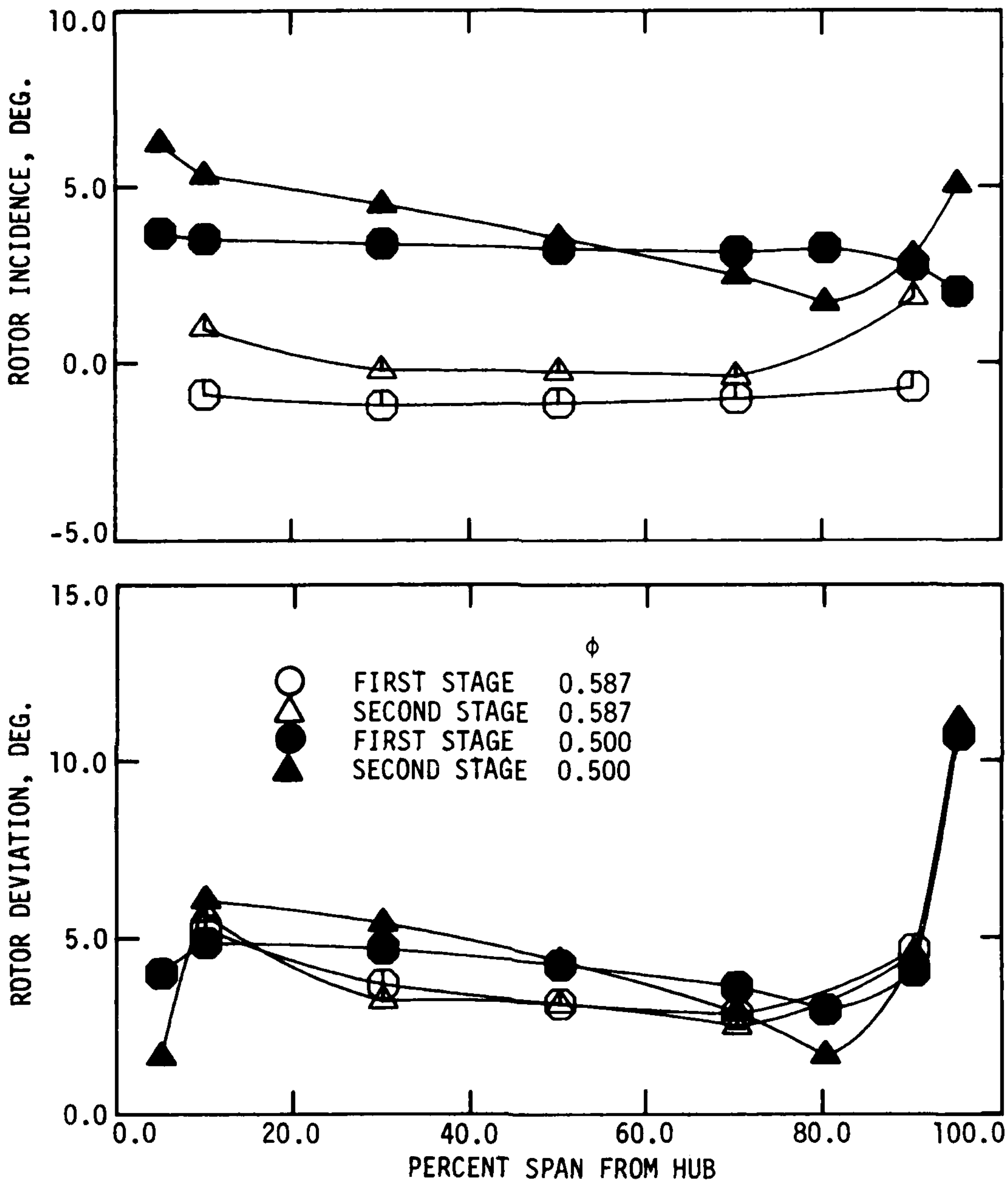

Figure 4.13 Spanwise distribution of circumferential-mean rotor incidence and deviation angles for the baseline 1 compressor build at the design (ϕ = 0.587) and the off-design (ϕ = 0.500) operating points.

Several characteristics of the ideal head-rise performance (Figure 4.11) are noteworthy:

- The first stage spanwise trend in ideal head-rise at design flow is similar to that at the off-design flow.
- The second stage spanwise trend in ideal head-rise at design flow is similar to that at the off-design flow.
- At off-design flow, the second stage spanwise distribution of ideal head-rise is similar to that of the first stage.
- At design flow, the second stage ideal head-rise is substantially higher than that of the first stage.

Some conclusions regarding rotor loss, incidence, and deviation follow:

- The first rotor loss curve for design flow is suspect because it indicates a negative rotor loss. This is probably due to calculated ideal head-rise, based on measured absolute flow angles, which was too low in the hub region.
- The spanwise trends in second rotor loss at design flow are similar to those at the off-design flow.
- At off-design flow, the spanwise distribution of second rotor loss is similar to that of the first rotor.
- There is no definite relationship between the spanwise trends in rotor incidence angle and those in rotor loss.
- There is no definite relationship between the spanwise trends in rotor deviation angle and those in rotor loss.

4.3.1.5. Hydraulic Efficiency

Spanwise variations in circumferential-mean hydraulic efficiency are presented in Figure 4.14. Conventional rotor, stage, and overall hydraulic efficiency curves are shown in Figure 4.14(a), (b), and (c), respectively. These data, like the rotor performance data, are included primarily for completeness and possible future reference. A few points on the overall efficiency data (Figure 4.14(c)) are worth mentioning:

- The overall compressor efficiency at the off-design flow is higher than that at design flow over most of the blade span.
- The spanwise trends in overall compressor efficiency differ for the two flow rates.
- The spanwise trends in overall compressor efficiency are similar to the spanwise trends in overall head-rise (Figure 4.4(c)).

4.3.1.6. Mass-Averaged Performance

Radially mass-averaged data for the baseline 1 compressor build at the two different flow rates are presented in Table 4.8. The following comparisons are significant:

- The mass-average stator loss is greater at the off-design flow than at design flow for both stages.
- The mass-average stage efficiency is higher at the off-design flow than at design flow for both stages.
- The mass-average overall compressor efficiency is higher at the off-design flow than at design flow.

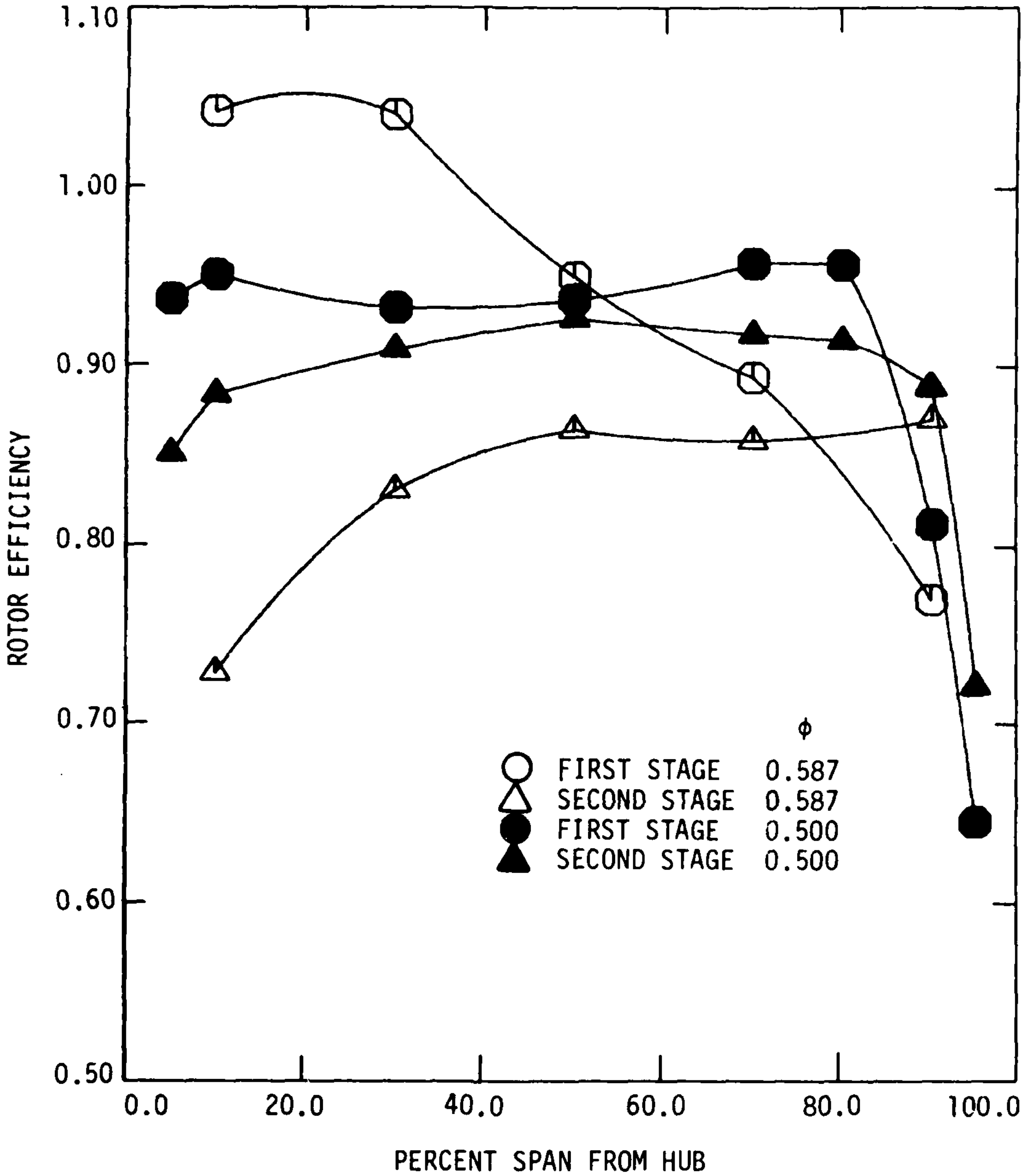

(a) ROTOR

Figure 4.14 Spanwise distribution of circumferential-mean hydraulic efficiences for the baseline 1 compressor build at the design (ϕ = 0.587) and the off-design (ϕ = 0.500) operating points.

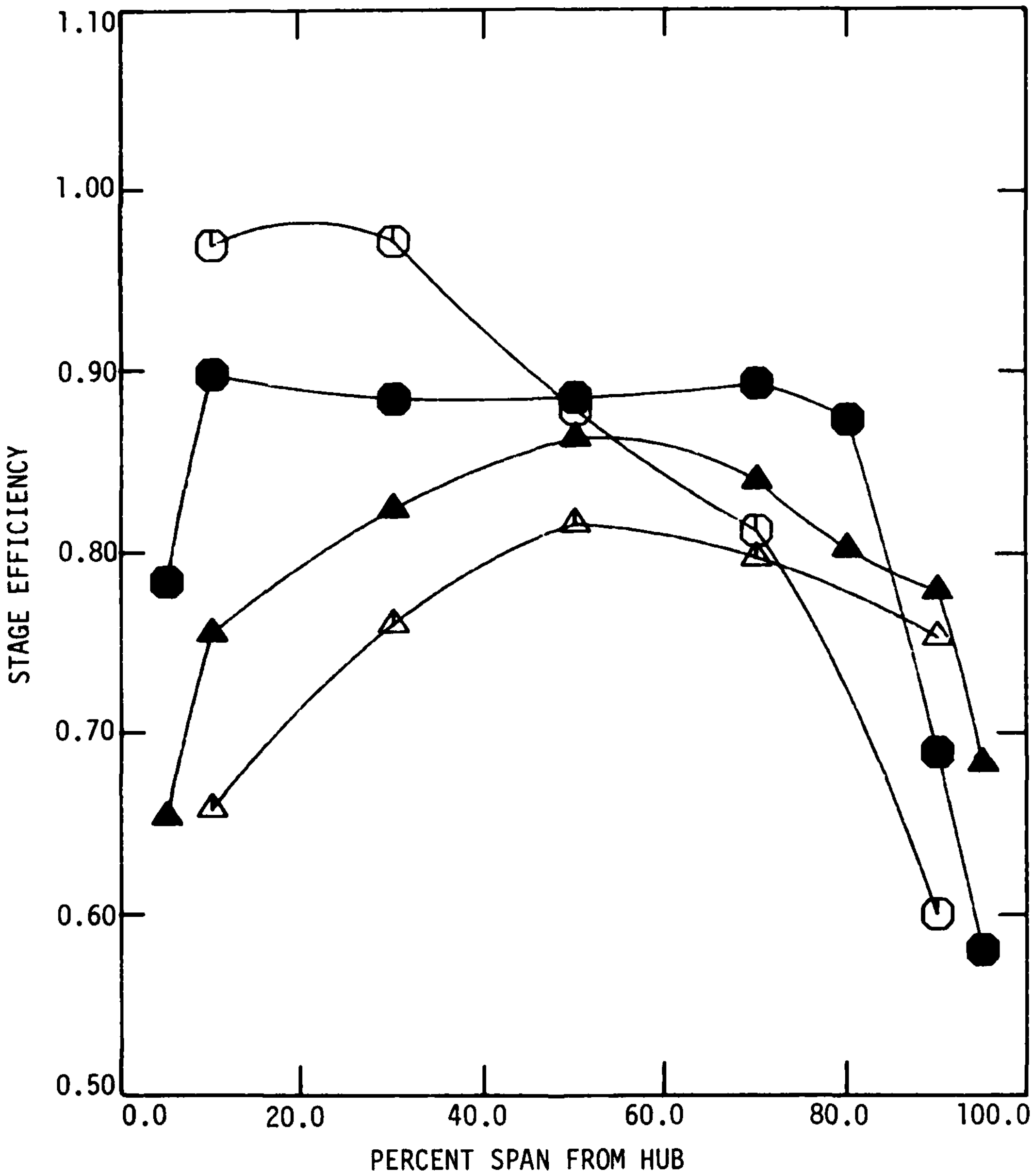

(b) STAGE

Figure 4.14 continued.

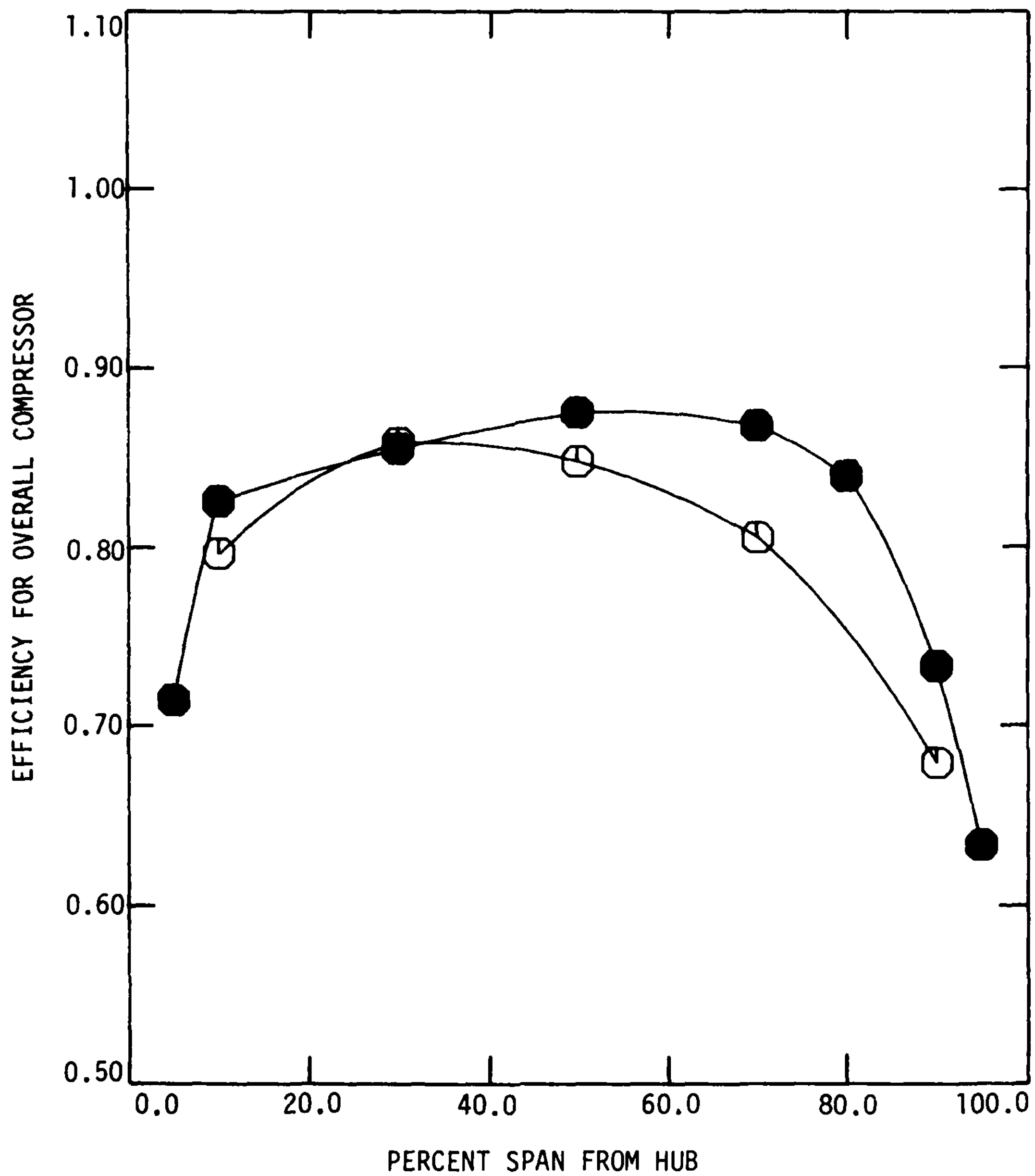

(c) OVERALL

Figure 4.14 concluded.

Table 4.8. Comparison of radially mass-averaged performance parameters for the baseline 1 compressor build at the design (ϕ = 0.587) and the off-design (ϕ = 0.500) operating points.

Flow Coefficient	Head Rise Coefficient		Loss Coefficient		Efficiency	
	Rotor	Stage	Rotor	Stator	Rotor	Stage
First Stage						
0.500	0.236	0.217	0.045	0.100	0.913	0.840
0.587	0.178	0.160	0.025	0.083	0.926	0.833
Second Stage						
0.500	0.226	0.204	0.051	0.116	0.899	0.813
0.587	0.175	0.159	0.063	0.071	0.833	0.760

Overall

Flow Coefficient	Head Rise Coefficient	Efficiency
0.500	0.421	0.827
0.587	0.319	0.795

The results listed in Table 4.8 reveal a peculiarity in the relationship between loss and efficiency. For example, at the off-design flow the first stage rotor and stator losses exceed those at design flow, yet the first stage efficiency is higher at the off-design flow. This apparent discrepancy is resolved by recognizing that efficiency depends on the losses as they relate to head-rise. The higher first stage rotor and stator row losses at the off-design flow are accompanied by a greater gain in stage head-rise over that at design flow.

4.3.2. First Stator Wake Tracking Through the Second Rotor

Contour maps of second rotor exit total-head for the baseline 1 compressor build at two flow coefficients (0.587 in Figure 4.6 and 0.500 in Figure 4.7) were presented in the preceding section. As was pointed out, the map for design flow (Figure 4.6) shows an interesting feature, namely, over most of the span and within one stator pitch there are two regions of lower total-head. In contrast, for the off-design flow (Figure 4.7) only one of these lower total-head regions exists.

When considering the first stator wake/second rotor blade row interaction, it seems reasonable to expect only one lower total-head region per stator pitch. Each first stator blade produces a continuous stream of low total-head wake fluid which enters the rotor row and is "chopped" into segments (see Smith [10] for a clear explanation of this concept of wake "chopping"). These "wake segments" are rotated within the rotor and are thus not reunited at the rotor exit. Upon exiting from the rotor row, these segments move downstream sequentially

within a stationary "wake avenue," with one avenue for each upstream stator. When time-averaged total-pressure is measured at the rotor exit, this "wake avenue" is expected to appear as a region of lower total-pressure relative to the no-stator-wake portion of the rotor exit flow. Therefore, only one lower total-head region per stator pitch is anticipated. More detailed discussion concerning this type of stator wake/rotor blade interaction is given by Smith [10], Wagner et al. [11], and Zierke and Okiishi [12].

Several experiments were carried out on the research compressor to better understand the unusual "two lower total-head region" pattern observed at design flow. Although most of the data obtained in this effort were acquired with the modified 1 compressor build, the general behavior observed applies to both the baseline and modified configurations.

The initial experiment consisted of making qualitative total-head surveys at mid-span of the second rotor exit within one stator pitch, over the entire range of compressor flow rates at design shaft speed. The results are presented in Figure 4.15.

Figure 4.15 demonstrates that the two-dip (two lower total-head region) pattern begins to appear at a flow coefficient of about 0.525, and remains for all higher flow rates. In general, both dips have similar magnitudes and move gradually to the right (rotor blades move left) as the flow coefficient increases. The single dip observed at lower flow coefficients also moves to the right as the flow coefficient increases.

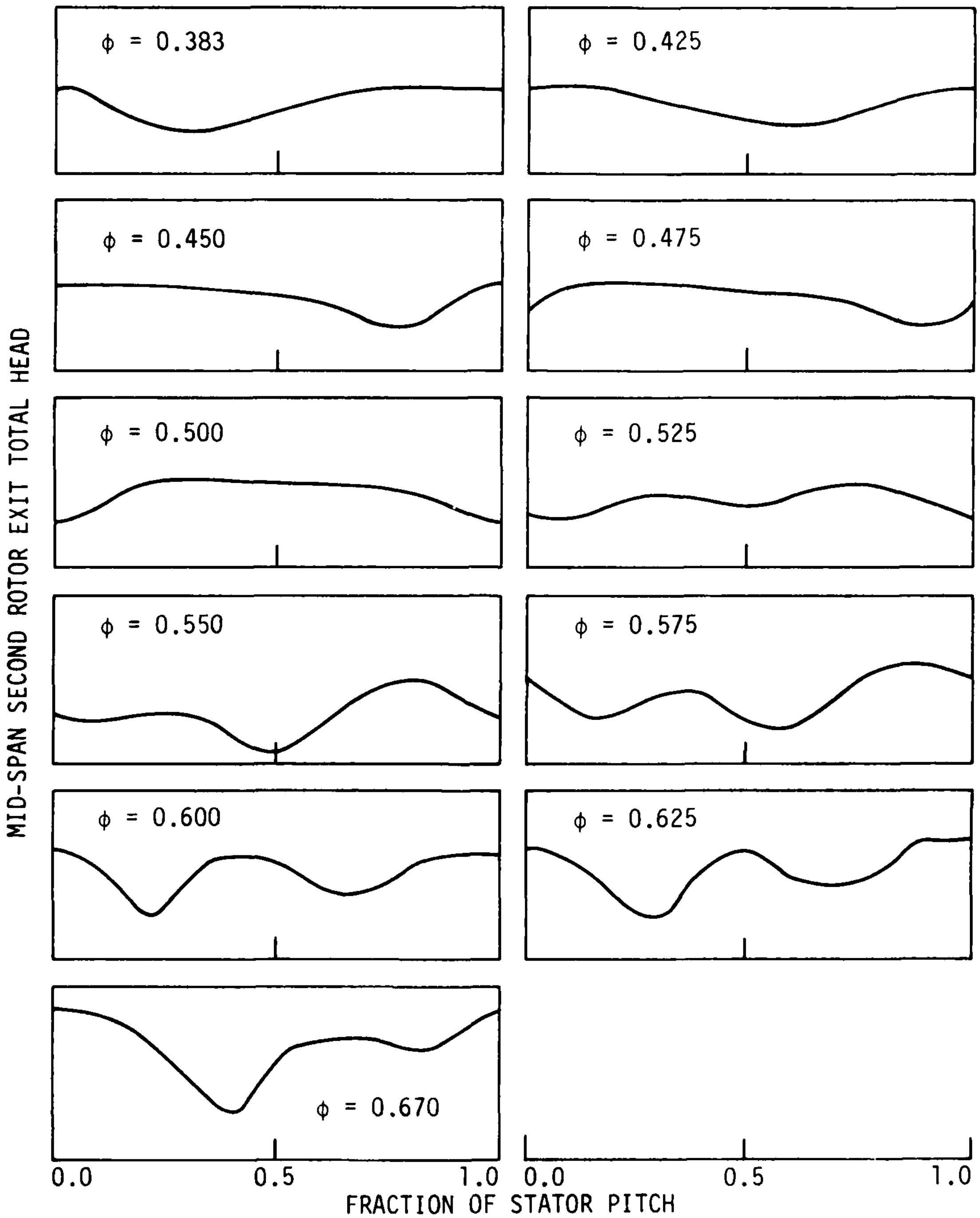

Figure 4.15 Qualitative variation of total head with circumferential extent at second rotor exit mid-span.

More qualitative data were obtained next. A specially constructed stator blade involving a wound heating element was used to produce a "warm" stator wake that could be tracked through the second stage rotor with a temperature survey at the second rotor exit. Details about the procedure and apparatus for obtaining these data were discussed earlier in the section on experimental procedure.

The variation of second rotor exit relative temperatures with circumferential extent at mid-span are presented in Figure 4.16. "Positions I and II" refer to the "warm" blade placement as illustrated in Figure 3.3. Figure 4.16(a) and (b) are for flow coefficients of 0.575 and 0.500, respectively, while in Figure 4.16(c) the results of three flow coefficients (0.575, 0.500, and 0.425) are compared. Included in Figure 4.16(a) and (b) are also total-head data which provide a means for comparing "normal wake" (no heating coil) data with "distorted wake" (cold heating coil) data, in order to ascertain the extent of wake distortion resulting from the heating coil. A relative temperature distribution is shown in Figure 4.16(b) for position II data taken with the heating coil turned off. These data illustrate that any significant increases in relative temperature are due solely to the fluid being heated by the coil.

At a flow coefficient of 0.575, the wake avenue (region of higher relative temperatures) extends over most, but not all, of the stator pitch. By comparing the circumferential wake distortion with the relative temperature distribution, a "corrected" wake avenue extent can be estimated. This corrected avenue extends

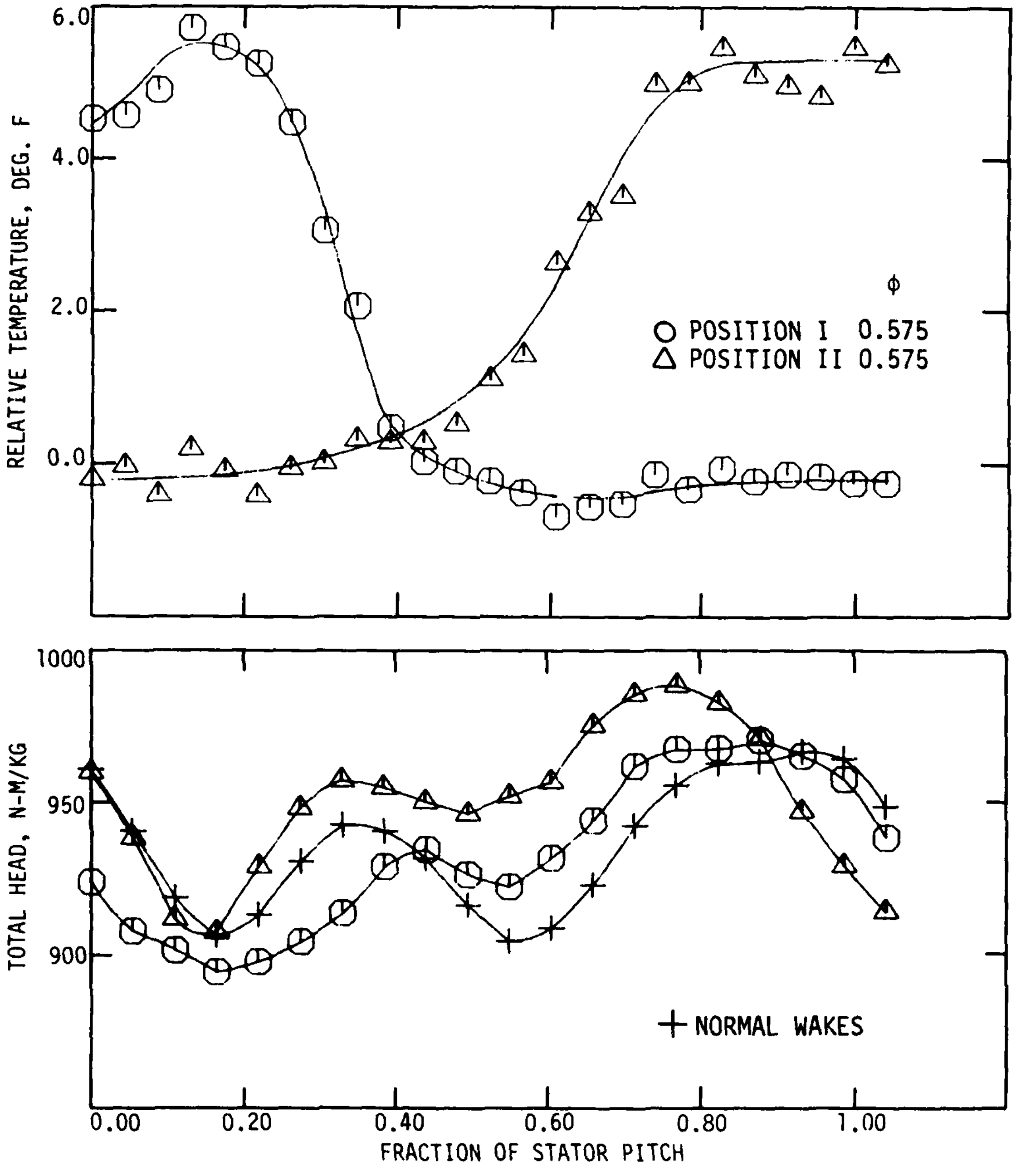

(a) ϕ = 0.575 (50 PERCENT SPAN)

Figure 4.16 First stator wake tracking data measured at the second rotor exit (50 percent span from hub).

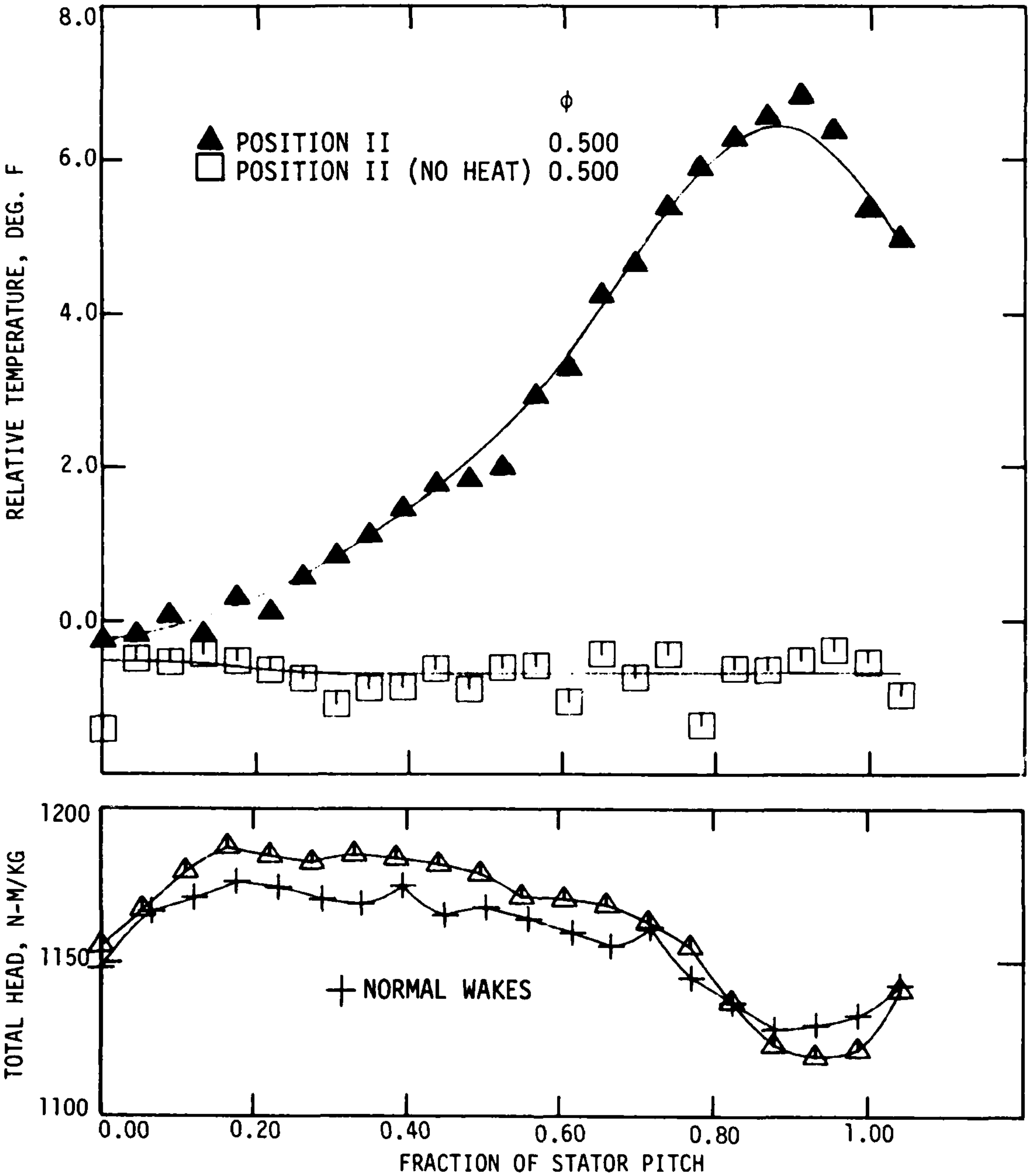

(b) ϕ = 0.500 (50 PERCENT SPAN)

Figure 4.16 continued.

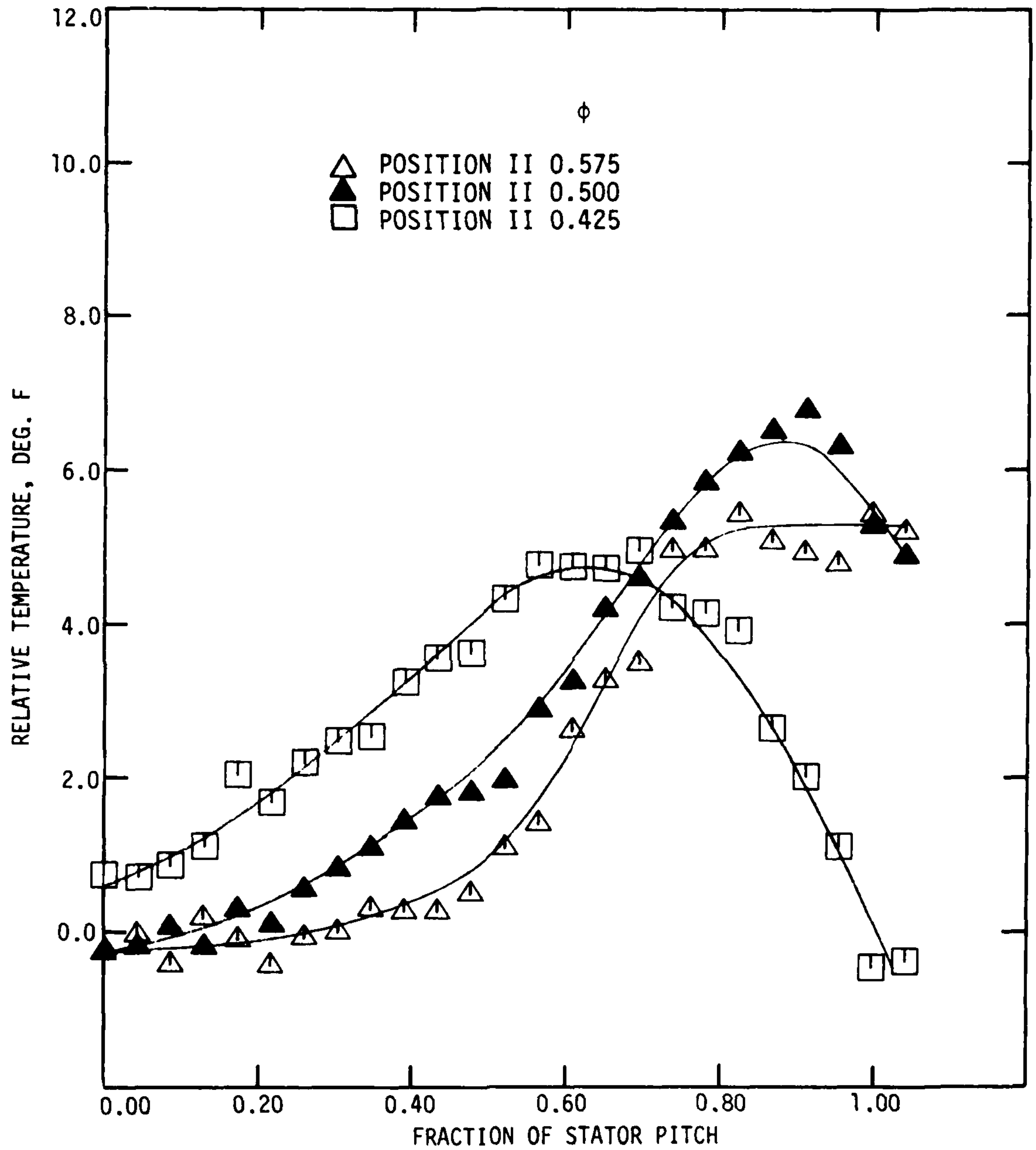

(c) FLOW COEFFICIENT COMPARISON (50 PERCENT SPAN)

Figure 4.16 concluded.

approximately from 0% to 35% and 55% to 100% of the stator pitch. Consequently, the region between wake avenues extends approximately from 35% to 55% of the stator pitch at this flow coefficient.

The wake avenue extent at flow coefficients of 0.500 or less can also be estimated by a similar analysis of data. From the data of Figure 4.15 and Figures 4.16(b) and (c), it is evident that for flow coefficients less than 0.5, the stator wake avenues overlap, and thus a region between wake avenues does not exist. At a flow coefficient of 0.500, one stator wake avenue extends from approximately 0% to 120% of the stator pitch. An overlap region between adjacent wake avenues extends from approximately 0% to 20% of the stator pitch.

Some general conclusions about changes in wake avenue extent and circumferential position with the flow rate variation are apparent from Figure 4.16(c):

- The "right-side" (as seen in Figure 4.16(c)) boundary of the wake avenue clearly shifts to the right (rotor blades move left) as the flow rate increases.
- The "left-side" boundary of the wake avenue shifts to the right as the flow rate increases, but in a much less definitive manner than the "right-side" boundary.
- At lower flow rates, the "left-side" boundary is spread out considerably (to the left) in circumferential extent.
- The "left-side" boundary becomes less spread out (more definite) as the flow rate increases.
- The "right-side" boundary maintains a somewhat definite form over the range of flow rates.

Figure 4.17(a) and (b) depict an interpretation--based on previously discussed data--of first stator wake/second rotor blade row interaction at mid-span for the two flow coefficients of 0.575 and 0.500, respectively. These drawings are similar to sketches presented by Smith [10], and, being approximately scaled, show the location of the circumferential measurement window with respect to the wake avenues.

The relationship between second rotor exit total-head variation and the blade-to-blade and wake-avenue widths is illustrated in Figure 4.18. This relationship at the flow coefficient of 0.575 is shown in Figure 4.18(a), while 4.18(b) shows it at the flow coefficient of 0.500. These drawings tend to illustrate clearly the previous results and conclusions.

For futher clarification of the observations made at mid-span, temperature data taken over the blade span were examined. Figures 4.19(a) and (b) represent second rotor exit relative temperature contour maps for the flow coefficients of 0.575 and 0.500, respectively. These two maps should be considered as they relate to the second rotor exit total-head contour maps (Figures 4.6 and 4.7) discussed earlier. The flow coefficient of 0.575 is not equal to the design value of 0.587 (for the total-head contour map). However, the temperature contours at a flow coefficient of 0.587 are not expected to be significantly different from those at the flow coefficient of 0.575. Also, as shown, some of the temperature contours for the flow coefficient of 0.500 are estimated, based on (1) the measured contours, (2) earlier conclusions on the extent of this wake

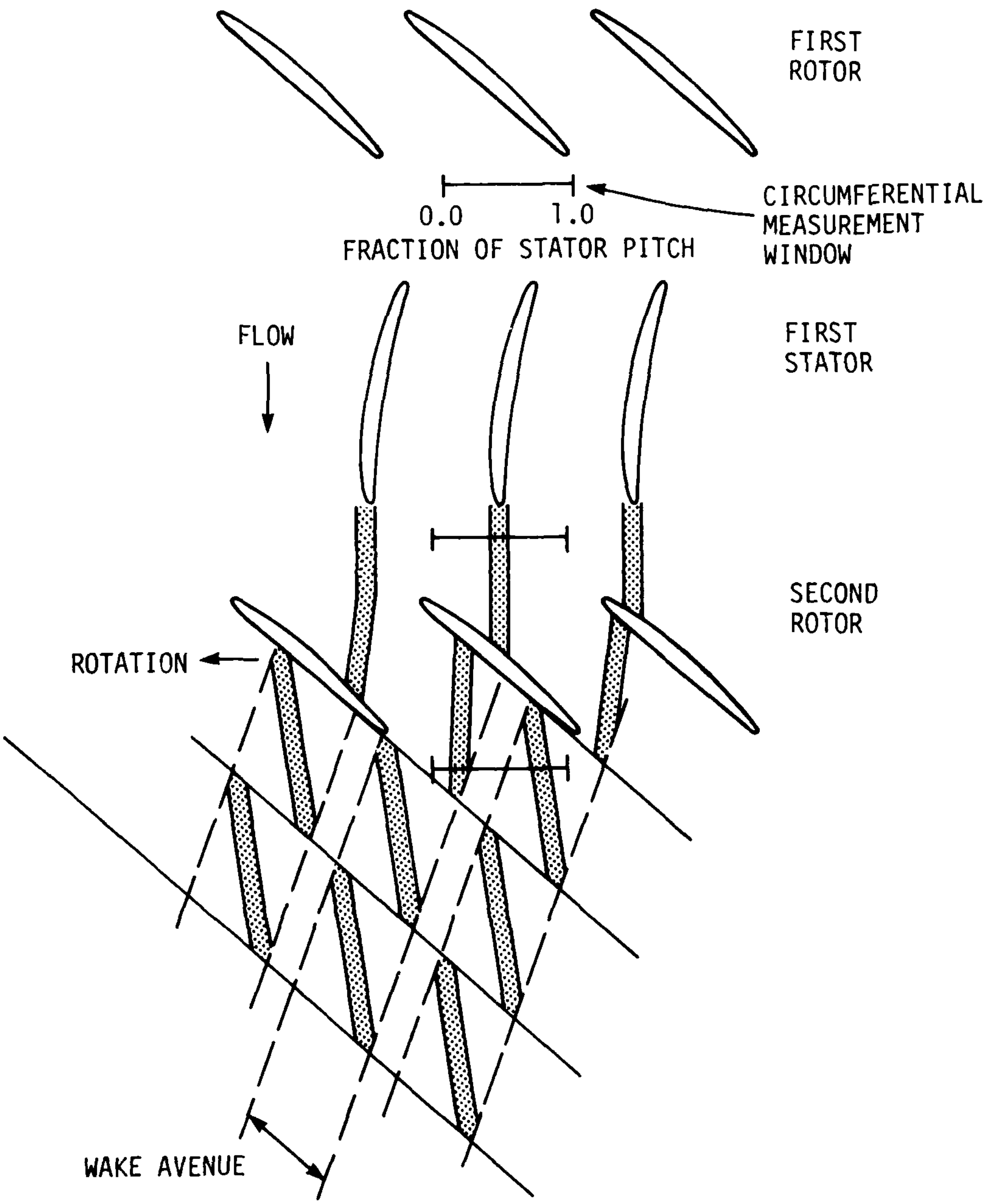

(a) $\phi = 0.575$

Figure 4.17 First stator wake/second rotor blade interaction at two operating points ($\phi = 0.575$ and $\phi = 0.500$).

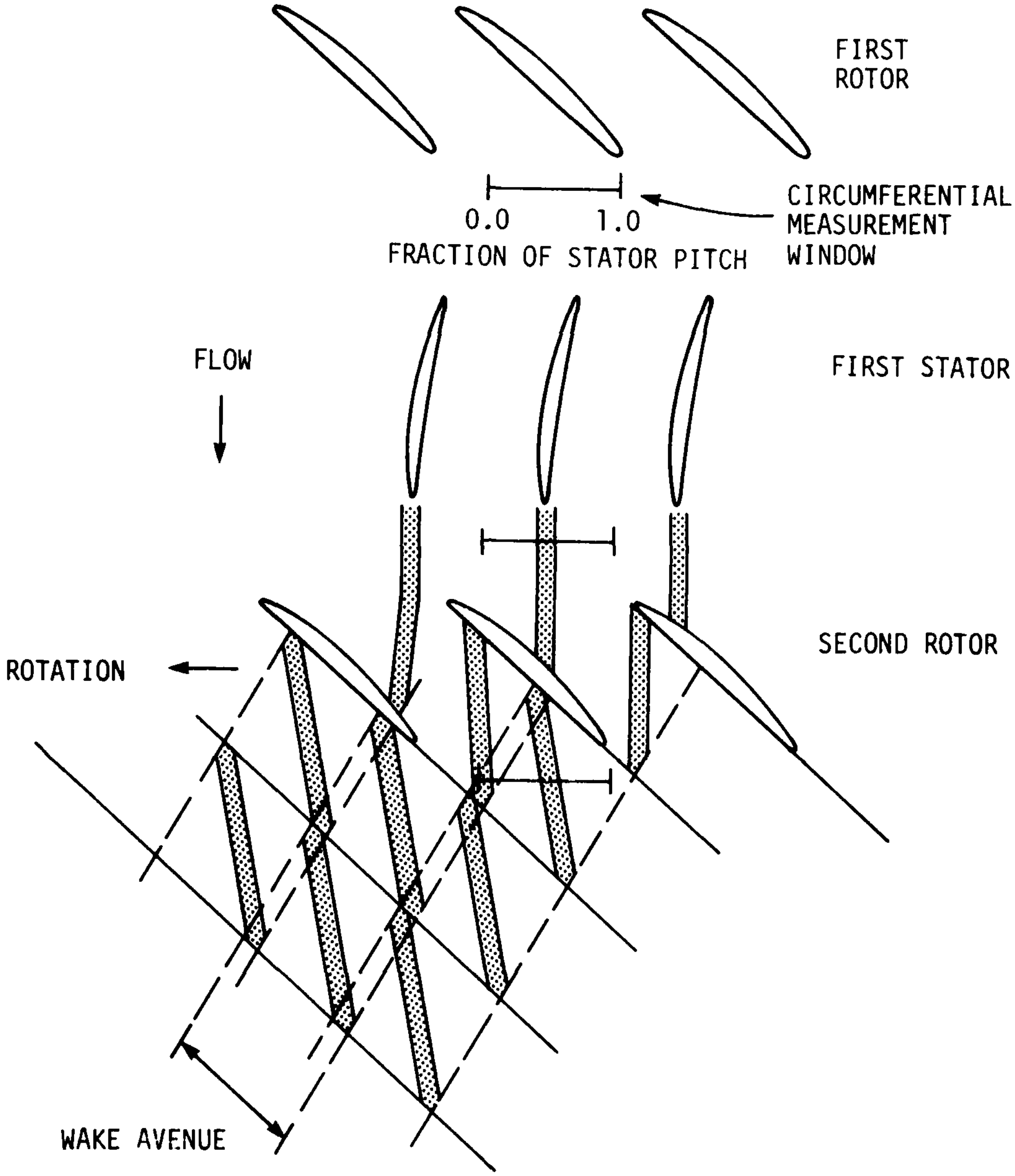

(b) ϕ = 0.500

Figure 4.17 concluded.

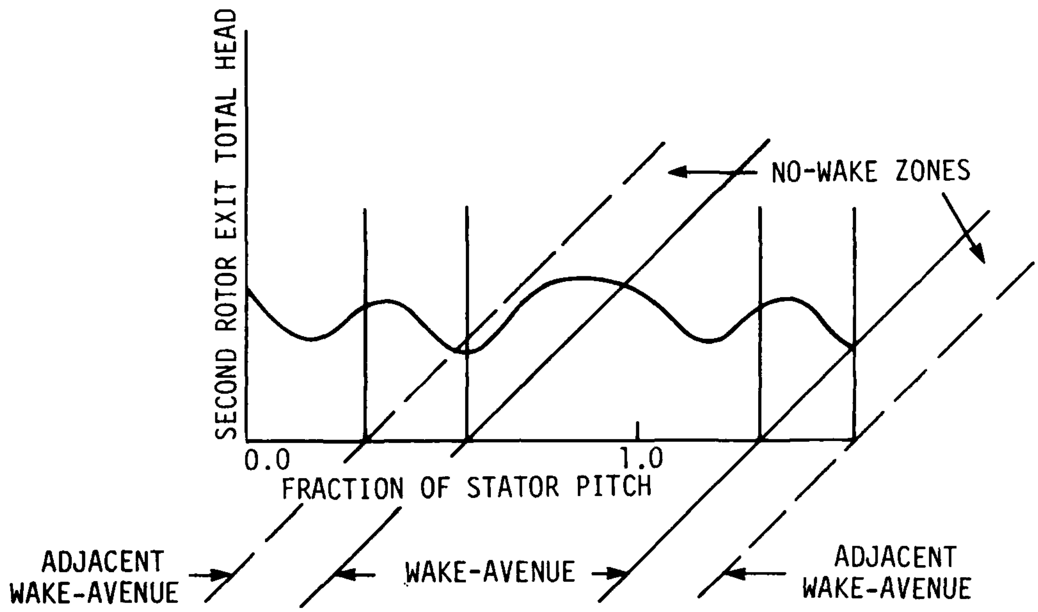

(a) ϕ = 0.575

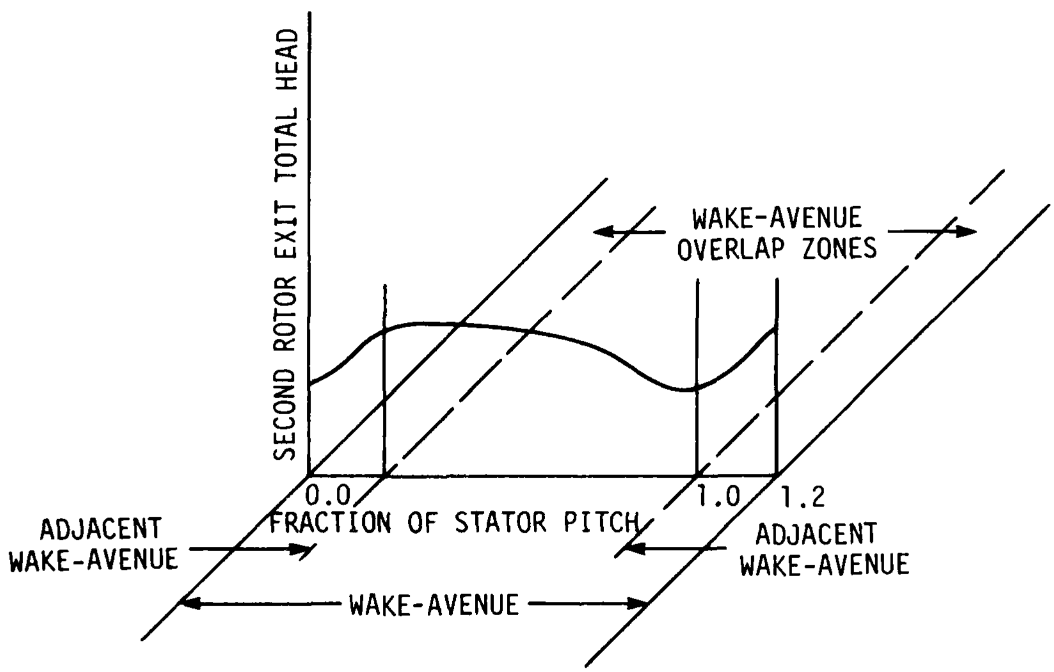

(b) ϕ = 0.500

Figure 4.18 Relationship between second rotor exit total-head variation and the blade-to-blade and wake-avenue widths.

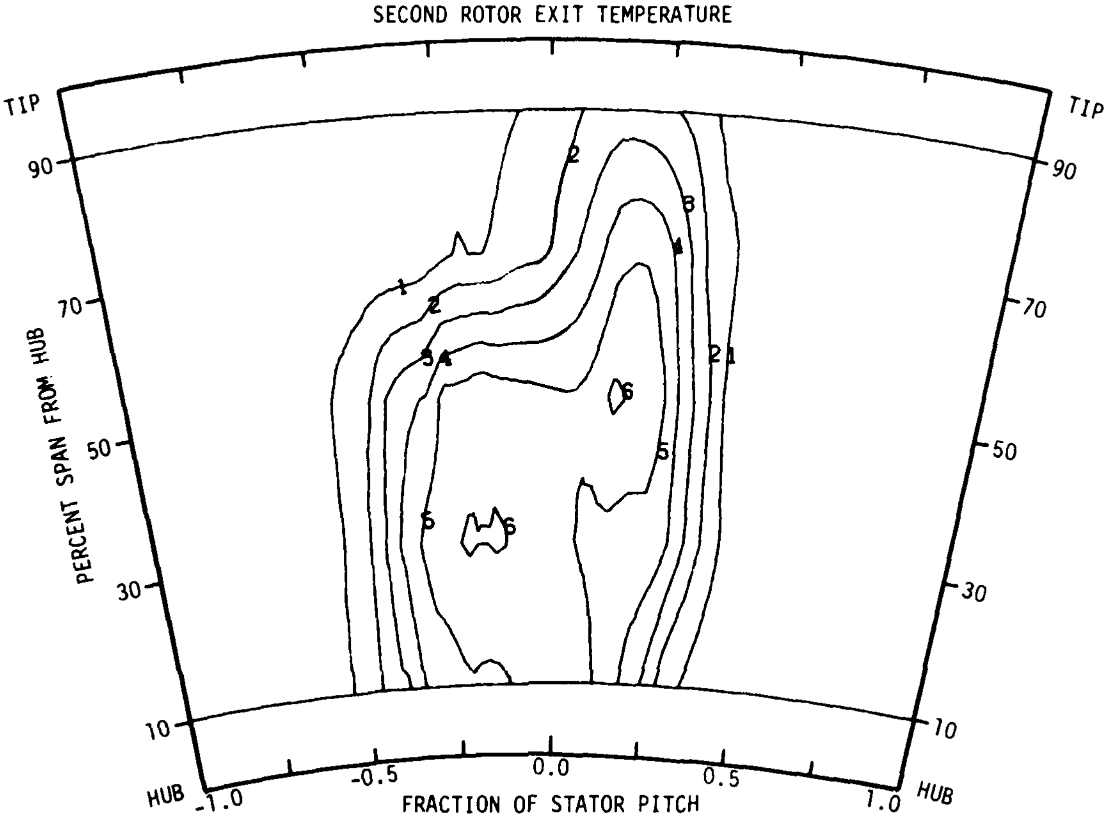

(a) ϕ = 0.575

CURVE LABEL	CURVE VALUE (DEG. F)
1	0.5
2	1.5
3	2.5
4	3.5
5	4.5
6	5.5

Figure 4.19 Contour maps of stator wake tracking temperatures measured at the second rotor exit.

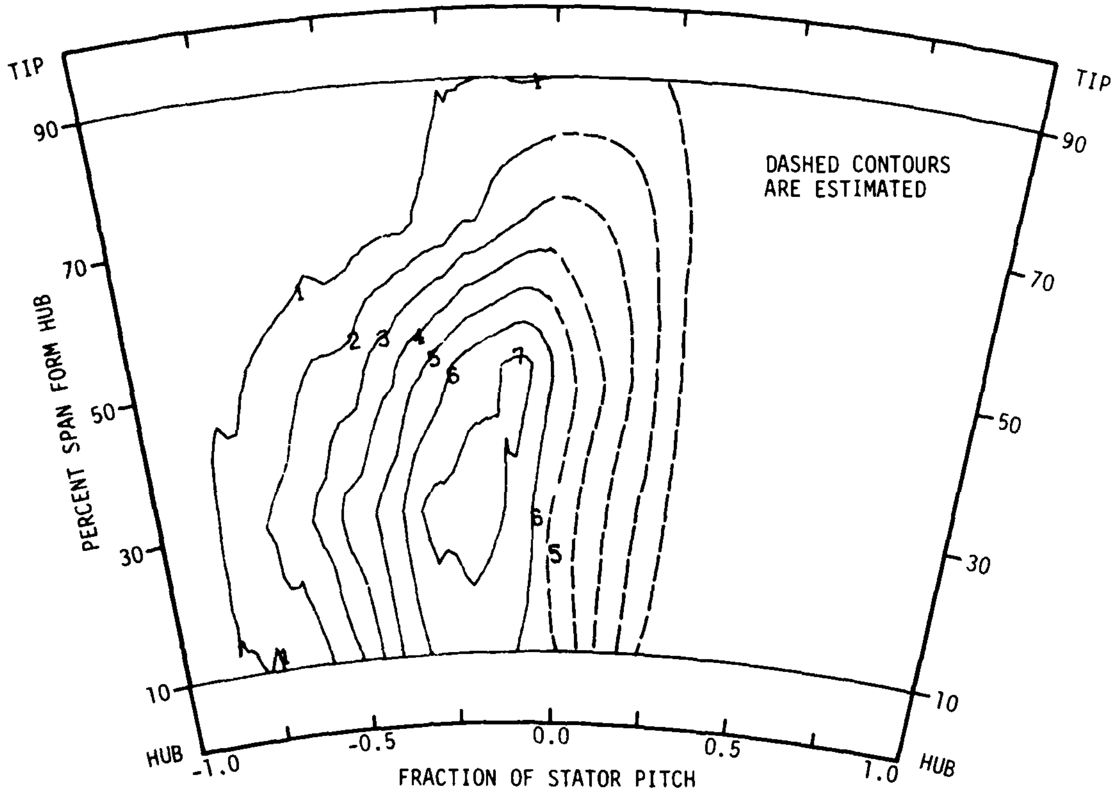

(b) ϕ = 0.500

CURVE LABEL	CURVE VALUE (DEG. F)
1	0.5
2	1.5
3	2.5
4	3.5
5	4.5
6	5.5
7	6.5

Figure 4.19 concluded.

avenue at mid-span, and (3) the spanwise behavior of corresponding contours for the flow coefficient of 0.575.

The following observations are based on the second rotor exit temperature and total-head contour maps:

- For each flow the wake avenue can be divided into two regions: (1) a "lower total-head sub-region" on the "right-side" portion of the wake avenue and (2) a "higher total-head sub-region" on the "left-side" portion of the wake avenue.
- At a flow coefficient of 0.500, adjacent wake avenues partially overlap from the hub to approximately 70% span from the hub. The single hub-to-tip valley in total head corresponds to the "lower total-head sub-region." The region of peak total head at 80% span is between wake avenues.
- At a flow coefficient of 0.587, adjacent wake avenues do not overlap at all over the entire span. The hub-to-tip valley in total head near 20% of the stator pitch corresponds to the "lower total-head sub-region" of a stator wake avenue. The second hub-to-tip valley crossing 50% of the stator pitch corresponds to the region between wake avenues. The region of peak total head from 30% to 50% span corresponds to the "higher total-head sub-region" of a stator wake avenue.
- At flow coefficients of 0.500 and less, adjacent wake avenues partially overlap over most of the span, and a single hub-to-tip valley in total head exists which corresponds to the "lower total-head sub-region" of a stator wake avenue.

- At flow coefficients of 0.525 and greater, adjacent wake avenues have a region between them which results in the formation of a second hub-to-tip valley in total head in one stator pitch.

An explanation of the variation in time-average total-head values within the wake avenues, and within the spaces between wake avenues, is beyond the scope of this study. Unsteady flow data would possibly clarify the physics involved. As pointed out by Zierke and Okiishi [12], the various kinds of fluid particles involved in chopped wake flow through a rotor (for example, freestream, stator wake, noninteracted rotor wake, interacted rotor wake) have different amounts of energy. The time-average total head at a point in space within the measurement window is a measure of the energy of the different kinds of particles that have passed through that measurement point.

4.4. Comparison of Compressor Builds

The detailed aerodynamic performance results obtained for the four different compressor builds at one operating point (venturi flow coefficient = 0.500 and shaft speed = 2400 rpm) are presented, compared, and analyzed in this section. Those data which most clearly show effects of stator geometry modification on the flow are emphasized. Two major subsections contained herein are:

1. Presentation and discussion of results
2. Analysis of stator geometry modification effects

The first major subsection proceeds in the following sequence:

- first stage performance
- second stage and overall performance
- first/second stage performance comparison
- mass-averaged performance

4.4.1. Presentation and Discussion of Results

4.4.1.1. First Stage Performance

Spanwise distributions of some first stage circumferential-mean performance parameters are presented in Figure 4.20. Conventional rotor and stage head-rise curves are shown in Figure 4.20(a) and (b), respectively. Figure 4.20(c) illustrates first stator loss variations, and Figure 4.20(d) involves first stator incidence and deviation angle data. First rotor head-rise performance is essentially unaffected by stator geometry modification. The differences between rotor head-rise curves in Figure 4.20(a) are not considered significant. This result is not surprising, since the upstream effect of the stator modification on rotor exit total head is expected to be small for the axial spacings involved. First rotor exit total-head contour maps for the baseline 1 and modified 1 builds are presented in Figure 4.21(a) and (b), respectively, and they demonstrate that first rotor exit total-head does not vary significantly with circumferential extent, thus substantiating the conclusion that stator blade influence on first rotor performance is nil. This constancy of first rotor head-rise performance between builds leads to the impression that the observed differences in first stage head-rise performance, indicated in

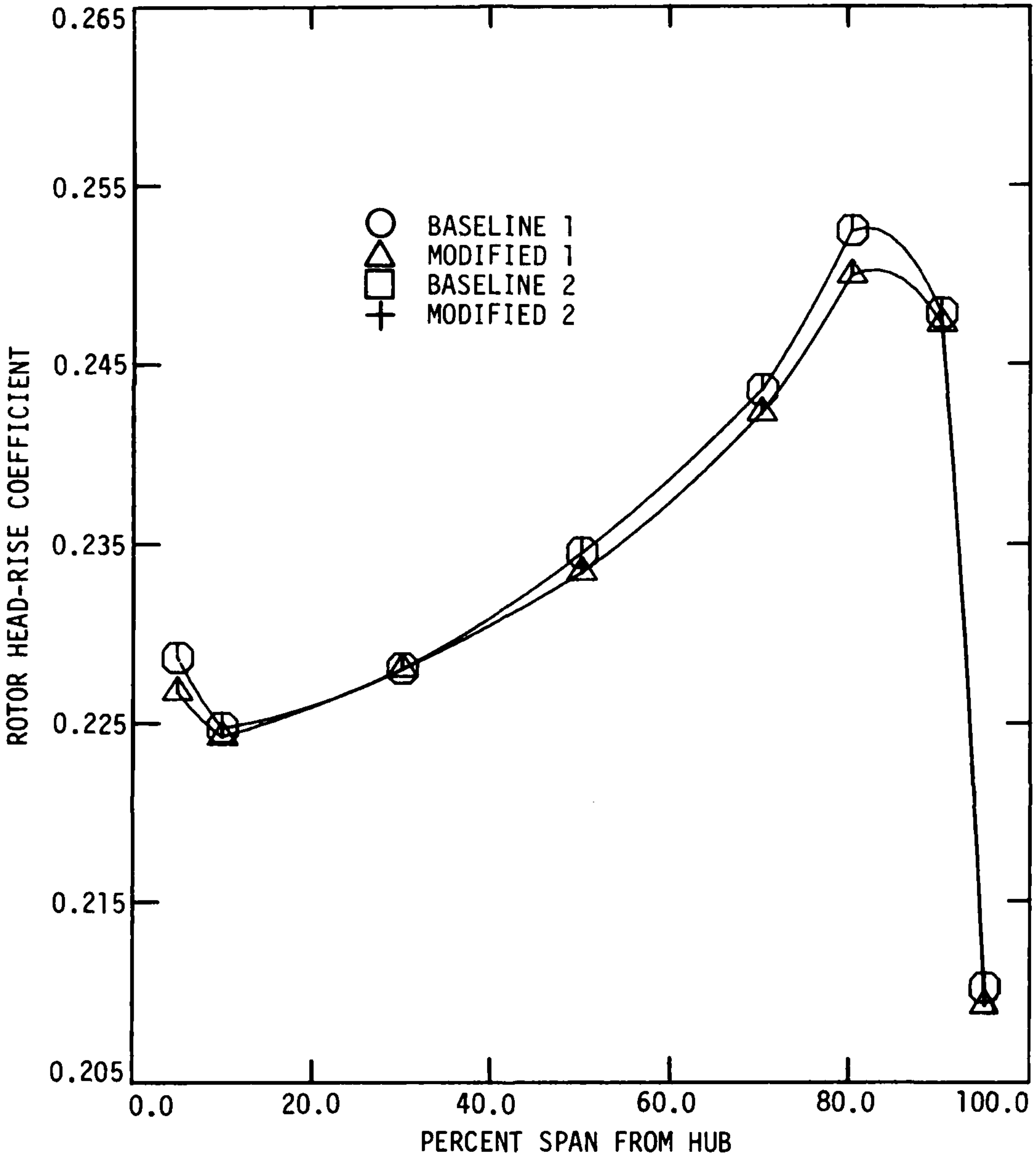

(a) ROTOR HEAD-RISE

Figure 4.20 Spanwise distribution of first stage circumferential-mean performance parameters for the different compressor builds (ϕ = 0.500).

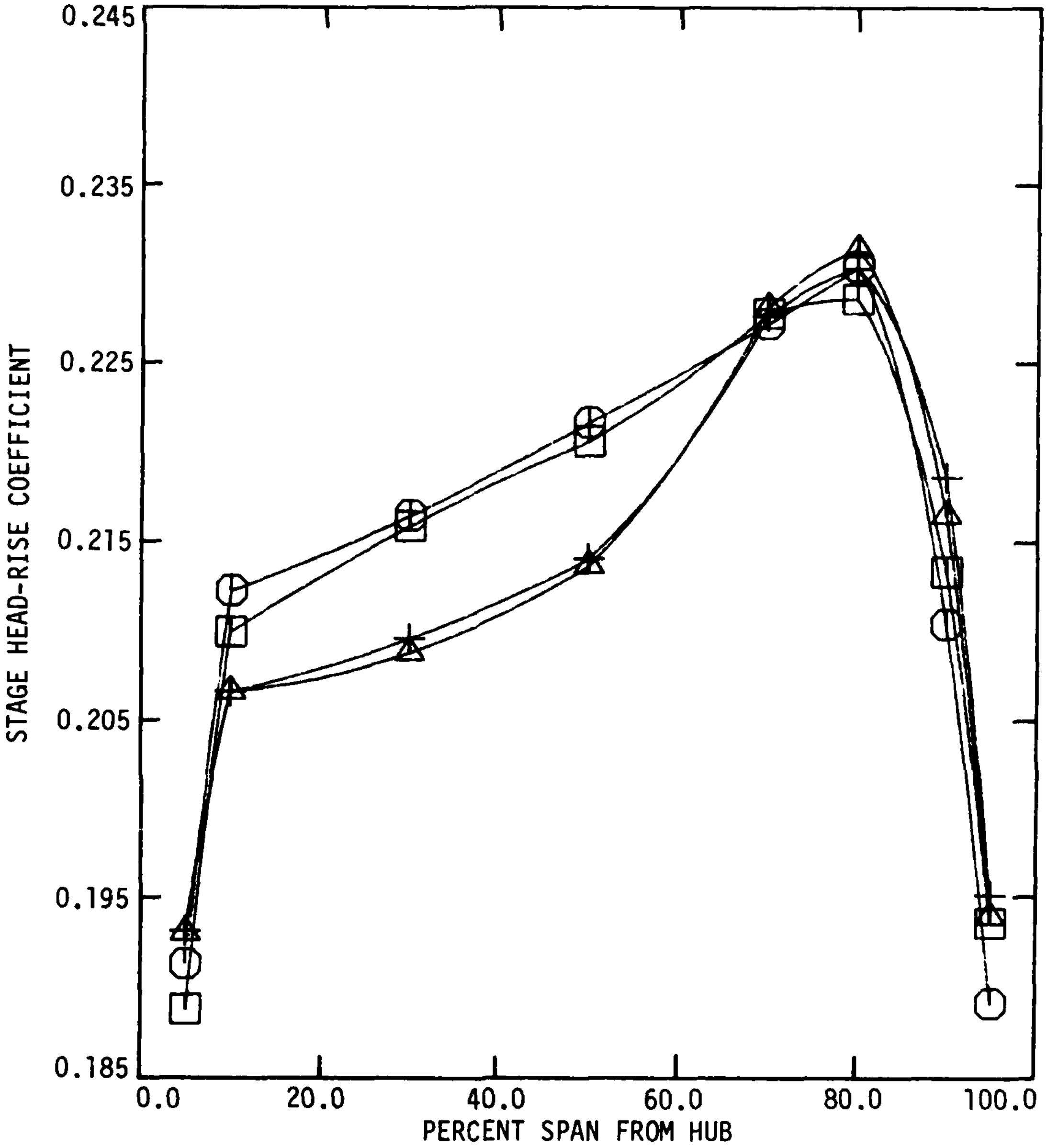

(b) STAGE HEAD-RISE

Figure 4.20 continued.

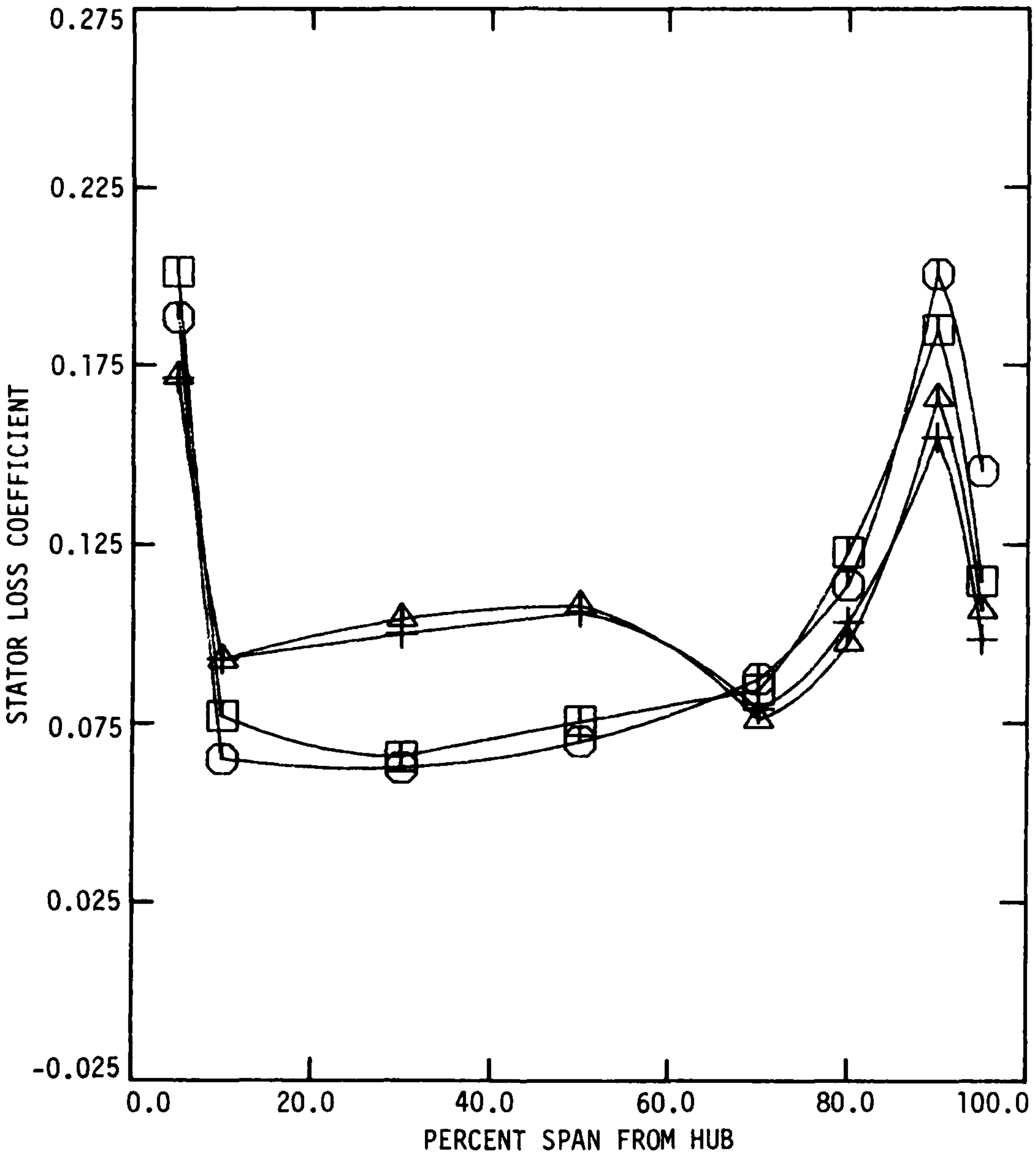

(c) STATOR LOSS

Figure 4.20 continued.

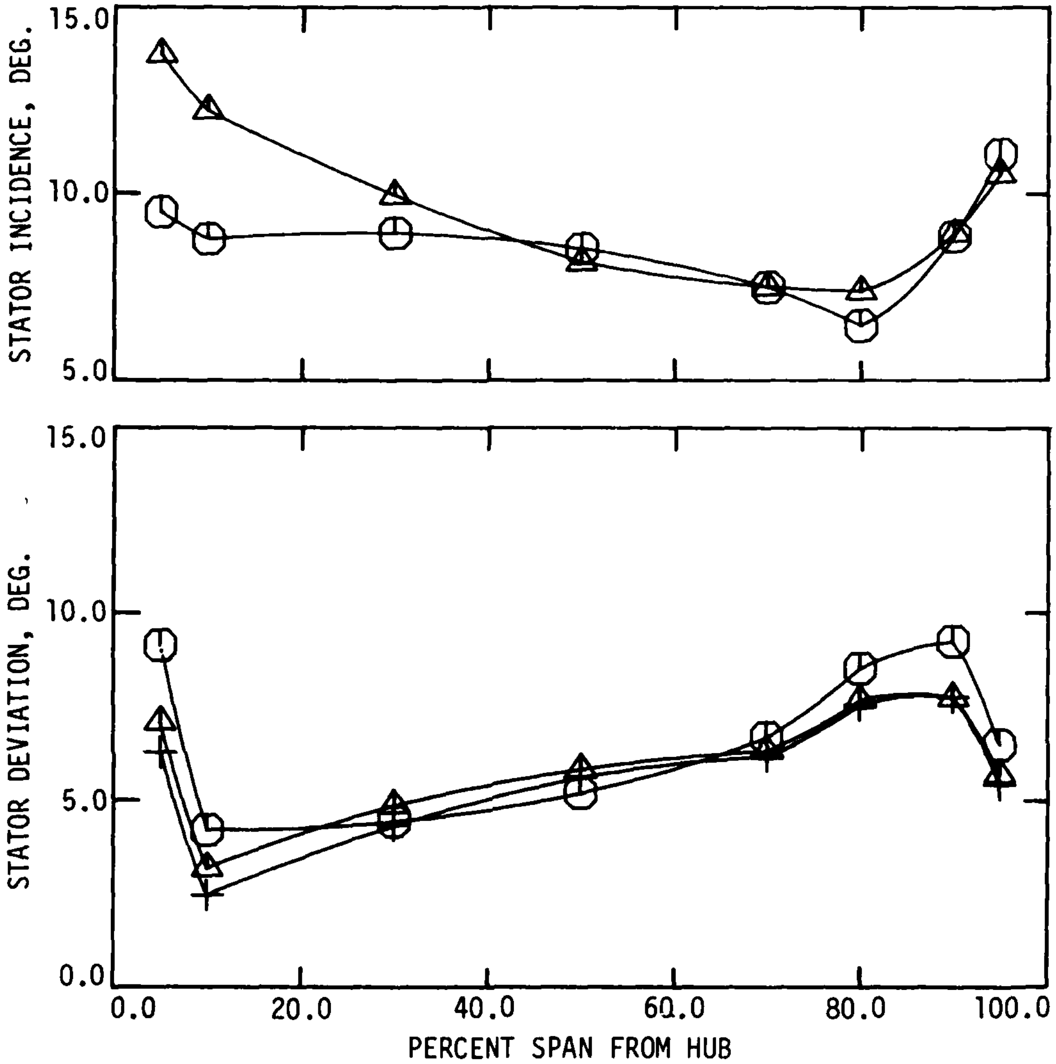

(d) STATOR INCIDENCE AND DEVIATION

Figure 4.20 concluded.

FIRST ROTOR EXIT TOTAL HEAD
BASELINE 1 COMPRESSOR BUILD

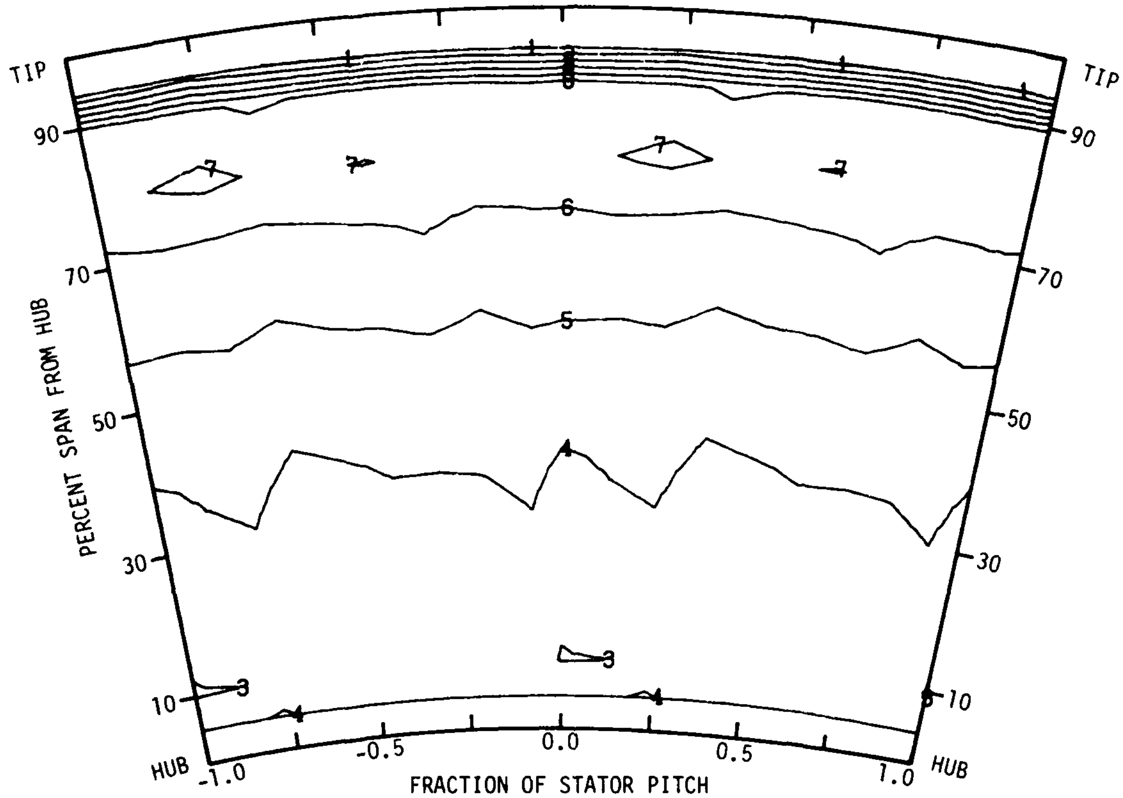

CURVE LABEL	CURVE VALUE (N-M/KG)
1	540
2	560
3	580
4	600
5	620
6	640
7	660

Figure 4.21 First rotor exit total-head contour maps for the baseline 1 and modified 1 compressor builds (ϕ = 0.500).

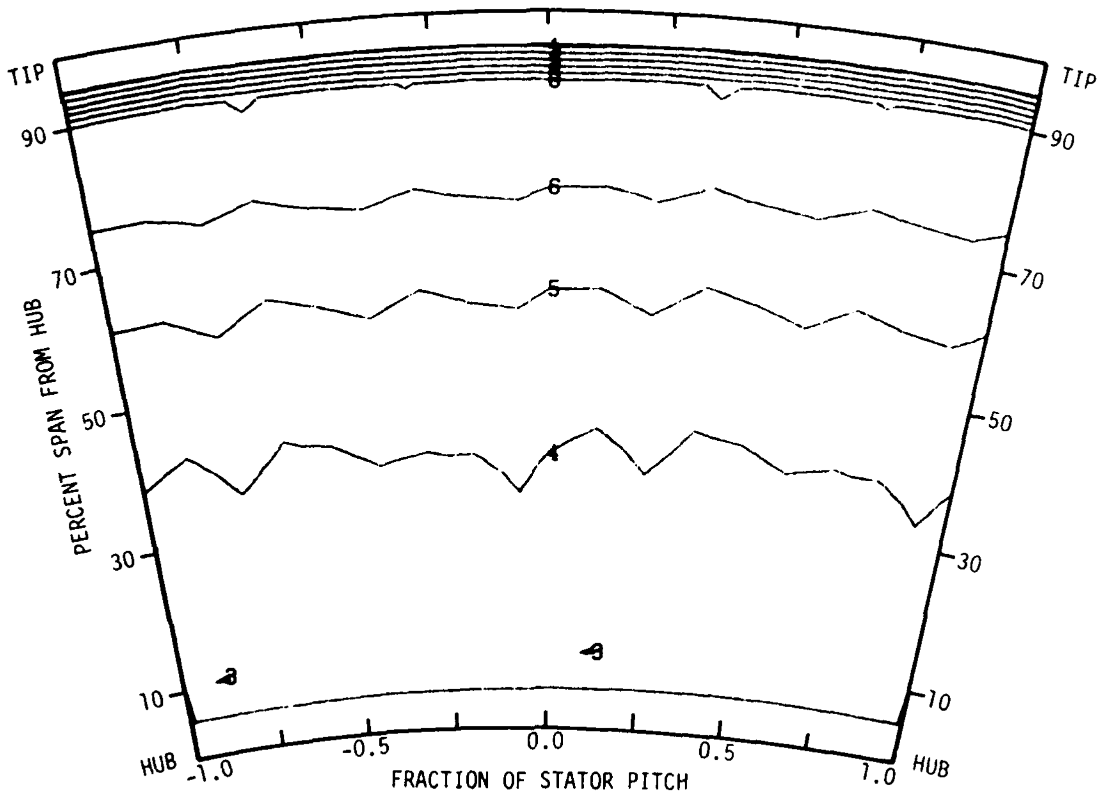

CURVE LABEL	CURVE VALUE (N-M/KG)
1	540
2	560
3	580
4	600
5	620
6	640

Figure 4.21 concluded.

Figure 4.20(b), can be directly attributed to the first stator loss performance shown in Figure 4.20(c).

The stator loss curves in Figure 4.20(c) suggest a significant difference in first stator loss performance by the baseline and modified stator blades. It should be noted (see Table 2.3 and Figure 2.5) that the two baseline builds, and similarly the two modified builds, are each pair identical in the first stage. Therefore, no difference .n stator loss performance is expected between the builds based on a common stator. The data verify this, with the differences between baseline 1 and 2, and between modified 1 and 2 first stator data in Figure 4.20(c) being insignificant.

The difference in spanwise distribution of first stator loss between each pair of builds can be readily described:

- The baseline stator loss is substantially less than the modified stator loss from 10% to 50% span from the hub.
- The modified stator loss is somewhat (significantly) less than the baseline stator loss from 70% to 95% span from the hub, and also at 5% span from the hub.

The first stator exit total-head contour maps for the different builds are presented in Figure 4.22. These maps allow one to relate the above observed stator loss behavior for the different build pairs to the wake behavior of each kind of stator blade geometry. Only a baseline/modified comparison is made for the first stator; however, maps for all four builds are included for completeness, and also to confirm data repeatability.

FIRST STATOR EXIT TOTAL HEAD
BASELINE 1 COMPRESSOR BUILD

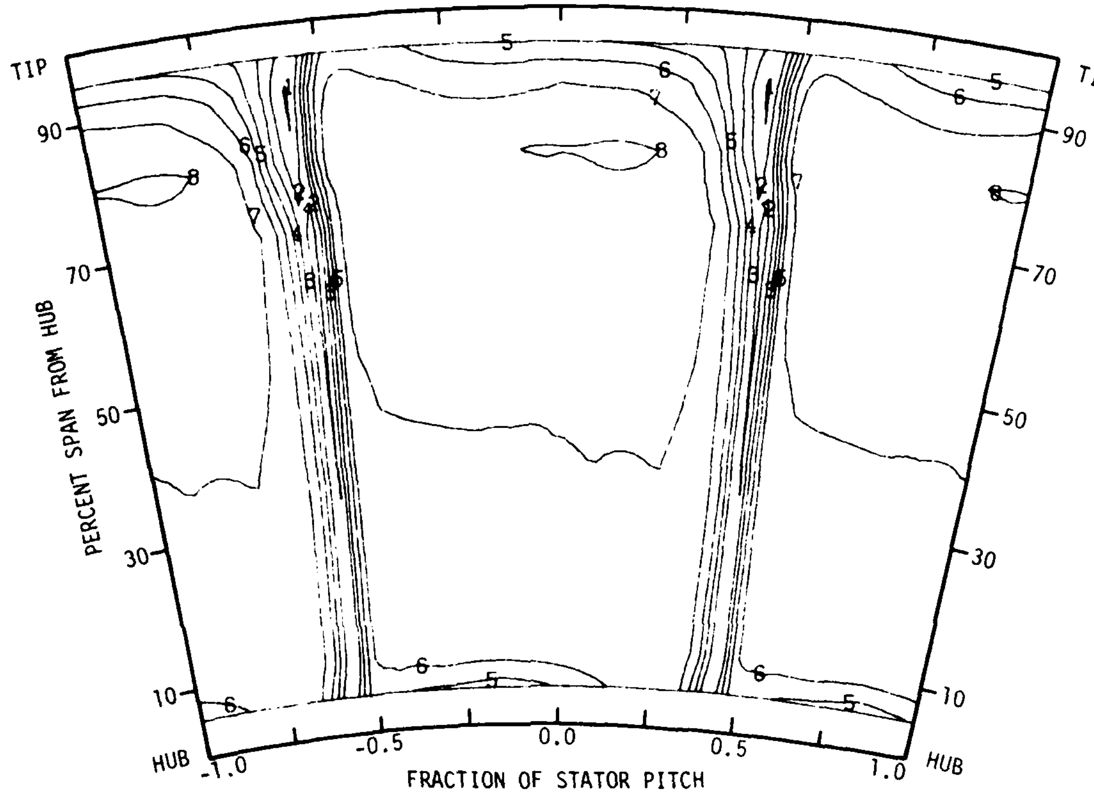

CURVE LABEL	CURVE VALUE (N-M/KG)
1	290
2	340
3	390
4	440
5	490
6	540
7	590
8	640

Figure 4.22 First stator exit total-head contour maps for each compressor build ($\phi = 0.500$).

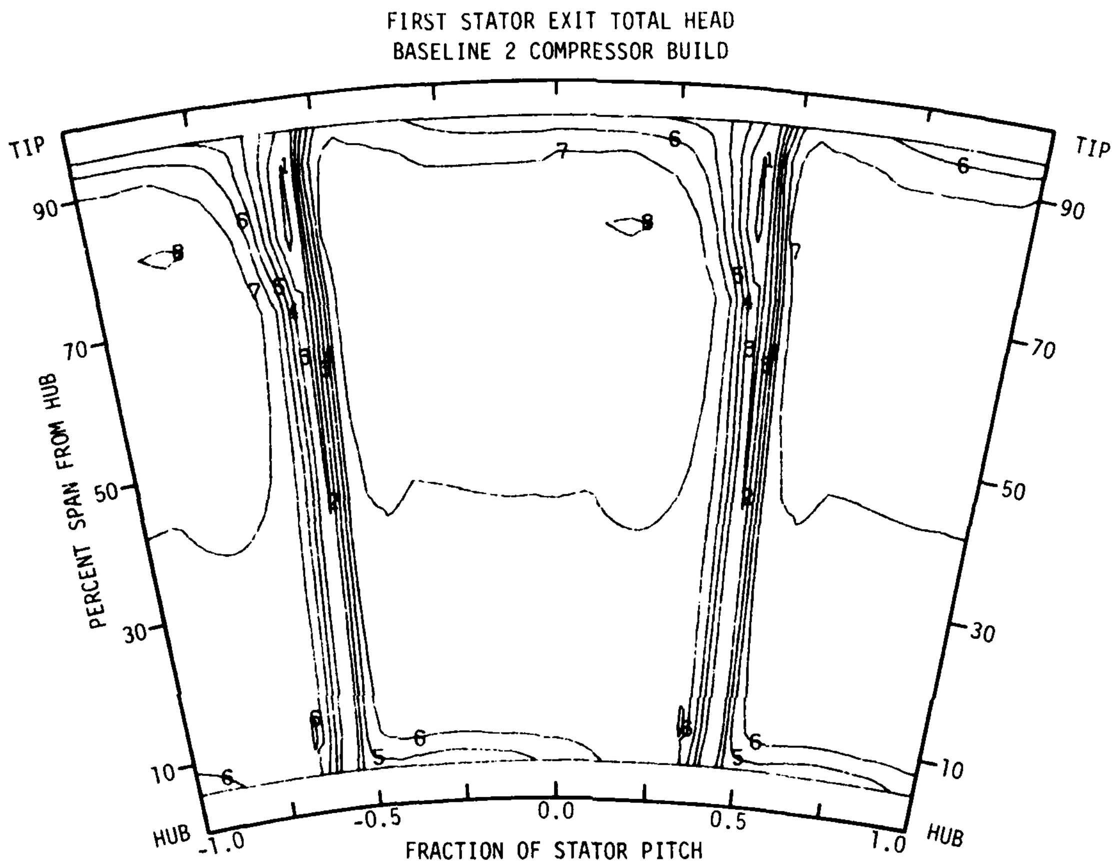

CURVE LABEL	CURVE VALUE (N-M/KG)
1	290
2	340
3	390
4	440
5	490
6	540
7	590
8	640

Figure 4.22 continued.

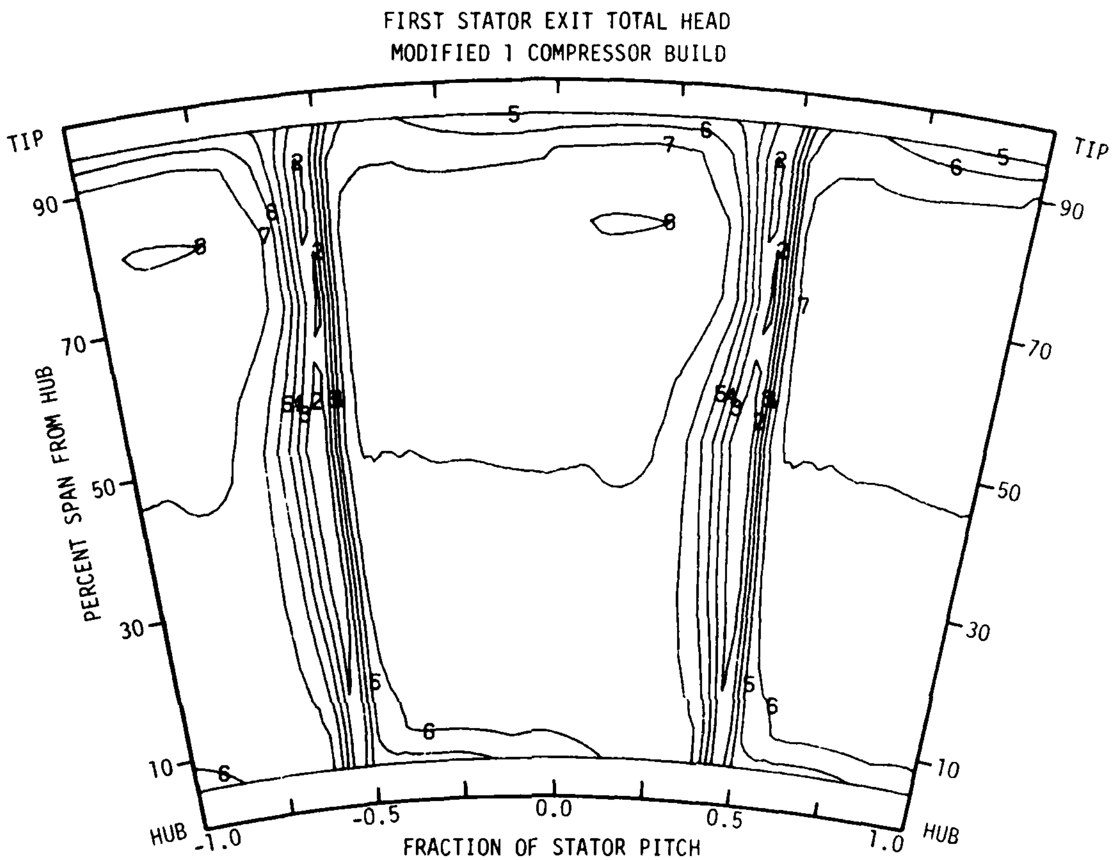

CURVE LABEL	CURVE VALUE (N-M/KG)
2	340
3	390
4	440
5	490
6	540
7	590
8	640

Figure 4.22 continued.

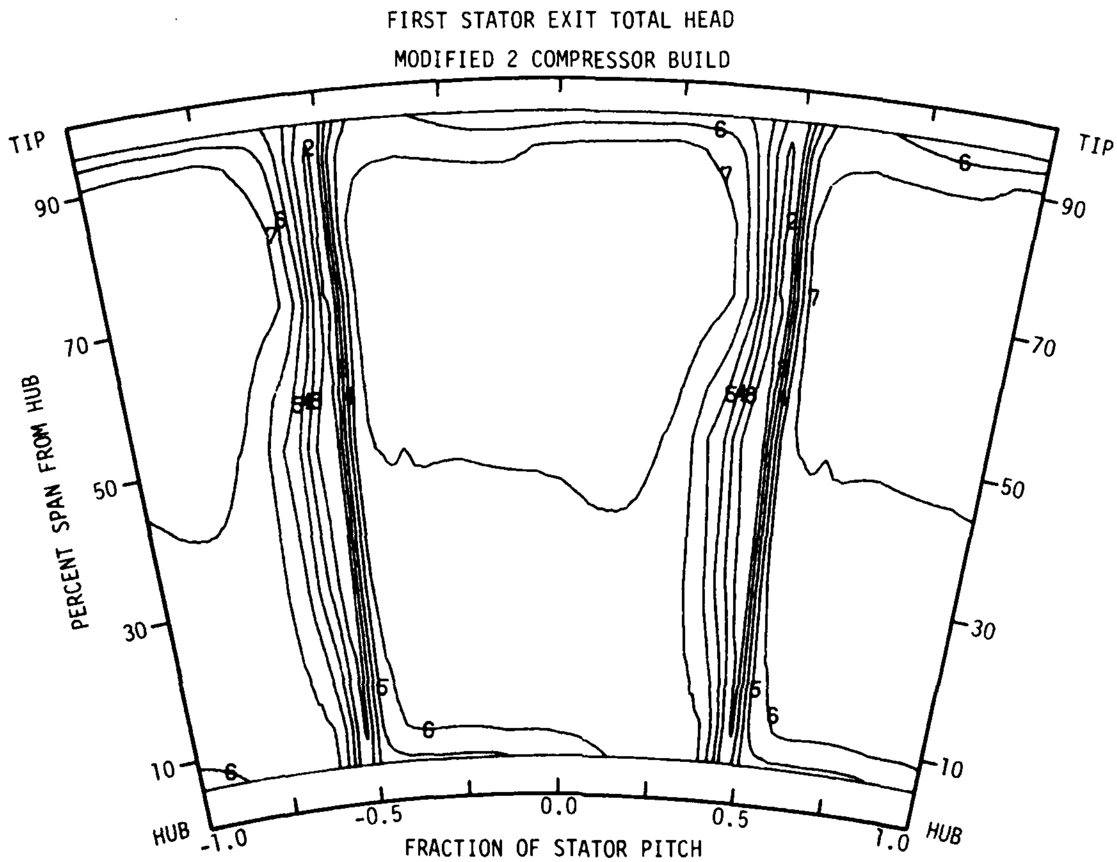

CURVE LABEL	CURVE VALUE (N-M/KG)
2	340
3	390
4	440
5	490
6	540
7	590

Figure 4.22 concluded.

The stator exit total-head contour maps display in some detail the stator exit wake and end-wall flows. On these maps, gradients in total head are easily discerned from the contours. From these gradients, the extent of the wake and end-wall flows can be inferred. Because stator row losses are generated mainly within these two flows, there exists a good correlation between the observed wake/end-wall region depth and extent and the corresponding circumferential-mean stator loss.

The following observations are based on the baseline first stator exit total-head contour map(s) (Figure 4.22) and the baseline first stator loss curve(s) (Figure 4.20(c)):

- The first stator wake is uniform in width and gradually increases in depth from 10% to 70% span from the hub. Correspondingly, the first stator loss gradually increases from 10% to 70% span from the hub.
- The first stator wake flairs out, mostly on the suction side, into an end-wall flow from 70% span to the tip. There is a corresponding increase in the first stator loss from 70% to 90% span from the hub. A probable reason for the drop in stator loss near the tip was previously discussed in section 4.3.1.
- Near the hub there is a "piling-up" of lower-momentum fluid on the pressure side of the stator blade. This is accompanied by a corresponding abrupt increase in stator loss near the hub. More detailed discussion concerning this was presented previously in section 4.3.1.

A comparison between the baseline and modified first stator exit total-head contour maps is shown in Figure 4.23. The following flow-field differences can be noted from this comparison, and related to corresponding first stator loss curves:

- The modified stator wake is substantially wider on the suction side, and somewhat deeper, than the baseline stator wake from 10% to 70% span from the hub. This is consistent with the first stator loss curves.
- The modified stator wake is similar in width and depth to the baseline stator wake at 70% span from the hub. Correspondingly, the first stator loss is almost the same for both geometries there.
- The modified stator wake "end-wall flair" on the suction side from 70% span to the tip, is substantially less than that for the baseline stator. The modified stator wake "end-wall flair" on the pressure side at both the hub and tip, is somewhat greater than that for the baseline stator. However, the net effect is seen as lower loss in the end-wall regions for the modified blade than for the baseline blade.

The first stator incidence and deviation angle results (Figure 4.20(d)) are discussed next. Only a few points seem salient:

- There is no recognizable relationship between the spanwise trends in first stator incidence angle and those in first stator loss.
- There is an approximate correlation between the spanwise trends in first stator deviation angle and those in first

FIRST STATOR EXIT TOTAL HEAD

BLACK BASELINE 1 BUILD
RED MODIFIED 1 BUILD

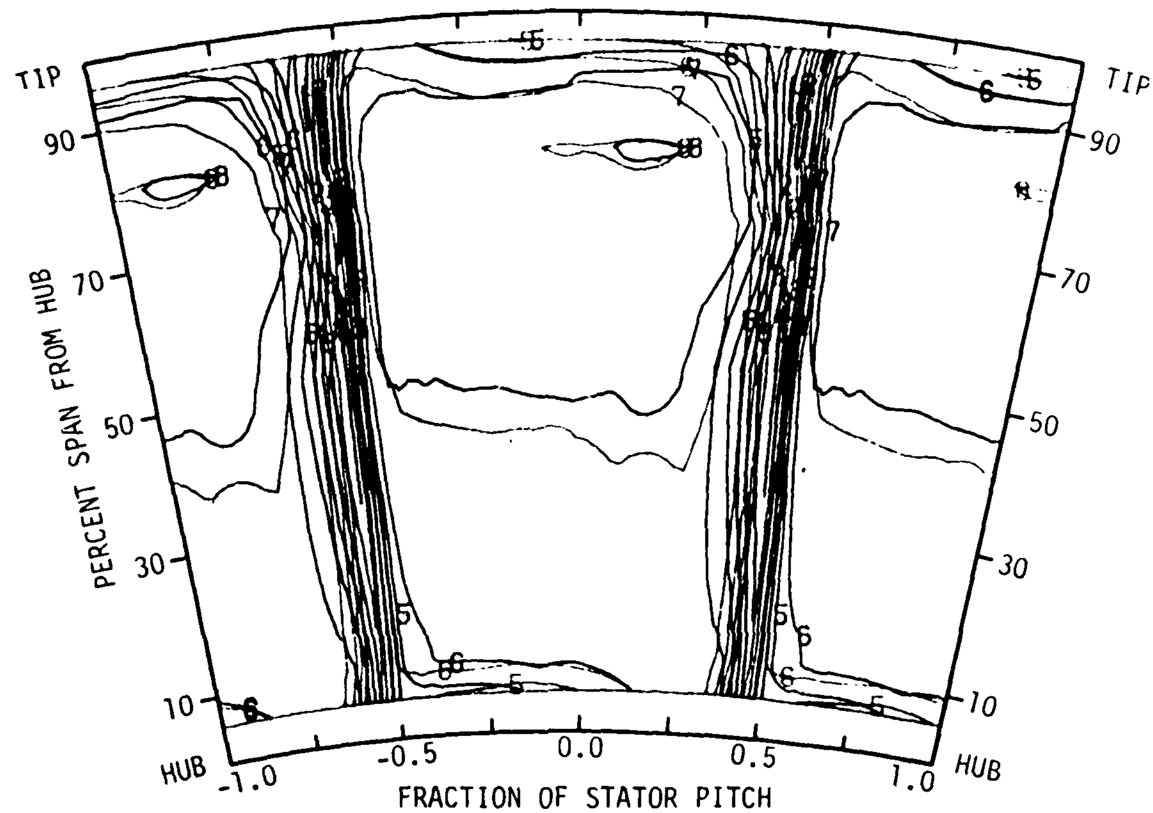

CURVE LABEL	CURVE VALUE (N-M/KG)
1	290
2	340
3	390
4	440
5	490
6	540
7	590
8	640

Figure 4.23 Map comparing the total-head contours at the first stator exit for the baseline 1 and modified 1 compressor builds (ϕ = 0.500).

stator loss. The modified stator tends to involve less deviation angle than the baseline stator in the end-wall regions.

- The difference between the baseline and modified first stator incidence angles near the hub indicates some upstream effect of the stator modification on first rotor exit absolute flow angle, but only near the hub.

4.4.1.2. Second Stage and Overall Performance

Spanwise distributions of second stage circumferential-mean performance parameters are presented in Figure 4.24. Conventional rotor and stage head-rise curves are included in Figure 4.24(a) and (b), respectively. In Figure 4.24(c) are found compressor-inlet to second-rotor-exit head-rise curves. Because the compressor-inlet total-head distribution is approximately uniform, Figure 4.24(c) actually provides an effective comparison of normalized second rotor exit total-head curves for the different builds. Figure 4.24(d) involves second stator loss data, and Figure 4.24(e) illustrates second stator incidence and deviation angle variations.

Results which show how first and second rotor head-rise values are related were discussed earlier (see section 4.3.1). First and second rotor exit total-head distributions over the blade span were shown to be similar, even though the head-rise distributions were not. Thus, it was concluded that the trends in the spanwise distribution of second rotor conventional head-rise coefficients were approximately similar to those of first stator loss. A comparison of the first stator loss curves in Figure 4.20(c) with the second

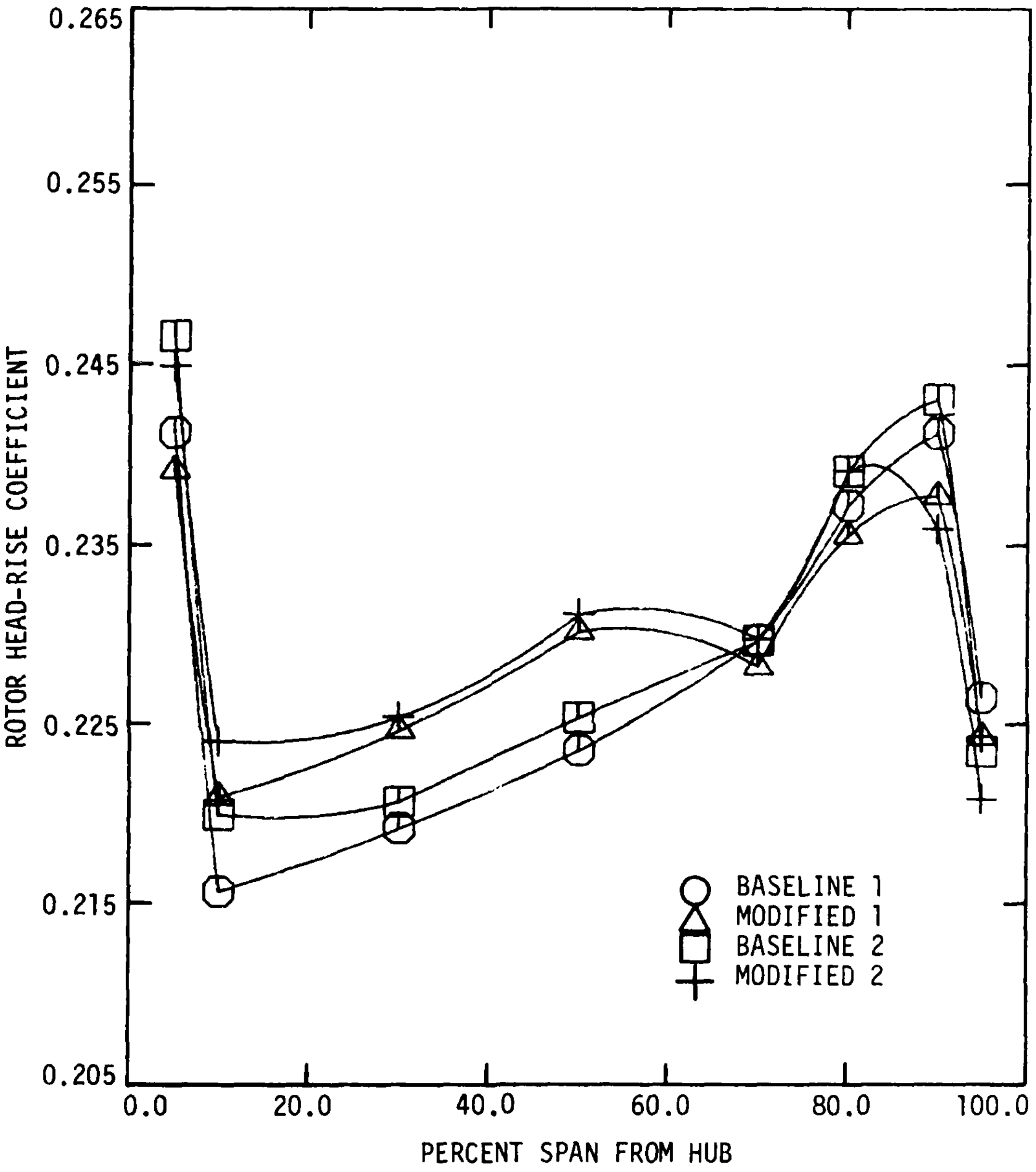

(a) ROTOR HEAD-RISE

Figure 4.24 Spanwise distribution of second stage circumferential-mean performance parameters for the different compressor builds (ϕ = 0.500).

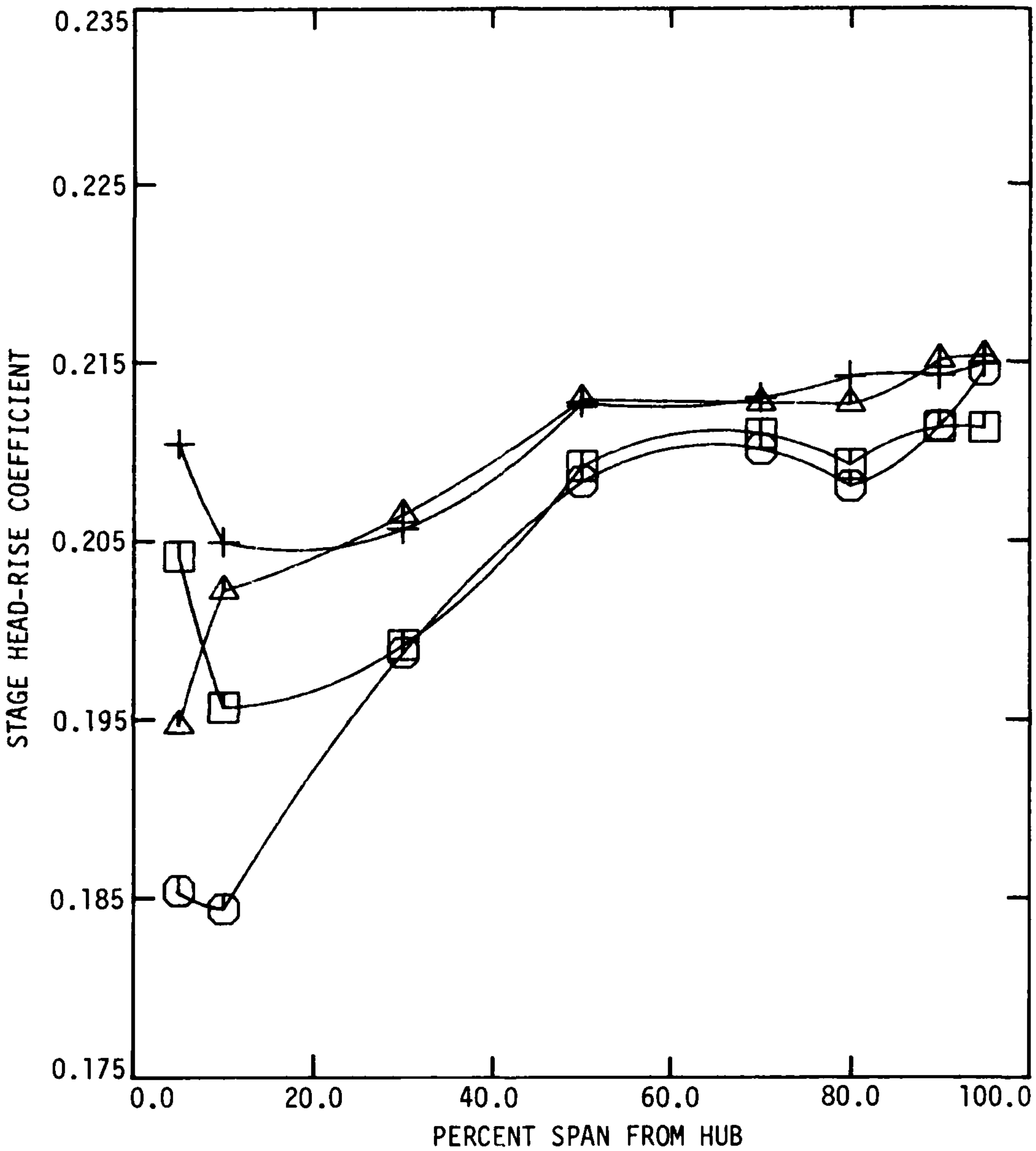

(b) STAGE HEAD-RISE

Figure 4.24 continued.

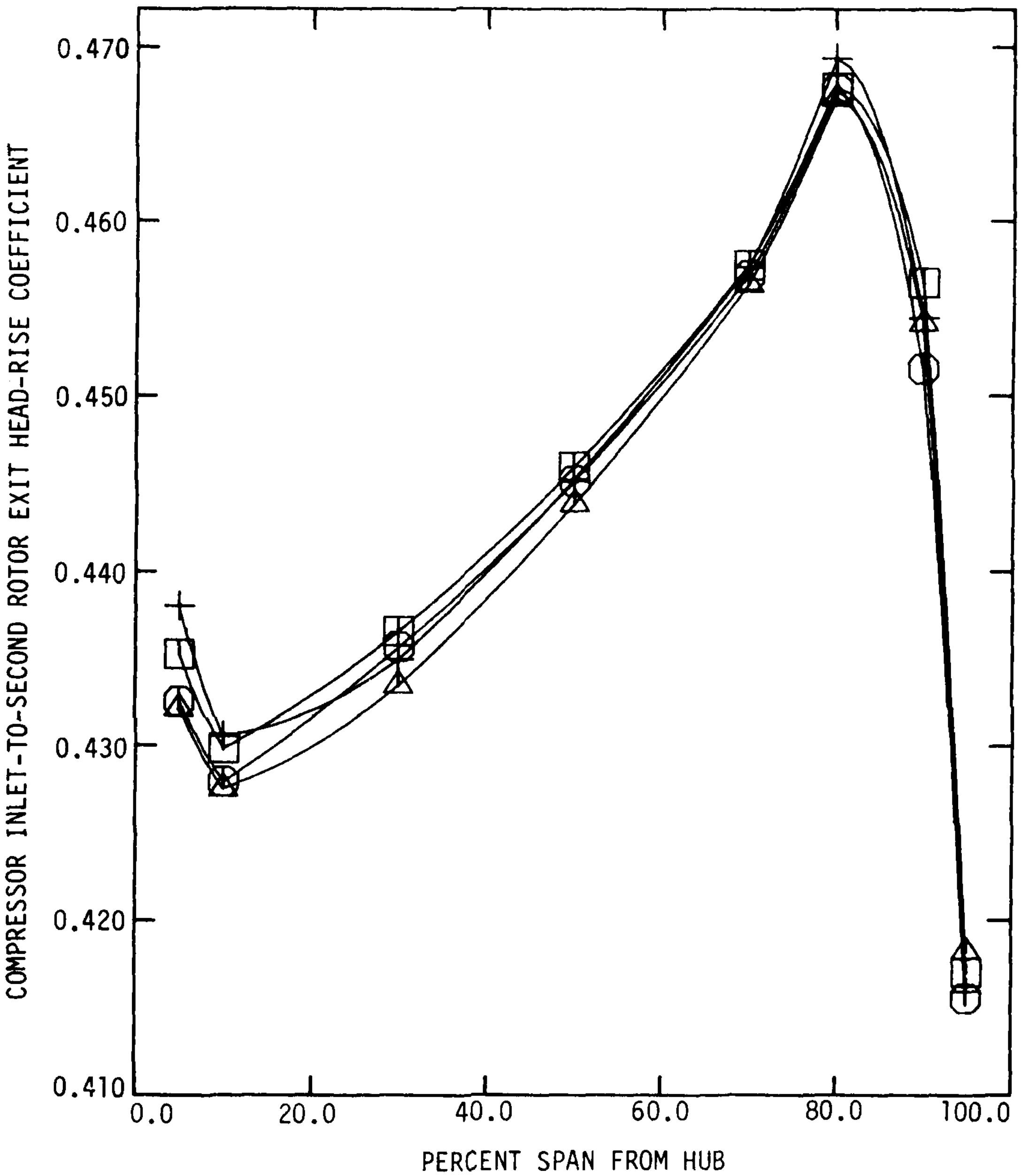

(c) COMPRESSOR INLET-TO-SECOND ROTOR EXIT HEAD-RISE

Figure 4.24 continued.

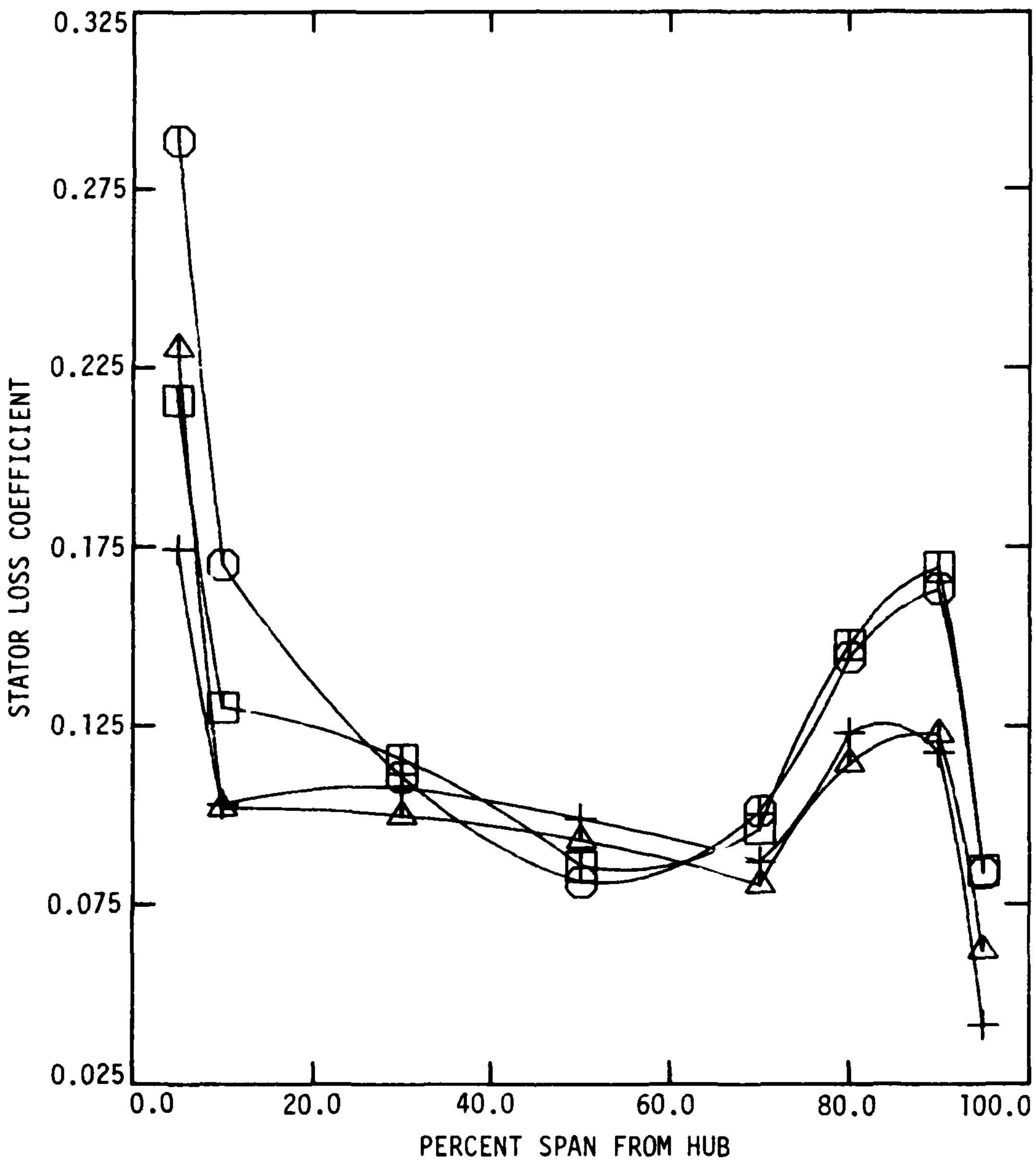

(d) STATOR LOSS

Figure 4.24 continued.

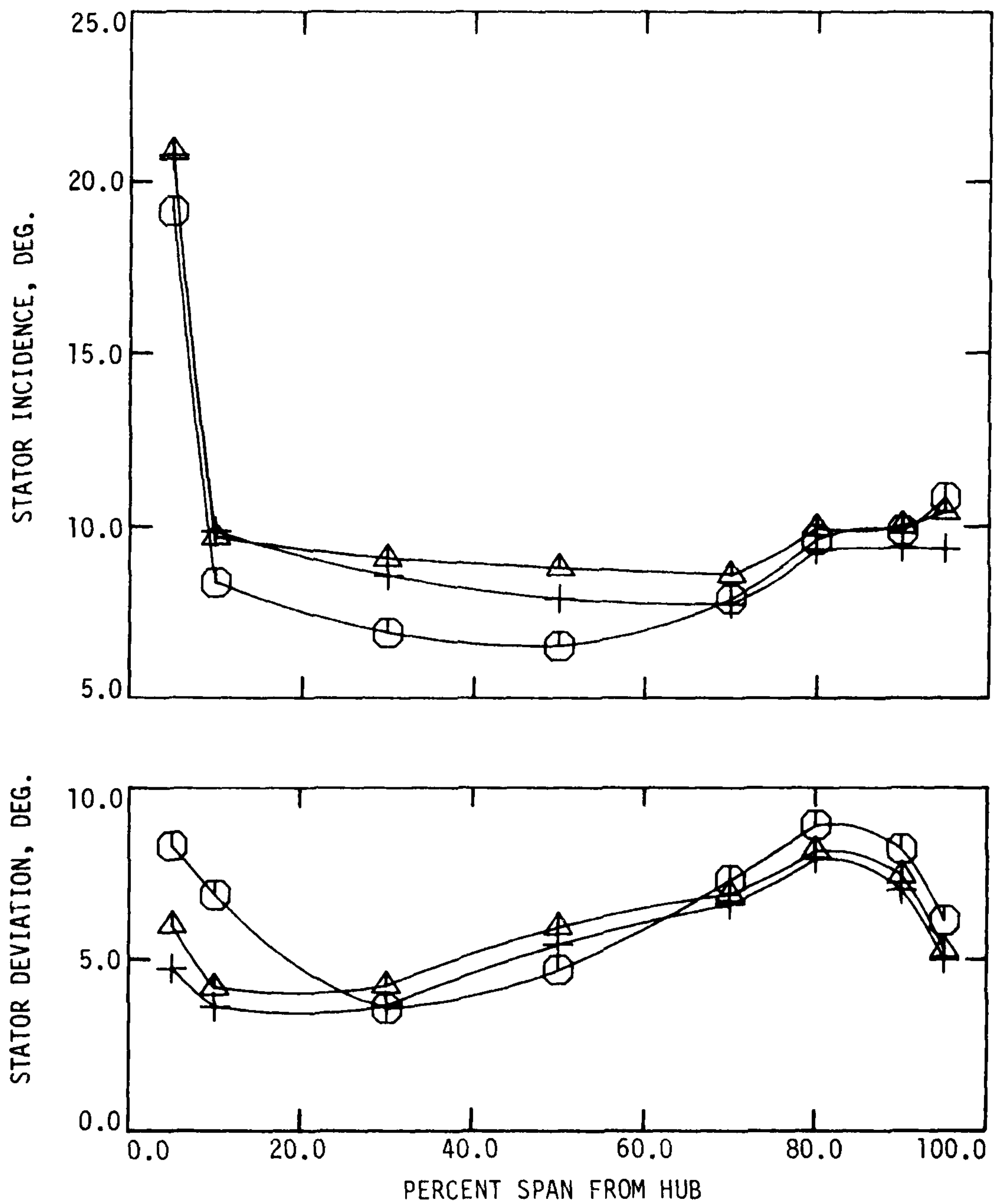

(e) STATOR INCIDENCE AND DEVIATION

Figure 4.24 concluded.

rotor head-rise curves in Figure 4.24(a) clearly verifies this relationship. Figure 4.24(c) can also be compared with Figure 4.20(a) to show the similarity in the first and second rotor exit total-head spanwise distributions, while also demonstrating the tendency of the second rotor row to compensate for variations in the spanwise distribution of total head at its inlet.

Second rotor exit total-head contour maps are presented in Figure 4.25. These maps demonstrate the general similarity of flow at the second rotor exit for the different builds, and confirm the trend indicated in Figure 4.24(c).

The second stage head-rise curves shown in Figure 4.24(b) contain a combination of second rotor and second stator performance information, and for that reason are difficult to analyze. Fortunately, it is not necessary to analyze these stage curves since enough useful information is obtained from an analysis of the second rotor and second stator flows. However, the stage curves do provide a comparison of the second stage head-rise performance. As is apparent by inspection of Figure 4.24(b), the two modified builds perform better in second stage head-rise than the two baseline builds over almost the entire span. The large differences between all four builds near the hub indicate that the second stator hub modifications decrease the near-hub losses considerably. This is clarified in some detail with the second stator loss curves (Figure 4.24(d)).

Curves showing the overall head-rise of the compressor for the different builds are presented in Figure 4.26. These curves are also closely related to the second stator loss curves. This follows

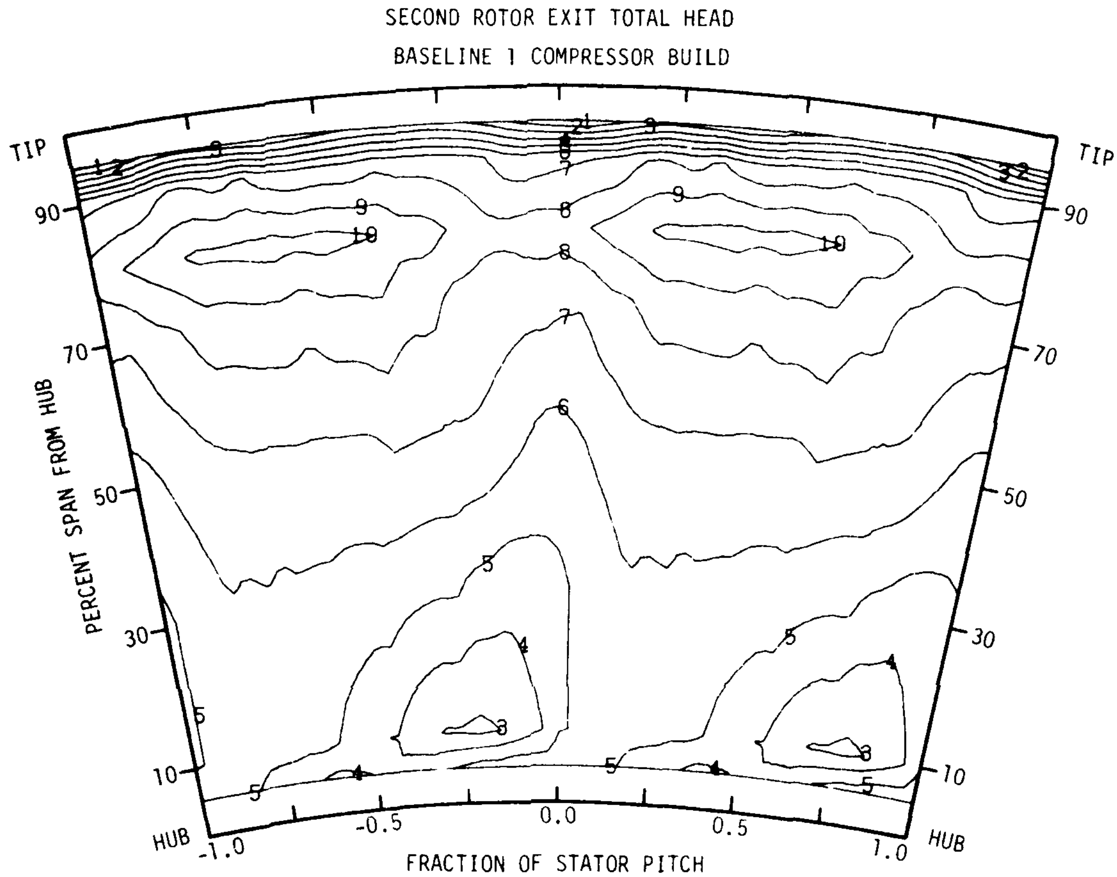

CURVE LABEL	CURVE VALUE (N-M/KG)
1	1050
2	1070
3	1090
4	1110
5	1130
6	1150
7	1170
8	1190
9	1210
10	1230

Figure 4.25 Second rotor exit total-head contour maps for each compressor build (ϕ = 0.500).

SECOND ROTOR EXIT TOTAL HEAD
BASELINE 2 COMPRESSOR BUILD

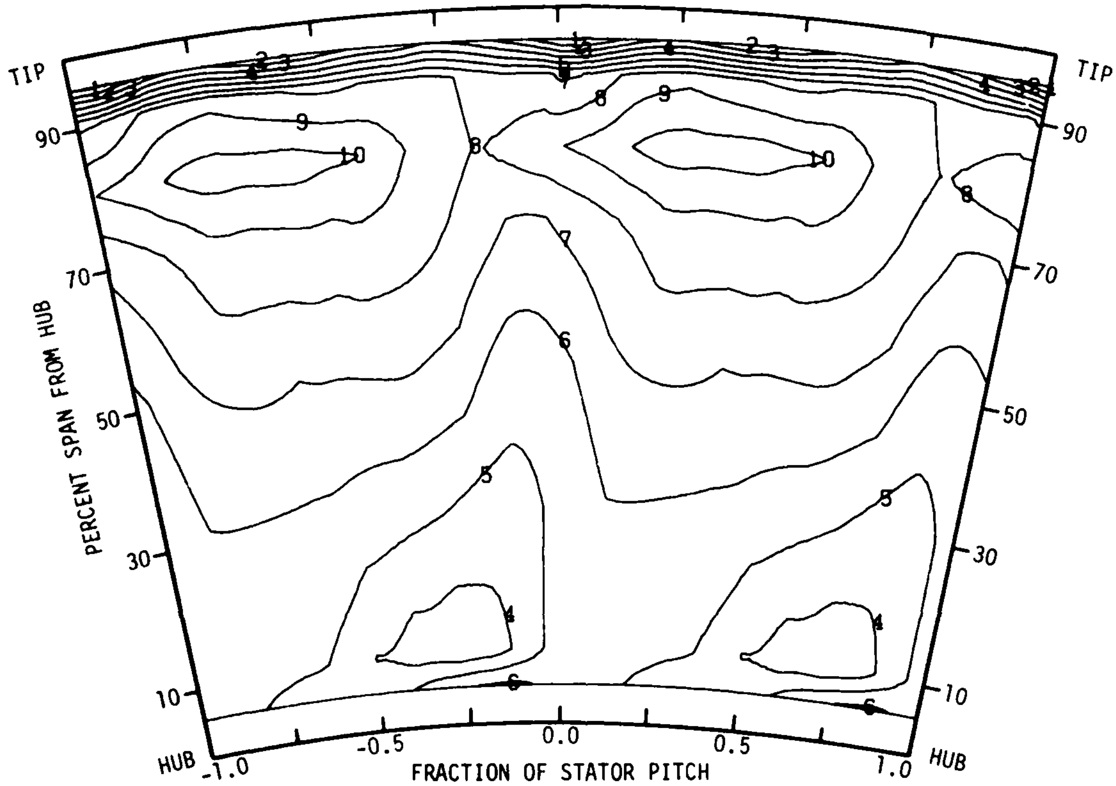

CURVE LABEL	CURVE VALUE (N-M/KG)
1	1050
2	1070
3	1090
4	1110
5	1130
6	1150
7	1170
8	1190
9	1200
10	1230

Figure 4.25 continued.

SECOND ROTOR EXIT TOTAL HEAD
MODIFIED 1 COMPRESSOR BUILD

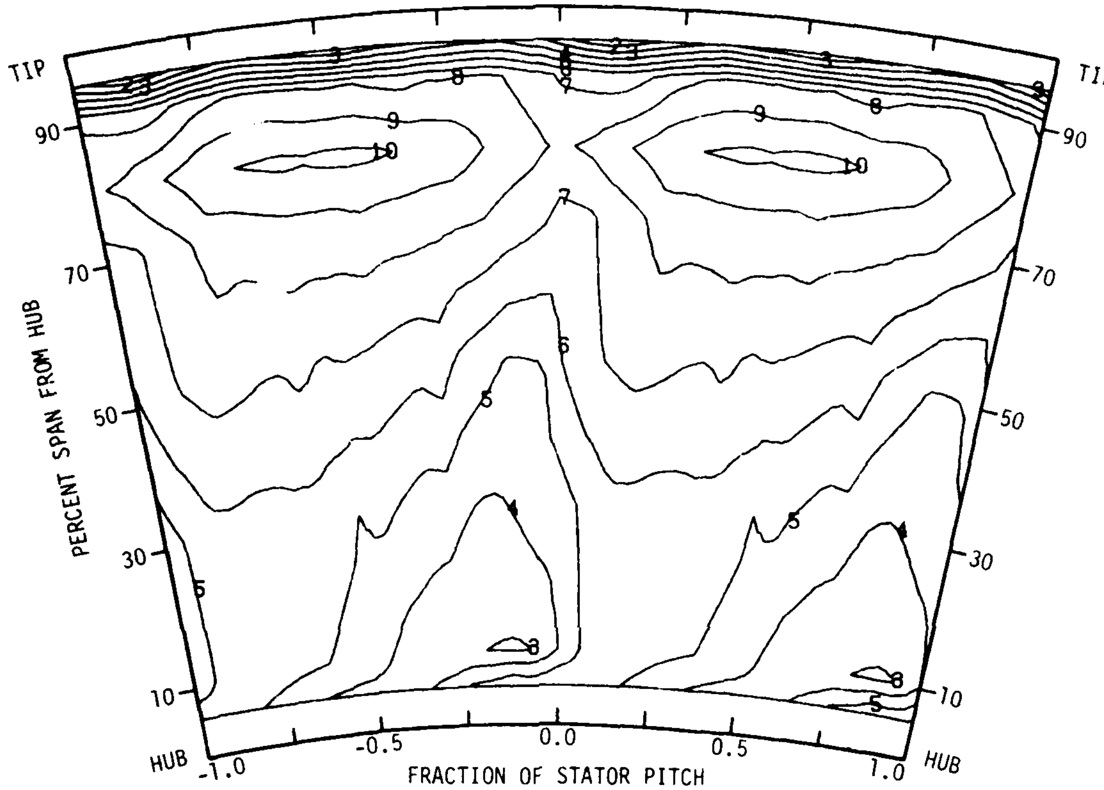

CURVE LABEL	CURVE VALUE (N-M/KG)
2	1070
3	1090
4	1110
5	1130
6	1150
7	1170
8	1190
9	1210
10	1230

Figure 4.25 continued.

SECOND ROTOR EXIT TOTAL HEAD

MODIFIED 2 COMPRESSOR BUILD

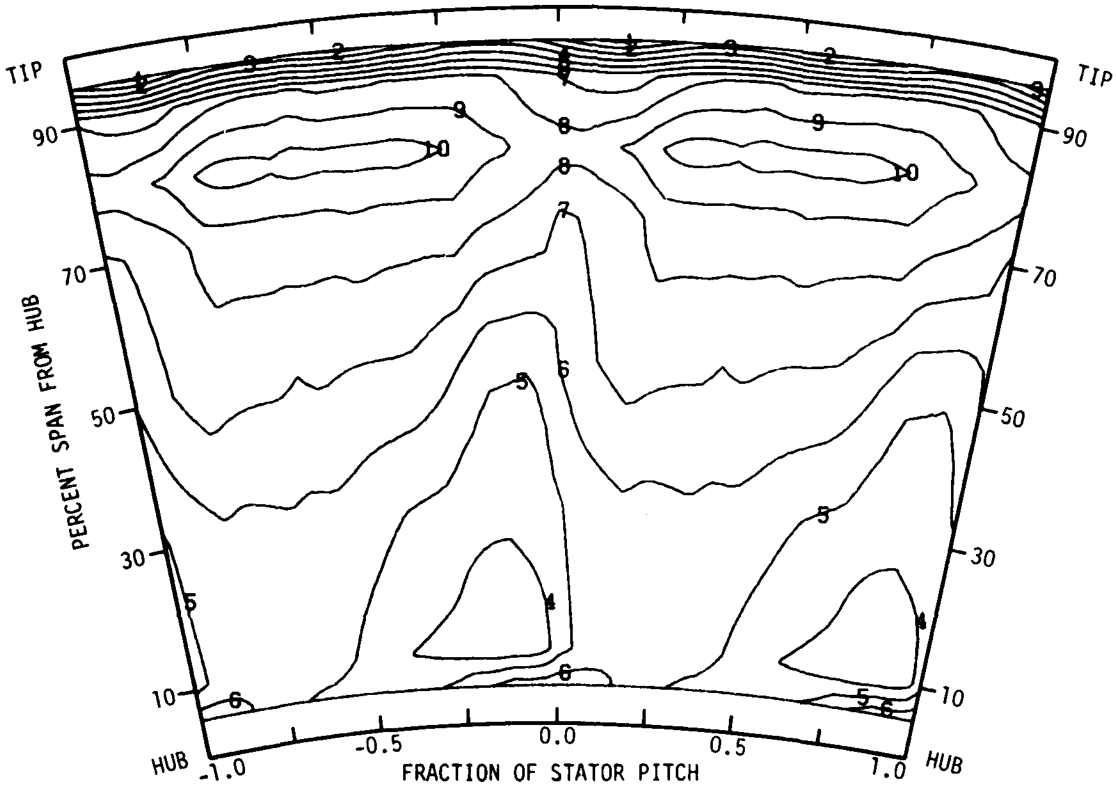

CURVE LABEL	CURVE VALUE (N-M/KG)
1	1050
2	1070
3	1090
4	1110
5	1130
6	1150
7	1170
8	1190
9	1210
10	1230

Figure 4.25 concluded.

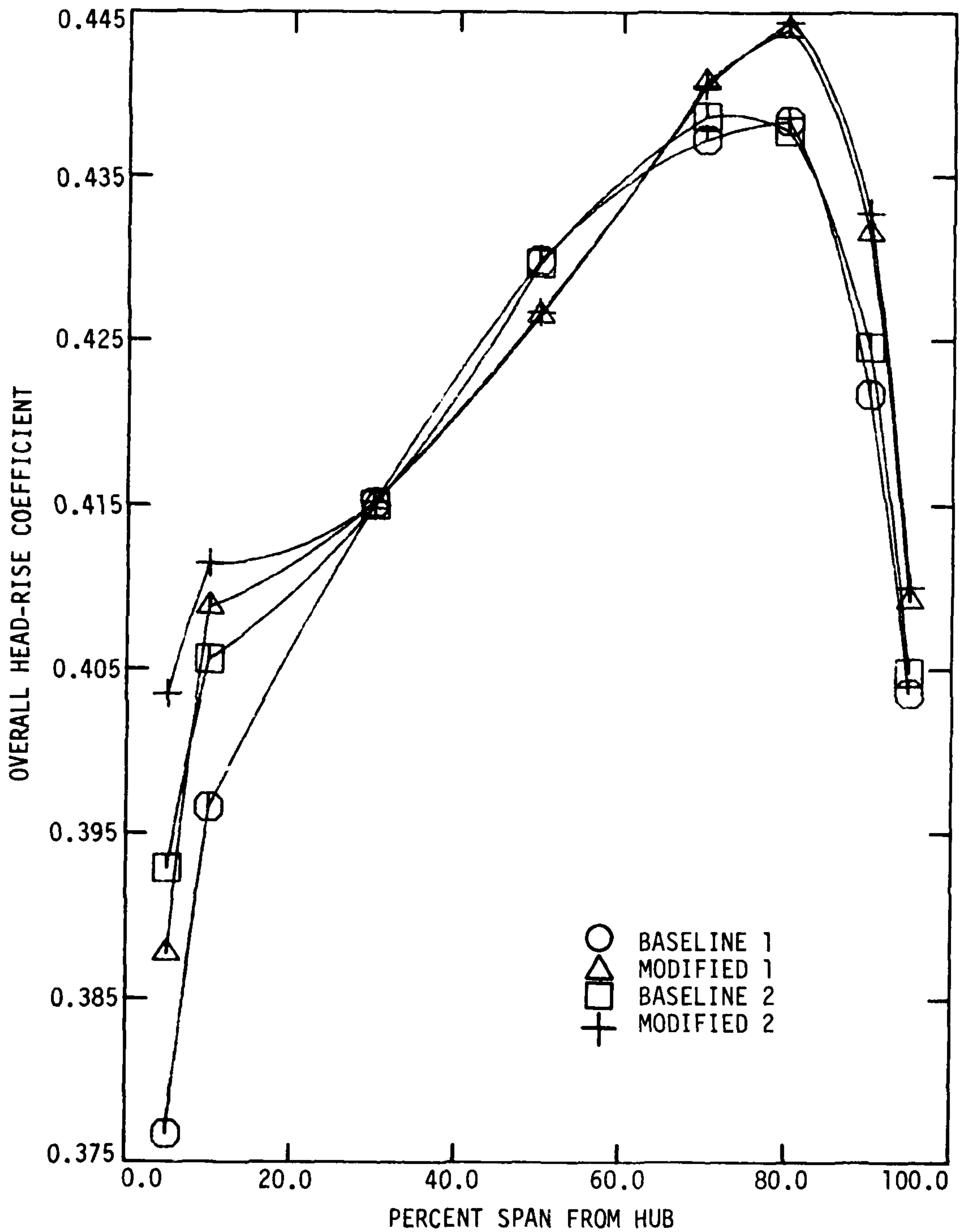

Figure 4.26 Spanwise distribution of circumferential-mean overall head-rise coefficients for the different compressor builds ($\phi = 0.500$).

from the similarity of all build spanwise distributions of second rotor exit total-head as shown in Figure 4.24(c).

The second stator loss curves in Figure 4.24(d) show significant differences in end-wall region loss performance between the different builds. Baseline 1 and 2 and modified 1 and 2 stator data differences from 30% to 90% span from the hub are not considered significant. The significant differences can be summarized as follows:

- The modified stator loss is substantially less than the baseline stator loss from 80% to 95% span from the hub, and also at 10% span from the hub.
- The modified stator loss is somewhat less than the baseline stator loss at 30% and 70% span from the hub, and somewhat greater at 50% span from the hub.
- The modified 2 build stator loss is substantially less than the modified 1 build stator loss at 5% and 95% span from the hub.
- The baseline 2 build stator loss is substantially less than the baseline 1 build stator loss at 5% and 10% span from the hub.

The second stator exit total-head contour maps for the different builds are presented separately in Figure 4.27. In Figure 4.28, second stator exit total-head contour maps are overlayed for more effective comparison of flow-field differences for the different builds. Specifically, Figure 4.28(a) compares the baseline 1 and modified 1 builds, Figure 4.28(b) compares the baseline 1 and 2 builds, and Figure 4.28(c) compares the modified 1 and 2 builds.

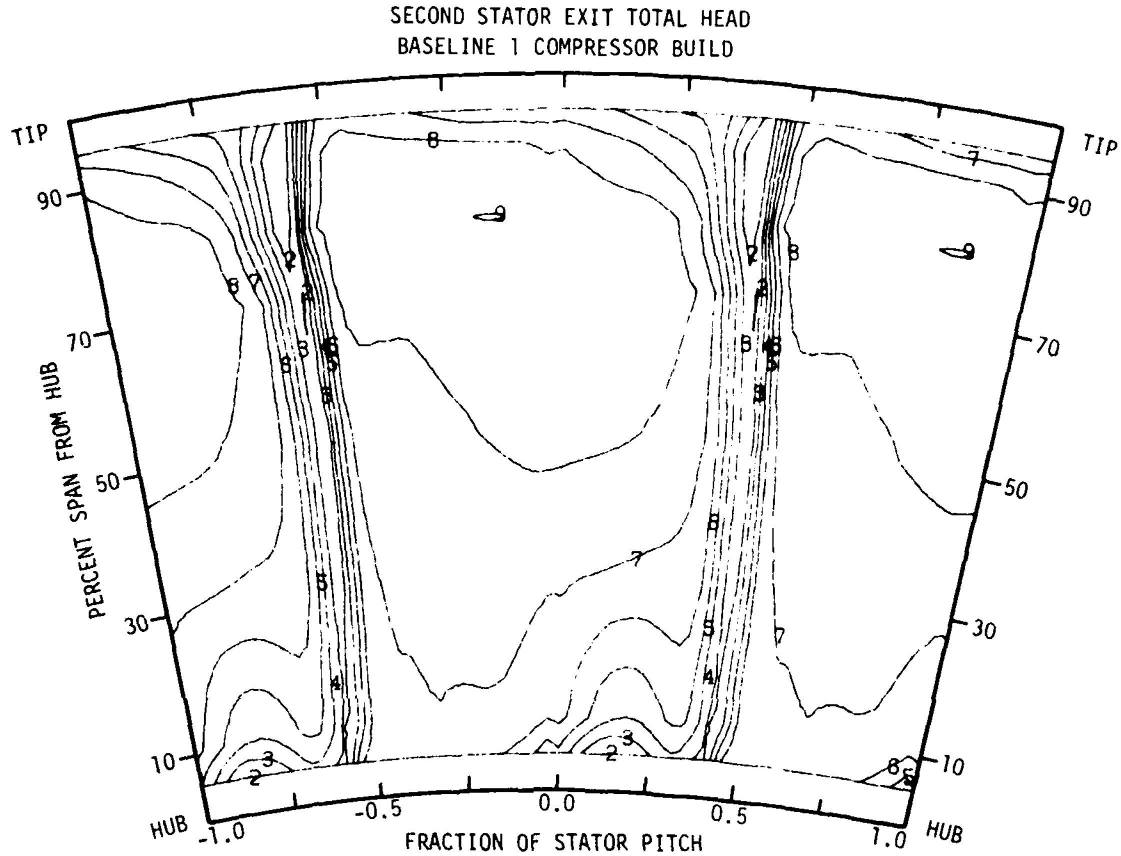

CURVE LABEL	CURVE VALUE (N-M/KG)
2	850
3	900
4	950
5	1000
6	1050
7	1100
8	1150
9	1200

Figure 4.27 Second stator exit total-head contour maps for each compressor build ($\phi = 0.500$).

SECOND STATOR EXIT TOTAL HEAD
BASELINE 2 COMPRESSOR BUILD

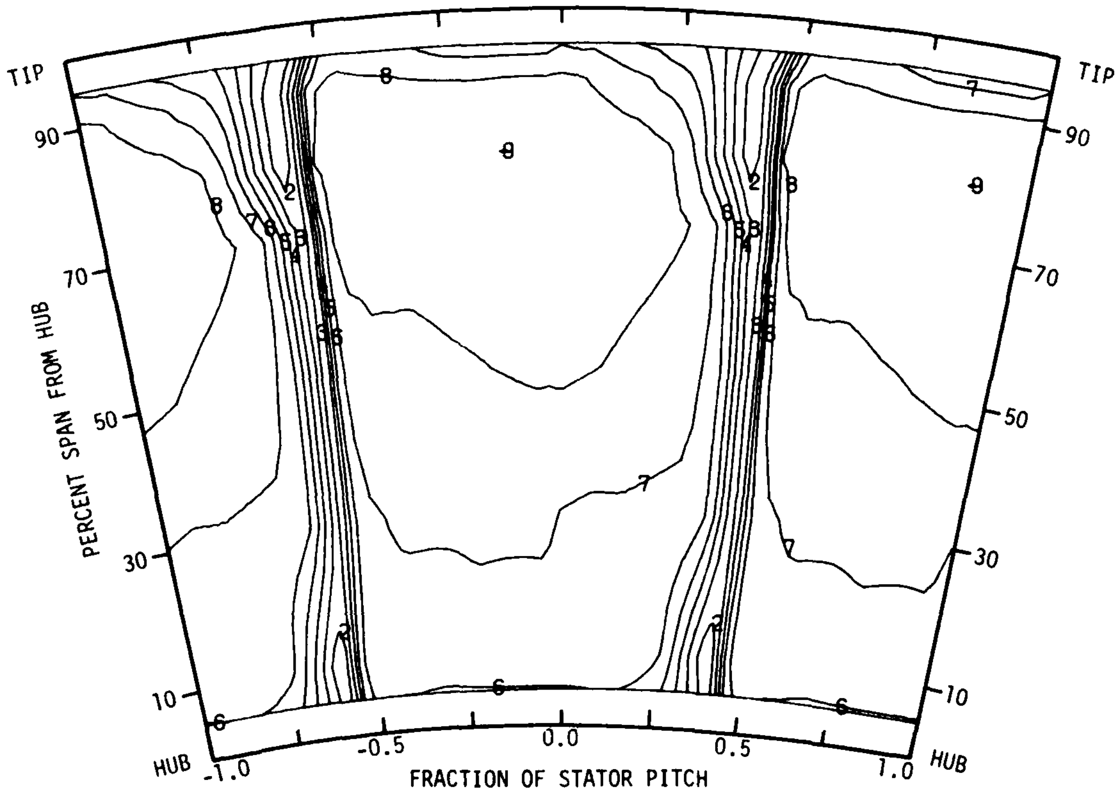

CURVE LABEL	CURVE VALUE (N-M/KG)
2	850
3	900
4	950
5	1000
6	1050
7	1100
8	1150
9	1200

Figure 4.27 continued.

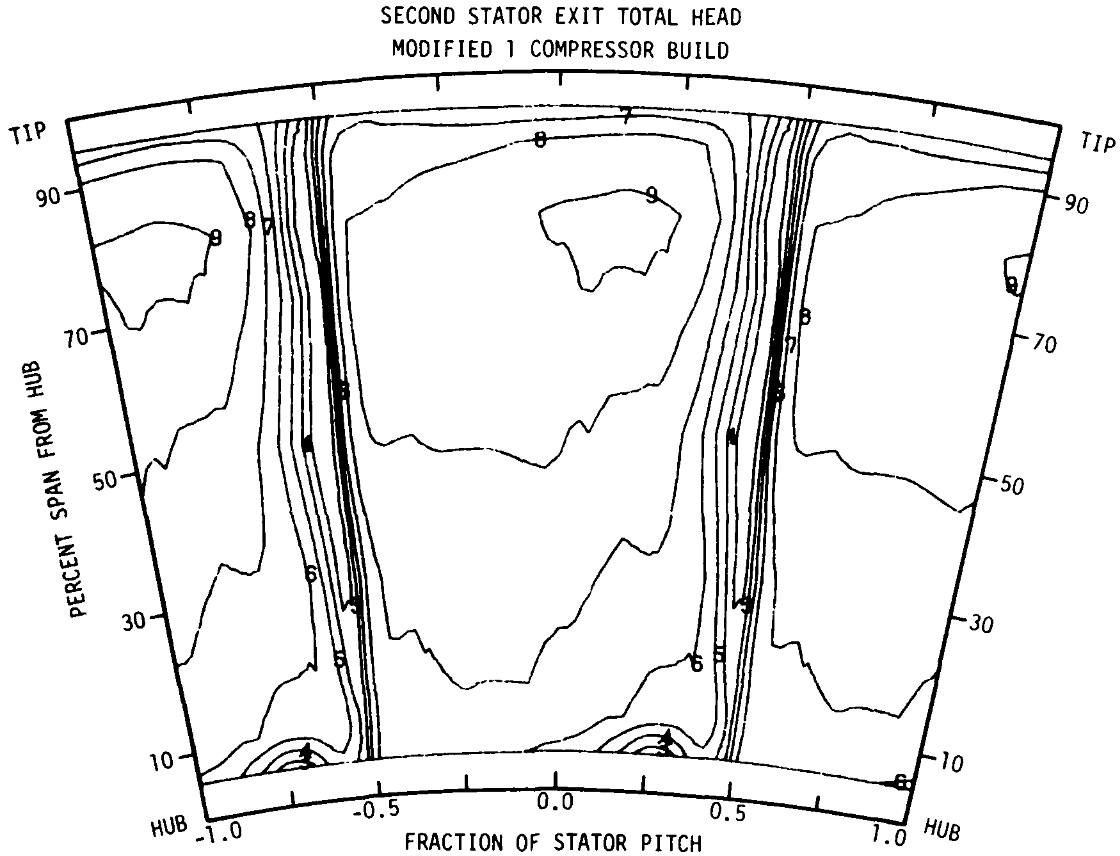

CURVE LABEL	CURVE VALUE (N-M/KG)
3	900
4	950
5	1000
6	1050
7	1100
8	1150
9	1200

Figure 4.27 continued.

SECOND STATOR EXIT TOTAL HEAD

MODIFIED 2 COMPRESSOR BUILD

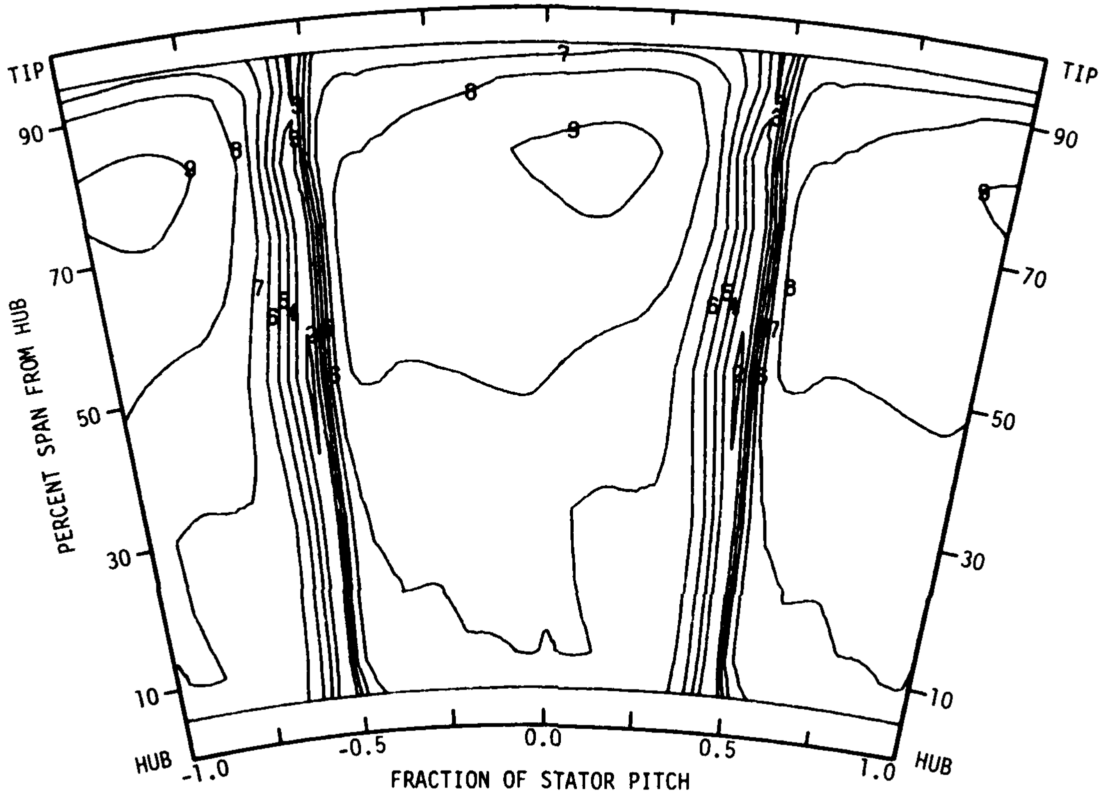

CURVE LABEL	CURVE VALUE (N-M/KG)
2	850
3	900
4	950
5	1000
6	1050
7	1100
8	1150
9	1200

Figure 4.27 concluded.

SECOND STATOR EXIT TOTAL HEAD

BLACK BASELINE 1 BUILD
RED MODIFIED 1 BUILD

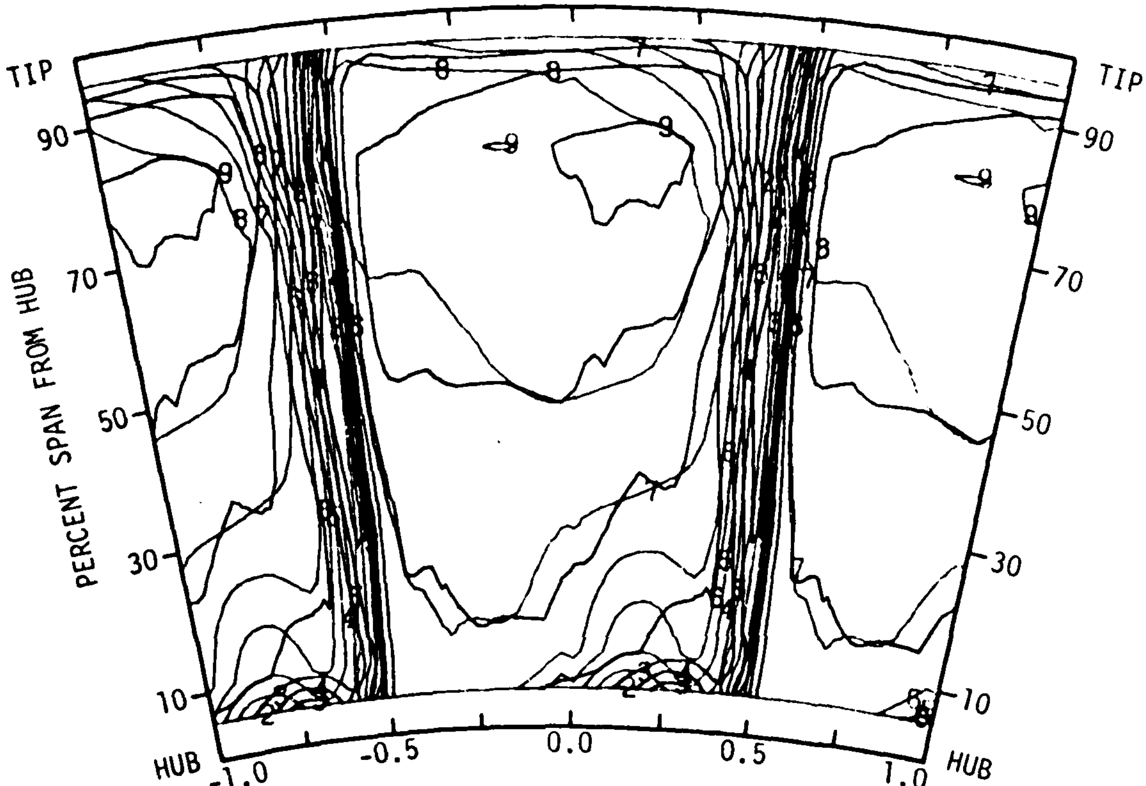

(a) BASELINE 1 AND MODIFIED 1 BUILDS

CURVE LABEL	CURVE VALUE (N-M/KG)
2	850
3	900
4	950
5	1000
6	1050
7	1100
8	1150
9	1200

Figure 4.28 Maps comparing the total-head contours at the second stator exit for the different compressor builds (ϕ = 0.500).

SECOND STATOR EXIT TOTAL HEAD

BLACK BASELINE 1 BUILD
RED BASELINE 2 BUILD

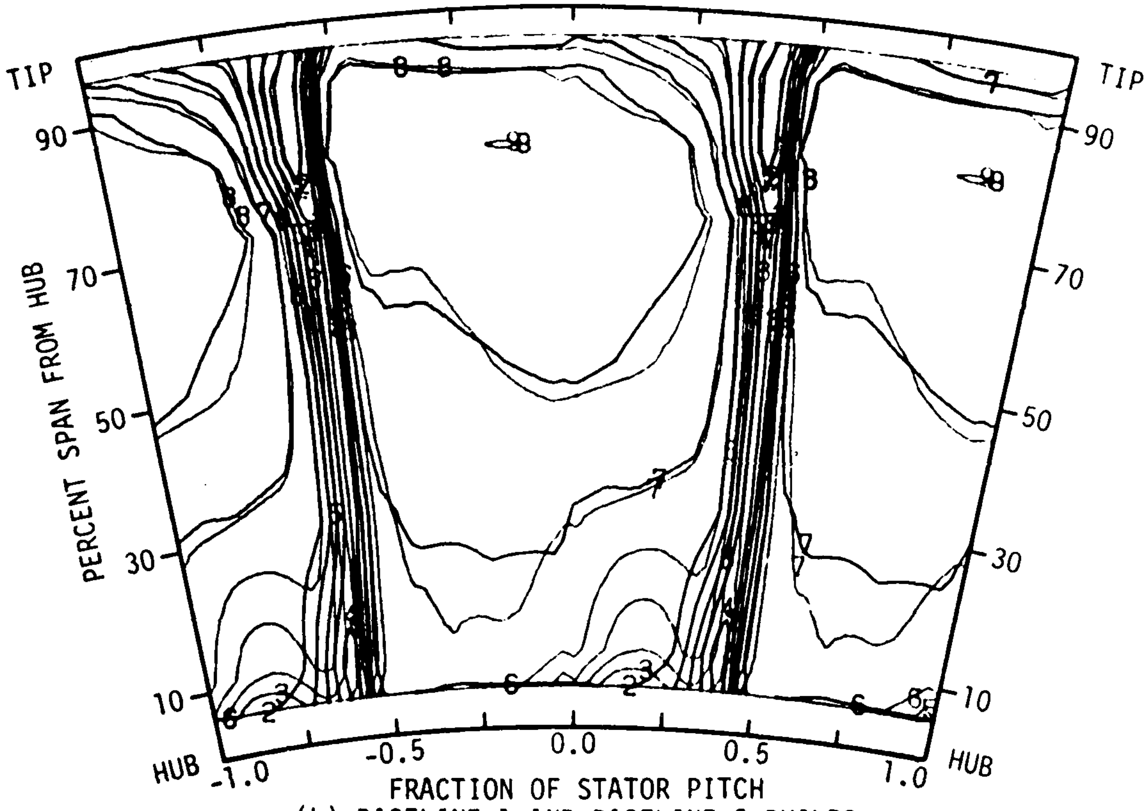

(b) BASELINE 1 AND BASELINE 2 BUILDS

CURVE LABEL	CURVE VALUE (N-M/KG)
2	850
3	900
4	950
5	1000
6	1050
7	1100
8	1150
9	1200

Figure 4.28 continued.

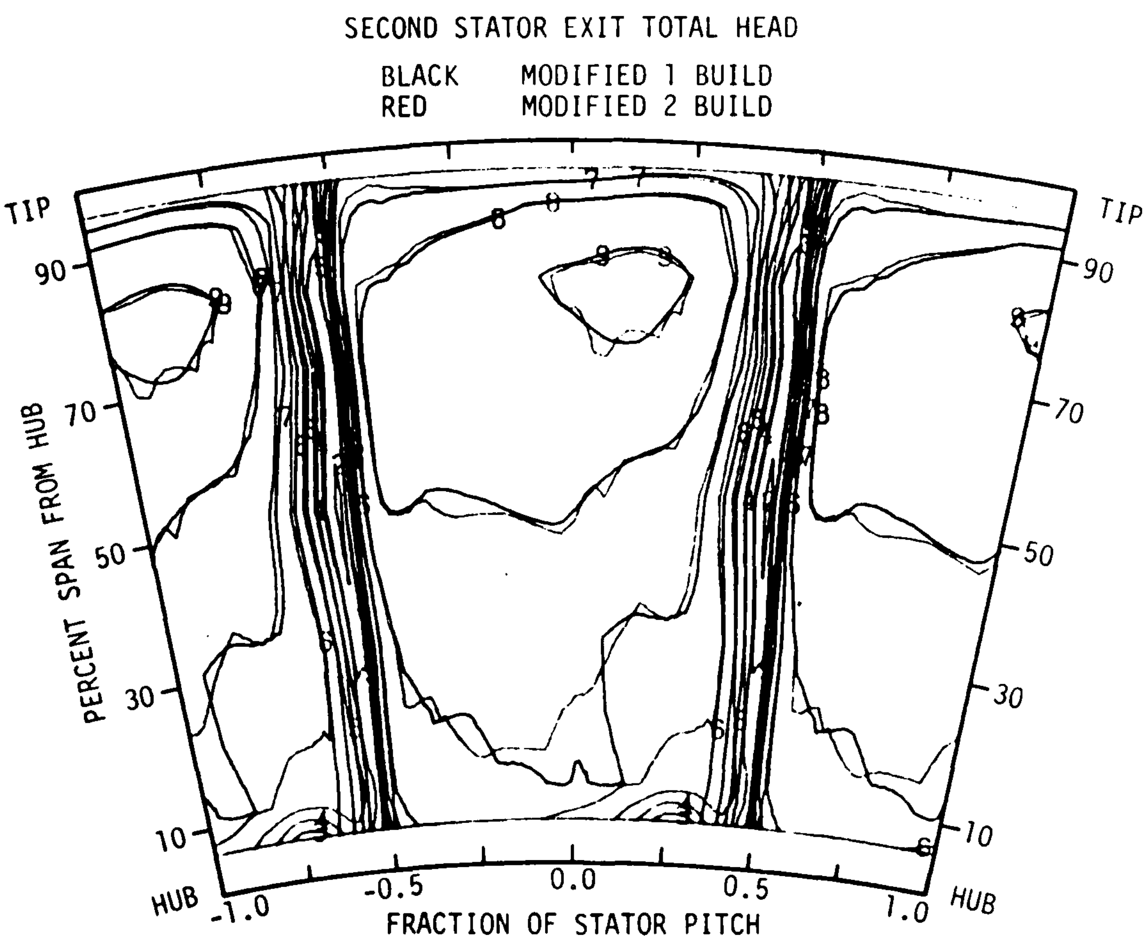

(c) MODIFIED 1 AND MODIFIED 2 BUILDS

CURVE LABEL	CURVE VALUE (N-M/KG)
2	850
3	900
4	950
5	1000
6	1050
7	1100
8	1150
9	1200

Figure 4.28 concluded.

In comparing the second stator exit flow fields for the different builds, it is convenient to divide the field into an outer (mid-span to tip) and an inner (mid-span to hub) flow portion. This is done mainly because the second stator exit outer portion flow field is similar to the first stator exit outer portion flow field for each build pair with a common stator geometry. Most of the baseline/modified differences observed for the first stator outer portion flow field also apply for the second stator, although only qualitatively.

The following characteristics about the second stator exit outer portion flow field and the corresponding second stator loss distributions can be noted:

- The second stator exit baseline/modified stator data differences (Figure 4.28(a)) are significantly larger than those for the first stator exit (Figure 4.23). Correspondingly, the baseline/modified second stator loss differences are larger (Figure 4.24(d)) than those for the first stator (Figure 4.20(c)) from 70% to 95% span.
- The baseline 1 and 2 builds have similar second stator exit outer portion flow fields (Figure 4.28(b)). The corresponding second stator loss distributions are similar (Figure 4.24(d)) from 30% to 95% span.
- The modified 1 and 2 builds have similar second stator exit outer portion flow fields (Figure 4.28(c)). The corresponding second stator loss distributions are similar (Figure 4.24(d)) from 10% to 90% span.

The second stator exit inner portion flow field (mid-span to hub) for the different builds (Figure 4.27) varies considerably. This corresponds to the noticeable variation in near-hub losses observed for the different builds (Figure 4.24(d)). Also, unlike the outer portion flow field, the second stator exit inner portion flow field is very different from that of the first stator. This difference is due to the second stator hub being stationary, while the first stator hub is moving.

The baseline 1 and modified 1 builds both indicate a substantial region of lower-momentum fluid adjacent to the second stator suction surface near the hub. This region was discussed earlier in some detail in section 4.3.1, where it was considered to be a "leakage vortex."

The following conclusions about the second stator exit inner portion flow field and the corresponding second stator loss distributions can be noted:

- The baseline 1 build leakage vortex is substantially larger than that of the modified 1 build (Figure 4.28(a)). Correspondingly, the baseline 1 build second stator loss is substantially greater than that of the modified 1 build at 5% and 10% span from the hub (Figure 4.24(d)).
- The baseline 2 and modified 2 builds eliminate the leakage vortex (Figure 4.28(b) and (c)). Correspondingly, the baseline 2 build second stator loss is substantially less than that of the baseline 1 build at 5% and 10% span from the hub. Similar loss behavior is seen for the modified 2

and modified 1 builds, but only at 5% span from the hub (Figure 4.24(d)).

- The baseline 2 and modified 2 build second stator wakes are approximately symmetrical about the mid-span. The baseline 2 build second stator wake is narrow over the mid-span and flairs out on its suction side near the hub and tip. Conversely, the modified 2 build second stator wake is relatively wide on its suction side over the mid-span and becomes narrower near the hub and tip (Figure 4.27). Correspondingly, the baseline 2 build second stator loss is less than that for the modified 2 build at mid-span, and is greater than that for the modified 2 build near the hub and tip (Figure 4.24(d)).

The second stator incidence and deviation results (Figure 4.24(e)) are similar to those for the first stator. Thus, most first stator comments made earlier apply again.

4.4.1.3. First/Second Stage Performance Comparison

Graphs useful for comparison of first and second stage performance data are provided in this subsection. The graphs are arranged into three groups:

1. Conventional head-rise and stator-related performance data in Figure 4.29
2. Ideal head-rise and rotor-related performance data in Figure 4.30
3. Hydraulic efficiency data in Figure 4.31

Most of these figures are not discussed, but are included for completeness and possible future reference.

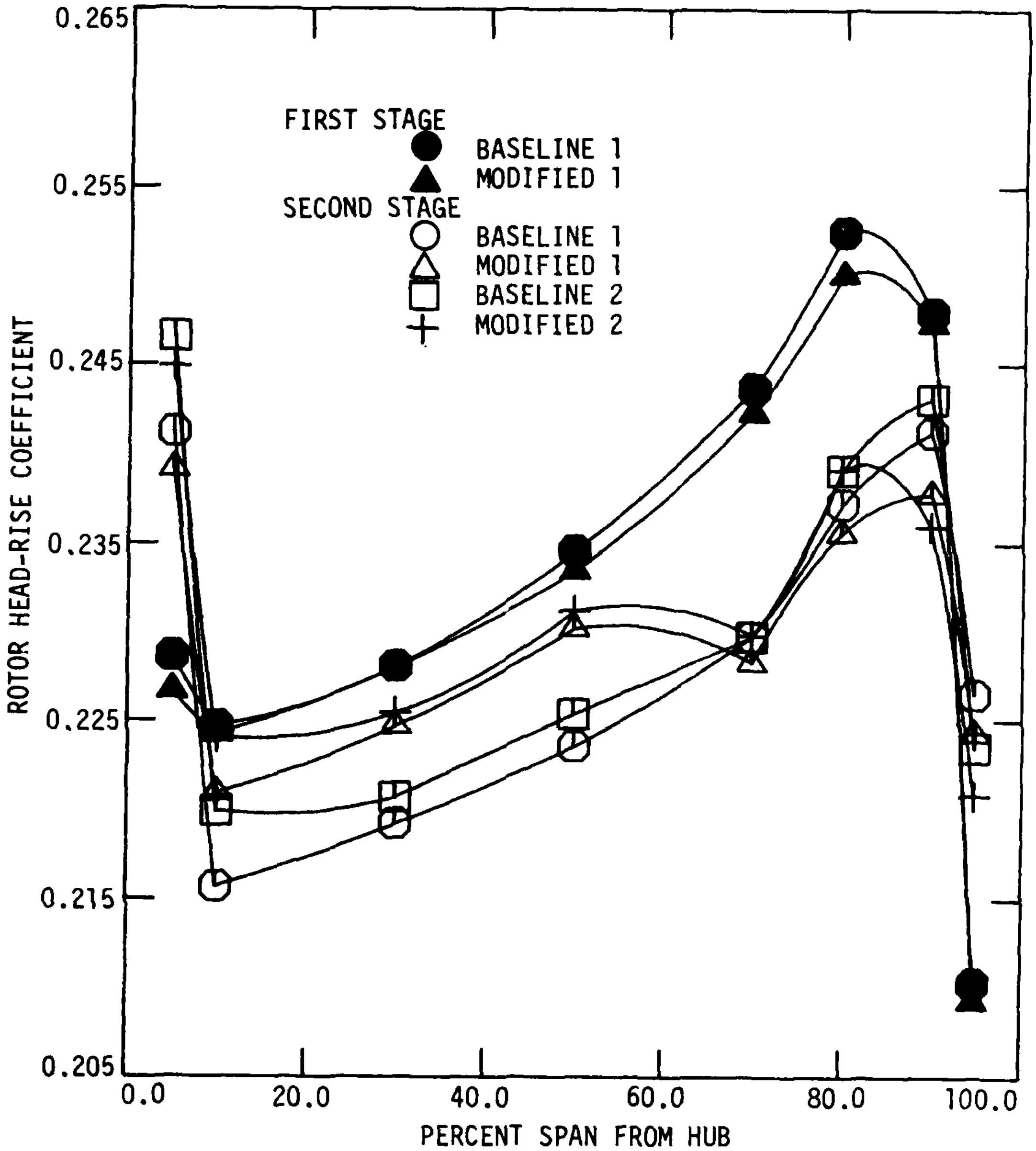

(a) ROTOR HEAD-RISE

Figure 4.29 Spanwise comparison between first and second stage circumferential-mean performance parameters for the different compressor builds (ϕ = 0.500).

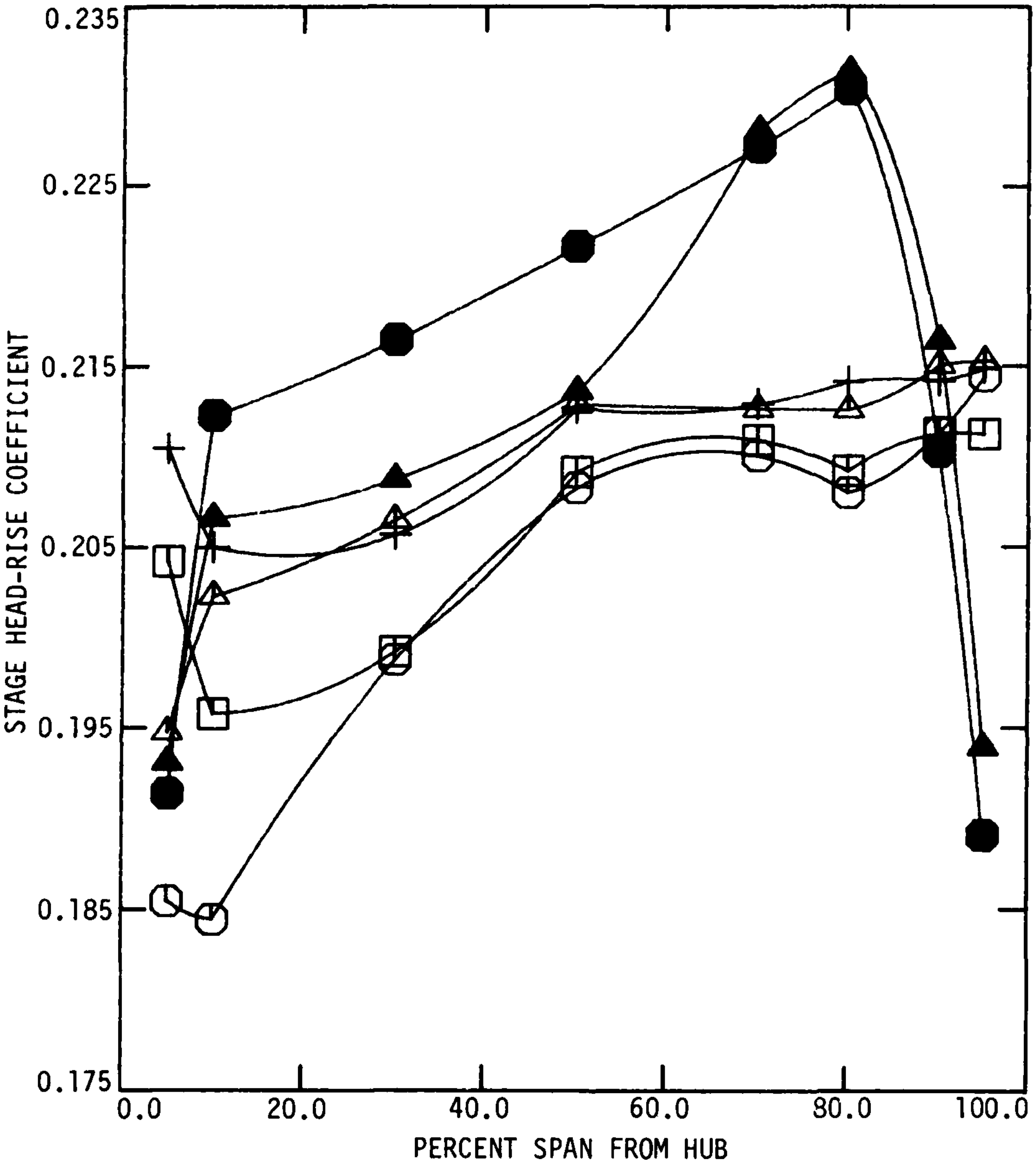

(b) STAGE HEAD-RISE

Figure 4.29 continued.

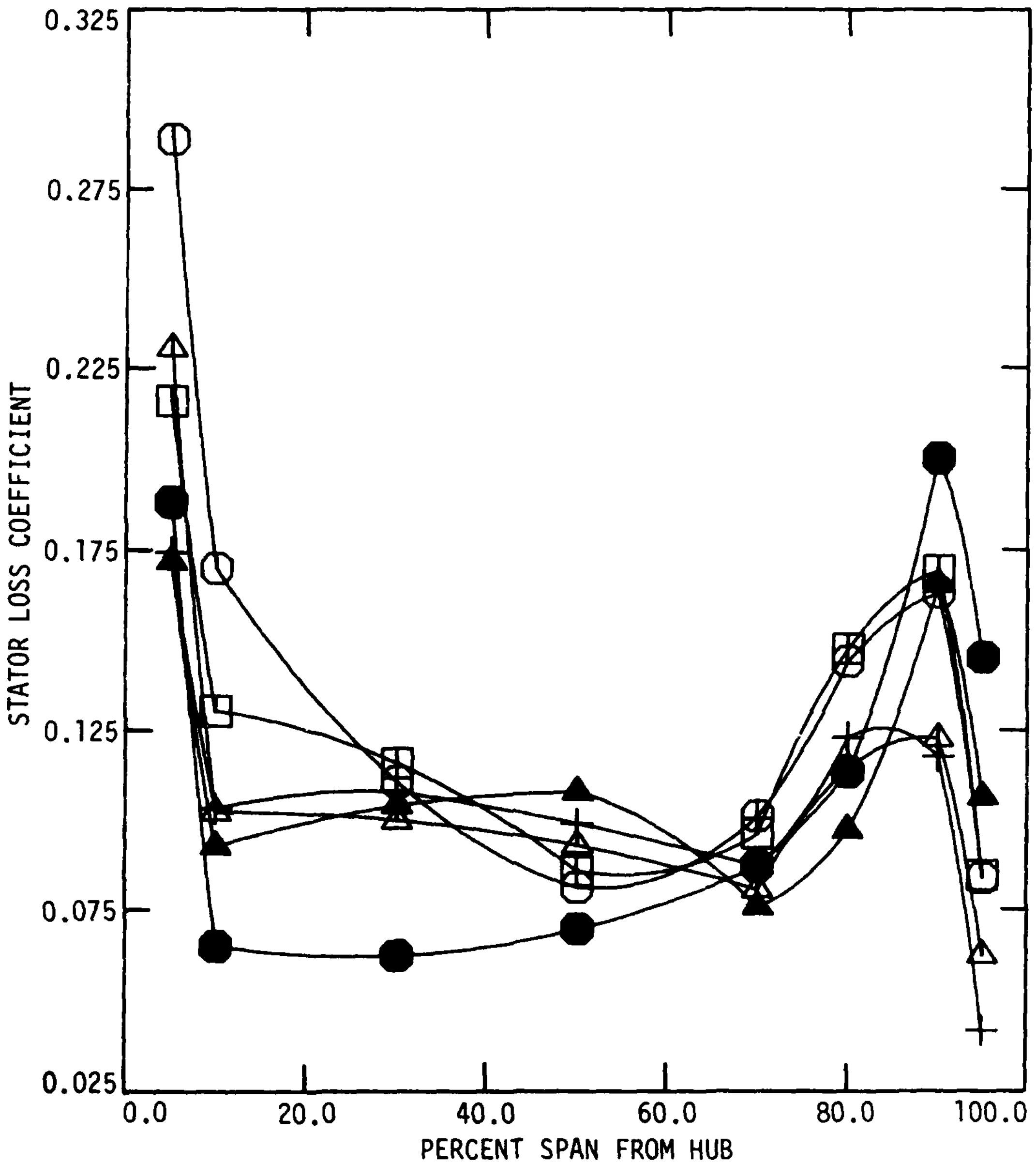

(c) STATOR LOSS

Figure 4.29 continued.

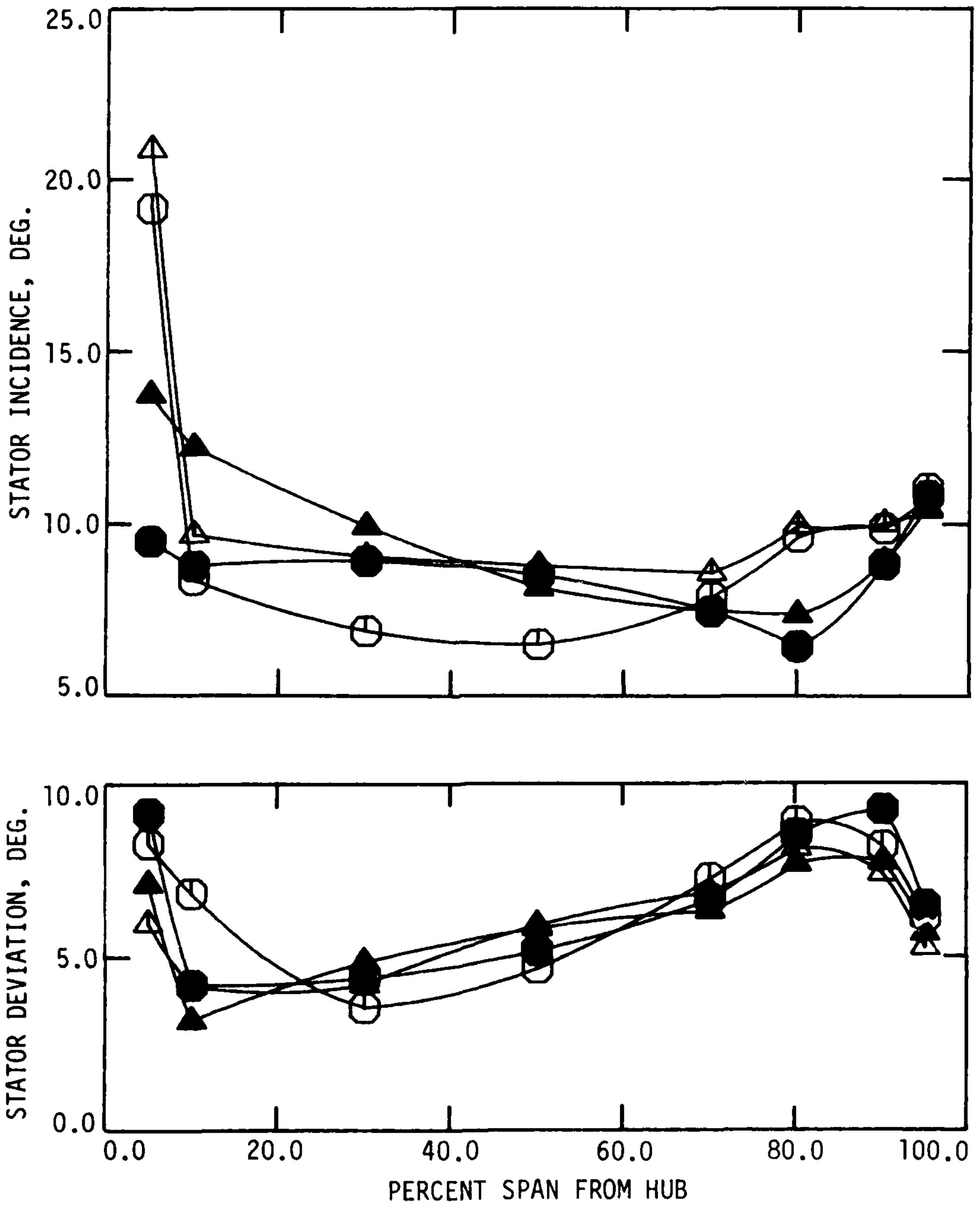

(d) STATOR INCIDENCE AND DEVIATION

Figure 4.29 continued.

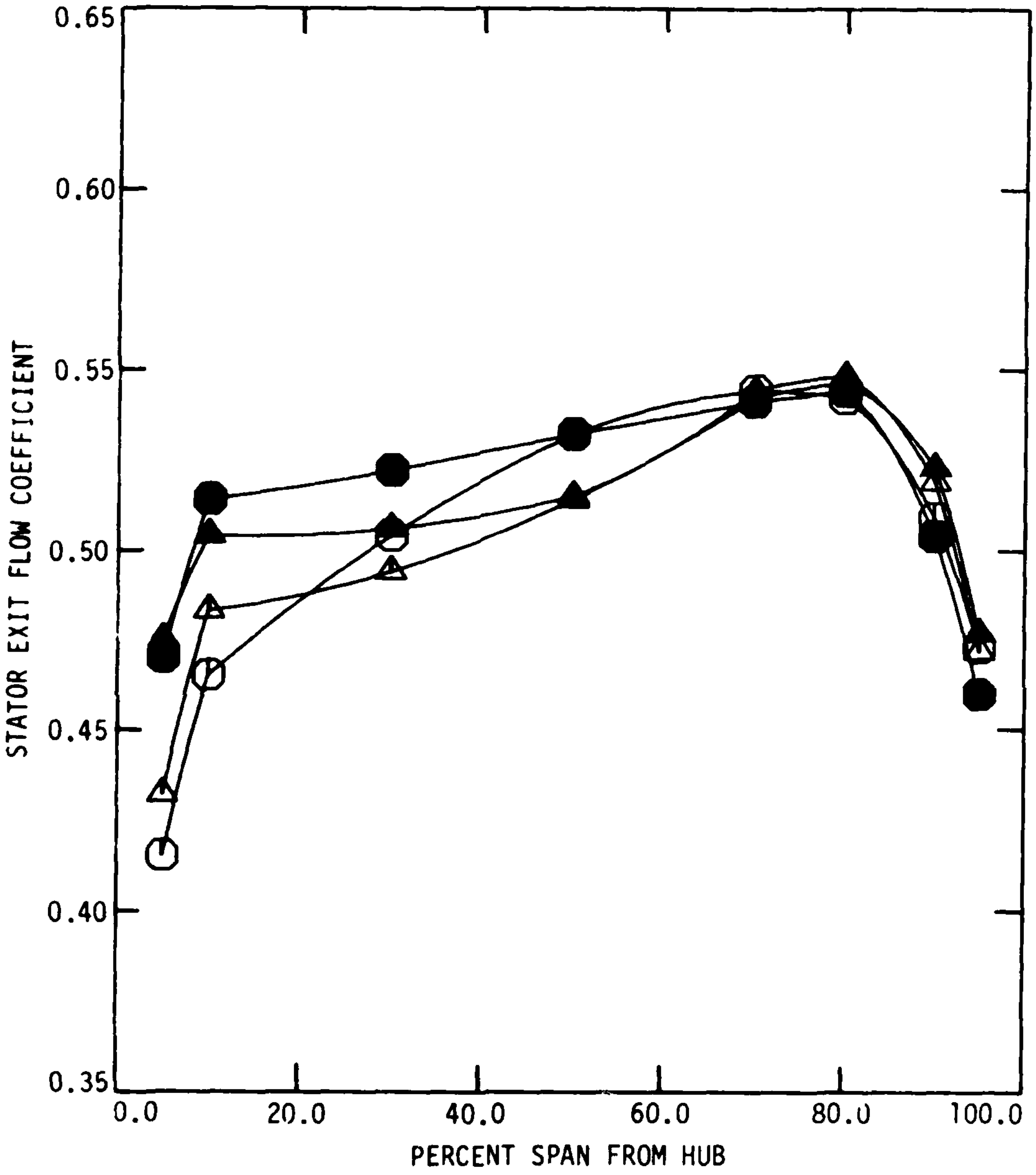

(e) STATOR EXIT FLOW COEFFICIENT

Figure 4.29 concluded.

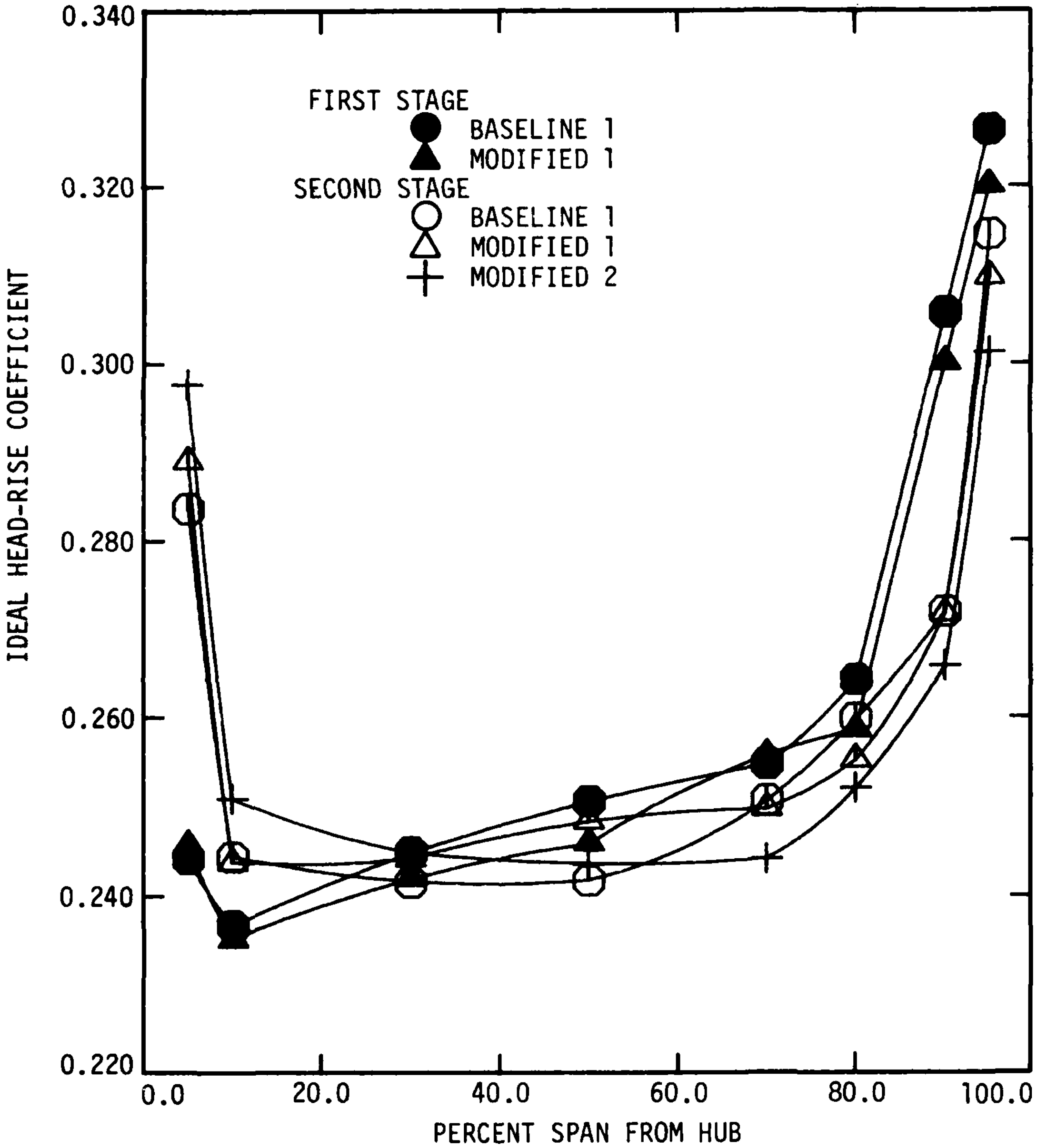

(a) IDEAL HEAD-RISE

Figure 4.30 Spanwise distribution of circumferential-mean rotor performance parameters for the different compressor builds ($\phi = 0.500$).

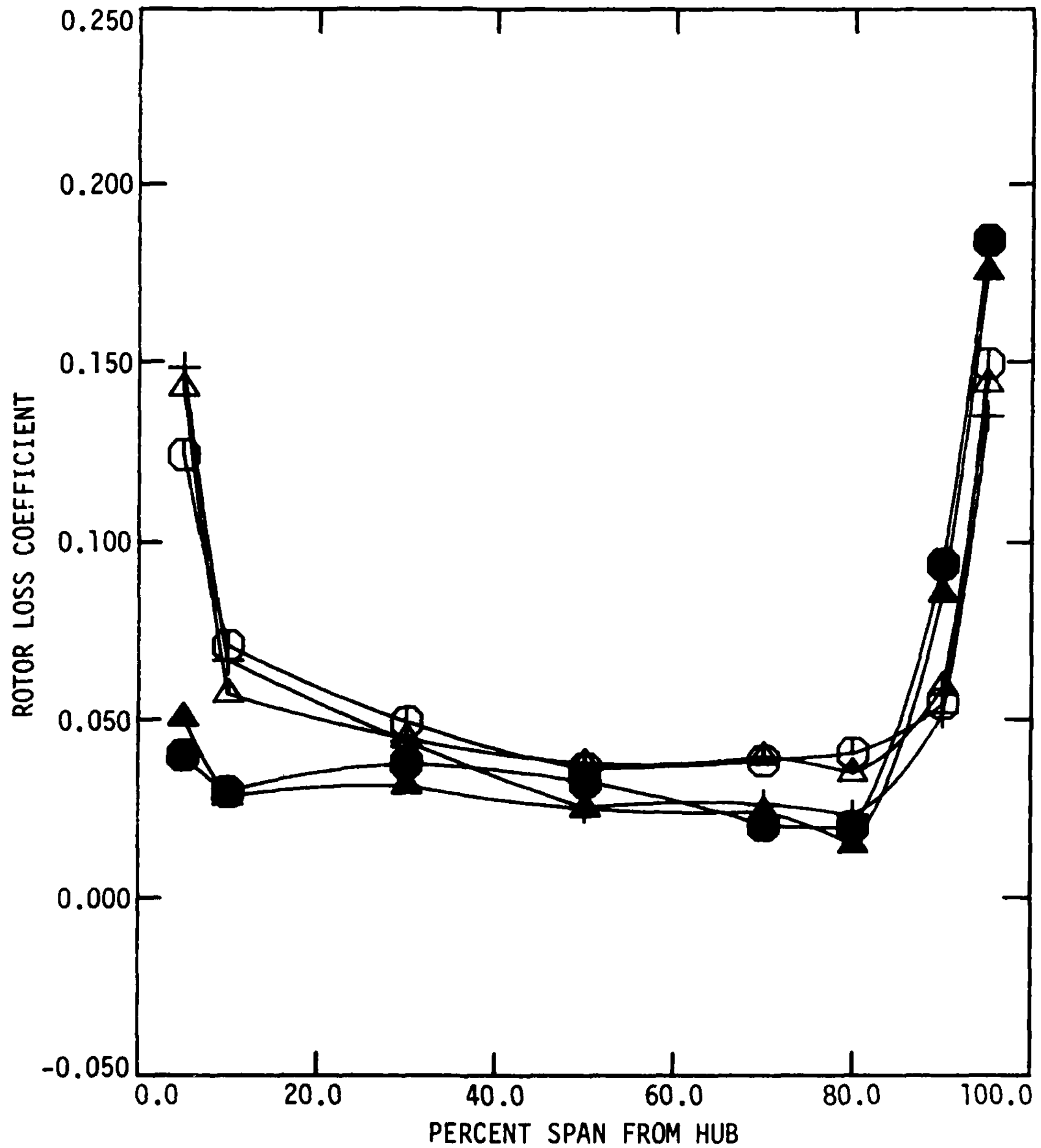

(b) ROTOR LOSS

Figure 4.30 continued.

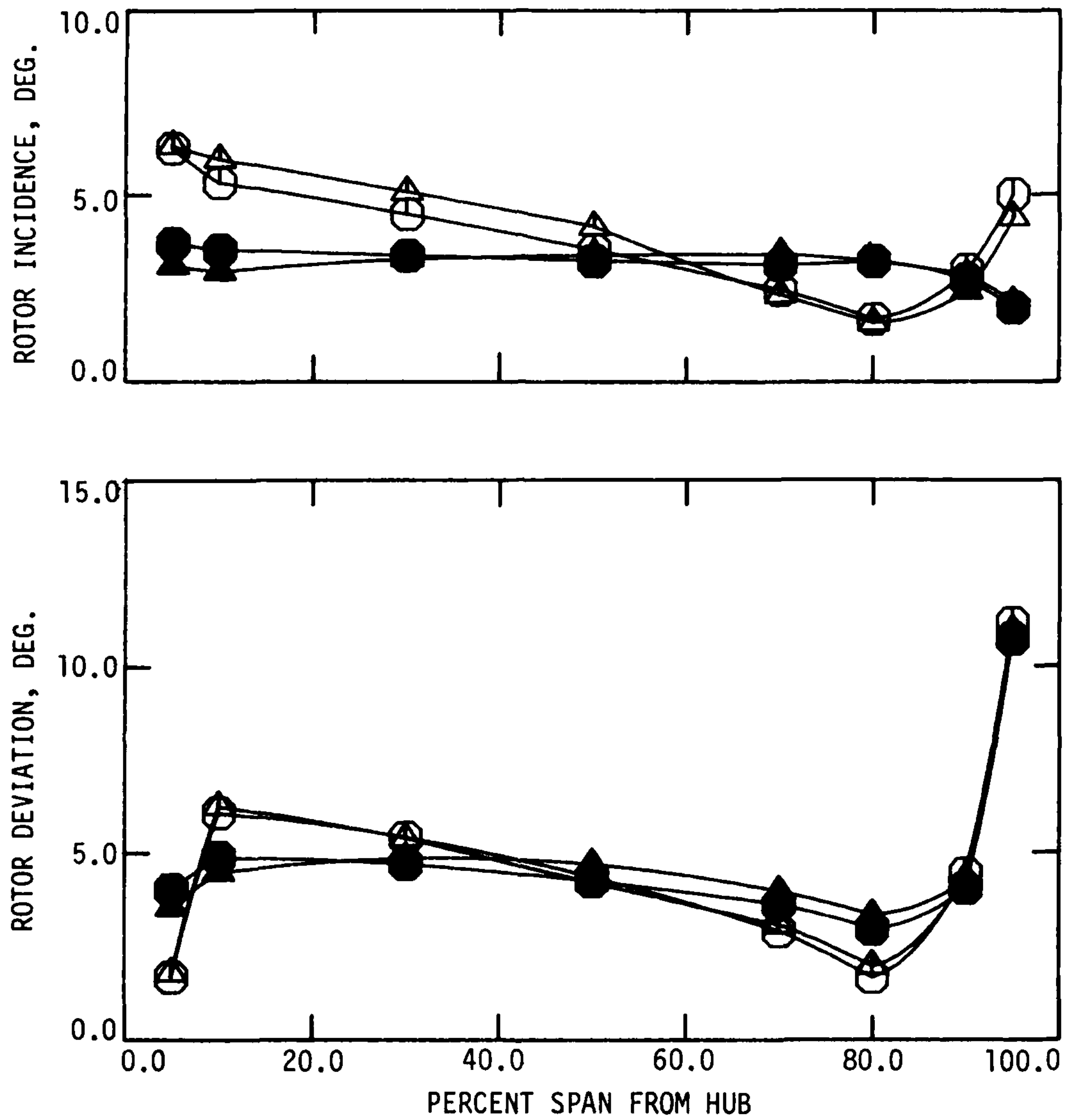

(c) ROTOR INCIDENCE AND DEVIATION

Figure 4.30 continued.

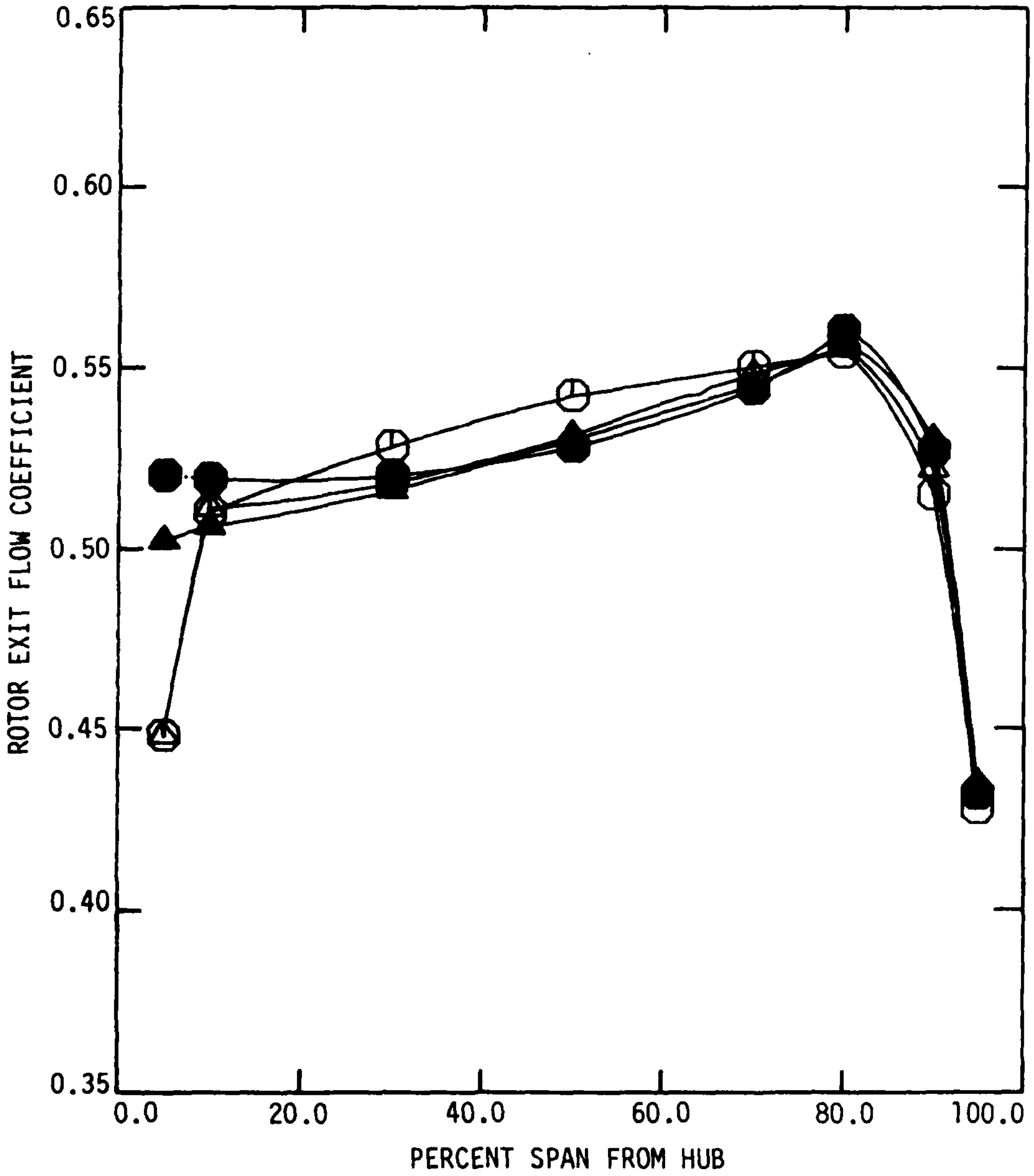

(d) ROTOR EXIT FLOW COEFFICIENT

Figure 4.30 concluded.

Some trends in conventional head-rise and stator loss are worth mentioning:

- For all builds, the first rotor and stage head-rise values are higher than those of the second stage over most of the span, the exceptions, occurring near the hub and tip (Figure 4.29(a) and (b)).
- The modified builds are somewhat close in head-rise performance between stages from 10% to 50% span from the hub. The baseline builds, conversely, are quite different in head-rise performance between stages over the entire span (Figure 4.29(b)).
- For all builds, the first stator loss is less than the second stator loss near the hub, whereas the opposite is observed near the tip (Figure 4.29(c)).
- The stator loss values are generally similar between stages for the modified builds, whereas they differ considerably between stages for the baseline builds (Figure 4.29(c)).

Ideal head-rise (Figure 4.30(a)), rotor loss (Figure 4.30(b)), and hydraulic efficiency (Figure 4.31) are affected considerably (see Figure 4.1) by the uncertainty in absolute flow angle measurement. Therefore, care should be exercised when drawing conclusions from these figures. Several general conclusions follow:

- Rotor loss is nearly constant over most of the blade span (Figure 4.30(b)).
- The rotor deviation angles (Figure 4.30(c)), like rotor loss data, are nearly constant over most of the blade span.

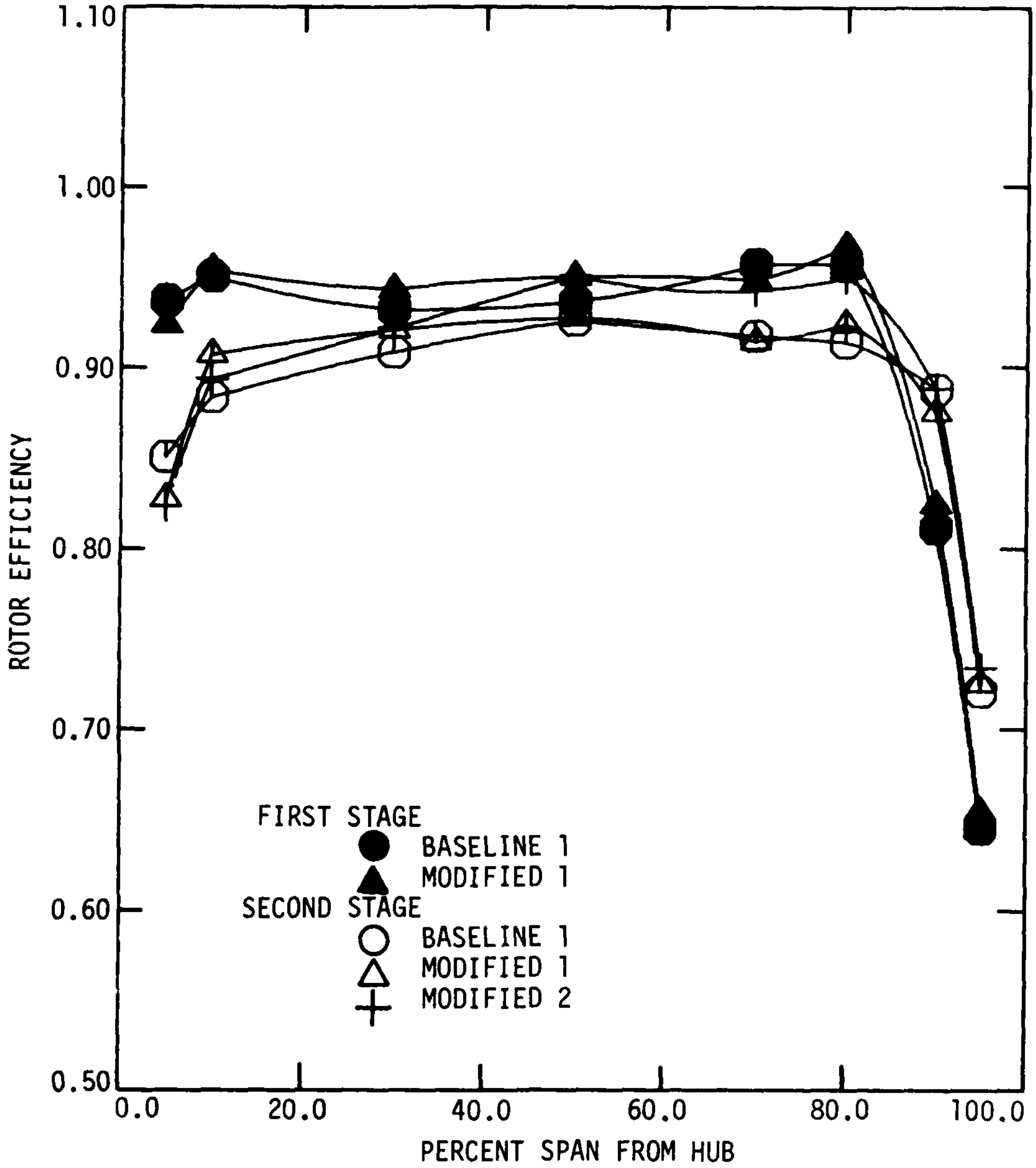

(a) ROTOR

Figure 4.31 Spanwise distribution of circumferential-mean hydraulic efficiencies for the different compressor builds (ϕ = 0.500).

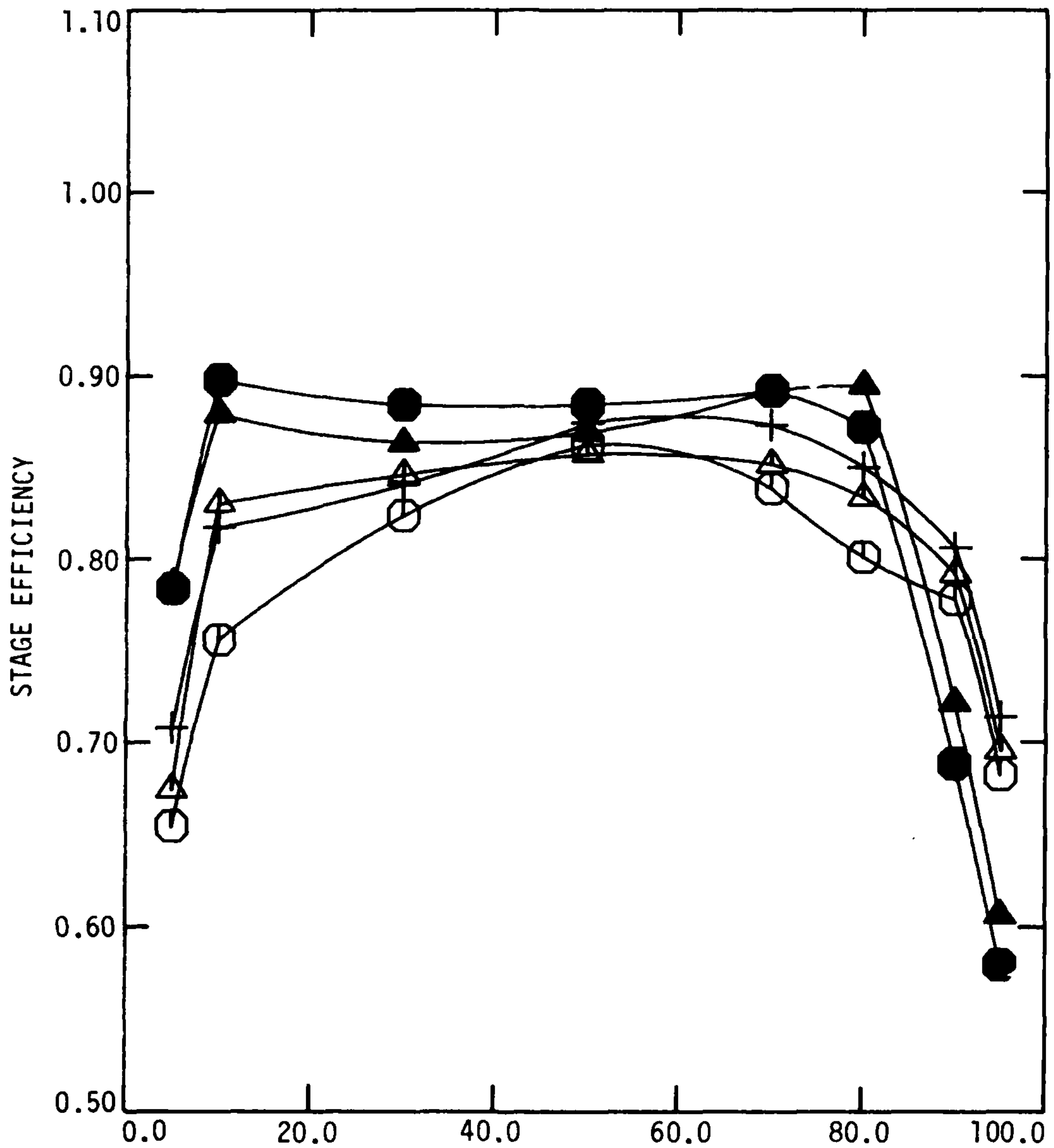

(b) STAGE

Figure 4.31 continued.

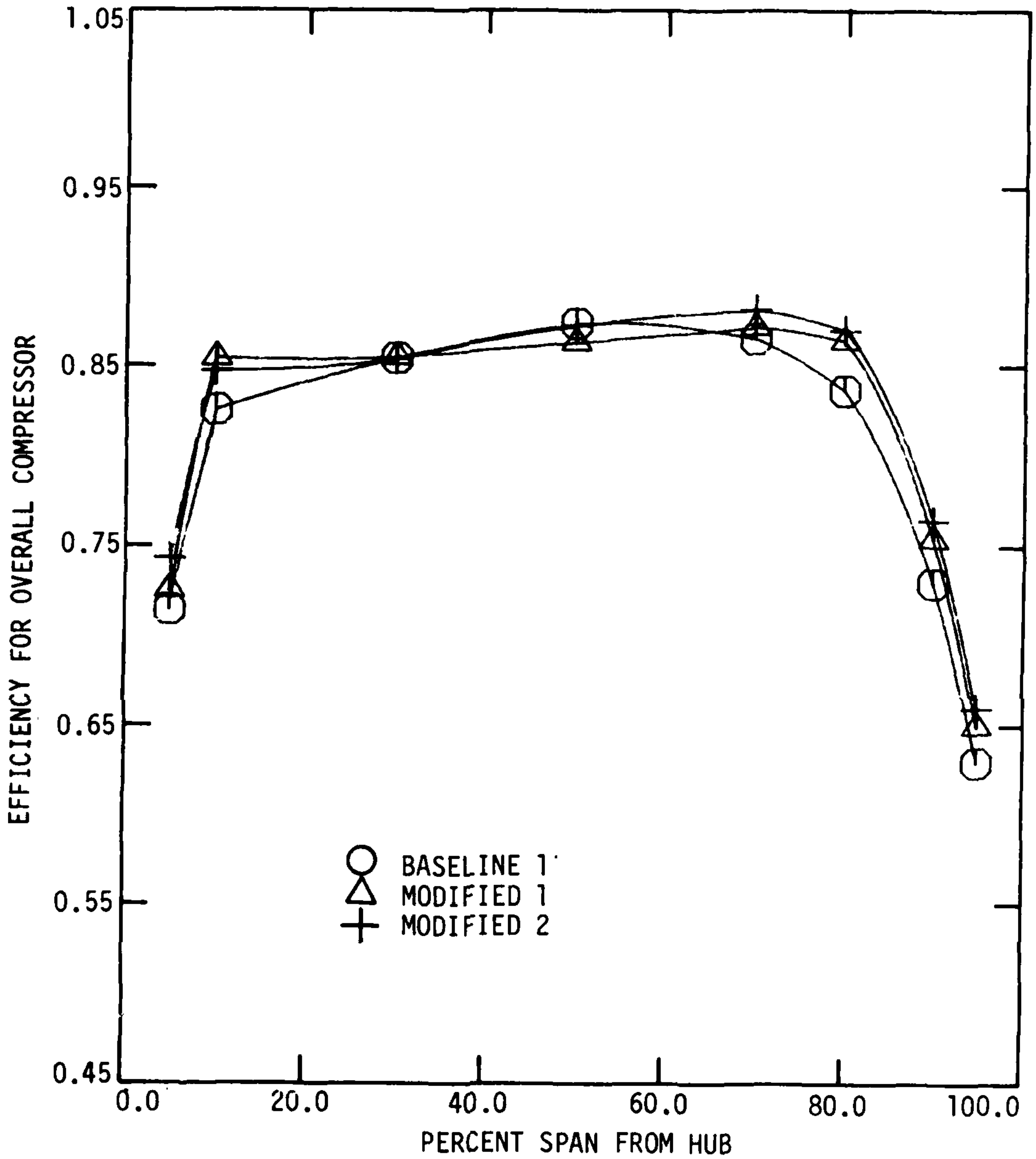

(c) OVERALL

Figure 4.31 concluded.

- The values of rotor loss (Figure 4.30(b)) are substantially less than those of stator loss (Figure 4.29(c)) over most of the blade span.
- The rotor efficiency curves (Figure 4.31(a)) reflect trends in the rotor loss curves (Figure 4.30(b)).
- The overall efficiency (Figure 4.31(c)) is nearly constant over most of the blade span for all builds. The modified 1 and 2 builds have higher overall efficiencies than does the baseline 1 build near the hub and tip.

4.4.1.4. Mass-Averaged Performance

Radially mass-averaged data for the different compressor builds are presented in Table 4.9. Of particular interest are the stator loss and overall efficiency data. Clearly, the modified stator overall efficiency is higher than the baseline stator value. The first stator loss values indicate a higher loss for the modified stator than for the baseline stator. The second stator loss values, however, reveal a higher loss for the baseline stator than for the modified stator. These results are consistent with the spanwise stator loss data presented earlier.

4.4.2. Analysis of Stator Geometry Modification Effects

The aerodynamic effects of three basic stator geometry modifications are analyzed in this section:

- symmetrical leading-edge sweep
- sealing of the clearance gap at a stationary end wall
- large corner fillets

Table 4.9. Comparison of radially mass-averaged performance parameters for the different compressor builds ($\phi = 0.500$).

Build	Head Rise Coefficient		(Shroud Static) Head Rise Coefficient		Loss Coefficient		Efficiency	
	Rotor	Stage	Rotor	Stage	Rotor	Stator	Rotor	Stage
First Stage								
Baseline 1	0.2357	0.2188	0.2066	0.2217	0.0447	0.0905	0.9125	0.8470
Baseline 2	--	0.2185	--	0.2242	--	0.0920	--	--
Modified 1	0.2349	0.2158	0.2063	0.2206	0.0403	0.1031	0.9202	0.8455
Modified 2	--	0.2161	--	0.2229	--	0.1016	--	0.8466
Second Stage								
Baseline 1	0.2258	0.2041	0.1932	0.2077	0.0505	0.1157	0.8998	0.8134
Baseline 2	0.2273	0.2060	0.1913	0.2052	--	0.1132	--	--
Modified 1	0.2282	0.2106	0.1942	0.2129	0.0480	0.0949	0.9058	0.8356
Modified 2	0.2294	0.2107	0.1946	0.2149	0.0408	0.1000	0.9188	0.8439

Overall

Build	Head Rise Coefficient	(Shroud Static) Head Rise Coefficient	Efficiency
Baseline 1	0.4229	0.4294	0.8304
Baseline 2	0.4245	0.4294	--
Modified 1	0.4264	0.4335	0.8406
Modified 2	0.4268	0.4378	0.8452

Expected effects of these types of stator geometry modifications are compared with the experimental results.

Symmetrical sweeping of the stator leading edges was done in this research project primarily to reduce stator blade suction-surface/end-wall corner losses by drawing higher-momentum fluid into those corner regions. The well-known beneficial effect of leading-edge sweep in reducing the Mach number component normal to the leading edge is not realized in low-speed flow research, and so was not considered in this project. The basic aerodynamics involved can be briefly described in the following way. Consider the static pressure distribution generated on and near the blade surfaces, particularly on the suction surface near the blade/end-wall corners. By extending the blade chord near the end walls, a lower-pressure region is generated on the suction surface of the extended section, which tends to draw the main flow toward the blade suction-surface/end-wall corner [13]. Normally, the pressure decrease on the extended suction surface is greater than the pressure rise on the pressure surface so the net effect is beneficial. The flow of higher-momentum fluid into the corner region reduces the thickness of the corner boundary layer, and thus the corner loss.

Reduction of blade/end-wall corner losses was also the objective in using large corner fillets; the function being to lessen interference drag and corner boundary layer growth. This idea stems from aircraft design experience with the fillet geometry at a wing/fuselage juncture [14,15]. The expected results of this modification in the present study, however, were uncertain since only low-speed flow was

involved. As Debruge [15] notes, it is possible for the large corner fillets to produce more loss than the small ones, particularly when a constant fillet radius is used around the entire airfoil circumference.

The sealing of the second stator/hub clearance gap was actually a modification resulting from the addition of large corner fillets at the hub for the modified stator blade geometry. However, after comparing results for the modified 1 and 2 builds, it was decided that additional useful data might be obtained by testing the baseline stator configuration with the second stator/hub clearance gap sealed. Thus, the effect of sealing a stationary blade/stationary end-wall clearance gap is apparent from the experimental results. Without sealing there is evidence of a substantial leakage vortex at the second stator exit hub (baseline 1 and modified 1 builds, Figure 4.28(a)), whereas with sealing, this leakage vortex is no longer present (baseline 2 and modified 2 builds, Figure 4.28(b) and (c)).

The experimental results show that symmetrically sweeping the stator blade leading edges affects the flow as anticipated. The previously discussed stator exit contour maps (Figures 4.23 and 4.28) indicate that the modified stator produces a flow field with substantially more higher-momentum fluid in the stator suction-surface/end-wall corners. This is accompanied by a small, but significant, reduction in higher-momentum fluid in the stator pressure-surface/end-wall corners. The increased flow into the suction-surface/end-wall corners, however, is associated with a

noticeable mid-span thickening of the stator wake on the suction side. This would seem to indicate a radial migration of lower-momentum boundary layer fluid from the stator suction-surface/end-wall corners toward mid-span, since the baseline and modified stators should have similar mid-span profile losses (equal chord lengths and similar blade profiles at mid-span). The data further indicate that at a stationary blade/stationary end-wall clearance gap the stator leading-edge sweep is beneficial in reducing the strength of the leakage vortex (Figure 4.28(a)). This seems reasonable in view of the foregoing discussion. The stator blade/end-wall corner flows produced by the symmetrically swept stator leading edge oppose the leakage-vortex flow.

Several factors should be considered when analyzing the stator loss performance of the baseline and modified builds:

- The modified stator has a longer blade chord, and thus higher solidity, than does the baseline stator except at mid-span where they are equal. Thus, higher profile losses are expected for the modified builds, especially near the hub and tip.
- If the modified builds are to have less "total" stator loss than the baseline builds, then the potentially higher modified stator profile losses must be compensated for by substantially lower end-wall losses.
- The experimental results obtained are for relatively low Reynolds number and Mach number levels.

AD-A141 793 STATOR BLADE ROW GEOMETRY MODIFICATION INFLUENCE ON TWO-STAGE AXIAL-FLOW..(U) IOWA STATE UNIV AMES ENGINEERING RESEARCH INST D L TWEEDT ET AL. DEC 83 3/3

UNCLASSIFIED ISU-ERI-AMES-84179 AFOSR-TR-84-0418 F/G 21/5 NL

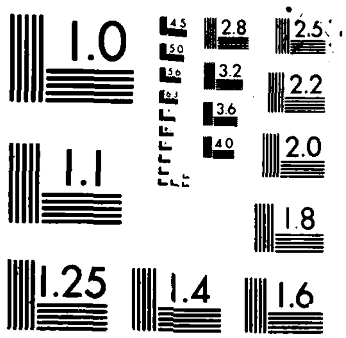

MICROCOPY RESOLUTION TEST CHART
NATIONAL BUREAU OF STANDARDS 1963 A

- The proportion of profile losses to end-wall losses may be considerably different at higher Reynolds number and Mach number levels.

As Table 4.9 indicates, the modified stator performed with higher mass-averaged (total) loss in the first stage and lower mass-averaged (total) loss in the second stage than did the baseline stator. However, the modified first stator might also have performed better than the baseline first stator if the expected profile losses were similar, instead of the mid-span chords. The better loss performance of the modified stator in the second stage is a strong indication that symmetrical leading-edge sweep is beneficial to stator loss performance. Also, the improvements in loss performance realized by symmetrically sweeping the stator leading edges may be greater where higher Reynolds number and Mach number levels are involved.

The experimental results do not show significant effects from using large corner fillets. The substantial improvement in second stator suction-surface/hub corner flow (Figure 4.28(c)) is considered to be primarily an effect of sealing the clearance gap. There is some evidence of a loss decrease near the casing end wall due to large corner fillets (Figure 4.24(d)), but the results are not conclusive. This general result, however, like the results concerning symmetrical leading-edge sweep, should be considered with Reynolds number and Mach number effects in mind.

5. CONCLUSIONS

Aerodynamic performance testing of four different builds of a two-stage axial-flow research compressor was accomplished in an effort to determine the effects of stator geometry modifications--symmetrical leading-edge sweep, large corner fillets, and hub clearance sealing--on flow management. An off-design operating point was selected for this comparative testing. Thus, a comparison of the baseline 1 compressor build performance at design and off-design operating points was also completed.

Substantial stator exit flow-field changes attributable to symmetrical sweeping of each stator leading edge were observed. These stator exit flow-field changes could be correlated with changes in the spanwise distributions of stator loss. The data clearly indicate that stator leading-edge sweep produced an increased flow of higher-momentum fluid into the stator blade suction-surface/end-wall corners with a resulting decrease in loss near the end walls. The increased flow into the stator suction-surface/end-wall corners, however, was accompanied by a substantial thickening of the stator wake (mainly on the suction side) over the mid-span portion of the blade with a resulting increase in loss there. Considering the above two changes together, it appears that symmetrically sweeping the stator leading edges induces an increased flow of higher-momentum fluid into the stator suction-surface/end-wall corners with an accompanying radial migration of stator suction-surface boundary layer fluid away from the end walls toward mid-span. The net effect of this secondary flow seems

to be a reduction in stator blade loss, especially so in the case where the stator hub is shrouded. For the case of a rotating stator hub, the hub-region flow behavior is less certain, but the data show a substantial deterioration of stator loss performance from mid-span to near-hub in going from the baseline to the modified stator.

No definite conclusions could be drawn from the data concerning large corner fillets. However, the data do indicate a slight decrease in stator loss near to the casing end wall. It is important to realize that the effects of stator fillet geometry and symmetrical leading-edge sweep may be largely affected by the levels of Reynolds number and Mach number involved. Qualitatively, these stator geometry modifications could be expected to improve stator loss performance more for higher Reynolds number and Mach number flows.

A curious result (peculiar total-head variations)--realized when comparing the performance of the compressor at different flow rates--led to the study of first stator wake movement and dispersion through the second rotor blade row. For compressor operation at lower flow rates, first stator wake avenues observed at the second rotor exit extended circumferentially over more than one stator pitch, resulting in adjacent avenues partially overlapping with each other. At higher flow rates these wake avenues did not overlap, but instead were with a narrow (no stator wake) region between. It was also observed that these wake avenues changed in circumferential extent with spanwise location, particularly near the tip where they became narrower. These basic differences in rotor exit wake avenue interaction provided a

reasonable explanation of the unusual second rotor exit total-head variations noted.

Some recommendations for further related research are in order. In the immediate future, it is recommended that time-average performance testing involving the different compressor builds continue at the maximum efficiency flow rate and at the design flow rate. Utilization of surface and through-flow flow visualization techniques could prove useful. These techniques may allow changes in the stator flow field produced by the geometry modifications--particularly symmetrical leading-edge sweep and clearance sealing--to be more clearly understood.

A final recommendation concerns stator solidity. For the present program, the mid-span stator solidity was kept constant between the baseline and modified stators, resulting in higher hub and tip solidities for the modified stators. However, if an "average" solidity was maintained constant between the baseline and modifed stators instead, a truer stator loss comparison could result since expected profile losses would be similar. That is, the relative effects of symmetrical leading-edge sweep on stator loss over the blade span could be more directly compared.

6. REFERENCES

1. Hathaway, M. D., and Okiishi, T. H. "Aerodynamic Design and Performance of a Two-Stage, Axial-Flow Compressor (Baseline)." ISU-ERI-Ames-84178, TCRL-24, December 1983.

2. Morgan, B. D. "A Water Column Balance Pressure Reference System." Unpublished Report. Department of Mechanical Engineering, Iowa State University, Ames, Iowa. 1979.

3. Greville, T. N. E. Theory and Applications of Spline Functions. New York: Academic Press, 1967.

4. Wylie, C. R. Advanced Engineering Mathematics. New York: McGraw-Hill Book Company, Inc., 1975.

5. Kline, S. J., and McClintock, F. A. "Describing Uncertainties in Single Sample Experiments." Mechanical Engineering, 75 (1953):3-8.

6. Moffat, R. J. "Contributions to the Theory of Single-Sample Uncertainty Analysis." Transactions of the ASME, Journal of Fluids Engineering, 104 (June 1982):250-260.

7. Smith, L. H., Jr. "Casing Boundary Layers in Multistage Axial-Flow Compressors," in Flow Research on Blading, L. S. Dzung, ed. New York: Elsevier Publishing Company, 1970.

8. Leboeuf, F., Bario, F., Boris, G., and Papailiou, K. D. "Experimental Study and Theoretical Prediction of Secondary Flows in a Transonic Axial Flow Compressor." ASME Paper No. 82-GT-14, 1982.

9. Johnsen, I. A., and Bullock, R. O., eds. "Aerodynamic Design of Axial-Flow Compressors." U.S. NASA SP-36, 1965.

10. Smith, L. H., Jr. "Wake Dispersion in Turbomachines." Transactions of the ASME, Journal of Basic Engineering, 88D (September 1966):688-690.

11. Wagner, J. H., Okiishi, T. H., and Holbrook, G. J. "Periodically Unsteady Flow in an Imbedded Stage of a Multistage, Axial-Flow Turbomachine." Transactions of the ASME, Journal of Engineering for Power, 101 (January 1979):42-51.

12. Zierke, W. C., and Okiishi, T. H. "Measurement and Analysis of Total-Pressure Unsteadiness Data from an Axial-Flow Compressor Stage." Transactions of the ASME, Journal of Engineering for Power, 104 (April 1982):479-488.

13. Senoo, Y., Taylor, E. S., Batra, S. K., and Hinck, E. "Control of Wall Boundary Layer in an Axial Compressor." Gas Turbine Laboratory Report No. 59. Massachusetts Institute of Technology. June 1960.

14. Wennerstrom, A. J. "Experimental Study of a High-Through-Flow Transonic Axial Compressor Stage." Paper scheduled for presentation at the 6th International Symposium on Air Breathing Engines, 6-10 June 1983, Paris, France.

15. Debruge, L. L. "The Aerodynamic Significane of Fillet Geometry in Turbocompressor Blade Rows." Transactions of the ASME, Journal of Engineering for Power, 102 (October 1980):984-993.

7. ACKNOWLEDGMENTS

The authors are grateful to their colleagues of the Iowa State University Engineering Research Institute/Mechanical Engineering Department Turbomachinery Components Research Laboratory for their helpful comments and assistance throughout. In particular, Mr. Jeffrey L. Hansen is appreciated for his help in obtaining some of the data. We remain indebted to Mr. Michael D. Hathaway for his fine related work. Mr. Leon Gerard and his associates are remembered for their dispatch of machining duties. To the staff of the Iowa State University Engineering Research Institute Office of Editorial Services and especially the technical editor and illustrators we offer thanks for patience and expertise. Finally, we sincerely acknowledge the support of the Air Force Office of Scientific Research (James D. Wilson--Contract Monitor) and the encouragement of George K. Serovy of Iowa State University and Arthur J. Wennerstrum of the Air Force Aero Propulsion Laboratory.

8. APPENDIX A: USER DEFINED CORRELATONS FOR NASA DESIGN CODE

Advanced compressor design codes frequently require the user to input various empirical correlations such as blade losses, incidence and deviation angle correlations, and annulus-wall blockage factors. The various user-defined correlations required as input to the NASA design code are presented in this section. The actual tabular input to the design code is given in Appendix B. The variables used in the correlation parameters are defined in the symbols and notation section.

8.1. Blade Loss

The blade loss correlations used are illustrated in Figure 8.1. The loss curves are typical of annular cascade tests of double-circular-arc blades. The correlating parameters are:

- Loss parameter $\equiv \dfrac{\bar{\omega}\cos\beta'_{y,2}}{2\sigma} \equiv$ approximate measure of blade wake momentum thickness to chord ratio.

  where $\sigma = c/S$

- D-factor $\equiv 1 - \dfrac{V'_2}{V'_1} + \dfrac{(rV_y)_2 - (rV_y)_1}{\sigma(r_1 + r_2)V'_1}$

- Percent span from hub

The trends shown are similar to those indicated in Figure 203 of Reference 9.

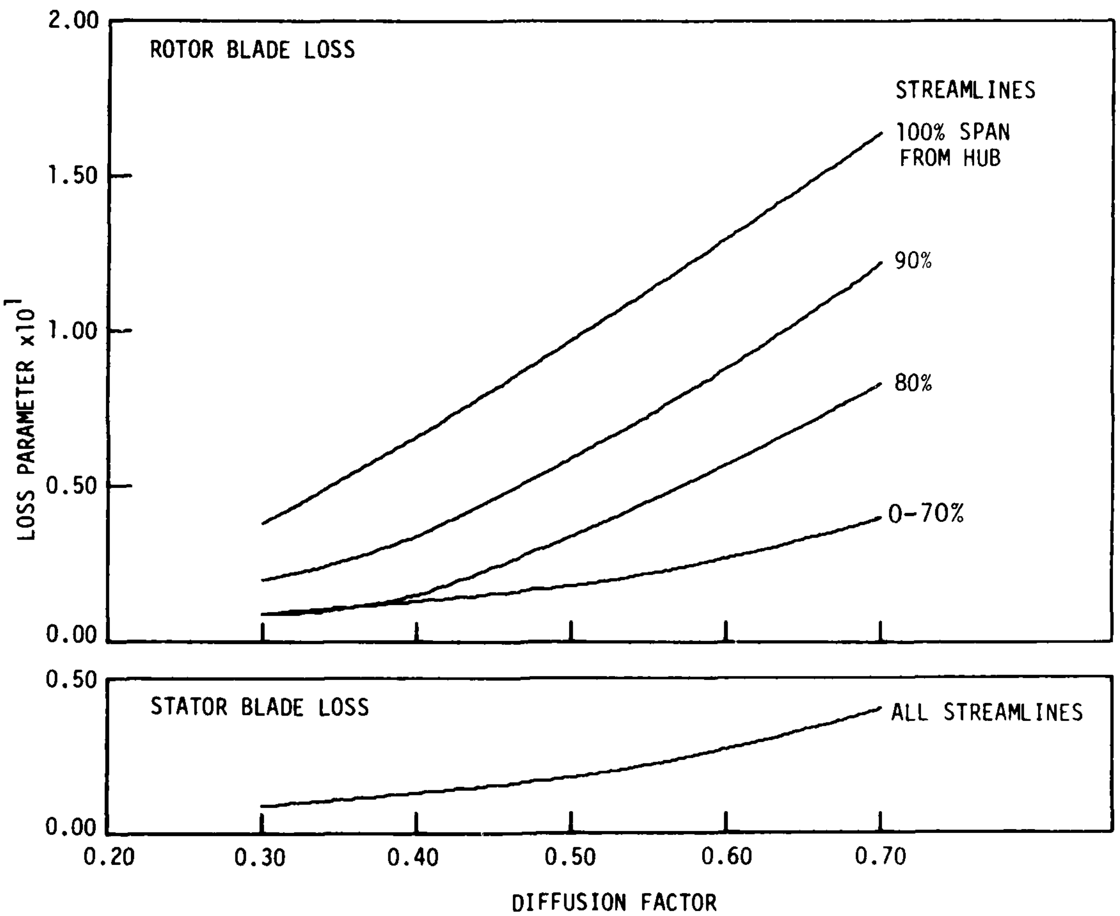

Figure 8.1 Blade loss correlation curves used in NASA design code.

8.2. Incidence and Deviation Angle

The design code provided several options for the incidence and deviation angle correlations. A two-dimensional incidence angle correlation was considered suitable for the baseline compressor design. Carter's rule was selected for the deviation angle correlation. Both correlations are described below.

The incidence angle correlation is described in Chapter VI of Reference 9 in the form of:

$$i = i_o + n\theta$$

where n is obtained from Figure 138 of Reference 9 as a function of

σ and κ_1

θ = blade camber angle

$i_o = (K_i)_{sh}\ (K_i)_t\ (i_o)_{10}$ = incidence angle for zero camber

where

$(i_o)_{10}$ is obtained from Figure 137 of Reference 9

$(K_i)_{sh}$ = 0.7 for double circular arc blades

$(K_i)_t$ is obtained from Figure 142 of Reference 9 as a function of t_{max}/c

The deviation angle correlation (Carter's rule) described in Chapter VII of Reference 9 is

$$\delta = \frac{m_c \theta}{\sqrt{\sigma}}$$

where m_c is obtained from Figure 160 of Reference 9 for circular arc blades.

9. APPENDIX B: NASA DESIGN CODE RESULTS

The output from the NASA design code is presented in the following tables. Table 9.1 lists in tabular form all input parameters and user defined correlations required for the design code analysis. Table 9.2 lists the aerodynamic output (e.g., velocity triangle information, blade element performance, etc.) for 11 streamlines at each axial computation station. The NASA design code gives the streamline radial positions as a percentage of the blade span measured from the shroud end-wall, whereas, the convention used for all data figures in this report is percent span measured from the hub end-wall. Table 9.3 lists the stage and overall mass-averaged aerodynamic performance parameters. Table 9.4 lists the manufacturing coordinates at 17 spanwise locations for the modified stator blade. Only the first stage stator blade manufacturing coordinates generated from the NASA design code are given as they were used for both stages of the modified compressor. Figure 9.1 shows a representative stator blade section and associated manufacturing coordinate nomenclature.

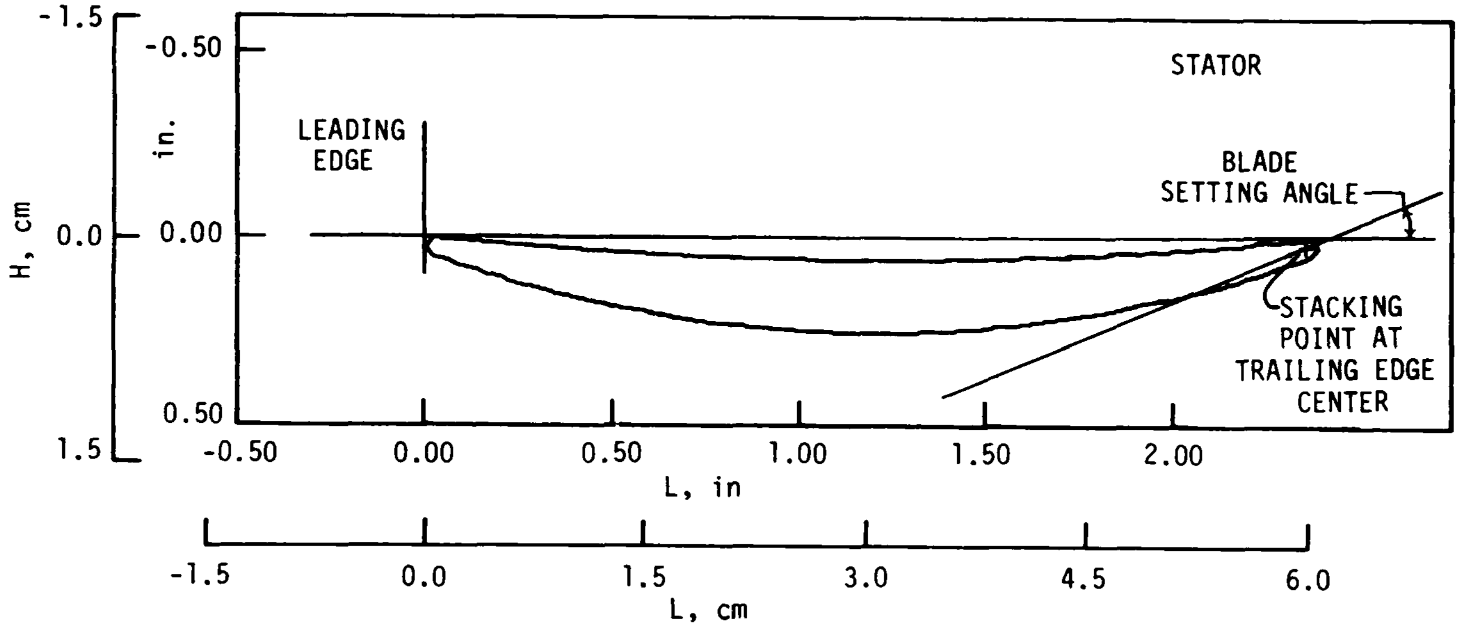

Figure 9.1. Typical modified stator blade section using manufacturing coordinates.

Table 9.1. Design code input parameters.

*** INPUT DATA FOR COMPRESSOR DESIGN PROGRAM ***

AFOSR/ISU TASK 4 2-STAGE HTF W/SP36 P248 LOSS 2400RPM 18MAR81

THE COMPRESSOR ROTATIONAL SPEED IS 2400.0 RPM.

THE DESIRED COMPRESSOR PRESSURE RATIO IS 1.019 .

CALCULATIONS WILL BE PERFORMED ON 11 STREAMLINES.

THE INLET FLOW RATE IS 5.250 (LB/SEC).

THE MOLECULAR WEIGHT IS 28.97 .

THE COMPRESSOR HAS 4 BLADE ROWS.

CALCULATIONS WILL BE MADE AT THE BLADE EDGES AND AT 7 ANNULAR STATIONS.

THE SPECIFIC HEAT POLYNOMIAL IS IN THE FOLLOWING FORM

```
CP = 0.23970D 00 +  0.0     *T +  0.0     *T**2 +  0.0     *T**3 +  0.0     *T**4 +  0.0     *T**5
```

INPUT DISTRIBUTIONS BY STREAMLINE OR STREAMTUBE

STREAMLINE NO.	INLET TOTAL TEMPERATURE (DEG. R.)	INLET TOTAL PRESSURE (PSIA)	INLET WHIRL VELOCITY (FT/SEC)	STREAMTUBE NO.	STREAMTUBE FLOW FRACTION
1	518.600	14.696	0.0	1	0.1000
2	518.600	14.696	0.0	2	0.2000
3	518.600	14.696	0.0	3	0.3000
4	518.600	14.696	0.0	4	0.4000
5	518.600	14.696	0.0	5	0.5000
6	518.600	14.696	0.0	6	0.6000
7	518.600	14.696	0.0	7	0.7000
8	518.600	14.696	0.0	8	0.8000
9	518.600	14.696	0.0	9	0.9000
10	518.600	14.696	0.0	10	1.0000
11	518.600	14.696	0.0		

Table 9.1. Continued.

INPUT DATA POINTS FOR TIP AND HUB CONTOURS.

TIP AXIAL COORDINATE (INCHES)	TIP RADIUS (INCHES)	HUB AXIAL COORDINATE (INCHES)	HUB RADIUS (INCHES)
-6.000	10.500	-11.530	8.150
-4.100	9.030	-9.100	6.050
-1.750	8.180	-6.100	5.600
0.0	8.000	-5.000	5.600
1.000	8.000	-3.400	5.600
2.500	8.000	0.0	5.600
4.000	8.000	8.000	5.600
7.500	8.000	17.000	5.600
10.500	8.000		
17.000	8.000		

Table 9.1. Continued.

THE INPUT PROFILE LOSS TABLES - OMEGA(BAR)*COS(BETA)/(2.0*SIGMA)

** PROFILE LOSS TABLE NO. 1 **

STREAMLINE	D-FACTOR	LOSS PARAM.	D-FACTOR	LOSS PARAM.	D-FACTOR	LOSS PARAM.	D-FACTOR	LOSS PARAM.	D-FACTOR	LOSS PARAM.
1	0.3000	0.0380	0.4000	0.0660	0.5000	0.0970	0.6000	0.1300	0.7000	0.1640
2	0.3000	0.0200	0.4000	0.0340	0.5000	0.0590	0.6000	0.0880	0.7000	0.1220
3	0.3000	0.0090	0.4000	0.0150	0.5000	0.0340	0.6000	0.0570	0.7000	0.0830
4	0.3000	0.0090	0.4000	0.0130	0.5000	0.0180	0.6000	0.0270	0.7000	0.0400
5	0.3000	0.0090	0.4000	0.0130	0.5000	0.0180	0.6000	0.0270	0.7000	0.0400
6	0.3000	0.0090	0.4000	0.0130	0.5000	0.0180	0.6000	0.0270	0.7000	0.0400
7	0.3000	0.0090	0.4000	0.0130	0.5000	0.0180	0.6000	0.0270	0.7000	0.0400
8	0.3000	0.0090	0.4000	0.0130	0.5000	0.0180	0.6000	0.0270	0.7000	0.0400
9	0.3000	0.0090	0.4000	0.0130	0.5000	0.0180	0.6000	0.0270	0.7000	0.0400
10	0.3000	0.0090	0.4000	0.0130	0.5000	0.0180	0.6000	0.0270	0.7000	0.0400
11	0.3000	0.0090	0.4000	0.0130	0.5000	0.0180	0.6000	0.0270	0.7000	0.0400

** PROFILE LOSS TABLE NO. 2 **

STREAMLINE	D-FACTOR	LOSS PARAM.	D-FACTOR	LOSS PARAM.	D-FACTOR	LOSS PARAM.	D-FACTOR	LOSS PARAM.	D-FACTOR	LOSS PARAM.
1	0.3000	0.0090	0.4000	0.0130	0.5000	0.0180	0.6000	0.0270	0.7000	0.0400
2	0.3000	0.0090	0.4000	0.0130	0.5000	0.0180	0.6000	0.0270	0.7000	0.0400
3	0.3000	0.0090	0.4000	0.0130	0.5000	0.0180	0.6000	0.0270	0.7000	0.0400
4	0.3000	0.0090	0.4000	0.0130	0.5000	0.0180	0.6000	0.0270	0.7000	0.0400
5	0.3000	0.0090	0.4000	0.0130	0.5000	0.0180	0.6000	0.0270	0.7000	0.0400
6	0.3000	0.0090	0.4000	0.0130	0.5000	0.0180	0.6000	0.0270	0.7000	0.0400
7	0.3000	0.0090	0.4000	0.0130	0.5000	0.0180	0.6000	0.0270	0.7000	0.0400
8	0.3000	0.0090	0.4000	0.0130	0.5000	0.0180	0.6000	0.0270	0.7000	0.0400
9	0.3000	0.0090	0.4000	0.0130	0.5000	0.0180	0.6000	0.0270	0.7000	0.0400
10	0.3000	0.0090	0.4000	0.0130	0.5000	0.0180	0.6000	0.0270	0.7000	0.0400
11	0.3000	0.0090	0.4000	0.0130	0.5000	0.0180	0.6000	0.0270	0.7000	0.0400

Table 9.1. Continued.

*** PRINTOUT OF INPUT STATION DATA ***

** INPUT SET NO. 1 IS AN ANNULAR STATION **

TIP AXIAL LOCATION (INCHES)	HUB AXIAL LOCATION (INCHES)	TIP BLOCKAGE FACTOR	HUB BLOCKAGE FACTOR	MASS BLEED FRACTION
-5.9500	-11.4000	0.0	0.0	0.0

** INPUT SET NO. 2 IS AN ANNULAR STATION **

TIP AXIAL LOCATION (INCHES)	HUB AXIAL LOCATION (INCHES)	TIP BLOCKAGE FACTOR	HUB BLOCKAGE FACTOR	MASS BLEED FRACTION
-4.7500	-8.3500	0.0030	0.0030	0.0

** INPUT SET NO. 3 IS AN ANNULAR STATION **

TIP AXIAL LOCATION (INCHES)	HUB AXIAL LOCATION (INCHES)	TIP BLOCKAGE FACTOR	HUB BLOCKAGE FACTOR	MASS BLEED FRACTION
-3.5800	-4.9500	0.0060	0.0060	0.0

** INPUT SET NO. 4 IS AN ANNULAR STATION **

TIP AXIAL LOCATION (INCHES)	HUB AXIAL LOCATION (INCHES)	TIP BLOCKAGE FACTOR	HUB BLOCKAGE FACTOR	MASS BLEED FRACTION
-1.4500	-1.6000	0.0080	0.0080	0.0

Table 9.1. Continued.

*** PRINTOUT OF INPUT STATION DATA ***

** INPUT SET NO. 5 IS ROTOR NO. 1 **

* ALL PROGRAM OPTIONS EXCEPT OFF - DESIGN PUNCH ARE DESIRED FOR THIS BLADE *

TIP C.G. AXIAL LOCATION (INCHES)	HUB C.G. AXIAL LOCATION (INCHES)	INLET TIP BLOCKAGE	INLET HUB BLOCKAGE	INLET MASS BLEED
1.8300	1.8300	0.0090	0.0090	0.0
LOSS SET USED	BLADE TILT ANGLE (DEGREES)	OUTLET TIP BLOCKAGE	OUTLET HUB BLOCKAGE	OUTLET MASS BLEED
1	C.0	0.0180	0.0090	0.0
TIP D FACTOR LIMIT	HUB FLOW ANGLE LIMIT (DEGREES)	TIP SOLIDITY	NUMBER OF BLADES	CUM ENERGY ADD FRACT
0.4000	0.0	1.0027	21	0.5000

* POLYNOMIAL CONSTANTS FOR THE FOLLOWING *

TERM	ROTOR OUTLET PRESSURE	L.E. RADIUS/CHORD	T.E. RADIUS/CHORD	MAX. THICKNESS/CHORD	CHORD/TIP CHORD
CONSTANT		0.0100	0.0100	0.0600	
LINEAR	0.0	0.0	0.0	0.0400	0.0
QUADRATIC	0.0	0.0	0.0	0.0	0.0
CUBIC	0.0	0.0	0.0	0.0	0.0
QUARTIC	0.0				
QUINTIC	0.0				

* INPUT BLADE ELEMENT DEFINITION OPTIONS *

INCIDENCE ANGLE	DEVIATION ANGLE	TURNING RATE RATIO	TRANSITION POINT	MAX. THICKNESS POINT	CHOKE MARGIN	BLADE MATERIAL DENSITY LB/(IN)**3
2-D	CARTERS RULE	CIRCULAR ARC	CIRCULAR ARC	TRANS. PT.	NONE	0.10000

Table 9.1. Continued.

*** PRINTOUT OF INPUT STATION DATA ***

** INPUT SET NO. 6 IS A GUIDE VANE OR STATOR **

* ALL PROGRAM OPTIONS EXCEPT OFF - DESIGN PUNCH ARE DESIRED FOR THIS BLADE *

TIP C.G. AXIAL LOCATION (INCHES)	HUB C.G. AXIAL LOCATION (INCHES)	INLET TIP BLOCKAGE	INLET HUB BLOCKAGE	INLET MASS BLEED
6.4600	6.4600	0.0180	0.0090	0.0
LOSS SET USED	**BLADE TILT ANGLE (DEGREES)**	**OUTLET TIP BLOCKAGE**	**OUTLET HUB BLOCKAGE**	**OUTLET MASS BLEED**
2	0.0	0.0180	0.0180	0.0
HUB D FACTOR LIMIT	**INLET HUB MACH LIMIT**	**TIP SOLIDITY**	**NUMBER OF BLADES**	**NTESTK NCVSTK**
0.5000	0.5000	1.8200	30	1 0

* POLYNOMIAL CONSTANTS FOR THE FOLLOWING *

TERM	STATOR OUTLET V(θ)	L.E. RADIUS/CHORD	T.E. RADIUS/CHORD	MAX. THICKNESS/CHORD	CHORD/TIP CHORD
INV.SQ.	0.0				
INVERSE	0.0				
CONSTANT	0.0	0.0100	0.0100	0.1000	
LINEAR	0.0	0.0	0.0	-0.0400	-0.8721
QUADRATIC	0.0	0.0	0.0	0.0	0.8721
CUBIC		0.0	0.0	0.0	0.0

* INPUT BLADE ELEMENT DEFINITION OPTIONS *

INCIDENCE ANGLE	DEVIATION ANGLE	TURNING RATE RATIO	TRANSITION POINT	MAX. THICKNESS POINT	CHOKE MARGIN
2-D	CARTERS RULE	CIRCULAR ARC	CIRCULAR ARC	TRANS. PT.	NONE

Table 9.1. Continued.

*** PRINTOUT OF INPUT STATION DATA ***

** INPUT SET NO. 7 IS ROTOR NO. 2 **

* ALL PROGRAM OPTIONS EXCEPT OFF - DESIGN PUNCH ARE DESIRED FOR THIS BLADE *

TIP C.G. AXIAL LOCATION (INCHES)	HUB C.G. AXIAL LOCATION (INCHES)	INLET TIP BLOCKAGE	INLET HUB BLOCKAGE	INLET MASS BLEED
8.2700	8.2700	0.0180	0.0180	0.0
LOSS SET USED	BLADE TILT ANGLE (DEGREES)	OUTLET TIP BLOCKAGE	OUTLET HUB BLOCKAGE	OUTLET MASS BLEED
1	0.0	0.0270	0.0180	0.0
TIP D FACTOR LIMIT	HUB FLOW ANGLE LIMIT (DEGREES)	TIP SOLIDITY	NUMBER OF BLADES	CUM ENERGY ADD FRACT
0.4000	0.0	1.0027	21	1.0000

* POLYNOMIAL CONSTANTS FOR THE FOLLOWING *

TERM	ROTOR OUTLET PRESSURE	L.E. RADIUS/CHORD	T.E. RADIUS/CHORD	MAX. THICKNESS/CHORD	CHORD/TIP CHORD
CONSTANT		0.0100	0.0100	0.0600	
LINEAR	0.0	0.0	0.0	0.0400	0.0
QUADRATIC	0.0	0.0	0.0	0.0	0.0
CUBIC	0.0	0.0	0.0	0.0	0.0
QUARTIC	0.0				
QUINTIC	0.0				

* INPUT BLADE ELEMENT DEFINITION OPTIONS *

INCIDENCE ANGLE	DEVIATION ANGLE	TURNING RATE RATIO	TRANSITION POINT	MAX. THICKNESS POINT	CHOKE MARGIN	BLADE MATERIAL DENSITY LB/(IN)**3
2-D	CARTERS RULE	CIRCULAR ARC	CIRCULAR ARC	TRANS. PT.	NONE	0.10000

Table 9.1. Continued.

*** PRINTOUT OF INPUT STATION DATA ***

** INPUT SET NO. 8 IS A GUIDE VANE OR STATOR **

* ALL PROGRAM OPTIONS EXCEPT OFF - DESIGN PUNCH ARE DESIRED FOR THIS BLADE *

TIP C.G. AXIAL LOCATION (INCHES)	HUB C.G. AXIAL LOCATION (INCHES)	INLET TIP BLOCKAGE	INLET HUB BLOCKAGE	INLET MASS BLEED
12.9000	12.9000	0.0270	0.0180	0.0
LOSS SET USED	**BLADE TILT ANGLE (DEGREES)**	**OUTLET TIP BLOCKAGE**	**OUTLET HUB BLOCKAGE**	**OUTLET MASS BLEED**
2	0.0	0.0270	0.0270	0.0
HUB D FACTOR LIMIT	**INLET HUB MACH LIMIT**	**TIP SOLIDITY**	**NUMBER OF BLADES**	**NTESTK NCVSTK**
0.5000	0.5000	1.8200	30	1 0

* POLYNOMIAL CONSTANTS FOR THE FOLLOWING *

TERM	STATOR OUTLET V(θ)	L.E. RADIUS/CHORD	T.E. RADIUS/CHORD	MAX. THICKNESS/CHORD	CHORD/TIP CHORD
INV.SQ.	0.0				
INVERSE	0.0				
CONSTANT	0.0	0.0100	0.0100	0.1000	
LINEAR	0.0	0.0	0.0	-0.0400	-0.8721
QUADRATIC	0.0	0.0	0.0	0.0	0.8721
CUBIC		0.0	0.0	0.0	0.0

* INPUT BLADE ELEMENT DEFINITION OPTIONS *

INCIDENCE ANGLE	DEVIATION ANGLE	TURNING RATE RATIO	TRANSITION POINT	MAX. THICKNESS POINT	CHOKE MARGIN
2-D	CARTERS RULE	CIRCULAR ARC	CIRCULAR ARC	TRANS. PT.	NONE

Table 9.1. Concluded.

*** PRINTOUT OF INPUT STATION DATA ***

** INPUT SET NO. 9 IS AN ANNULAR STATION **

TIP AXIAL LOCATION (INCHES)	HUB AXIAL LOCATION (INCHES)	TIP BLOCKAGE FACTOR	HUB BLOCKAGE FACTOR	MASS BLEED FRACTION
14.5000	14.5000	0.0270	0.0270	0.0

** INPUT SET NO. 10 IS AN ANNULAR STATION **

TIP AXIAL LOCATION (INCHES)	HUB AXIAL LOCATION (INCHES)	TIP BLOCKAGE FACTOR	HUB BLOCKAGE FACTOR	MASS BLEED FRACTION
15.5000	15.5000	0.0270	0.0270	0.0

** INPUT SET NO. 11 IS AN ANNULAR STATION **

TIP AXIAL LOCATION (INCHES)	HUB AXIAL LOCATION (INCHES)	TIP BLOCKAGE FACTOR	HUB BLOCKAGE FACTOR	MASS BLEED FRACTION
16.5000	16.5000	0.0270	0.0270	0.0

I	IFT	Z(IFT,JM)	AR	I	Z(I,J)	AR
1	1	-8.4947	0.0	1	-8.4947	0.0
2	2	-6.3346	1.6969	2	-6.3345	1.6969
3	3	-4.1903	1.4520	3	-4.1903	1.4520
4	4	-1.5182	0.9303	4	-1.5182	0.9303
5	5	1.0003	0.9356	5	1.0003	0.9356
6	6	2.7808	1.3125	6	2.7808	1.3125
7	7	3.8350	2.2171	7	3.8350	2.2171
8	8	6.4600	0.8805	8	6.4600	0.8805
9	9	7.4405	2.3566	9	7.4405	2.3566
10	10	9.2206	1.2875	10	9.2206	1.2875
11	11	10.2750	2.1739	11	10.2750	2.1739
12	12	12.9000	0.8634	12	12.9000	0.8634
13	13	14.5000	1.4166	13	14.5000	1.4166
14	14	15.5000	2.2666	14	15.5000	2.2666
15	15	16.5000	2.2666	15	16.5000	2.2666

FACT1 = 1.2548 FACT2 = 1.0193

Table 9.2. Design code predictions of aerodynamic parameters.

** VALUES OF PARAMETERS ON STREAMLINES AT STATION, 1, WHICH IS AN ANNULUS **

STREAMLINE NO.	RADIUS (IN.)	AXIAL COORD. (IN.)	AXIAL VEL. (FT/SEC)	MERD. VEL. (FT/SEC)	TANG. VEL. (FT/SEC)	ABS. VEL. (FT/SEC)	ABS. MACH NO.	ABS.FLOW ANGLE (DEG)	STREAM. SLOPE (DEG)	STREAM. CURV. (1./IN.)	TOTAL PRESS. (PSIA)	TOTAL TEMP. (DEG.R.)	STATIC PRESS. (PSIA)	STATIC TEMP. (DEG.R.)
TIP	10.454	-5.950												
1	10.454	-5.950	30.91	42.24	0.0	42.24	0.0378	0.0	-42.97	0.044	14.696	518.60	14.681	518.45
2	10.289	-6.317	30.58	40.32	0.0	40.32	0.0361	0.0	-40.68	0.040	14.696	518.60	14.683	518.46
3	10.110	-6.715	30.02	38.40	0.0	38.40	0.0344	0.0	-38.58	0.037	14.696	518.60	14.684	518.48
4	9.914	-7.150	29.27	36.51	0.0	36.51	0.0327	0.0	-36.70	0.035	14.696	518.60	14.685	518.49
5	9.700	-7.624	28.35	34.64	0.0	34.64	0.0310	0.0	-35.07	0.034	14.696	518.60	14.686	518.50
6	9.466	-8.144	27.29	32.84	0.0	32.84	0.0294	0.0	-33.80	0.034	14.696	518.60	14.687	518.51
7	9.210	-8.714	26.10	31.14	0.0	31.14	0.0279	0.0	-33.06	0.035	14.696	518.60	14.688	518.52
8	8.931	-9.333	24.79	29.62	0.0	29.62	0.0265	0.0	-33.18	0.038	14.696	518.60	14.689	518.53
9	8.632	-9.999	23.34	28.38	0.0	28.38	0.0254	0.0	-34.65	0.042	14.696	518.60	14.689	518.53
10	8.319	-10.695	21.63	27.58	0.0	27.58	0.0247	0.0	-38.35	0.048	14.696	518.60	14.690	518.54
11	8.001	-11.400	19.00	27.20	0.0	27.20	0.0244	0.0	-45.69	0.050	14.696	518.60	14.690	518.54
HUB	8.001	-11.400												

** VALUES OF PARAMETERS ON STREAMLINES AT STATION, 2, WHICH IS AN ANNULUS **

STREAMLINE NO.	RADIUS (IN.)	AXIAL COORD. (IN.)	AXIAL VEL. (FT/SEC)	MERD. VEL. (FT/SEC)	TANG. VEL. (FT/SEC)	ABS. VEL. (FT/SEC)	ABS. MACH NO.	ABS.FLOW ANGLE (DEG)	STREAM. SLOPE (DEG)	STREAM. CURV. (1./IN.)	TOTAL PRESS. (PSIA)	TOTAL TEMP. (DEG.R.)	STATIC PRESS. (PSIA)	STATIC TEMP. (DEG.R.)
TIP	9.459	-4.750												
1	9.450	-4.759	47.63	59.06	0.0	59.06	0.0529	0.0	-36.24	0.117	14.696	518.60	14.667	518.31
2	9.238	-4.965	46.94	56.62	0.0	56.62	0.0507	0.0	-33.99	0.104	14.696	518.60	14.670	518.33
3	9.011	-5.187	46.05	54.20	0.0	54.20	0.0486	0.0	-31.82	0.095	14.696	518.60	14.672	518.36
4	8.764	-5.427	44.96	51.76	0.0	51.76	0.0464	0.0	-29.70	0.089	14.696	518.60	14.674	518.38
5	8.496	-5.689	43.64	49.25	0.0	49.25	0.0441	0.0	-27.62	0.086	14.696	518.60	14.676	518.40
6	8.200	-5.978	42.03	46.59	0.0	46.59	0.0417	0.0	-25.56	0.086	14.696	518.60	14.678	518.42
7	7.870	-6.300	40.05	43.68	0.0	43.68	0.0391	0.0	-23.53	0.092	14.696	518.60	14.680	518.44
8	7.494	-6.666	37.55	40.37	0.0	40.37	0.0362	0.0	-21.55	0.104	14.696	518.60	14.683	518.46
9	7.054	-7.096	34.27	36.40	0.0	36.40	0.0326	0.0	-19.74	0.127	14.696	518.60	14.685	518.49
10	6.513	-7.623	29.74	31.35	0.0	31.35	0.0281	0.0	-18.46	0.169	14.696	518.60	14.688	518.52
11	5.784	-8.334	22.97	24.31	0.0	24.31	0.0218	0.0	-19.13	0.248	14.696	518.60	14.691	518.55
HUB	5.769	-8.350												

Table 9.2. Continued.

** VALUES OF PARAMETERS ON STREAMLINES AT STATION. 3. WHICH IS AN ANNULUS **

STREAMLINE NO.	RADIUS (IN.)	AXIAL COORD. (IN.)	AXIAL VEL. (FT/SEC)	MERD. VEL. (FT/SEC)	TANG. VEL. (FT/SEC)	ABS. VEL. (FT/SEC)	ABS. MACH NO.	ABS.FLOW ANGLE (DEG)	STREAM. SLOPE (DEG)	STREAM. CURV. (1./IN.)	TOTAL PRESS. (PSIA)	TOTAL TEMP. (DEG.R.)	STATIC PRESS. (PSIA)	STATIC TEMP. (DEG.R.)
TIP	8.755	-3.580												
1	8.740	-3.587	70.43	78.16	0.0	78.16	0.0700	0.0	-25.70	0.152	14.696	518.60	14.646	518.09
2	8.522	-3.681	69.13	75.61	0.0	75.61	0.0678	0.0	-23.91	0.135	14.696	518.60	14.649	518.12
3	8.290	-3.782	67.82	73.18	0.0	73.18	0.0656	0.0	-22.07	0.121	14.696	518.60	14.652	518.15
4	8.044	-3.889	66.51	70.86	0.0	70.86	0.0635	0.0	-20.16	0.106	14.696	518.60	14.655	518.18
5	7.782	-4.003	65.19	68.61	0.0	68.61	0.0615	0.0	-18.16	0.093	14.696	518.60	14.657	518.21
6	7.500	-4.125	63.87	66.44	0.0	66.44	0.0595	0.0	-16.00	0.079	14.696	518.60	14.660	518.23
7	7.195	-4.257	62.53	64.33	0.0	64.33	0.0576	0.0	-13.61	0.064	14.696	518.60	14.662	518.26
8	6.864	-4.401	61.17	62.28	0.0	62.28	0.0558	0.0	-10.84	0.047	14.696	518.60	14.664	518.28
9	6.500	-4.559	59.79	60.30	0.0	60.30	0.0540	0.0	-7.50	0.026	14.696	518.60	14.666	518.30
10	6.093	-4.735	58.31	58.40	0.0	58.40	0.0523	0.0	-3.17	-0.006	14.696	518.60	14.668	518.32
11	5.626	-4.939	56.62	56.70	0.0	56.70	0.0508	0.0	3.10	-0.058	14.696	518.60	14.669	518.33
HUB	5.600	-4.950												

** VALUES OF PARAMETERS ON STREAMLINES AT STATION. 4. WHICH IS AN ANNULUS **

STREAMLINE NO.	RADIUS (IN.)	AXIAL COORD. (IN.)	AXIAL VEL. (FT/SEC)	MERD. VEL. (FT/SEC)	TANG. VEL. (FT/SEC)	ABS. VEL. (FT/SEC)	ABS. MACH NO.	ABS.FLOW ANGLE (DEG)	STREAM. SLOPE (DEG)	STREAM. CURV. (1./IN.)	TOTAL PRESS. (PSIA)	TOTAL TEMP. (DEG.R.)	STATIC PRESS. (PSIA)	STATIC TEMP. (DEG.R.)
TIP	8.128	-1.450												
1	8.111	-1.451	99.08	100.07	0.0	100.07	0.0897	0.0	-8.06	0.108	14.696	518.60	14.613	517.77
2	7.912	-1.463	97.24	98.11	0.0	98.11	0.0879	0.0	-7.66	0.098	14.696	518.60	14.617	517.80
3	7.704	-1.475	95.53	96.30	0.0	96.30	0.0863	0.0	-7.24	0.088	14.696	518.60	14.620	517.83
4	7.486	-1.488	94.00	94.66	0.0	94.66	0.0848	0.0	-6.73	0.077	14.696	518.60	14.622	517.85
5	7.258	-1.502	92.64	93.18	0.0	93.18	0.0835	0.0	-6.12	0.067	14.696	518.60	14.624	517.88
6	7.019	-1.516	91.45	91.86	0.0	91.86	0.0823	0.0	-5.42	0.057	14.696	518.60	14.626	517.90
7	6.769	-1.531	90.41	90.70	0.0	90.70	0.0813	0.0	-4.63	0.048	14.696	518.60	14.628	517.91
8	6.505	-1.546	89.52	89.71	0.0	89.71	0.0804	0.0	-3.73	0.038	14.696	518.60	14.630	517.93
9	6.228	-1.563	88.77	88.87	0.0	88.87	0.0796	0.0	-2.76	0.029	14.696	518.60	14.631	517.94
1(	5.936	-1.580	88.13	88.17	0.0	88.17	0.0790	0.0	-1.71	0.022	14.696	518.60	14.632	517.95
1.	5.625	-1.599	87.54	87.54	0.0	87.54	0.0785	0.0	-0.66	0.019	14.696	518.60	14.633	517.96
HUB	5.600	-1.600												

Table 9.2. Continued.

** VALUES OF PARAMETERS ON STREAMLINES AT STATION, 5, WHICH IS THE INLET OF ROTOR NUMBER, 1 **

STREAMLINE NO.	RADIUS (IN.)	AXIAL COORD. (IN.)	AXIAL VEL. (FT/SEC)	MERD. VEL. (FT/SEC)	TANG. VEL. (FT/SEC)	ABS. VEL. (FT/SEC)	ABS. MACH NO.	ABS.FLOW ANGLE (DEG)	STREAM. SLOPE (DEG)	STREAM. CURV. (1./IN.)	TOTAL PRESS. (PSIA)	TOTAL TEMP. (DEG.R.)	STATIC PRESS. (PSIA)	STATIC TEMP. (DEG.R.)
TIP	8.001	1.145												
1	7.982	1.144	98.25	98.26	0.0	98.26	0.0881	0.0	-0.52	-0.009	14.696	518.60	14.616	517.80
2	7.779	1.129	98.45	98.47	0.0	98.47	0.0883	0.0	-0.90	-0.009	14.696	518.60	14.616	517.79
3	7.570	1.114	98.59	98.60	0.0	98.60	0.0884	0.0	-0.96	-0.004	14.696	518.60	14.616	517.79
4	7.356	1.098	98.63	98.64	0.0	98.64	0.0884	0.0	-0.94	0.000	14.696	518.60	14.616	517.79
5	7.135	1.081	98.59	98.60	0.0	98.60	0.0884	0.0	-0.90	0.003	14.696	518.60	14.616	517.79
6	6.907	1.062	98.50	98.51	0.0	98.51	0.0883	0.0	-0.84	0.004	14.696	518.60	14.616	517.79
7	6.671	1.043	98.38	98.39	0.0	98.39	0.0882	0.0	-0.74	0.005	14.696	518.60	14.616	517.79
8	6.426	1.022	98.25	98.25	0.0	98.25	0.0881	0.0	-0.61	0.004	14.696	518.60	14.616	517.80
9	6.171	0.998	98.14	98.15	0.0	98.15	0.0880	0.0	-0.45	0.002	14.696	518.60	14.617	517.80
10	5.905	0.972	98.11	98.11	0.0	98.11	0.0879	0.0	-0.25	-0.002	14.696	518.60	14.617	517.80
11	5.625	0.944	98.25	98.25	0.0	98.25	0.0881	0.0	-0.03	-0.011	14.696	518.60	14.616	517.80
HUB	5.600	0.941												

STREAMLINE NO.	R/RTIP	REL.FLOW ANGLE (DEG)	REL. TANG.VEL. (FT/SEC)	REL. VEL. (FT/SEC)	REL.MACH NUMBER	WHEEL SPEED (FT/SEC)	FLOW COEF.	L.E.RAD. /CHORD	MAX.TH. /CHORD	MAX.TH. PT.LOC. /CHORD	TRAN.PT. LOCATION /CHORD	SEGMENT IN/OUT TURN.RATE	LAYOUT CONE ANG. (DEG)
TIP	1.0000					167.57							
1	0.9977	59.56	167.19	193.92	0.1738	167.19	0.5863	0.0100	0.0600	0.5000	0.5000	1.0000	-0.77
2	0.9723	58.85	162.92	190.37	0.1706	162.92	0.5875	0.0100	0.0635	0.5000	0.5000	1.0000	-1.05
3	0.9462	58.12	158.55	186.71	0.1674	158.55	0.5883	0.0100	0.0670	0.5000	0.5000	1.0000	-0.96
4	0.9194	57.37	154.07	182.94	0.1640	154.07	0.5886	0.0100	0.0706	0.5000	0.5000	1.0000	-0.83
5	0.8918	56.58	149.44	179.04	0.1605	149.44	0.5884	0.0100	0.0744	0.5000	0.5000	1.0000	-0.70
6	0.8633	55.75	144.67	175.02	0.1569	144.67	0.5878	0.0100	0.0782	0.5000	0.5000	1.0000	-0.59
7	0.8338	54.85	139.73	170.89	0.1532	139.73	0.5871	0.0100	0.0823	0.5000	0.5000	1.0000	-0.47
8	0.8032	53.87	134.60	166.64	0.1494	134.60	0.5863	0.0100	0.0864	0.5000	0.5000	1.0000	-0.34
9	0.7713	52.79	129.25	162.29	0.1455	129.25	0.5857	0.0100	0.0907	0.5000	0.5000	1.0000	-0.22
10	0.7380	51.57	123.67	157.87	0.1415	123.67	0.5855	0.0100	0.0953	0.5000	0.5000	1.0000	-0.10
11	0.7032	50.18	117.83	153.42	0.1375	117.83	0.5863	0.0100	0.1000	0.5000	0.5000	1.0000	-0.00
HUB	0.6999												

--- INLET STREAMLINE --- ++++++++++++++++++++++++++++++++++ LAYOUT CONE ++

STREAMLINE NO.	PCT. SPAN	INC. ANGLE (DEG)	S.S.INC. ANGLE (DEG)	IN.BLADE ANGLE (DEG)	IN.BLADE ANGLE (DEG)	TRAN.PT. BL.ANGLE (DEG)	BLD.SET ANGLE (DEG)	1ST SEG. S.S.CAM. (DEG)	MACH NO. AT SHOCK LOCATION	SH.LOC. AS FRACT OF S.S.	COV.CHAN. AS FRACT OF S.S.	MIN.CHK. AREA MARGIN	MIN.CHK. PT.LOC.IN COV.CHAN.	L.E.EDGE CIR.CENT. R*DB/DR
1	0.77	-1.94	-6.58	61.50	61.50	53.07	53.06	13.07	0.2739	0.7925	0.2075	2.6806	0.0	-0.0646
2	9.24	0.22	-4.95	58.64	58.64	53.15	53.15	10.55	0.2526	0.7668	0.2332	2.6555	0.0	-0.0459
3	17.93	0.72	-4.76	57.40	57.40	52.32	52.32	10.56	0.2447	0.7366	0.2634	2.6635	0.0	-0.0407
4	26.85	0.84	-5.06	56.53	56.53	51.21	51.21	11.22	0.2396	0.7052	0.2948	2.7131	0.0	-0.0419
5	36.05	0.94	-5.39	55.65	55.65	49.99	49.99	11.98	0.2343	0.6730	0.3270	2.7712	0.0	-0.0434
6	45.54	1.04	-5.72	54.70	54.70	48.66	48.66	12.81	0.2287	0.6402	0.3598	2.8321	0.0	-0.0460
7	55.37	1.16	-6.07	53.69	53.69	47.20	47.20	13.71	0.2228	0.6066	0.3934	2.8969	0.0	-0.0505
8	65.57	1.28	-6.42	52.59	52.59	45.58	45.58	14.71	0.2164	0.5720	0.4280	2.9662	0.0	-0.0567
9	76.19	1.41	-6.78	51.38	51.37	43.75	43.75	15.81	0.2097	0.5363	0.4637	3.0404	0.0	-0.0650
10	87.29	1.56	-7.13	50.02	50.01	41.67	41.67	17.03	0.2025	0.4993	0.5007	3.1186	0.0474	-0.0762
11	98.90	1.74	-7.48	48.44	48.44	39.28	39.28	18.38	0.1947	0.4606	0.5394	3.1933	0.0960	-0.0884

Table 9.2. Continued.

** VALUES OF PARAMETERS ON STREAMLINES AT STATION, 6, WHICH IS THE OUTLET OF ROTOR NUMBER, 1 **

STREAMLINE NO.	RADIUS (IN.)	AXIAL COORD. (IN.)	AXIAL VEL. (FT/SEC)	MERD. VEL. (FT/SEC)	TANG. VEL. (FT/SEC)	ABS. VEL. (FT/SEC)	ABS. MACH NO.	ABS.FLOW ANGLE (DEG)	STREAM. SLOPE (DEG)	STREAM. CURV. (1./IN.)	TOTAL PRESS. (PSIA)	TOTAL TEMP. (DEG.R.)	STATIC PRESS. (PSIA)	STATIC TEMP. (DEG.R.)
TIP	8.000	2.603												
1	7.963	2.600	90.29	90.30	54.52	105.48	0.0944	31.12	-0.91	-0.001	14.786	520.12	14.694	519.19
2	7.752	2.582	98.38	98.39	39.45	106.00	0.0949	21.85	-0.93	0.007	14.786	519.67	14.693	518.73
3	7.546	2.594	100.14	100.14	36.95	106.75	0.0956	20.25	-0.77	0.008	14.786	519.57	14.692	518.62
4	7.334	2.614	100.08	100.08	37.89	107.02	0.0958	20.74	-0.59	0.007	14.786	519.57	14.691	518.62
5	7.116	2.635	99.93	99.93	39.16	107.33	0.0961	21.40	-0.44	0.007	14.786	519.57	14.691	518.61
6	6.891	2.658	99.79	99.79	40.44	107.67	0.0964	22.06	-0.31	0.007	14.786	519.57	14.690	518.61
7	6.659	2.683	99.65	99.65	41.86	108.09	0.0968	22.79	-0.17	0.007	14.786	519.57	14.689	518.60
8	6.416	2.710	99.51	99.51	43.44	108.58	0.0972	23.59	-0.04	0.007	14.786	519.57	14.688	518.59
9	6.165	2.739	99.33	99.33	45.22	109.13	0.0977	24.48	0.12	0.009	14.786	519.57	14.687	518.58
10	5.902	2.771	99.07	99.07	47.24	109.76	0.0983	25.49	0.30	0.013	14.786	519.57	14.686	518.57
11	5.626	2.806	98.62	98.63	49.59	110.39	0.0989	26.69	0.60	0.022	14.786	519.57	14.685	518.56
HUB	5.600	2.809												

STREAMLINE NO.	R/RTIP	REL.FLOW ANGLE (DEG)	REL. TANG.VEL. (FT/SEC)	REL. VEL. (FT/SEC)	REL.MACH NUMBER	WHEEL SPEED (FT/SEC)	FLOW COEF.	HEAD COEF.	IDEAL HEAD COEF.	ADIAB. EFF.	DIFFUSION FACTOR	LOSS COEF.	SHOCK LOSS COEF.	ELEMENT SOLIDITY
TIP	1.0000													
1	0.9954	51.19	112.26	144.07	0.1290	166.77	0.5388	0.1933	0.3238	0.5969	0.3971	0.1964	0.0	1.0027
2	0.9691	51.32	122.92	157.44	0.1410	162.36	0.5871	0.1933	0.2281	0.8474	0.2734	0.0544	0.0	1.0295
3	0.9432	50.41	121.08	157.13	0.1407	158.03	0.5976	0.1933	0.2080	0.9293	0.2519	0.0239	0.0	1.0577
4	0.9168	49.14	115.71	152.99	0.1370	153.61	0.5972	0.1933	0.2073	0.9324	0.2587	0.0237	0.0	1.0884
5	0.8896	47.72	109.89	148.53	0.1330	149.04	0.5963	0.1933	0.2078	0.9299	0.2678	0.0257	0.0	1.1219
6	0.8614	46.15	103.88	144.05	0.1290	144.33	0.5955	0.1933	0.2079	0.9297	0.2766	0.0270	0.0	1.1587
7	0.8323	44.40	97.58	139.48	0.1249	139.45	0.5947	0.1933	0.2079	0.9296	0.2858	0.0283	0.0	1.1995
8	0.8021	42.42	90.94	134.80	0.1207	134.38	0.5938	0.1933	0.2079	0.9296	0.2957	0.0298	0.0	1.2449
9	0.7706	40.19	83.90	130.02	0.1164	129.11	0.5927	0.1933	0.2079	0.9296	0.3063	0.0314	0.0	1.2960
10	0.7378	37.63	76.37	125.09	0.1120	123.61	0.5912	0.1933	0.2079	0.9294	0.3181	0.0333	0.0	1.3541
11	0.7033	34.68	68.24	119.93	0.1074	117.83	0.5885	0.1933	0.2081	0.9288	0.3320	0.0355	0.0	1.4209
HUB	0.7000													

STREAMLINE NO.	PCT. SPAN	PRESS. RATIO	TEMP. RATIO	AERO. CHORD (IN.)	MEAN SPACING (IN.)	LOCAL BLADE FORCES RADIUS (IN.)	LOCAL BLADE FORCES FOR.AXIAL (LBS/IN)	LOCAL BLADE FORCES TANG. (LBS/IN)	--- OUTLET STREAMLINE --- T.E.RAD. /CHORD	DEV. ANGLE (DEG)	OUT.BLADE ANGLE (DEG)	++ LAYOUT CONE +++ OUT.BLADE ANGLE (DEG)	MAX.CAMB. PT.LOC. /CHORD	T.E.EDGE CIR.CENT R*DΘ/DR
1	1.54	1.0061	1.0029	2.3919	2.3854	7.973	0.1549	-0.2046	0.0100	6.53	44.66	44.63	0.5000	-0.3871
2	10.31	1.0061	1.0021	2.3919	2.3235	7.766	0.1783	-0.1478	0.0100	3.66	47.66	47.67	0.5000	-0.1348
3	18.92	1.0061	1.0019	2.3919	2.2613	7.558	0.1769	-0.1366	0.0100	3.17	47.24	47.24	0.5000	0.0262
4	27.73	1.0061	1.0019	2.3919	2.1977	7.345	0.1706	-0.1363	0.0100	3.24	45.90	45.89	0.5000	0.0618
5	36.81	1.0061	1.0019	2.3919	2.1320	7.126	0.1638	-0.1365	0.0100	3.38	44.34	44.33	0.5000	0.0675
6	46.19	1.0061	1.0019	2.3918	2.0643	6.899	0.1568	-0.1364	0.0100	3.51	42.64	42.63	0.5000	0.0725
7	55.90	1.0061	1.0019	2.3918	1.9941	6.665	0.1496	-0.1362	0.0100	3.66	40.73	40.72	0.5000	0.0799
8	65.97	1.0061	1.0019	2.3918	1.9213	6.421	0.1420	-0.1360	0.0100	3.84	38.59	38.57	0.5000	0.0888
9	76.46	1.0061	1.0019	2.3918	1.8455	6.168	0.1340	-0.1357	0.0100	4.04	36.15	36.13	0.5000	0.0996
10	87.41	1.0061	1.0019	2.3918	1.7663	5.903	0.1255	-0.1355	0.0100	4.26	33.37	33.34	0.5000	0.1129
11	98.90	1.0061	1.0019	2.3918	1.6833	5.626	0.1164	-0.1389	0.0100	4.51	30.17	30.12	0.5000	0.1265

Table 9.2. Continued.

** VALUES OF PARAMETERS ON STREAMLINES AT STATION. 7. WHICH IS THE INLET OF STATOR NUMBER. 1. OF STAGE NUMBER. 1 **

STREAMLINE NO.	RADIUS (IN.)	AXIAL COORD. (IN.)	AXIAL VEL. (FT/SEC)	MERD. VEL. (FT/SEC)	TANG. VEL. (FT/SEC)	ABS. VEL. (FT/SEC)	ABS. MACH NO.	ABS.FLOW ANGLE (DEG)	STREAM. SLOPE (DEG)	STREAM. CURV. (1./IN.)	TOTAL PRESS. (PSIA)	TOTAL TEMP. (DEG.R.)	STATIC PRESS. (PSIA)	STATIC TEMP. (DEG.R.)
TIP	8.000	3.470												
1	7.951	3.512	91.79	91.79	54.60	106.80	0.0956	30.75	-0.48	0.017	14.786	520.12	14.692	519.16
2	7.742	3.695	99.75	99.75	39.50	107.29	0.0961	21.60	-0.15	0.016	14.786	519.67	14.691	518.71
3	7.537	3.861	101.33	101.33	37.00	107.88	0.0966	20.06	0.01	0.013	14.786	519.57	14.690	518.60
4	7.329	3.993	101.16	101.16	37.92	108.04	0.0968	20.55	0.11	0.010	14.786	519.57	14.689	518.60
5	7.113	4.085	100.96	100.96	39.18	108.29	0.0970	21.21	0.17	0.007	14.786	519.57	14.689	518.60
6	6.890	4.131	100.82	100.82	40.45	108.63	0.0973	21.86	0.21	0.005	14.786	519.57	14.688	518.59
7	6.660	4.128	100.72	100.72	41.85	109.07	0.0977	22.57	0.26	0.003	14.786	519.57	14.687	518.58
8	6.421	4.071	100.63	100.63	43.41	109.60	0.0982	23.34	0.31	0.001	14.786	519.57	14.686	518.57
9	6.171	3.953	100.56	100.57	45.17	110.24	0.0987	24.19	0.40	-0.001	14.786	519.57	14.685	518.56
10	5.911	3.766	100.48	100.49	47.17	111.01	0.0994	25.15	0.55	-0.004	14.786	519.57	14.684	518.55
11	5.635	3.499	100.41	100.42	49.50	111.96	0.1003	26.24	0.84	-0.010	14.786	519.57	14.682	518.53
HUB	5.600	3.464												

STREAMLINE NO.	R/RTIP	FLOW COEF.	REL.FLOW ANGLE (DEG)	L.E.RAD. /CHORD	MAX.TH. /CHORD	MAX.TH. PT.LOC. /CHORD	TRAN.PT. LOCATION /CHORD	SEGMENT IN/OUT TURN.RATE	LAYOUT CONE ANG. (DEG)
TIP	1.0000								
1	0.9939	0.5478	50.64	0.0100	0.1000	0.5000	0.5000	1.0000	0.25
2	0.9678	0.5953	50.98	0.0100	0.0964	0.5000	0.5000	1.0000	0.41
3	0.9422	0.6047	50.02	0.0100	0.0929	0.5000	0.5000	1.0000	0.40
4	0.9161	0.6037	48.80	0.0100	0.0892	0.5000	0.5000	1.0000	0.36
5	0.8892	0.6025	47.40	0.0100	0.0855	0.5000	0.5000	1.0000	0.33
6	0.8614	0.6016	45.85	0.0100	0.0817	0.5000	0.5000	1.0000	0.30
7	0.8325	0.6010	44.11	0.0100	0.0777	0.5000	0.5000	1.0000	0.28
8	0.8026	0.6005	42.14	0.0100	0.0736	0.5000	0.5000	1.0000	0.27
9	0.7715	0.6001	39.90	0.0100	0.0693	0.5000	0.5000	1.0000	0.27
10	0.7389	0.5996	37.33	0.0100	0.0647	0.5000	0.5000	1.0000	0.28
11	0.7045	0.5992	34.31	0.0100	0.0600	0.5000	0.5000	1.0000	0.31
HUB	0.7000								

--- INLET STREAMLINE --- ++++++++++++++++++++++++++++++++ LAYOUT CONE ++

STREAMLINE NO.	PCT. SPAN	INC. ANGLE (DEG)	S.S.INC. ANGLE (DEG)	IN.BLADE ANGLE (DEG)	IN.BLADE ANGLE (DEG)	TRAN.PT. BL.ANGLE (DEG)	BLD.SET ANGLE (DEG)	1ST SEG. S.S.CAM. (DEG)	MACH NO. AT SHOCK LOCATION	SH.LOC. AS FRACT OF S.S.	COV.CHAN. AS FRACT OF S.S.	MIN.CHK. AREA MARGIN	MIN.CHK. PT.LOC.IN COV.CHAN.	L.E.EDGE CIR.CENT. R*D0/DR
1	2.04	2.07	-6.95	28.68	28.05	11.04	11.05	26.02	0.1187	0.2099	0.7453	4.5402	0.3568	-1.1351
2	10.74	1.47	-7.27	20.14	19.97	7.88	7.89	20.82	0.0961	0.1648	0.8005	4.3192	0.4151	-0.3404
3	19.26	1.21	-7.14	18.85	18.90	7.44	7.45	19.80	0.0966	0.1625	0.8031	4.3750	0.3927	0.1472
4	27.96	1.09	-6.84	19.46	19.50	7.65	7.65	19.79	0.0968	0.1708	0.7923	4.4434	0.3758	0.2085
5	36.94	1.04	-6.46	20.17	20.19	7.90	7.91	19.79	0.1022	0.1776	0.7837	4.4887	0.3616	0.1689
6	46.21	1.07	-5.99	20.79	20.80	8.15	8.16	19.71	0.1060	0.1810	0.7797	4.5146	0.3485	0.1199
7	55.82	1.20	-5.41	21.37	21.37	8.42	8.42	19.55	0.1090	0.1805	0.7810	4.5209	0.3376	0.0723
8	65.79	1.45	-4.68	21.88	21.88	8.70	8.71	19.31	0.1117	0.1757	0.7881	4.5079	0.3305	0.0309
9	76.18	1.85	-3.79	22.34	22.33	9.00	9.00	18.98	0.1142	0.1665	0.8008	4.4749	0.3288	0.0042
10	87.04	2.41	-2.72	22.74	22.74	9.30	9.30	18.56	0.1170	0.1536	0.8181	4.4217	0.3331	0.0025
11	98.48	3.12	-1.47	23.12	23.11	9.62	9.62	18.08	0.1202	0.1379	0.8386	4.3501	0.3386	0.0256

Table 9.2. Continued.

** VALUES OF PARAMETERS ON STREAMLINES AT STATION. 8. WHICH IS THE OUTLET OF STATOR NUMBER. 1. OF STAGE NUMBER. 1 **

STREAMLINE NO.	RADIUS (IN.)	AXIAL COORD. (IN.)	AXIAL VEL. (FT/SEC)	MERD. VEL. (FT/SEC)	TANG. VEL. (FT/SEC)	ABS. VEL. (FT/SEC)	ABS. MACH NO.	ABS.FLOW ANGLE (DEG)	STREAM. SLOPE (DEG)	STREAM. CURV. (1./IN.)	TOTAL PRESS. (PSIA)	TOTAL TEMP. (DEG.R.)	STATIC PRESS. (PSIA)	STATIC TEMP. (DEG.R.)
TIP	8.000	6.491												
1	7.963	6.490	99.05	99.05	0.0	99.05	0.0887	0.0	0.24	-0.009	14.784	520.12	14.703	519.30
2	7.762	6.488	99.50	99.50	0.0	99.50	0.0891	0.0	0.31	-0.010	14.784	519.67	14.703	518.84
3	7.556	6.486	99.74	99.75	0.0	99.75	0.0893	0.0	0.27	-0.009	14.784	519.57	14.702	518.74
4	7.344	6.485	99.90	99.90	0.0	99.90	0.0895	0.0	0.22	-0.008	14.784	519.57	14.702	518.74
5	7.127	6.484	100.02	100.02	0.0	100.02	0.0896	0.0	0.18	-0.007	14.784	519.57	14.702	518.74
6	6.903	6.484	100.12	100.12	0.0	100.12	0.0897	0.0	0.15	-0.006	14.784	519.57	14.701	518.74
7	6.671	6.484	100.19	100.19	0.0	100.19	0.0897	0.0	0.12	-0.005	14.784	519.57	14.701	518.74
8	6.432	6.484	100.23	100.23	0.0	100.23	0.0898	0.0	0.10	-0.004	14.784	519.57	14.701	518.74
9	6.183	6.486	100.22	100.22	0.0	100.22	0.0897	0.0	0.08	-0.003	14.784	519.57	14.701	518.74
10	5.924	6.488	100.13	100.13	0.0	100.13	0.0897	0.0	0.07	-0.002	14.784	519.57	14.701	518.74
11	5.652	6.490	99.91	99.91	0.0	99.91	0.0899	0.0	0.13	0.002	14.783	519.57	14.701	518.74
HUB	5.600	6.491												

STREAMLINE NO.	R/RTIP	FLOW COEF.	HEAD COEF.	IDEAL HEAD COEF.	STATOR PO.RATIO	STAGE PO.RATIO	STAGE AD.EFF.	DIFFUSION FACTOR	STATOR LOSS COEF.	SHOCK LOSS COEF.	ELEMENT SOLIDITY	AERO. CHORD (IN.)	MEAN SPACING (IN.)
TIP	1.0000												
1	0.9954	0.5911	0.1892	0.3238	0.9999	1.0060	0.5843	0.2129	0.0201	0.0	1.8200	3.0331	1.6665
2	0.9702	0.5938	0.1903	0.2281	0.9999	1.0060	0.8345	0.1785	0.0144	0.0	1.7365	2.8192	1.6235
3	0.9444	0.5952	0.1904	0.2080	0.9999	1.0060	0.9156	0.1776	0.0138	0.0	1.6747	2.6470	1.5805
4	0.9180	0.5961	0.1903	0.2073	0.9999	1.0060	0.9183	0.1825	0.0141	0.0	1.6360	2.5138	1.5365
5	0.8908	0.5969	0.1902	0.2078	0.9999	1.0060	0.9152	0.1876	0.0146	0.0	1.6244	2.4222	1.4912
6	0.8628	0.5975	0.1901	0.2079	0.9999	1.0060	0.9143	0.1914	0.0153	0.0	1.6452	2.3764	1.4444
7	0.8339	0.5979	0.1898	0.2079	0.9999	1.0060	0.9132	0.1938	0.0162	0.0	1.7054	2.3808	1.3961
8	0.8040	0.5981	0.1896	0.2079	0.9999	1.0060	0.9118	0.1946	0.0173	0.0	1.8137	2.4411	1.3459
9	0.7729	0.5981	0.1892	0.2079	0.9999	1.0060	0.9100	0.1942	0.0189	0.0	1.9818	2.5639	1.2937
10	0.7404	0.5975	0.1887	0.2079	0.9999	1.0060	0.9073	0.1933	0.0210	0.0	2.2252	2.7576	1.2393
11	0.7065	0.5962	0.1878	0.2081	0.9998	1.0059	0.9028	0.1937	0.0243	0.0	2.5659	3.0331	1.1821
HUB	0.7000												

STREAMLINE NO.	PCT. SPAN	LOCAL BLADE FORCES RADIUS (IN.)	FOR.AXIAL (LBS/IN)	TANG. (LBS/IN)	--- OUTLET STREAMLINE --- T.E.RAD. /CHORD	DEV. ANGLE (DEG)	OUT.BLADE ANGLE (DEG)	++ LAYOUT CONE +++ OUT.BLADE ANGLE (DEG)	MAX.CAMB. PT.LOC. /CHORD	T.E.EDGE CIR.CENT R*DB/DR
1	1.53	7.957	0.0380	0.1447	0.0100	5.96	-5.96	-5.96	0.5000	0.0
2	9.93	7.752	0.0186	0.1047	0.0100	4.21	-4.21	-4.21	0.5000	0.0
3	18.52	7.547	0.0157	0.0969	0.0100	4.01	-4.01	-4.01	0.5000	0.0
4	27.33	7.336	0.0161	0.0967	0.0100	4.21	-4.21	-4.21	0.5000	0.0
5	36.39	7.120	0.0167	0.0969	0.0100	4.39	-4.39	-4.39	0.5000	0.0
6	45.72	6.897	0.0173	0.0969	0.0100	4.50	-4.50	-4.50	0.5000	0.0
7	55.36	6.666	0.0179	0.0968	0.0100	4.53	-4.53	-4.53	0.5000	0.0
8	65.34	6.426	0.0186	0.0967	0.0100	4.48	-4.48	-4.48	0.5000	0.0
9	75.70	6.177	0.0193	0.0966	0.0100	4.34	-4.34	-4.34	0.5000	0.0
10	86.51	5.917	0.0201	0.0963	0.0100	4.14	-4.14	-4.14	0.5000	0.0
11	97.82	5.644	0.0209	0.0986	0.0100	3.88	-3.88	-3.88	0.5000	0.0

Table 9.2. Continued.

** VALUES OF PARAMETERS ON STREAMLINES AT STATION. 9. WHICH IS THE INLET OF ROTOR NUMBER. 2 **

STREAMLINE NO.	RADIUS (IN.)	AXIAL COORD. (IN.)	AXIAL VEL. (FT/SEC)	MERD. VEL. (FT/SEC)	TANG. VEL. (FT/SEC)	ABS. VEL. (FT/SEC)	ABS. MACH NO.	ABS.FLOW ANGLE (DEG)	STREAM. SLOPE (DEG)	STREAM. CURV. (1./IN.)	TOTAL PRESS. (PSIA)	TOTAL TEMP. (DEG.R.)	STATIC PRESS. (PSIA)	STATIC TEMP. (DEG.R.)
TIP	8.000	7.581												
1	7.963	7.578	98.90	98.91	0.0	98.91	0.0885	0.0	-0.27	-0.008	14.784	520.12	14.703	519.30
2	7.761	7.563	99.38	99.38	0.0	99.38	0.0890	0.0	-0.39	-0.012	14.784	519.67	14.703	518.84
3	7.555	7.547	99.67	99.67	0.0	99.67	0.0893	0.0	-0.36	-0.011	14.784	519.57	14.702	518.75
4	7.344	7.530	99.86	99.86	0.0	99.86	0.0894	0.0	-0.31	-0.010	14.784	519.57	14.702	518.74
5	7.126	7.513	100.02	100.02	0.0	100.02	0.0896	0.0	-0.25	-0.008	14.784	519.57	14.702	518.74
6	6.902	7.494	100.12	100.13	0.0	100.13	0.0897	0.0	-0.21	-0.006	14.784	519.57	14.701	518.74
7	6.671	7.474	100.19	100.19	0.0	100.19	0.0897	0.0	-0.17	-0.005	14.784	519.57	14.701	518.74
8	6.431	7.453	100.22	100.22	0.0	100.22	0.0897	0.0	-0.15	-0.004	14.784	519.57	14.701	518.74
9	6.183	7.430	100.23	100.23	0.0	100.23	0.0898	0.0	-0.14	-0.005	14.784	519.57	14.701	518.74
10	5.923	7.404	100.23	100.23	0.0	100.23	0.0898	0.0	-0.16	-0.007	14.784	519.57	14.701	518.74
11	5.652	7.376	100.33	100.33	0.0	100.33	0.0898	0.0	-0.23	-0.016	14.783	519.57	14.700	518.73
HUB	5.600	7.371												

STREAMLINE NO.	R/RTIP	REL.FLOW ANGLE (DEG)	REL. TANG.VEL. (FT/SEC)	REL. VEL. (FT/SEC)	REL.MACH NUMBER	WHEEL SPEED (FT/SEC)	FLOW COEF.	L.E.RAD. /CHORD	MAX.TH. /CHORD	MAX.TH. PT.LOC. /CHORD	TRAN.PT. LOCATION /CHORD	SEGMENT IN/OUT TURN.RATE	LAYOUT CONE ANG. (DEG)
TIP	1.0000					167.55							
1	0.9954	59.33	166.78	193.90	0.1735	166.78	0.5903	0.0100	0.0600	0.5000	0.5000	1.0000	-0.72
2	0.9702	58.56	162.55	190.53	0.1706	162.55	0.5931	0.0100	0.0635	0.5000	0.5000	1.0000	-0.94
3	0.9444	57.79	158.23	187.01	0.1675	158.23	0.5949	0.0100	0.0671	0.5000	0.5000	1.0000	-0.83
4	0.9180	57.00	153.80	183.38	0.1642	153.80	0.5960	0.0100	0.0707	0.5000	0.5000	1.0000	-0.68
5	0.8908	56.17	149.25	179.66	0.1609	149.25	0.5969	0.0100	0.0745	0.5000	0.5000	1.0000	-0.53
6	0.8628	55.29	144.56	175.85	0.1575	144.56	0.5976	0.0100	0.0784	0.5000	0.5000	1.0000	-0.40
7	0.8339	54.35	139.71	171.93	0.1540	139.71	0.5980	0.0100	0.0824	0.5000	0.5000	1.0000	-0.28
8	0.8039	53.35	134.70	167.89	0.1503	134.70	0.5982	0.0100	0.0865	0.5000	0.5000	1.0000	-0.17
9	0.7725	52.26	129.49	163.74	0.1466	129.49	0.5982	0.0100	0.0908	0.5000	0.5000	1.0000	-0.07
10	0.7404	51.06	124.06	159.49	0.1428	124.06	0.5982	0.0100	0.0953	0.5000	0.5000	1.0000	-0.00
11	0.7066	49.72	118.38	155.18	0.1390	118.38	0.5988	0.0100	0.1000	0.5000	0.5000	1.0000	0.01
HUB	0.7000												

--- INLET STREAMLINE --- ++++++++++++++++++++++++++++++++++++ LAYOUT CONE ++

STREAMLINE NO.	PCT. SPAN	INC. ANGLE (DEG)	S.S.INC. ANGLE (DEG)	IN.BLADE ANGLE (DEG)	IN.BLADE ANGLE (DEG)	TRAN.PT. BL.ANGLE (DEG)	BLD.SET ANGLE (DEG)	1ST SEG. S.S.CAM. (DEG)	MACH NO. AT SHOCK LOCATION	SH.LOC. AS FRACT OF S.S.	COV.CHAN. AS FRACT OF S.S.	MIN.CHK. AREA MARGIN	MIN.CHK. PT.LOC.IN COV.CHAN.	L.E.EDGE CIR.CENT. R*D0/DR
1	1.54	-1.91	-6.55	61.24	61.24	52.60	52.60	13.28	0.2749	0.7883	0.2117	2.6871	0.0	-0.0386
2	9.94	-0.02	-5.08	58.58	58.58	52.53	52.52	11.12	0.2556	0.7619	0.2381	2.6616	0.0	-0.0409
3	18.54	0.51	-4.97	57.28	57.29	51.68	51.66	11.08	0.2474	0.7318	0.2682	2.6672	0.0	-0.0480
4	27.35	0.63	-5.27	56.38	56.38	50.51	50.50	11.78	0.2425	0.7002	0.2998	2.7131	0.0	-0.0518
5	36.41	0.73	-5.61	55.45	55.45	49.24	49.23	12.55	0.2372	0.6681	0.3319	2.7662	0.0	-0.0525
6	45.74	0.83	-5.94	54.46	54.46	47.86	47.86	13.38	0.2316	0.6354	0.3646	2.8223	0.0	-0.0547
7	55.38	0.94	-6.29	53.41	53.42	46.36	46.36	14.28	0.2257	0.6019	0.3981	2.8820	0.0	-0.0581
8	65.36	1.06	-6.64	52.29	52.29	44.70	44.70	15.29	0.2195	0.5677	0.4323	2.9464	0.0	-0.0629
9	75.72	1.18	-7.00	51.08	51.08	42.86	42.86	16.40	0.2128	0.5326	0.4674	3.0163	0.0	-0.0697
10	86.52	1.32	-7.36	49.74	49.74	40.77	40.77	17.65	0.2058	0.4963	0.5037	3.0933	0.0052	-0.0799
11	97.81	1.48	-7.72	48.24	48.23	38.37	38.37	19.06	0.1984	0.4586	0.5414	3.1695	0.0557	-0.0917

Table 9.2. Continued.

** VALUES OF PARAMETERS ON STREAMLINES AT STATION, 10, WHICH IS THE OUTLET OF ROTOR NUMBER, 2 **

STREAMLINE NO.	RADIUS (IN.)	AXIAL COORD. (IN.)	AXIAL VEL. (FT/SEC)	MERD. VEL. (FT/SEC)	TANG. VEL. (FT/SEC)	ABS. VEL. (FT/SEC)	ABS. MACH NO.	ABS.FLOW ANGLE (DEG)	STREAM. SLOPE (DEG)	STREAM. CURV. (1./IN.)	TOTAL PRESS. (PSIA)	TOTAL TEMP. (DEG.R.)	STATIC PRESS. (PSIA)	STATIC TEMP. (DEG.R.)
TIP	8.000	9.050												
1	7.945	9.046	92.20	92.22	54.42	107.08	0.0957	30.54	-1.30	-0.017	14.879	521.62	14.784	520.67
2	7.737	9.033	99.45	99.47	41.45	107.76	0.0964	22.62	-1.14	-0.006	14.879	520.79	14.783	519.82
3	7.533	9.045	101.44	101.45	38.80	108.62	0.0972	20.93	-0.90	-0.001	14.879	520.59	14.781	519.61
4	7.325	9.065	101.60	101.60	39.84	109.13	0.0976	21.41	-0.66	0.001	14.879	520.59	14.780	519.60
5	7.112	9.087	101.55	101.55	41.13	109.56	0.0980	22.05	-0.46	0.003	14.879	520.59	14.779	519.59
6	6.891	9.111	101.48	101.48	42.49	110.02	0.0984	22.72	-0.26	0.005	14.879	520.59	14.779	519.59
7	6.663	9.136	101.36	101.36	44.00	110.50	0.0989	23.47	-0.08	0.007	14.879	520.60	14.778	519.58
8	6.426	9.163	101.16	101.16	45.70	111.01	0.0993	24.31	0.13	0.010	14.879	520.60	14.777	519.57
9	6.180	9.192	100.86	100.86	47.62	111.54	0.0998	25.27	0.37	0.015	14.879	520.60	14.776	519.56
10	5.923	9.223	100.34	100.35	49.85	112.05	0.1003	26.42	0.72	0.024	14.879	520.60	14.775	519.56
11	5.653	9.258	99.35	99.37	52.52	112.40	0.1006	27.86	1.34	0.045	14.879	520.61	14.774	519.56
HUB	5.600	9.264												

STREAMLINE NO.	R/RTIP	REL.FLOW ANGLE (DEG)	REL. TANG.VEL. (FT/SEC)	REL. VEL. (FT/SEC)	REL.MACH NUMBER	WHEEL SPEED (FT/SEC)	FLOW COEF.	HEAD COEF.	IDEAL HEAD COEF.	ADIAB. EFF.	DIFFUSION FACTOR	LOSS COEF.	SHOCK LOSS COEF.	ELEMENT SOLIDITY
TIP	1.0000													
1	0.9931	50.53	111.97	145.06	0.1297	166.39	0.5503	0.2043	0.3225	0.6335	0.3917	0.1779	0.0	1.0027
2	0.9672	50.43	120.59	156.32	0.1398	162.05	0.5935	0.2030	0.2393	0.8484	0.2851	0.0566	0.0	1.0292
3	0.9417	49.55	118.98	156.36	0.1399	157.78	0.6054	0.2029	0.2181	0.9303	0.2619	0.0246	0.0	1.0572
4	0.9157	48.19	113.59	152.40	0.1364	153.42	0.6064	0.2030	0.2177	0.9322	0.2687	0.0248	0.0	1.0874
5	0.8890	46.71	107.81	148.11	0.1325	148.94	0.6061	0.2031	0.2182	0.9306	0.2777	0.0265	0.0	1.1203
6	0.8614	45.10	101.83	143.76	0.1286	144.32	0.6057	0.2033	0.2185	0.9304	0.2869	0.0278	0.0	1.1564
7	0.8329	43.31	95.54	139.29	0.1246	139.55	0.6049	0.2035	0.2187	0.9302	0.2968	0.0292	0.0	1.1962
8	0.8033	41.31	88.90	134.67	0.1205	134.59	0.6038	0.2037	0.2191	0.9300	0.3075	0.0308	0.0	1.2405
9	0.7725	39.05	81.82	129.87	0.1162	129.44	0.6020	0.2041	0.2196	0.9296	0.3195	0.0325	0.0	1.2902
10	0.7404	36.48	74.21	124.81	0.1117	124.06	0.5989	0.2047	0.2203	0.9291	0.3335	0.0347	0.0	1.3464
11	0.7066	33.54	65.87	119.22	0.1067	118.39	0.5929	0.2055	0.2215	0.9277	0.3516	0.0375	0.0	1.4109
HUB	0.7000													

STREAMLINE NO.	PCT. SPAN	PRESS. RATIO	TEMP. RATIO	AERO. CHORD (IN.)	MEAN SPACING (IN.)	LOCAL BLADE FORCES RADIUS (IN.)	LOCAL BLADE FORCES FOR.AXIAL (LBS/IN)	LOCAL BLADE FORCES TANG. (LBS/IN)	--- OUTLET STREAMLINE --- T.E.RAD. /CHORD	--- OUTLET STREAMLINE --- DEV. ANGLE (DEG)	--- OUTLET STREAMLINE --- OUT.BLADE ANGLE (DEG)	++ LAYOUT CONE +++ OUT.BLADE ANGLE (DEG)	++ LAYOUT CONE +++ MAX.CAMB. PT.LOC. /CHORD	++ LAYOUT CONE +++ T.E.EDGE CIR.CENT RΦDΘ/DR
1	2.31	1.0064	1.0029	2.3862	2.3798	7.954	0.1674	-0.2067	0.0100	6.48	44.04	43.96	0.5000	-0.2969
2	10.95	1.0064	1.0022	2.3862	2.3186	7.749	0.1859	-0.1573	0.0100	4.00	46.48	46.47	0.5000	-0.1022
3	19.44	1.0064	1.0020	2.3862	2.2572	7.544	0.1848	-0.1454	0.0100	3.47	46.08	46.08	0.5000	0.0335
4	28.11	1.0064	1.0020	2.3862	2.1945	7.335	0.1782	-0.1456	0.0100	3.56	44.63	44.63	0.5000	0.0718
5	37.02	1.0064	1.0020	2.3862	2.1300	7.119	0.1712	-0.1460	0.0100	3.69	43.03	43.02	0.5000	0.0760
6	46.21	1.0064	1.0020	2.3862	2.0634	6.897	0.1640	-0.1461	0.0100	3.83	41.27	41.26	0.5000	0.0810
7	55.72	1.0064	1.0020	2.3861	1.9947	6.667	0.1566	-0.1463	0.0100	3.99	39.32	39.31	0.5000	0.0878
8	65.57	1.0064	1.0020	2.3861	1.9235	6.429	0.1488	-0.1464	0.0100	4.17	37.13	37.12	0.5000	0.0962
9	75.82	1.0064	1.0020	2.3861	1.8495	6.181	0.1407	-0.1465	0.0100	4.36	34.67	34.64	0.5000	0.1069
10	86.54	1.0065	1.0020	2.3861	1.7722	5.923	0.1320	-0.1466	0.0100	4.62	31.86	31.80	0.5000	0.1209
11	97.81	1.0065	1.0020	2.3861	1.6912	5.653	0.1227	-0.1507	0.0100	4.90	28.64	28.51	0.5000	0.1358

Table 9.2. Continued.

** VALUES OF PARAMETERS ON STREAMLINES AT STATION, 11, WHICH IS THE INLET OF STATOR NUMBER, 1, OF STAGE NUMBER, 2 **

STREAMLINE NO.	RADIUS (IN.)	AXIAL COORD. (IN.)	AXIAL VEL. (FT/SEC)	MERD. VEL. (FT/SEC)	TANG. VEL. (FT/SEC)	ABS. VEL. (FT/SEC)	ABS. MACH NO.	ABS.FLOW ANGLE (DEG)	STREAM. SLOPE (DEG)	STREAM. CURV. (1./IN.)	TOTAL PRESS. (PSIA)	TOTAL TEMP. (DEG.R.)	STATIC PRESS. (PSIA)	STATIC TEMP. (DEG.R.)
TIP	8.000	9.885												
1	7.924	9.956	96.11	96.12	54.56	110.53	0.0988	29.58	-0.92	0.031	14.879	521.62	14.778	520.61
2	7.721	10.145	102.55	102.55	41.54	110.64	0.0990	22.05	-0.48	0.026	14.879	520.79	14.777	519.77
3	7.521	10.311	103.97	103.97	38.86	110.99	0.0993	20.49	-0.21	0.020	14.879	520.59	14.777	519.57
4	7.317	10.442	103.75	103.75	39.87	111.15	0.0995	21.02	-0.03	0.014	14.879	520.59	14.777	519.56
5	7.108	10.533	103.48	103.48	41.15	111.36	0.0996	21.68	0.08	0.010	14.879	520.59	14.776	519.56
6	6.891	10.579	103.32	103.32	42.48	111.72	0.1000	22.35	0.17	0.005	14.879	520.59	14.775	519.55
7	6.667	10.575	103.22	103.22	43.97	112.20	0.1004	23.07	0.25	0.001	14.879	520.60	14.775	519.55
8	6.435	10.519	103.17	103.17	45.63	112.81	0.1009	23.86	0.36	-0.004	14.879	520.60	14.773	519.54
9	6.194	10.401	103.18	103.18	47.51	113.59	0.1016	24.73	0.55	-0.010	14.879	520.60	14.772	519.52
10	5.941	10.215	103.18	103.19	49.70	114.54	0.1025	25.71	0.89	-0.018	14.879	520.60	14.770	519.51
11	5.674	9.950	103.20	103.25	52.32	115.75	0.1036	26.88	1.61	-0.032	14.879	520.61	14.768	519.49
HUB	5.600	9.877												

STREAMLINE NO.	R/RTIP	FLOW COEF.	REL.FLOW ANGLE (DEG)	L.E.RAD. /CHORD	MAX.TH. /CHORD	MAX.TH. PT.LOC. /CHORD	TRAN.PT. LOCATION /CHORD	SEGMENT IN/OUT TURN.RATE	LAYOUT CONE ANG. (DEG)
TIP	1.0000								
1	0.9905	0.5736	49.21	0.0100	0.1000	0.5000	0.5000	1.0000	0.41
2	0.9651	0.6120	49.52	0.0100	0.0964	0.5000	0.5000	1.0000	0.54
3	0.9401	0.6205	48.78	0.0100	0.0928	0.5000	0.5000	1.0000	0.51
4	0.9147	0.6192	47.54	0.0100	0.0892	0.5000	0.5000	1.0000	0.45
5	0.8885	0.6176	46.15	0.0100	0.0855	0.5000	0.5000	1.0000	0.39
6	0.8614	0.6167	44.59	0.0100	0.0816	0.5000	0.5000	1.0000	0.32
7	0.8334	0.6161	42.83	0.0100	0.0777	0.5000	0.5000	1.0000	0.26
8	0.8044	0.6158	40.83	0.0100	0.0735	0.5000	0.5000	1.0000	0.19
9	0.7742	0.6158	38.54	0.0100	0.0692	0.5000	0.5000	1.0000	0.13
10	0.7426	0.6158	35.91	0.0100	0.0648	0.5000	0.5000	1.0000	0.09
11	0.7092	0.6160	32.79	0.0100	0.0600	0.5000	0.5000	1.0000	0.09
HUB	0.7000								

		--- INLET STREAMLINE ---					+++++ LAYOUT CONE +++++						
STREAMLINE NO.	PCT. SPAN	INC. ANGLE (DEG)	S.S.INC. ANGLE (DEG)	IN.BLADE ANGLE (DEG)	IN.BLADE ANGLE (DEG)	TRAN.PT. BL.ANGLE (DEG)	BLD.SET ANGLE (DEG)	1ST SEG. S.S.CAM. (DEG)	MACH NO. AT SHOCK LOCATION	SH.LOC. AS FRACT OF S.S.	COV.CHAN. AS FRACT OF S.S.	MIN.CHK. AREA MARGIN	MIN.CHK. PT.LOC.IN COV.CHAN.	L.E.EDGE CIR.CENT. R*DB/DR
1	3.18	2.05	-6.99	27.53	26.60	10.45	10.46	25.19	0.1202	0.2010	0.7558	4.3399	0.3662	-0.8856
2	11.64	1.48	-7.24	20.57	20.35	8.02	8.03	21.05	0.0990	0.1675	0.7971	4.1950	0.4044	-0.2458
3	19.96	1.22	-7.12	19.27	19.37	7.63	7.64	20.08	0.0993	0.1661	0.7986	4.2540	0.3821	0.1567
4	28.44	1.10	-6.92	19.92	20.02	7.85	7.85	20.09	0.1013	0.1749	0.7873	4.3251	0.3618	0.2167
5	37.18	1.04	-6.45	20.64	20.69	8.09	8.10	20.09	0.1067	0.1817	0.7786	4.3741	0.3445	0.1737
6	46.20	1.06	-5.99	21.29	21.31	8.34	8.35	20.01	0.1103	0.1852	0.7745	4.4014	0.3283	0.1234
7	55.53	1.19	-5.41	21.88	21.88	8.61	8.62	19.87	0.1134	0.1848	0.7756	4.4085	0.3143	0.0738
8	65.21	1.45	-4.58	22.41	22.41	8.90	8.90	19.63	0.1161	0.1800	0.7827	4.3947	0.3050	0.0307
9	75.27	1.85	-3.79	22.88	22.88	9.20	9.20	19.31	0.1188	0.1709	0.7954	4.3582	0.3031	0.0037
10	85.80	2.41	-2.71	23.30	23.30	9.52	9.52	18.91	0.1217	0.1579	0.8128	4.2971	0.3115	0.0035
11	96.94	3.14	-1.44	23.74	23.71	9.85	9.85	18.44	0.1254	0.1421	0.8335	4.2183	0.3205	0.0298

Table 9.2. Continued.

** VALUES OF PARAMETERS ON STREAMLINES AT STATION. 12. WHICH IS THE OUTLET OF STATOR NUMBER. 1. OF STAGE NUMBER. 2 **

STREAMLINE NO.	RADIUS (IN.)	AXIAL COORD. (IN.)	AXIAL VEL. (FT/SEC)	MERD. VEL. (FT/SEC)	TANG. VEL. (FT/SEC)	ABS. VEL. (FT/SEC)	ABS. MACH NO.	ABS.FLOW ANGLE (DEG)	STREAM. SLOPE (DEG)	STREAM. CURV. (1./IN.)	TOTAL PRESS. (PSIA)	TOTAL TEMP. (DEG.R.)	STATIC PRESS. (PSIA)	STATIC TEMP. (DEG.R.)
TIP	8.000	12.931												
1	7.945	12.930	100.54	100.54	0.0	100.54	0.0899	0.0	0.40	-0.016	14.877	521.62	14.793	520.76
2	7.747	12.928	101.06	101.07	0.0	101.07	0.0904	0.0	0.44	-0.014	14.877	520.79	14.793	519.94
3	7.544	12.926	101.39	101.40	0.0	101.40	0.0907	0.0	0.41	-0.012	14.878	520.59	14.792	519.74
4	7.337	12.925	101.59	101.59	0.0	101.59	0.0909	0.0	0.36	-0.009	14.877	520.59	14.792	519.73
5	7.124	12.924	101.72	101.72	0.0	101.72	0.0910	0.0	0.30	-0.006	14.877	520.59	14.791	519.73
6	6.904	12.924	101.79	101.79	0.0	101.79	0.0911	0.0	0.23	-0.004	14.877	520.59	14.791	519.73
7	6.678	12.924	101.80	101.80	0.0	101.80	0.0911	0.0	0.16	-0.002	14.877	520.60	14.791	519.73
8	6.443	12.924	101.73	101.73	0.0	101.73	0.0910	0.0	0.07	-0.000	14.877	520.60	14.791	519.74
9	6.199	12.926	101.56	101.56	0.0	101.56	0.0909	0.0	-0.02	0.002	14.877	520.60	14.791	519.74
10	5.945	12.927	101.25	101.25	0.0	101.25	0.0906	0.0	-0.12	0.005	14.876	520.60	14.791	519.75
11	5.678	12.930	100.72	100.72	0.0	100.72	0.0901	0.0	-0.25	0.010	14.876	520.61	14.792	519.76
HUB	5.600	12.931												

STREAMLINE NO.	R/RTIP	FLOW COEF.	HEAD COEF.	IDEAL HEAD COEF.	STATOR PO.RATIO	STAGE PO.RATIO	STAGE AD.EFF.	DIFFUSION FACTOR	STATOR LOSS COEF.	SHOCK LOSS COEF.	ELEMENT SOLIDITY	AERO. CHORD (IN.)	MEAN SPACING (IN.)
TIP	1.0000												
1	0.9931	0.6000	0.1996	0.3225	0.9999	1.0063	0.6187	0.2258	0.0220	0.0	1.8200	3.0244	1.6617
2	0.9683	0.6032	0.1994	0.2393	0.9999	1.0063	0.8332	0.1945	0.0166	0.0	1.7354	2.8109	1.6197
3	0.9430	0.6051	0.1995	0.2181	0.9999	1.0063	0.9147	0.1910	0.0155	0.0	1.6726	2.6387	1.5776
4	0.9171	0.6053	0.1995	0.2177	0.9999	1.0063	0.9163	0.1957	0.0158	0.0	1.6330	2.5059	1.5346
5	0.8905	0.6071	0.1995	0.2182	0.9999	1.0063	0.9142	0.2004	0.0163	0.0	1.6204	2.4149	1.4903
6	0.8630	0.6075	0.1995	0.2185	0.9999	1.0063	0.9132	0.2047	0.0170	0.0	1.6401	2.3694	1.4447
7	0.8347	0.6076	0.1994	0.2187	0.9999	1.0063	0.9117	0.2079	0.0181	0.0	1.6988	2.3740	1.3975
8	0.8054	0.6071	0.1993	0.2191	0.9999	1.0063	0.9098	0.2102	0.0195	0.0	1.8049	2.4342	1.3486
9	0.7749	0.6062	0.1992	0.2196	0.9998	1.0063	0.9071	0.2120	0.0216	0.0	1.9698	2.5565	1.2978
10	0.7431	0.6043	0.1989	0.2203	0.9998	1.0063	0.9031	0.2141	0.0246	0.0	2.2088	2.7493	1.2447
11	0.7098	0.6011	0.1985	0.2215	0.9998	1.0063	0.8964	0.2186	0.0292	0.0	2.5441	3.0243	1.1888
HUB	0.7000												

STREAMLINE		LOCAL BLADE FORCES			--- OUTLET STREAMLINE ---			++ LAYOUT CONE +++		
NO.	PCT. SPAN	RADIUS (IN.)	FOR.AXIAL (LBS/IN)	TANG. (LBS/IN)	T.E.RAD. /CHORD	DEV. ANGLE (DEG)	OUT.BLADE ANGLE (DEG)	OUT.BLADE ANGLE (DEG)	MAX.CAMB. PT.LOC. /CHORD	T.E.EDGE CIR.CENT R*D@/DR
1	2.30	7.934	0.0372	0.1479	0.0100	5.70	-5.70	-5.70	0.5000	0.0
2	10.56	7.734	0.0204	0.1125	0.0100	4.30	-4.30	-4.30	0.5000	0.0
3	18.99	7.533	0.0172	0.1040	0.0100	4.11	-4.11	-4.11	0.5000	0.0
4	27.64	7.327	0.0177	0.1041	0.0100	4.32	-4.32	-4.32	0.5000	0.0
5	36.51	7.116	0.0184	0.1043	0.0100	4.50	-4.50	-4.50	0.5000	0.0
6	45.66	6.898	0.0190	0.1043	0.0100	4.62	-4.62	-4.62	0.5000	0.0
7	55.10	6.673	0.0197	0.1043	0.0100	4.66	-4.66	-4.66	0.5000	0.0
8	64.87	6.439	0.0205	0.1043	0.0100	4.61	-4.61	-4.61	0.5000	0.0
9	75.03	6.197	0.0213	0.1042	0.0100	4.47	-4.47	-4.47	0.5000	0.0
10	85.63	5.943	0.0222	0.1039	0.0100	4.26	-4.26	-4.26	0.5000	0.0
11	96.74	5.676	0.0231	0.1066	0.0100	4.01	-4.01	-4.01	0.5000	0.0

Table 9.2. Continued.

** VALUES OF PARAMETERS ON STREAMLINES AT STATION, 13, WHICH IS AN ANNULUS **

STREAMLINE NO.	RADIUS (IN.)	AXIAL COORD. (IN.)	AXIAL VEL. (FT/SEC)	MERD. VEL. (FT/SEC)	TANG. VEL. (FT/SEC)	ABS. VEL. (FT/SEC)	ABS. MACH NO.	ABS.FLOW ANGLE (DEG)	STREAM. SLOPE (DEG)	STREAM. CURV. (1./IN.)	TOTAL PRESS. (PSIA)	TOTAL TEMP. (DEG.R.)	STATIC PRESS. (PSIA)	STATIC TEMP. (DEG.R.)
TIP	8.000	14.500												
1	7.945	14.500	101.51	101.51	0.0	101.51	0.0907	0.0	-0.09	0.005	14.877	521.62	14.791	520.77
2	7.748	14.500	101.66	101.66	0.0	101.66	0.0909	0.0	-0.06	0.003	14.877	520.79	14.792	519.93
3	7.547	14.500	101.67	101.67	0.0	101.67	0.0910	0.0	-0.04	0.002	14.878	520.59	14.792	519.73
4	7.340	14.500	101.63	101.63	0.0	101.63	0.0909	0.0	-0.01	0.000	14.877	520.59	14.792	519.73
5	7.127	14.500	101.60	101.60	0.0	101.60	0.0909	0.0	0.00	-0.000	14.877	520.59	14.792	519.73
6	6.907	14.500	101.56	101.56	0.0	101.56	0.0909	0.0	0.01	-0.001	14.877	520.59	14.792	519.74
7	6.680	14.500	101.50	101.50	0.0	101.50	0.0908	0.0	0.02	-0.001	14.877	520.60	14.792	519.74
8	6.445	14.500	101.41	101.41	0.0	101.41	0.0907	0.0	0.02	-0.001	14.877	520.60	14.792	519.74
9	6.200	14.500	101.28	101.28	0.0	101.28	0.0906	0.0	0.03	-0.001	14.877	520.60	14.792	519.75
10	5.945	14.500	101.09	101.09	0.0	101.09	0.0904	0.0	0.03	-0.001	14.876	520.60	14.792	519.75
11	5.678	14.500	100.82	100.82	0.0	100.82	0.0902	0.0	0.05	-0.003	14.876	520.61	14.791	519.76
HUB	5.600	14.500												

** VALUES OF PARAMETERS ON STREAMLINES AT STATION, 14, WHICH IS AN ANNULUS **

STREAMLINE NO.	RADIUS (IN.)	AXIAL COORD. (IN.)	AXIAL VEL. (FT/SEC)	MERD. VEL. (FT/SEC)	TANG. VEL. (FT/SEC)	ABS. VEL. (FT/SEC)	ABS. MACH NO.	ABS.FLOW ANGLE (DEG)	STREAM. SLOPE (DEG)	STREAM. CURV. (1./IN.)	TOTAL PRESS. (PSIA)	TOTAL TEMP. (DEG.R.)	STATIC PRESS. (PSIA)	STATIC TEMP. (DEG.R.)
TIP	8.000	15.500												
1	7.945	15.500	101.39	101.39	0.0	101.39	0.0906	0.0	0.02	-0.001	14.877	521.62	14.792	520.77
2	7.748	15.500	101.63	101.63	0.0	101.63	0.0909	0.0	0.01	-0.001	14.877	520.79	14.792	519.93
3	7.547	15.500	101.69	101.69	0.0	101.69	0.0910	0.0	0.00	-0.000	14.878	520.59	14.792	519.73
4	7.340	15.500	101.68	101.68	0.0	101.68	0.0910	0.0	-0.00	0.000	14.877	520.59	14.792	519.73
5	7.127	15.500	101.64	101.64	0.0	101.64	0.0909	0.0	-0.00	0.000	14.877	520.59	14.792	519.73
6	6.907	15.500	101.59	101.59	0.0	101.59	0.0909	0.0	-0.00	0.000	14.877	520.59	14.792	519.73
7	6.680	15.500	101.52	101.52	0.0	101.52	0.0908	0.0	-0.00	-0.000	14.877	520.60	14.792	519.74
8	6.445	15.500	101.42	101.42	0.0	101.42	0.0907	0.0	-0.00	-0.000	14.877	520.60	14.792	519.74
9	6.200	15.500	101.27	101.27	0.0	101.27	0.0906	0.0	-0.00	-0.000	14.877	520.60	14.792	519.75
10	5.945	15.500	101.05	101.05	0.0	101.05	0.0904	0.0	-0.01	0.000	14.876	520.60	14.792	519.75
11	5.678	15.500	100.71	100.71	0.0	100.71	0.0901	0.0	-0.02	0.001	14.876	520.61	14.792	519.76
HUB	5.600	15.500												

Table 9.2. Concluded.

** VALUES OF PARAMETERS ON STREAMLINES AT STATION, 15, WHICH IS AN ANNULUS **

STREAMLINE NO.	RADIUS (IN.)	AXIAL COORD. (IN.)	AXIAL VEL. (FT/SEC)	MERD. VEL. (FT/SEC)	TANG. VEL. (FT/SEC)	ABS. VEL. (FT/SEC)	ABS. MACH NO.	ABS.FLOW ANGLE (DEG)	STREAM. SLOPE (DEG)	STREAM. CURV. (1./IN.)	TOTAL PRESS. (PSIA)	TOTAL TEMP. (DEG.R.)	STATIC PRESS. (PSIA)	STATIC TEMP. (DEG.R.)
TIP	8.000	16.500												
1	7.945	16.500	101.40	101.40	0.0	101.40	0.0906	0.0	-0.02	-0.001	14.877	521.62	14.792	520.77
2	7.748	16.500	101.63	101.63	0.0	101.63	0.0909	0.0	-0.01	-0.000	14.877	520.79	14.792	519.93
3	7.546	16.500	101.69	101.69	0.0	101.69	0.0910	0.0	-0.01	-0.000	14.878	520.59	14.792	519.73
4	7.340	16.500	101.68	101.68	0.0	101.68	0.0910	0.0	-0.00	0.000	14.877	520.59	14.792	519.73
5	7.127	16.500	101.64	101.64	0.0	101.64	0.0909	0.0	-0.00	0.000	14.877	520.59	14.792	519.73
6	6.907	16.500	101.59	101.59	0.0	101.59	0.0909	0.0	-0.00	0.000	14.877	520.59	14.792	519.73
7	6.680	16.500	101.52	101.52	0.0	101.52	0.0908	0.0	-0.00	-0.000	14.877	520.60	14.792	519.74
8	6.445	16.500	101.41	101.41	0.0	101.41	0.0907	0.0	-0.00	-0.000	14.877	520.60	14.792	519.74
9	6.200	16.500	101.27	101.27	0.0	101.27	0.0906	0.0	-0.00	-0.000	14.877	520.60	14.792	519.75
10	5.945	16.500	101.05	101.05	0.0	101.05	0.0904	0.0	-0.00	0.000	14.876	520.60	14.792	519.75
11	5.678	16.500	100.71	100.71	0.0	100.71	0.0901	0.0	0.01	0.000	14.876	520.61	14.792	519.76
HUB	5.600	16.500												

Table 9.3. Design code stage and overall performance predictions.

*** COMPUTED COMPRESSOR DESIGN PARAMETERS FOR A ROTATIONAL SPEED OF. 2400.0. RPM ***

** THE CORRECTED WEIGHTFLOW PER UNIT OF CASING ANNULAR AREA AT THE INLET FACE OF THE FIRST BLADE ROW IS 7.37 LBS/SEC/FT SQ **

** MASS AVERAGED ROTOR AND STAGE AERODYNAMIC PARAMETERS **

STAGE NO.	BLADE TYPE	FLOW COEF.	HEAD COEF.	ID. HEAD COEF.	PRESS. RATIO	TEMP. RATIO	ADIA. EFF.	POLY. EFF.	ASPECT RATIO	FOR. AX. THRUST (LBS)	GAS BENDING MOMENTS FOR. AX. (FT-LBS)	GAS BENDING MOMENTS TANG. (FT-LBS)	TORQUE (FT-LBS)	POWER (HP)
1	ROTOR	0.5871	0.1933	0.2157	1.0061	1.0019	0.8962	0.8962	1.00	7.54	0.037	-0.033		
1	STATOR	0.5983	0.1897	0.2157	1.0060	1.0019	0.8797	0.8798	1.01	-13.59	0.004	0.022	3.93	1.8[illegible]
2	ROTOR	0.5966	0.2036	0.2261	1.0064	1.0020	0.9003	0.9004	1.01	7.51	0.038	-0.034		
2	STATOR	0.6144	0.1993	0.2261	1.0063	1.0020	0.8814	0.8815	1.01	-13.46	0.004	0.022	4.12	1.88

** CUMULATIVE SUMS OF MASS AVERAGED ROTOR AND STAGE AERODYDAMIC PARAMETERS **

STAGE NO.	BLADE TYPE	WEIGHT FLOW (LBS/SEC)	TOTAL PRESS. (PSIA)	TOTAL TEMP. (DEG. R.)	PRESS. RATIO	TEMP. RATIO	HEAD COEF.	IDEAL HEAD COEF.	ADIA. EFF.	POLY. EFF.	FOR. AX. THRUST (LBS)	TORQUE (FT-LBS)	POWER (HP)	FRACT ENERGY
1	INLET	5.25	14.696	518.60										
1	ROTOR	5.25	14.786	519.61	1.0061	1.0019	0.1933	0.2157	0.8962	0.8962	7.54			
1	STATOR	5.25	14.784	519.61	1.0060	1.0019	0.1897	0.2157	0.8797	0.8798	-6.05	3.93	1.80	0.4882
2	ROTOR	5.25	14.879	520.67	1.0125	1.0040	0.3932	0.4418	0.8902	0.8903	1.27			
2	STATOR	5.25	14.877	520.67	1.0123	1.0040	0.3889	0.4418	0.8805	0.8807	-12.20	8.05	3.68	1.0000

Table 9.4 Modified-stator blade manufacturing coordinates generated by NASA design code.

** BLADE SECTION PROPERTIES OF STATOR NO. 1 FOLLOWING ROTOR NO. 1 **

NUMBER OF BLADES = 30.0 AXIAL LOCATION OF STACKING LINE IN COMPRESSOR = 5.460 IN.

BLADE SECTION NO.	RAD. LOC. (IN.)	STACKING POINT COORDINATES L (IN.)	STACKING POINT COORDINATES H (IN.)	SECTION SETTING ANGLE (DEG.)	BLADE SECTION C.G. COORDINATES L (IN.)	BLADE SECTION C.G. COORDINATES H (IN.)	SECTION AREA (IN.)**2	MOMENTS OF INERTIA THROUGH C.G. IMIN (IN.)**4	MOMENTS OF INERTIA THROUGH C.G. IMAX (IN.)**4	IMAX SETTING ANGLE (DEG.)	SECTION TORSION CONSTANT (IN.)**4	SECTION TWIST STIFFNESS (IN.)**6
1	8.020	3.1244	0.0310	13.813	1.5758	0.2547	0.73732	0.000000	0.01432	13.860	0.016801	0.137932
2	7.840	2.8999	0.0290	9.181	1.4640	0.1650	0.61107	0.000199	-1.48665	0.910	0.011383	14.271236
3	7.660	2.7251	0.0273	7.496	1.3774	0.1302	0.52229	0.000065	-1.07957	2.046	0.008090	8.936669
4	7.480	2.5947	0.0259	7.447	1.3066	0.1232	0.45653	0.000035	-0.82823	3.048	0.005978	6.046024

SECTION NO. 1 COORDINATES

L (IN.)	HP (IN.)	HS (IN.)
0.0	0.0346	0.0346
0.0346	0.0000	0.0747
0.1000	0.0157	0.1132
0.2000	0.0387	0.1672
0.3000	0.0593	0.2157
0.4000	0.0778	0.2591
0.5000	0.0943	0.2979
0.6000	0.1088	0.3324
0.7000	0.1215	0.3628
0.8000	0.1325	0.3895
0.9000	0.1418	0.4125
1.0000	0.1495	0.4320
1.1000	0.1556	0.4481
1.2000	0.1603	0.4610
1.3000	0.1636	0.4706
1.4000	0.1655	0.4770
1.5000	0.1660	0.4802
1.6000	0.1652	0.4803
1.7000	0.1631	0.4773
1.8000	0.1597	0.4711
1.9000	0.1551	0.4617
2.0000	0.1492	0.4491
2.1000	0.1421	0.4333
2.2000	0.1337	0.4142
2.3000	0.1242	0.3918
2.4000	0.1134	0.3659
2.5000	0.1014	0.3366
2.6000	0.0882	0.3036
2.7000	0.0738	0.2669
2.8000	0.0582	0.2264
2.9000	0.0415	0.1820
3.0000	0.0235	0.1333
3.1000	0.0043	0.0803
3.1244	-0.0000	0.0667
3.15 4	0.0310	0.0310

SECTION NO. 2 COORDINATES

L (IN.)	HP (IN.)	HS (IN.)
0.0	0.0301	0.0301
0.0301	0.0000	0.0629
0.1000	0.0070	0.0922
0.2000	0.0163	0.1308
0.3000	0.0247	0.1657
0.4000	0.0321	0.1972
0.5000	0.0387	0.2255
0.6000	0.0445	0.2506
0.7000	0.0494	0.2728
0.8000	0.0537	0.2920
0.9000	0.0572	0.3083
1.0000	0.0600	0.3219
1.1000	0.0622	0.3327
1.2000	0.0637	0.3409
1.3000	0.0646	0.3463
1.4000	0.0648	0.3490
1.5000	0.0644	0.3491
1.6000	0.0635	0.3465
1.7000	0.0619	0.3413
1.8000	0.0598	0.3334
1.9000	0.0571	0.3227
2.0000	0.0538	0.3094
2.1000	0.0500	0.2933
2.2000	0.0456	0.2744
2.3000	0.0407	0.2528
2.4000	0.0353	0.2282
2.5000	0.0292	0.2007
2.6000	0.0227	0.1703
2.7000	0.0156	0.1368
2.8000	0.0080	0.1002
2.8999	0.0000	0.0603
2.9000	0.0000	0.0603
2.9289	0.0290	0.0290

SECTION NO. 3 COORDINATES

L (IN.)	HP (IN.)	HS (IN.)
0.0	0.0275	0.0275
0.0275	0.0000	0.0566
0.1000	0.0034	0.0817
0.2000	0.0079	0.1139
0.3000	0.0119	0.1433
0.4000	0.0157	0.1699
0.5000	0.0190	0.1939
0.6000	0.0220	0.2152
0.7000	0.0246	0.2338
0.8000	0.0269	0.2498
0.9000	0.0288	0.2633
1.0000	0.0303	0.2742
1.1000	0.0314	0.2825
1.2000	0.0322	0.2883
1.3000	0.0327	0.2916
1.4000	0.0328	0.2924
1.5000	0.0325	0.2906
1.6000	0.0318	0.2862
1.7000	0.0308	0.2794
1.8000	0.0295	0.2700
1.9000	0.0278	0.2580
2.0000	0.0257	0.2434
2.1000	0.0232	0.2262
2.2000	0.0205	0.2063
2.3000	0.0173	0.1837
2.4000	0.0138	0.1584
2.5000	0.0100	0.1302
2.6000	0.0057	0.0992
2.7000	0.0012	0.0653
2.7251	0.0000	0.0563
2.7523	0.0273	0.0273

SECTION NO. 4 COORDINATES

L (IN.)	HP (IN.)	HS (IN.)
0.0	0.0259	0.0259
0.0259	0.0	0.0534
0.1000	0.0038	0.0784
0.2000	0.0086	0.1097
0.3000	0.0130	0.1382
0.4000	0.0171	0.1639
0.5000	0.0207	0.1868
0.6000	0.0239	0.2069
0.7000	0.0267	0.2244
0.8000	0.0291	0.2392
0.9000	0.0311	0.2513
1.0000	0.0326	0.2607
1.1000	0.0338	0.2675
1.2000	0.0345	0.2717
1.3000	0.0347	0.2733
1.4000	0.0346	0.2722
1.5000	0.0340	0.2686
1.6000	0.0330	0.2622
1.7000	0.0316	0.2533
1.8000	0.0297	0.2416
1.9000	0.0275	0.2273
2.0000	0.0247	0.2103
2.1000	0.0216	0.1905
2.2000	0.0179	0.1678
2.3000	0.0139	0.1423
2.4000	0.0094	0.1139
2.5000	0.0045	0.0825
2.5847	0.0000	0.0535
2.6000	0.0050	0.0469
2.6107	0.0259	0.0259

Table 9.4. Continued.

** BLADE SECTION PROPERTIES OF STATOR NO. 1 FOLLOWING ROTOR NO. 1 **

NUMBER OF BLADES = 30.0 AXIAL LOCATION OF STACKING LINE IN COMPRESSOR = 6.460 IN.

BLADE SECTION NO.	SECTION RAD. LOC. (IN.)	STACKING POINT COORDINATES L (IN.)	STACKING POINT COORDINATES H (IN.)	SECTION SETTING ANGLE (DEG.)	BLADE SECTION C.G. COORDINATES L (IN.)	BLADE SECTION C.G. COORDINATES H (IN.)	SECTION AREA (IN.)**2	MOMENTS OF INERTIA THROUGH C.G. IMIN (IN.)**4	MOMENTS OF INERTIA THROUGH C.G. IMAX (IN.)**4	IMAX SETTING ANGLE (DEG.)	SECTION TORSION CONSTANT (IN.)**4	SECTION TWIST STIFFNESS (IN.)**6
5	7.300	2.4774	0.0249	7.666	1.2521	0.1213	0.40737	0.000030	-0.66451	3.283	0.004594	4.366084
6	7.120	2.4024	0.0242	7.877	1.2139	0.1204	0.37168	0.000028	-0.55715	3.342	0.003686	3.365907
7	6.940	2.3594	0.0238	8.081	1.1919	0.1205	0.34744	0.000028	-0.48988	3.412	0.003099	2.786083
8	6.760	2.3483	0.0237	8.285	1.1860	0.1218	0.33315	0.000029	-0.45316	3.505	0.002738	2.488973

SECTION NO. 5 COORDINATES L (IN.)	HP (IN.)	HS (IN.)	SECTION NO. 6 COORDINATES L (IN.)	HP (IN.)	HS (IN.)	SECTION NO. 7 COORDINATES L (IN.)	HP (IN.)	HS (IN.)	SECTION NO. 8 COORDINATES L (IN.)	HP (IN.)	HS (IN.)
0.0	0.0249	0.0249	0.0	0.0241	0.0241	0.0	0.0237	0.0237	0.0	0.0237	0.0237
0.0249	0.0	0.0512	0.0241	0.0	0.0497	0.0237	0.0	0.0489	0.0237	0.0	0.0487
0.1000	0.0048	0.0767	0.1000	0.0058	0.0755	0.1000	0.0066	0.0749	0.1000	0.0074	0.0747
0.2000	0.0108	0.1080	0.2000	0.0129	0.1068	0.2000	0.0148	0.1060	0.2000	0.0166	0.1057
0.3000	0.0163	0.1363	0.3000	0.0194	0.1349	0.3000	0.0222	0.1340	0.3000	0.0249	0.1336
0.4000	0.0212	0.1616	0.4000	0.0252	0.1600	0.4000	0.0289	0.1588	0.4000	0.0323	0.1583
0.5000	0.0256	0.1841	0.5000	0.0304	0.1820	0.5000	0.0347	0.1806	0.5000	0.0388	0.1798
0.6000	0.0295	0.2036	0.6000	0.0349	0.2011	0.6000	0.0398	0.1993	0.6000	0.0445	0.1984
0.7000	0.0329	0.2204	0.7000	0.0387	0.2173	0.7000	0.0441	0.2151	0.7000	0.0493	0.2140
0.8000	0.0357	0.2343	0.8000	0.0419	0.2306	0.8000	0.0476	0.2279	0.8000	0.0531	0.2266
0.9000	0.0380	0.2455	0.9000	0.0444	0.2409	0.9000	0.0504	0.2378	0.9000	0.0562	0.2363
1.0000	0.0397	0.2538	1.0000	0.0462	0.2485	1.0000	0.0523	0.2448	1.0000	0.0583	0.2431
1.1000	0.0409	0.2595	1.1000	0.0474	0.2532	1.1000	0.0535	0.2489	1.1000	0.0595	0.2470
1.2000	0.0415	0.2623	1.2000	0.0479	0.2550	1.2000	0.0539	0.2502	1.2000	0.0599	0.2481
1.3000	0.0415	0.2625	1.3000	0.0477	0.2541	1.3000	0.0534	0.2485	1.3000	0.0594	0.2463
1.4000	0.0410	0.2599	1.4000	0.0468	0.2503	1.4000	0.0522	0.2440	1.4000	0.0579	0.2416
1.5000	0.0400	0.2545	1.5000	0.0452	0.2437	1.5000	0.0502	0.2366	1.5000	0.0556	0.2340
1.6000	0.0384	0.2464	1.6000	0.0430	0.2342	1.6000	0.0474	0.2263	1.6000	0.0524	0.2235
1.7000	0.0362	0.2355	1.7000	0.0400	0.2218	1.7000	0.0438	0.2131	1.7000	0.0483	0.2101
1.8000	0.0335	0.2218	1.8000	0.0364	0.2065	1.8000	0.0394	0.1969	1.8000	0.0433	0.1938
1.9000	0.0302	0.2052	1.9000	0.0321	0.1883	1.9000	0.0342	0.1777	1.9000	0.0374	0.1744
2.0000	0.0263	0.1857	2.0000	0.0271	0.1670	2.0000	0.0282	0.1554	2.0000	0.0306	0.1519
2.1000	0.0219	0.1634	2.1000	0.0214	0.1427	2.1000	0.0214	0.1301	2.1000	0.0229	0.1264
2.2000	0.0168	0.1380	2.2000	0.0150	0.1153	2.2000	0.0137	0.1015	2.2000	0.0143	0.0976
2.3000	0.0113	0.1096	2.3000	0.0079	0.0847	2.3000	0.0053	0.0696	2.3000	0.0048	0.0656
2.4000	0.0051	0.0780	2.4000	0.0001	0.0508	2.3594	0.0000	0.0491	2.3483	0.0000	0.0489
2.4774	0.0000	0.0514	2.4024	0.0000	0.0499	2.3833	0.0238	0.0238	2.3720	0.0237	0.0237
2.5000	0.0143	0.0355	2.4266	0.0242	0.0242						
2.5024	0.0249	0.0249									

Table 9.4. Continued.

** BLADE SECTION PROPERTIES OF STATOR NO. 1 FOLLOWING ROTOR NO. 1 **

NUMBER OF BLADES = 30.0 AXIAL LOCATION OF STACKING LINE IN COMPRESSOR = 6.460 IN.

BLADE SECTION NO.	RAD. LOC. (IN.)	STACKING POINT COORDINATES L (IN.)	H (IN.)	SECTION SETTING ANGLE (DEG.)	BLADE SECTION C.G. COORDINATES L (IN.)	H (IN.)	SECTION AREA (IN.)**2	MOMENTS OF INERTIA THROUGH C.G. IMIN (IN.)**4	IMAX (IN.)**4	IMAX SETTING ANGLE (DEG.)	SECTION TORSION CONSTANT (IN.)**4	SECTION TWIST STIFFNESS (IN.)**6
9	6.580	2.3687	0.0240	8.493	1.1959	0.1243	0.32773	0.000032	-0.44163	3.623	0.002542	2.406001
10	6.400	2.4204	0.0245	8.703	1.2216	0.1281	0.33046	0.000036	-0.45310	3.760	0.002475	2.515519
11	6.240	2.4924	0.0253	8.888	1.2575	0.1327	0.33936	0.000042	-0.48596	3.893	0.002509	2.821126
12	6.080	2.5886	0.0263	9.072	1.3056	0.1383	0.35418	0.000051	-0.53786	4.043	0.002623	3.316427

SECTION NO. 9 COORDINATES L (IN.)	HP (IN.)	HS (IN.)	SECTION NO. 10 COORDINATES L (IN.)	HP (IN.)	HS (IN.)	SECTION NO. 11 COORDINATES L (IN.)	HP (IN.)	HS (IN.)	SECTION NO. 12 COORDINATES L (IN.)	HP (IN.)	HS (IN.)
0.0	0.0239	0.0239	0.0	0.0245	0.0245	0.0	0.0253	0.0253	0.0	0.0263	0.0263
0.0239	0.0	0.0492	0.0245	0.0000	0.0504	0.0253	0.0	0.0520	0.0263	0.0000	0.0541
0.1000	0.0082	0.0750	0.1000	0.0088	0.0758	0.1000	0.0092	0.0770	0.1000	0.0096	0.0786
0.2000	0.0182	0.1060	0.2000	0.0197	0.1067	0.2000	0.0210	0.1077	0.2000	0.0221	0.1092
0.3000	0.0274	0.1337	0.3000	0.0297	0.1343	0.3000	0.0316	0.1354	0.3000	0.0335	0.1369
0.4000	0.0355	0.1583	0.4000	0.0386	0.1590	0.4000	0.0412	0.1601	0.4000	0.0437	0.1617
0.5000	0.0427	0.1798	0.5000	0.0465	0.1806	0.5000	0.0497	0.1819	0.5000	0.0529	0.1837
0.6000	0.0490	0.1984	0.6000	0.0534	0.1993	0.6000	0.0572	0.2008	0.6000	0.0610	0.2029
0.7000	0.0543	0.2140	0.7000	0.0592	0.2151	0.7000	0.0636	0.2170	0.7000	0.0681	0.2196
0.8000	0.0586	0.2257	0.8000	0.0641	0.2281	0.8000	0.0690	0.2304	0.8000	0.0740	0.2336
0.9000	0.0620	0.2365	0.9000	0.0679	0.2383	0.9000	0.0733	0.2412	0.9000	0.0789	0.2450
1.0000	0.0644	0.2435	1.0000	0.0707	0.2458	1.0000	0.0766	0.2493	1.0000	0.0827	0.2539
1.1000	0.0658	0.2476	1.1000	0.0725	0.2505	1.1000	0.0788	0.2547	1.1000	0.0855	0.2602
1.2000	0.0663	0.2489	1.2000	0.0733	0.2524	1.2000	0.0799	0.2575	1.2000	0.0872	0.2640
1.3000	0.0658	0.2474	1.3000	0.0730	0.2516	1.3000	0.0801	0.2576	1.3000	0.0878	0.2654
1.4000	0.0644	0.2430	1.4000	0.0717	0.2481	1.4000	0.0791	0.2552	1.4000	0.0873	0.2642
1.5000	0.0619	0.2359	1.5000	0.0694	0.2418	1.5000	0.0771	0.2501	1.5000	0.0858	0.2606
1.6000	0.0585	0.2258	1.6000	0.0661	0.2328	1.6000	0.0740	0.2424	1.6000	0.0832	0.2544
1.7000	0.0542	0.2129	1.7000	0.0617	0.2210	1.7000	0.0699	0.2320	1.7000	0.0795	0.2457
1.8000	0.0488	0.1971	1.8000	0.0563	0.2064	1.8000	0.0648	0.2189	1.8000	0.0748	0.2345
1.9000	0.0425	0.1783	1.9000	0.0499	0.1890	1.9000	0.0585	0.2032	1.9000	0.0690	0.2208
2.0000	0.0352	0.1566	2.0000	0.0425	0.1687	2.0000	0.0512	0.1847	2.0000	0.0621	0.2045
2.1000	0.0269	0.1317	2.1000	0.0340	0.1454	2.1000	0.0429	0.1634	2.1000	0.0542	0.1855
2.2000	0.0177	0.1038	2.2000	0.0245	0.1192	2.2000	0.0335	0.1393	2.2000	0.0451	0.1640
2.3000	0.0075	0.0727	2.3000	0.0139	0.0899	2.3000	0.0230	0.1123	2.3000	0.0350	0.1397
2.3687	0.0000	0.0494	2.4000	0.0023	0.0575	2.4000	0.0114	0.0824	2.4000	0.0238	0.1127
2.3926	0.0240	0.0240	2.4204	0.0000	0.0505	2.4924	-0.0000	0.0521	2.5000	0.0116	0.0829
			2.4449	0.0245	0.0245	2.5000	0.0012	0.0494	2.5886	-0.0000	0.0541
						2.5177	0.0253	0.0253	2.6000	0.0026	0.0501
									2.6150	0.0263	0.0263

Table 9.4. Continued.

** BLADE SECTION PROPERTIES OF STATOR NO. 1 FOLLOWING ROTOR NO. 1 **

NUMBER OF BLADES = 30.0 AXIAL LOCATION OF STACKING LINE IN COMPRESSOR = 6.460 IN.

BLADE SECTION NO.	RAD. LOC. (IN.)	STACKING POINT COORDINATES L (IN.)	STACKING POINT COORDINATES H (IN.)	SECTION SETTING ANGLE (DEG.)	BLADE SECTION C.G. COORDINATES L (IN.)	BLADE SECTION C.G. COORDINATES H (IN.)	SECTION AREA (IN.)**2	MOMENTS OF INERTIA THROUGH C.G. IMIN (IN.)**4	MOMENTS OF INERTIA THROUGH C.G. IMAX (IN.)**4	IMAX SETTING ANGLE (DEG.)	SECTION TORSION CONSTANT (IN.)**4	SECTION TWIST STIFFNESS (IN.)**6
13	5.920	2.7087	0.0276	9.254	1.3655	0.1450	0.37484	0.000062	-0.61413	4.203	0.002815	4.092050
14	5.760	2.8522	0.0291	9.433	1.4370	0.1529	0.40131	0.000078	-0.72005	4.370	0.003087	5.263619
15	5.600	3.0185	0.0309	9.610	1.5199	0.1619	0.43360	0.000099	-0.86280	4.541	0.003442	7.007969
16	5.560	3.0536	0.0314	9.654	1.5423	0.1643	0.44258	0.000106	-0.98861	4.592	0.003544	8.984628

SECTION NO. 13 COORDINATES L (IN.)	HP (IN.)	HS (IN.)	SECTION NO. 14 COORDINATES L (IN.)	HP (IN.)	HS (IN.)	SECTION NO. 15 COORDINATES L (IN.)	HP (IN.)	HS (IN.)	SECTION NO. 16 COORDINATES L (IN.)	HP (IN.)	HS (IN.)
0.0	0.0276	0.0276	0.0	0.0292	0.0292	0.0	0.0310	0.0310	0.0	0.0315	0.0315
0.0276	0.0	0.0567	0.0292	0.0	0.0599	0.0310	0.0	0.0636	0.0315	0.0000	0.0646
0.1000	0.0100	0.0807	0.1000	0.0102	0.0832	0.1000	0.0105	0.0861	0.1000	0.0105	0.0870
0.2000	0.0231	0.1112	0.2000	0.0241	0.1136	0.2000	0.0251	0.1165	0.2000	0.0253	0.1173
0.3000	0.0352	0.1388	0.3000	0.0369	0.1413	0.3000	0.0386	0.1443	0.3000	0.0390	0.1451
0.4000	0.0462	0.1638	0.4000	0.0486	0.1664	0.4000	0.0510	0.1695	0.4000	0.0516	0.1704
0.5000	0.0560	0.1860	0.5000	0.0592	0.1889	0.5000	0.0623	0.1923	0.5000	0.0631	0.1933
0.6000	0.0648	0.2057	0.6000	0.0687	0.2090	0.6000	0.0726	0.2128	0.6000	0.0736	0.2139
0.7000	0.0725	0.2228	0.7000	0.0771	0.2266	0.7000	0.0817	0.2311	0.7000	0.0829	0.2323
0.8000	0.0792	0.2374	0.8000	0.0844	0.2420	0.8000	0.0898	0.2471	0.8000	0.0912	0.2484
0.9000	0.0847	0.2496	0.9000	0.0907	0.2550	0.9000	0.0969	0.2609	0.9000	0.0985	0.2625
1.0000	0.0892	0.2594	1.0000	0.0959	0.2657	1.0000	0.1028	0.2726	1.0000	0.1046	0.2744
1.1000	0.0925	0.2668	1.1000	0.1000	0.2741	1.1000	0.1077	0.2821	1.1000	0.1097	0.2842
1.2000	0.0949	0.2718	1.2000	0.1030	0.2804	1.2000	0.1116	0.2896	1.2000	0.1138	0.2920
1.3000	0.0961	0.2744	1.3000	0.1050	0.2844	1.3000	0.1144	0.2950	1.3000	0.1168	0.2977
1.4000	0.0963	0.2747	1.4000	0.1059	0.2862	1.4000	0.1162	0.2983	1.4000	0.1188	0.3015
1.5000	0.0954	0.2727	1.5000	0.1058	0.2858	1.5000	0.1169	0.2996	1.5000	0.1198	0.3032
1.6000	0.0934	0.2682	1.6000	0.1046	0.2832	1.6000	0.1166	0.2989	1.6000	0.1197	0.3029
1.7000	0.0904	0.2615	1.7000	0.1023	0.2785	1.7000	0.1152	0.2961	1.7000	0.1186	0.3006
1.8000	0.0863	0.2523	1.8000	0.0990	0.2715	1.8000	0.1128	0.2913	1.8000	0.1164	0.2963
1.9000	0.0811	0.2408	1.9000	0.0947	0.2623	1.9000	0.1094	0.2844	1.9000	0.1132	0.2900
2.0000	0.0749	0.2269	2.0000	0.0892	0.2508	2.0000	0.1049	0.2754	2.0000	0.1090	0.2816
2.1000	0.0676	0.2105	2.1000	0.0828	0.2372	2.1000	0.0994	0.2644	2.1000	0.1037	0.2713
2.2000	0.0592	0.1917	2.2000	0.0752	0.2212	2.2000	0.0928	0.2514	2.2000	0.0974	0.2589
2.3000	0.0497	0.1704	2.3000	0.0666	0.2030	2.3000	0.0852	0.2362	2.3000	0.0901	0.2445
2.4000	0.0392	0.1466	2.4000	0.0569	0.1825	2.4000	0.0765	0.2189	2.4000	0.0817	0.2280
2.5000	0.0275	0.1202	2.5000	0.0461	0.1596	2.5000	0.0668	0.1995	2.5000	0.0723	0.2094
2.6000	0.0148	0.0913	2.6000	0.0343	0.1343	2.6000	0.0561	0.1779	2.6000	0.0618	0.1887
2.7000	0.0010	0.0596	2.7000	0.0214	0.1067	2.7000	0.0443	0.1541	2.7000	0.0503	0.1659
2.7087	-0.0000	0.0567	2.8000	0.0074	0.0765	2.8000	0.0314	0.1281	2.8000	0.0378	0.1409
2.7363	0.0276	0.0276	2.8522	-0.0000	0.0598	2.9000	0.0175	0.0999	2.9000	0.0242	0.1137
			2.8813	0.0291	0.0291	3.0000	0.0025	0.0694	3.0000	0.0095	0.0843
						3.0185	-0.0000	0.0634	3.0636	-0.0000	0.0644
						3.0495	0.0309	0.0309	3.0951	0.0314	0.0314

Table 9.4. Concluded.

** BLADE SECTION PROPERTIES OF STATOR NO. 1 FOLLOWING ROTOR NO. 1 **

NUMBER OF BLADES = 30.0   AXIAL LOCATION OF STACKING LINE IN COMPRESSOR = 6.460 IN.

BLADE SECTION NO.	RAD. LOC. (IN.)	STACKING POINT COORDINATES L (IN.)	STACKING POINT COORDINATES H (IN.)	SECTION SETTING ANGLE (DEG.)	BLADE SECTION C.G. COORDINATES L (IN.)	BLADE SECTION C.G. COORDINATES H (IN.)	SECTION AREA (IN.)**2	MOMENTS OF INERTIA THROUGH C.G. IMIN (IN.)**4	MOMENTS OF INERTIA THROUGH C.G. IMAX (IN.)**4	IMAX SETTING ANGLE (DEG.)	SECTION TORSION CONSTANT (IN.)**4	SECTION TWIST STIFFNESS (IN.)**6
17	8.000	3.0961	0.0308	13.137	1.5615	0.2415	0.72073	0.000106	-1.66722	8.103	0.016047	15.533062

SECTION NO. 17 COORDINATES

L (IN.)	HP (IN.)	HS (IN.)
0.0	0.0340	0.0340
0.0340	0.0	0.0730
0.1000	0.0146	0.1104
0.2000	0.0356	0.1623
0.3000	0.0545	0.2088
0.4000	0.0714	0.2505
0.5000	0.0863	0.2878
0.6000	0.0995	0.3209
0.7000	0.1111	0.3502
0.8000	0.1210	0.3757
0.9000	0.1293	0.3978
1.0000	0.1363	0.4164
1.1000	0.1417	0.4317
1.2000	0.1459	0.4438
1.3000	0.1487	0.4528
1.4000	0.1503	0.4586
1.5000	0.1505	0.4613
1.6000	0.1496	0.4610
1.7000	0.1474	0.4576
1.8000	0.1441	0.4511
1.9000	0.1397	0.4415
2.0000	0.1341	0.4288
2.1000	0.1273	0.4129
2.2000	0.1195	0.3938
2.3000	0.1105	0.3714
2.4000	0.1004	0.3456
2.5000	0.0892	0.3165
2.6000	0.0768	0.2838
2.7000	0.0634	0.2476
2.8000	0.0489	0.2076
2.9000	0.0333	0.1637
3.0000	0.0166	0.1158
3.0961	-0.0000	0.0658
3.1000	0.0002	0.0637
3.1269	0.0308	0.0308

10. APPENDIX C: PARAMETER EQUATIONS

The equations used for computing the time-averaged flow quantities and performance parameters are presented in this appendix. Sign conventions are shown in Figure 10.1. Circumferential-mean and radial mass-average parameters were computed using a spline-fit integration scheme [3].

10.1. General Parameters

10.1.1. Basic Fluid Properties

Barometric pressure, N/m^2:

$$P_{atm} = h_{hg@t_{baro}} \left(1.0 - 0.00018 \left(t_{baro} - 273.15\right)\right) \gamma_{hg@273°K} \tag{10.1}$$

Density of air, kg/m^3:

$$\rho = \frac{P_{atm}}{R\ t} \tag{10.2}$$

Specific weight of water, N/m^3:

$$\gamma_{H_2O} = g\left(996.86224 + 0.1768124\left(\frac{9}{5}\ t - 459.67\right) - 2.64966 \times 10^{-3}\left(\frac{9}{5}\ t - 459.67\right)^2 + 5.00063 \times 10^{-6}\left(\frac{9}{5}\ t - 459.67\right)^3\right) \tag{10.3}$$

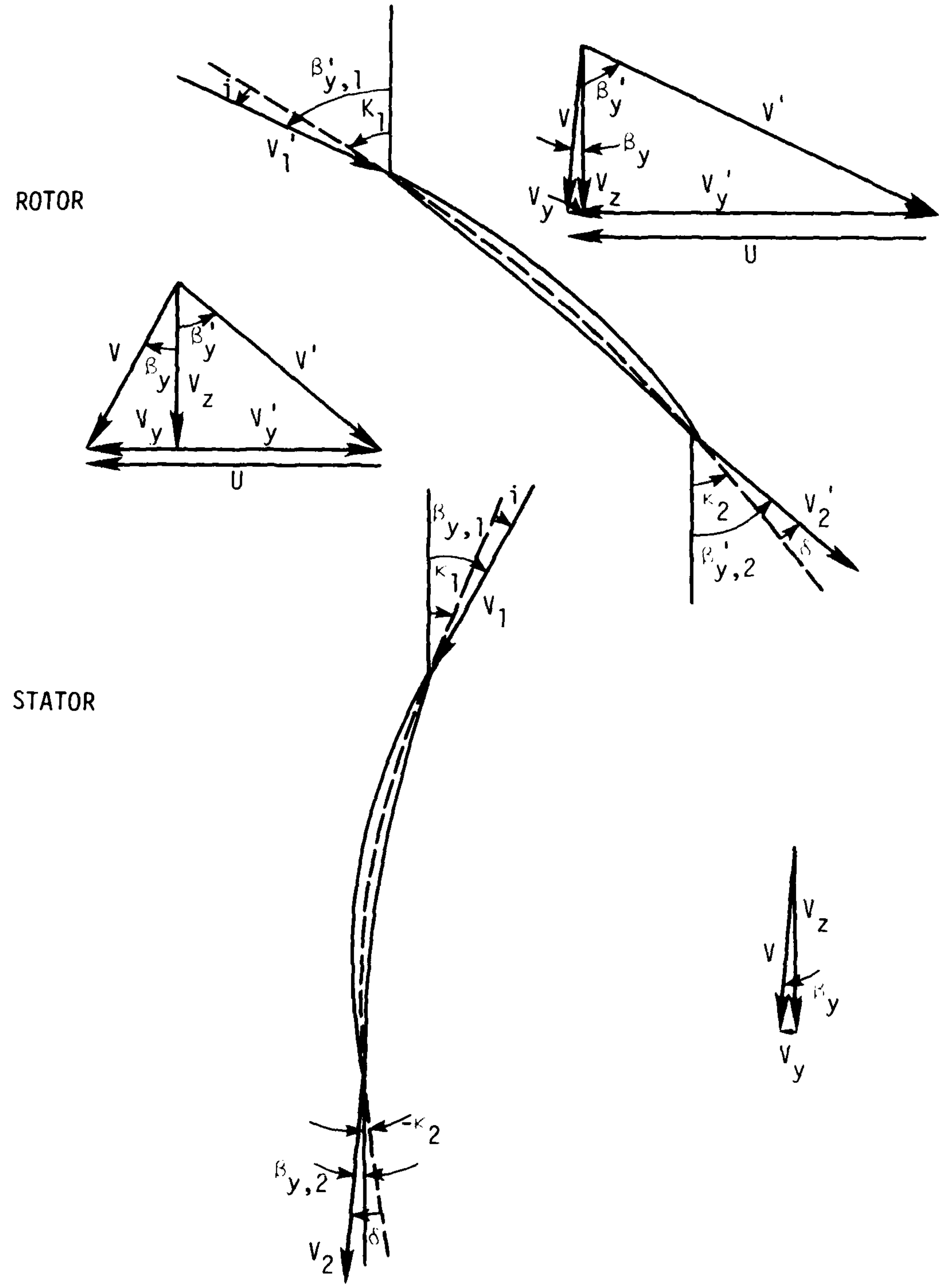

Figure 10.1. Notation and sign conventions (all positive except as noted) for flow-field parameters.

10.1.2. Spanwise Measurement Location

Percent passage height from hub:

$$PHH = \frac{r - 0.14224}{0.06096} \times 100 \tag{10.4}$$

10.2. Flow-Field Parameters

10.2.1. Point and Circumferential-Mean Quantities

Total head, N-m/kg:

$$H = \frac{P_t \gamma_{H_2O}}{\rho} \tag{10.5}$$

and

$$\bar{H} = \frac{1}{S_S} \int_0^{S_S} H \, dY \tag{10.6}$$

Absolute flow angle behind rotors (see Figure 8.1 for sign convention), degrees:

$$\overline{\beta_y} = \frac{1}{S_S} \int_0^{S_S} \beta_y dY \tag{10.7}$$

Absolute flow angle behind stators (see Figure 8 ' ˜or sign convention), degrees:

$$\bar{\beta}_y = \frac{1}{\Delta Y_{fs}} \int_{\substack{\text{across} \\ \Delta Y_{fs}}} \beta_y dY \tag{10.8}$$

Casing static head, N-m/kg:

$$h_w = \frac{P_w \gamma_{H_2O}}{\rho} \tag{10.9}$$

and

$$\overline{h_w} = \frac{1}{S_S}\int_0^{S_S} h_w dY \tag{10.10}$$

Static head (radial equilibrium equation), N-m/kg:

$$\frac{d\bar{h}}{dr} = \frac{2 \sin^2 \bar{\beta}_y(\bar{H} - \bar{h})}{r} \tag{10.11}$$

Absolute fluid velocity, m/s:

$$V = \sqrt{2(H \cdot \bar{h})} \tag{10.12}$$

and

$$\bar{V} = \frac{1}{S_S} \int_0^{S_S} V \; dY \tag{10.13}$$

Blade velocity, m/s:

$$U = \frac{\pi r(RPM)}{30.0} \tag{10.14}$$

Axial component of absolute fluid velocity, m/s:

$$V_z = V\cos \beta_y \tag{10.15}$$

and

$$\bar{V}_z = \bar{V}\cos\,\bar{\beta}_y \tag{10.16}$$

Tangential component of absolute fluid velocity (see Figure 8.1 for sign convention), m/s:

$$V_y = V\sin\,\beta_y \tag{10.17}$$

and

$$\bar{V}_y = \bar{V}\sin\,\bar{\beta}_y \tag{10.18}$$

Tangential component of relative fluid velocity (see Figure 8.1 for sign convention), m/s:

$$V_y' = U - V_y \tag{10.19}$$

and

$$\overline{V_y'} = U - \bar{V}_y \tag{10.20}$$

Relative fluid velocity, m/s:

$$V' = \sqrt{(V_y')^2 + (\bar{V}_z)^2} \tag{10.21}$$

and

$$\overline{V'} = \sqrt{(\overline{V_y'})^2 + (\bar{V}_z)^2} \tag{10.22}$$

Relative tangential flow angle (see Figure 8.1 for sign convention), degrees:

$$\beta_y' = \tan^{-1}\left(\frac{V_y'}{V_z}\right) \tag{10.23}$$

and

$$\overline{\beta_y'} = \tan^{-1}\left(\frac{\overline{V_y'}}{\overline{V_z}}\right) \tag{10.24}$$

Incidence angle for rotors (see Figure 8.1 for sign convention), degrees:

$$\bar{i}_R = \overline{\beta'}_{y,1,R} - \kappa_{1,R} \tag{10.25}$$

Deviation angle for rotors (see Figure 8.1 for sign convention), degrees:

$$\bar{\delta}_R = \overline{\beta'}_{y,2,R} - \kappa_{2,R} \tag{10.26}$$

Incidence angle for stators (see Figure 8.1 for sign convention), degrees:

$$\bar{i}_S = \bar{\beta}_{y,1,S} - \kappa_{1,S} \tag{10.27}$$

Deviation angle for stators (see Figure 10.1 for sign convention), degrees:

$$\bar{\delta} = \bar{\beta}_{y,2,S} - \kappa_{2,S} \tag{10.28}$$

Flow coefficient:

$$\bar{\phi} = \frac{\bar{V}_z}{U_t} \tag{10.29}$$

10.2.2. Global Parameters

Venturi volumetric flow rate, m^3/s:

$$Q_v = 0.05229 \sqrt{\frac{2\gamma_{H_2O}\Delta P_v}{\rho}} \tag{10.30}$$

Venturi flow coefficient:

$$\phi = \frac{Q_v}{A\ U_t} \tag{10.31}$$

Integrated volumetric flow rate at each axial measurement station, m^3/s:

$$Q_a = 2\pi \int_{r_h}^{r_t} \bar{V}_z\ r\ dr \tag{10.32}$$

Integrated flow coefficient at each axial measurement station:

$$\phi_a = \frac{Q_a}{A\ U_t} \tag{10.33}$$

Integrated and venturi flow-coefficient comparison, percent:

$$FCC = \frac{\phi_a - \phi}{\phi} \times 100 \tag{10.34}$$

General radial mass-average parameter equation (let ξ be any general parameter):

$$\dot{\xi} = \frac{\int_{r_h}^{r_t} \xi \, \bar{V}_z \, r \, dr}{\int_{r_h}^{r_t} \bar{V}_z \, r \, dr} \tag{10.35}$$

10.2.3. Performance Parameters (Based on Kiel and Cobra Probe Data)

Actual total-head rise coefficient for rotor:

$$\psi_R = \frac{(\bar{H}_{2,R} - \bar{H}_{1,R})}{U_t^2} \tag{10.36}$$

Actual total-head rise coefficient for stage:

$$\psi_{stage} = \frac{(\bar{H}_{2,S} - \bar{H}_{1,R})}{U_t^2} \tag{10.37}$$

Actual total-head rise coefficient for overall compressor:

$$\psi_{overall} = \frac{(\bar{H}_{2,2S} - \bar{H}_{1,1R})}{U_t^2} \tag{10.38}$$

Ideal total-head rise (aerodynamic work-input) coefficient for rotor:

$$\psi_{i,R} = \frac{U(\bar{V}_{y,2,R} - \bar{V}_{y,1,R})}{U_t^2} \tag{10.39}$$

Ideal total-head rise coefficient for stage:

$$\psi_{i,stage} = \psi_{i,R} \tag{10.40}$$

Ideal total-head rise (aerodynamic work-input) coefficient for overall compressor:

$$\psi_{i,overall} = \psi_{i,1R} + \psi_{i,2R} \tag{10.41}$$

Hydraulic efficiency for rotor:

$$\eta_R = \frac{\psi_R}{\psi_{i,R}} \tag{10.42}$$

Hydraulic efficiency for stage:

$$\eta_{stage} = \frac{\psi_{stage}}{\psi_{i,stage}} \tag{10.43}$$

Hydraulic efficiency for overall compressor:

$$\eta_{overall} = \frac{\psi_{overall}}{\psi_{i,overall}} \tag{10.44}$$

Total-head loss coefficient for rotor:

$$\omega_R = 2(\psi_{i,R} - \psi_R) \frac{U_t^2}{(\overline{V'}_{1,R})^2} \tag{10.45}$$

Total-head loss coefficient for stator:

$$\omega_S = -2 \frac{(\bar{H}_{2,S} - \bar{H}_{1,S})}{(\bar{V}_{1,S})^2} \tag{10.46}$$

10.2.4. Overall Performance Parameters (Performance Map Parameters)

Cross-section average absolute velocity at the second stator exit assuming zero swirl, m/s:

$$\bar{\bar{V}}_{2,2S} = \frac{Q_v}{A} \tag{10.47}$$

Cross-section average absolute velocity at the venturi, m/s:

$$\bar{\bar{V}}_v = \frac{Q_v}{A_v} \tag{10.48}$$

Cross-section average total-head at the second stator exit assuming constant flow passage annulus static-head, N-m/kg:

$$\bar{\bar{H}}_{2,2S} = h_{w,2,2S} = \frac{\bar{\bar{V}}^2_{2,2S}}{2} \tag{10.49}$$

Cross-section average total-head at the venturi assuming constant venturi flow passage static-head, N-m/kg:

$$\bar{\bar{H}}_v = \frac{\gamma_{H_2O} P_v}{\rho} + \frac{\bar{\bar{V}}_v^2}{2} \tag{10.50}$$

Actual head-rise coefficient for overall compressor:

$$\psi_{overall,2,2S} = \frac{\bar{\bar{H}}_{2,2S}}{U_t^2} \tag{10.51}$$

Actual head-rise coefficent for overall compressor incuding losses between the second stator exit and the venturi:

$$\psi_{overall,v} = \frac{\bar{\bar{H}}_v}{U_t^2} \tag{10.52}$$

Work-input coefficient for overall compressor including mechanical losses:

$$\psi_{i,overall,m} = \frac{\pi T(RPM)}{(30)\rho Q_v U_t^2} \tag{10.53}$$

Efficiency for overall compressor including mechanical losses:

$$\eta_{m,overall,2,2S} = \frac{\psi_{overall,2,2S}}{\psi_{i,overall,m}} \tag{10.54}$$

11. APPENDIX D: TABULATION OF EXPERIMENTAL DATA

Circumferential-mean data for the four different compressor builds are tabulated in Tables 11.1 through 11.10 in this section. All data in the following tables pertain to compressor operation at the design shaft speed of 2400 rpm and the off-design flow coefficient of 0.500. The data for the Baseline 1 build at design point operation (flow coefficient = 0.587 and shaft speed = 2400 rpm) are tabulated in Appendix E of Reference 1. The column headings in Tables 11.1 through 11.4 are defined as follows:

- BETA R = Relative flow angle, β_y'
- BETA Y = Absolute flow angle, β_y
- FC = Flow coefficient, $\bar{\phi}$
- HS = Static head, h
- HT = Total head H
- PHH = Percent passage height from hub, PHH
- V = Absolute velocity, V
- VR = Relative velocity, V'
- VY = Tangential component of absolute velocity, V_y
- VZ = Axial component of absolute velocity, V_z
- VYR = Tangential component of relative velocity, V_y'
- Y/SS = Fraction of stator pitch, Y/S_s

PREVIOUS PAGE IS BLANK

Table 11.1 Circumferential-mean flow-field quantities for the baseline 1 compressor build ($\phi = 0.500$).

STATION 1 : ROTOR 1 INLET

PHH	HT N*M/KG	HS N*M/KG	BETA Y DEG.	V M/S	VZ M/S	VY M/S	BETA R DEG.	VR M/S	VYR M/S	FC
5.00	-1.409	-372.234	1.480	27.233	27.224	0.703	52.758	44.985	35.811	0.533
10.00	-0.494	-372.226	1.640	27.266	27.255	0.780	53.251	45.554	36.501	0.534
30.00	-0.254	-372.185	1.350	27.274	27.266	0.643	55.520	48.164	39.702	0.534
50.00	0.019	-372.161	1.190	27.283	27.277	0.567	57.516	50.789	42.843	0.534
70.00	-0.113	-372.146	0.760	27.277	27.275	0.362	59.396	53.574	46.112	0.534
80.00	-0.245	-372.144	-0.340	27.273	27.272	-0.162	60.482	55.352	48.167	0.534
90.00	-2.449	-372.143	-0.330	27.192	27.191	-0.157	61.314	56.647	49.694	0.532
95.00	-7.508	-372.143	-0.510	27.005	27.004	-0.240	61.886	57.305	50.544	0.529

STATION 2 : ROTOR 1 EXIT / STATOR 1 INLET

PHH	HT N*M/KG	HS N*M/KG	BETA Y DEG.	V M/S	VZ M/S	VY M/S	BETA R DEG.	VR M/S	VYR M/S	FC
5.00	594.832	77.270	34.310	32.173	26.575	18.135	34.669	32.312	18.380	0.520
10.00	585.442	84.411	33.170	31.655	26.497	17.319	36.993	33.175	19.962	0.519
30.00	594.488	106.947	31.820	31.226	26.533	16.464	41.989	35.697	23.881	0.520
50.00	611.740	126.055	30.070	31.167	26.972	15.616	45.859	38.729	27.793	0.528
70.00	635.336	142.071	27.810	31.409	27.781	14.654	48.876	42.241	31.820	0.544
80.00	658.262	148.907	26.390	31.917	28.591	14.186	49.788	44.285	33.819	0.560
90.00	644.064	155.372	30.640	31.263	26.898	15.933	51.325	43.044	33.605	0.527
95.00	541.040	158.941	37.110	27.644	22.045	16.679	56.750	40.207	33.625	0.432

Table 11.1 concluded.

STATION 3 : STATOR 1 EXIT / ROTOR 2 INLET

PHH	HT N*M/KG	HS N*M/KG	BETA Y DEG.	V M/S	VZ M/S	VY M/S	BETA R DEG.	VR M/S	VYR M/S	FC
5.00	497.470	205.571	4.280	24.078	24.010	1.797	55.333	42.212	34.718	0.470
10.00	552.993	205.705	-0.650	26.265	26.264	-0.298	55.050	45.847	37.579	0.514
30.00	564.111	205.877	-0.320	26.673	26.672	-0.149	56.628	48.489	40.494	0.522
50.00	577.833	205.890	0.550	27.166	27.164	0.261	57.807	50.987	43.148	0.532
70.00	592.276	205.904	2.130	27.632	27.613	1.027	58.718	53.177	45.446	0.541
80.00	600.512	205.939	4.000	27.844	27.776	1.942	58.910	53.790	46.063	0.544
90.00	546.118	206.035	4.260	25.830	25.759	1.919	61.590	54.139	47.619	0.504
95.00	485.554	206.088	0.300	23.477	23.477	0.123	64.928	55.401	50.181	0.460

STATION 4 : ROTOR 2 EXIT / STATOR 2 INLET

PHH	HT N*M/KG	HS N*M/KG	BETA Y DEG.	V M/S	VZ M/S	VY M/S	BETA R DEG.	VR M/S	VYR M/S	FC
5.00	1126.535	621.723	43.950	31.772	22.874	22.051	32.307	27.063	14.464	0.448
10.00	1115.447	634.703	32.770	31.002	26.068	16.780	38.182	33.163	20.501	0.510
30.00	1135.789	652.201	29.790	31.098	26.988	15.450	42.689	36.717	24.895	0.528
50.00	1160.897	668.311	28.070	31.386	27.694	14.769	45.962	39.840	28.641	0.542
70.00	1191.417	682.863	28.230	31.890	28.097	15.084	48.168	42.127	31.389	0.550
80.00	1219.137	690.127	29.570	32.524	28.288	16.050	48.484	42.677	31.955	0.554
90.00	1175.189	698.048	31.690	30.890	26.284	16.227	51.724	42.432	33.311	0.515
95.00	1076.326	702.117	36.910	27.351	21.870	16.426	57.156	40.323	33.878	0.428

STATION 5 : STATOR 2 EXIT

PHH	HT N*M/KG	HS N*M/KG	BETA Y DEG.	V M/S	VZ M/S	VY M/S	BETA R DEG.	VR M/S	VYR M/S	FC
5.00	980.943	747.531	3.390	21.232	21.195	1.255	58.989	41.139	35.259	0.415
10.00	1033.804	747.566	2.003	23.768	23.753	0.831	56.909	43.507	36.450	0.465
30.00	1082.361	747.592	-1.190	25.758	25.753	-0.535	57.791	48.315	40.880	0.504
50.00	1120.967	747.609	0.030	27.167	27.167	0.014	57.952	51.197	43.395	0.532
70.00	1140.072	747.622	2.734	27.793	27.761	1.325	58.413	53.000	45.148	0.544
80.00	1143.003	747.674	4.350	27.783	27.703	2.107	58.886	53.611	45.898	0.542
90.00	1097.334	747.783	3.193	26.023	25.983	1.450	61.617	54.659	48.088	0.509
95.00	1044.936	747.821	-0.060	24.137	24.137	-0.025	64.378	55.817	50.329	0.473

Table 11.2 Circumferential-mean flow-field quantities for the baseline 2 compressor build ($\phi = 0.500$).

STATION 3 : STATOR 1 EXIT / ROTOR 2 INLET

PHH	HT N*M/KG	HS N*M/KG	BETA Y DEG.	V M/S	VZ M/S	VY M/S	BETA R DEG.	VR M/S	VYR M/S	FC
5.00	490.805	205.550	4.280	23.778	23.712	1.775	55.685	42.061	34.740	0.464
10.00	546.940	205.682	-0.650	26.029	26.027	-0.295	55.291	45.710	37.576	0.510
30.00	562.609	205.851	-0.320	26.604	26.603	-0.149	56.696	48.451	40.494	0.521
50.00	575.090	205.865	0.550	27.059	27.058	0.260	57.909	50.931	43.149	0.530
70.00	593.734	205.879	2.130	27.694	27.674	1.029	58.659	53.208	45.444	0.542
80.00	595.792	205.913	4.000	27.630	27.563	1.927	59.113	53.693	46.078	0.540
90.00	553.782	206.009	4.260	26.132	26.060	1.941	61.299	54.263	47.596	0.510
95.00	497.289	206.062	0.300	23.995	23.995	0.126	64.443	55.620	50.178	0.470

STATION 4 : ROTOR 2 EXIT / STATOR 2 INLET

PHH	HT N*M/KG	HS N*M/KG	BETA Y DEG.	V M/S	VZ M/S	VY M/S	BETA R DEG.	VR M/S	VYR M/S	FC
5.00	1133.810	621.083	43.950	32.020	23.053	22.223	31.798	27.124	14.292	0.451
10.00	1120.490	634.247	32.770	31.180	26.218	16.877	37.892	33.222	20.404	0.513
30.00	1138.156	652.048	29.790	31.179	27.059	15.490	42.569	36.741	24.855	0.530
50.00	1162.882	668.219	28.070	31.451	27.752	14.799	45.872	39.858	28.610	0.543
70.00	1192.792	682.818	28.230	31.934	28.135	15.105	48.110	42.138	31.368	0.551
80.00	1219.412	690.098	29.570	32.532	28.295	16.054	48.473	42.679	31.951	0.554
90.00	1187.770	698.041	31.690	31.294	26.629	16.440	51.182	42.480	33.098	0.521
95.00	1080.189	702.174	36.910	27.488	21.979	16.508	56.962	40.314	33.795	0.430

STATION 5 : STATOR 2 EXIT

PHH	HT N*M/KG	HS N*M/KG	BETA Y DEG.	V M/S	VZ M/S	VY M/S	BETA R DEG.	VR M/S	VYR M/S	FC
5.00	1023.191	747.573	3.390	23.305	23.264	1.378	56.491	42.141	35.137	0.456
10.00	1057.305	747.617	2.003	24.637	24.622	0.861	55.938	43.962	36.420	0.482
30.00	1082.034	747.645	-1.190	25.767	25.761	-0.535	57.782	48.320	40.880	0.504
50.00	1120.536	747.662	0.030	27.187	27.187	0.014	57.933	51.208	43.395	0.532
70.00	1143.802	747.675	2.734	27.973	27.941	1.334	58.242	53.087	45.139	0.547
80.00	1141.375	747.728	4.350	27.689	27.610	2.100	58.975	53.569	45.905	0.541
90.00	1104.853	747.837	3.193	26.378	26.338	1.469	61.281	54.811	48.068	0.516
95.00	1048.241	747.875	-0.060	24.200	24.200	-0.025	64.320	55.845	50.329	0.474

Table 11.3 Circumferential-mean flow-field quantities for the modified 1 compressor build (ϕ = 0.500).

STATION 1 : ROTOR 1 INLET

PHH	HT N*M/KG	HS N*M/KG	BETA Y DEG.	V M/S	VZ M/S	VY M/S	BETA R DEG.	VR M/S	VYR M/S	FC
5.00	-1.805	-370.849	3.330	27.168	27.122	1.578	52.177	44.229	34.937	0.531
10.00	-0.912	-370.809	3.520	27.199	27.148	1.670	52.680	44.779	35.611	0.532
30.00	-0.858	-370.645	1.790	27.195	27.182	0.849	55.463	47.945	39.496	0.532
50.00	0.002	-370.611	0.680	27.225	27.223	0.323	57.714	50.966	43.086	0.533
70.00	-0.023	-370.608	-0.260	27.224	27.224	-0.124	59.705	53.967	46.597	0.533
80.00	-0.762	-370.608	-0.100	27.197	27.197	-0.047	60.491	55.216	48.053	0.533
90.00	-2.625	-370.608	-0.670	27.129	27.127	-0.317	61.449	56.757	49.855	0.531
95.00	-8.700	-370.608	-0.740	26.904	26.901	-0.347	62.027	57.352	50.651	0.527

STATION 2 : ROTOR 1 EXIT / STATOR 1 INLET

PHH	HT N*M/KG	HS N*M/KG	BETA Y DEG.	V M/S	VZ M/S	VY M/S	BETA R DEG.	VR M/S	VYR M/S	FC
5.00	589.344	78.299	36.720	31.970	25.626	19.115	34.176	30.975	17.400	0.502
10.00	583.848	86.291	35.040	31.545	25.828	18.112	36.583	32.164	19.169	0.506
30.00	593.780	110.321	32.000	31.095	26.370	16.478	42.148	35.567	23.867	0.516
50.00	608.828	129.152	29.150	30.973	27.050	15.087	46.316	39.165	28.322	0.530
70.00	631.861	143.916	27.080	31.239	27.814	14.221	49.225	42.589	32.252	0.545
80.00	651.366	150.422	26.250	31.652	28.388	14.000	50.145	44.298	34.006	0.556
90.00	642.311	156.711	29.780	31.164	27.048	15.478	51.545	43.493	34.059	0.530
95.00	537.182	160.135	36.270	27.461	22.140	16.245	56.974	40.622	34.058	0.434

STATION 3 : STATOR 1 EXIT / ROTOR 2 INLET

PHH	HT N*M/KG	HS N*M/KG	BETA Y DEG.	V M/S	VZ M/S	VY M/S	BETA R DEG.	VR M/S	VYR M/S	FC
5.00	501.594	204.326	3.150	24.310	24.273	1.336	55.395	42.740	35.179	0.475
10.00	537.819	204.412	-0.910	25.728	25.725	-0.409	55.685	45.632	37.689	0.504
30.00	543.525	204.525	0.430	25.850	25.850	0.194	57.226	47.753	40.151	0.506
50.00	557.122	204.537	1.320	26.300	26.293	0.606	58.439	50.234	42.803	0.515
70.00	594.810	204.567	2.060	27.790	27.772	0.999	58.586	53.284	45.474	0.544
80.00	602.675	204.600	3.630	28.039	27.983	1.775	58.814	54.039	46.230	0.548
90.00	561.813	204.679	3.530	26.574	26.523	1.636	61.027	54.754	47.901	0.519
95.00	497.058	204.718	0.450	24.098	24.097	0.189	64.320	55.607	50.114	0.472

Table 11.3 concluded.

STATION 4 : ROTOR 2 EXIT / STATOR 2 INLET

PHH	HT N*M/KG	HS N*M/KG	BETA Y DEG.	V M/S	VZ M/S	VY M/S	BETA R DEG.	VR M/S	VYR M/S	FC
5.00	1125.282	621.825	43.860	31.728	22.877	21.984	32.423	27.101	14.531	0.448
10.00	1113.947	634.791	32.510	30.950	26.100	16.634	38.346	33.279	20.647	0.511
30.00	1129.481	652.168	31.120	30.894	26.448	15.967	42.667	35.969	24.378	0.518
50.00	1157.493	669.375	29.790	31.241	27.112	15.521	45.808	38.895	27.888	0.531
70.00	1190.043	685.428	28.200	31.766	27.995	15.011	48.337	42.114	31.463	0.548
80.00	1217.026	692.640	28.860	32.381	28.359	15.629	48.784	43.040	32.376	0.555
90.00	1181.857	700.069	30.900	31.039	26.634	15.940	51.595	42.874	33.598	0.522
95.00	1082.090	703.829	36.200	27.499	22.191	16.241	56.916	40.653	34.062	0.435

STATION 5 : STATOR 2 EXIT

PHH	HT N*M/KG	HS N*M/KG	BETA Y DEG.	V M/S	VZ M/S	VY M/S	BETA R DEG.	VR M/S	VYR M/S	FC
5.00	1009.314	759.842	2.010	22.097	22.084	0.775	58.288	42.012	35.740	0.432
10.00	1065.226	759.864	0.080	24.648	24.648	0.034	56.505	44.663	37.246	0.483
30.00	1081.969	759.883	-0.220	25.253	25.253	-0.097	58.018	47.679	40.442	0.494
50.00	1112.264	759.887	1.400	26.273	26.265	0.642	58.445	50.188	42.767	0.514
70.00	1149.449	759.928	2.600	27.711	27.682	1.257	58.524	53.017	45.216	0.542
80.00	1157.128	759.977	4.080	27.954	27.883	1.989	58.787	53.805	46.017	0.546
90.00	1122.771	760.074	3.190	26.768	26.726	1.490	60.915	54.981	48.048	0.523
95.00	1058.519	760.111	0.020	24.353	24.353	0.009	64.163	55.881	50.295	0.477

Table 11.4 Circumferential-mean flow-field quantities for the modified 2 compressor build (ϕ = 0.500).

STATION 3 : STATOR 1 EXIT / ROTOR 2 INLET

PHH	HT N*M/KG	HS N*M/KG	BETA Y DEG.	V M/S	VZ M/S	VY M/S	BETA R DEG.	VR M/S	VYR M/S	FC
5.00	501.800	204.278	2.330	24.321	24.301	0.989	55.626	43.042	35.526	0.476
10.00	537.711	204.340	-1.630	25.726	25.716	-0.732	55.921	45.894	38.013	0.504
30.00	545.536	204.497	-0.120	25.935	25.935	-0.054	57.301	48.008	40.399	0.508
50.00	558.048	204.508	1.090	26.337	26.333	0.501	58.463	50.344	42.908	0.516
70.00	593.404	204.532	1.910	27.736	27.721	0.924	58.676	53.321	45.549	0.543
80.00	599.742	204.560	3.500	27.944	27.892	1.706	58.934	54.052	46.300	0.546
90.00	567.253	204.634	3.540	26.784	26.733	1.654	60.825	54.841	47.884	0.523
95.00	500.171	204.673	0.160	24.235	24.235	0.068	64.246	55.776	50.236	0.475

STATION 4 : ROTOR 2 EXIT / STATOR 2 INLET

PHH	HT N*M/KG	HS N*M/KG	BETA Y DEG.	V M/S	VZ M/S	VY M/S	BETA R DEG.	VR M/S	VYR M/S	FC
5.00	1140.473	623.468	43.770	32.152	23.218	22.242	31.582	27.254	14.273	0.455
10.00	1121.970	636.873	32.680	31.142	26.212	16.815	37.982	33.256	20.466	0.513
30.00	1133.469	654.658	30.620	30.943	26.629	15.761	42.714	36.242	24.584	0.521
50.00	1161.029	671.370	28.890	31.290	27.396	15.117	45.922	39.382	28.292	0.536
70.00	1192.709	686.542	27.340	31.815	28.261	14.612	48.427	42.590	31.862	0.553
80.00	1223.407	693.444	28.220	32.553	28.684	15.393	48.668	43.432	32.613	0.562
90.00	1182.564	700.667	30.260	31.042	26.813	15.643	51.654	43.218	33.895	0.525
95.00	1076.089	704.319	35.120	27.261	22.298	15.683	57.215	41.180	34.620	0.437

STATION 5 : STATOR 2 EXIT

PHH	HT N*M/KG	HS N*M/KG	BETA Y DEG.	V M/S	VZ M/S	VY M/S	BETA R DEG.	VR M/S	VYR M/S	FC
5.00	1050.475	759.868	0.750	23.949	23.947	0.313	56.516	43.405	36.201	0.469
10.00	1072.131	759.874	-0.480	24.859	24.858	-0.208	56.452	44.982	37.489	0.487
30.00	1081.867	759.893	-0.810	25.232	25.230	-0.357	58.206	47.887	40.702	0.494
50.00	1112.710	759.899	0.890	26.310	26.307	0.409	58.542	50.409	43.001	0.515
70.00	1148.731	759.923	2.300	27.692	27.670	1.111	58.618	53.135	45.362	0.542
80.00	1158.303	759.962	3.850	27.988	27.925	1.879	58.809	53.921	46.126	0.547
90.00	1125.946	760.048	2.780	26.939	26.908	1.307	60.843	55.229	48.231	0.527
95.00	1060.663	760.078	-0.270	24.451	24.451	-0.115	64.129	56.035	50.419	0.479

Table 11.5 Circumferential-mean incidence angles (deg.) for the different compressor builds (ϕ = 0.500).

BASELINE 1 BUILD

PHH	STATION 1 (ROTOR 1)	STATION 2 (STATOR 1)	STATION 3 (ROTOR 2)	STATION 4 (STATOR 2)
5.00	3.668	9.480	6.243	19.120
10.00	3.501	8.750	5.300	8.350
30.00	3.350	8.910	4.458	6.880
50.00	3.206	8.490	3.497	6.490
70.00	3.116	7.450	2.438	7.870
80.00	3.232	6.440	1.660	9.620
90.00	2.724	8.830	3.000	9.880
95.00	1.976	11.020	5.018	10.820

MODIFIED 1 BUILD

PHH	STATION 1 (ROTOR 1)	STATION 2 (STATOR 1)	STATION 3 (ROTOR 2)	STATION 4 (STATOR 2)
5.00	3.087	13.720	6.305	20.860
10.00	2.930	12.200	5.935	9.670
30.00	3.293	9.930	5.056	9.050
50.00	3.404	8.130	4.129	8.770
70.00	3.425	7.460	2.306	8.580
80.00	3.241	7.350	1.564	9.960
90.00	2.859	8.910	2.437	10.030
95.00	2.117	10.500	4.410	10.430

MODIFIED 2 BUILD

PHH	STATION 1 (ROTOR 1)	STATION 2 (STATOR 1)	STATION 3 (ROTOR 2)	STATION 4 (STATOR 2)
5.00	3.087	13.720	6.536	20.770
10.00	2.930	12.200	6.171	9.840
30.00	3.293	9.930	5.131	8.550
50.00	3.404	8.130	4.153	7.870
70.00	3.425	7.460	2.396	7.720
80.00	3.241	7.350	1.684	9.320
90.00	2.859	8.910	2.235	9.390
95.00	2.117	10.500	4.336	9.350

Table 11.6 Circumferential-mean deviation angles (deg.) for the different compressor builds (ϕ = 0.500).

BASELINE 1 BUILD

PHH	STATION 2 (ROTOR 1)	STATION 3 (STATOR 1)	STATION 4 (ROTOR 2)	STATION 5 (STATOR 2)
5.00	3.999	9.140	1.637	8.250
10.00	4.863	4.180	6.052	6.833
30.00	4.679	4.400	5.379	3.530
50.00	4.209	5.180	4.312	4.660
70.00	3.566	6.660	2.858	7.264
80.00	2.929	8.520	1.624	8.870
90.00	4.005	9.250	4.404	8.183
95.00	10.700	6.470	11.106	6.110

MODIFIED 1 BUILD

PHH	STATION 2 (ROTOR 1)	STATION 3 (STATOR 1)	STATION 4 (ROTOR 2)	STATION 5 (STATOR 2)
5.00	3.506	7.090	1.753	5.950
10.00	4.453	3.150	6.216	4.140
30.00	4.838	4.850	5.357	4.200
50.00	4.666	5.830	4.158	5.910
70.00	3.915	6.320	3.027	6.860
80.00	3.285	7.670	1.924	8.120
90.00	4.225	7.740	4.275	7.400
95.00	10.924	5.690	10.866	5.260

MODIFIED 2 BUILD

PHH	STATION 2 (ROTOR 1)	STATION 3 (STATOR 1)	STATION 4 (ROTOR 2)	STATION 5 (STATOR 2)
5.00	3.506	6.270	0.912	4.690
10.00	4.453	2.430	5.852	3.580
30.00	4.838	4.300	5.404	3.610
50.00	4.666	5.600	4.272	5.400
70.00	3.915	6.170	3.117	6.560
80.00	3.285	7.540	1.808	7.890
90.00	4.225	7.750	4.334	6.990
95.00	10.924	5.400	11.165	4.970

Table 11.7 Circumferential-mean performance parameters for the baseline 1 compressor build (ϕ = 0.500).

*** FIRST STAGE ***

PHH	HEAD RISE COEFFICIENT ROTOR	HEAD RISE COEFFICIENT STAGE	LOSS COEFFICIENT ROTOR	LOSS COEFFICIENT STATOR	EFFICIENCY ROTOR	EFFICIENCY STAGE
5.00	0.2286	0.1913	0.0398	0.1881	0.9367	0.7838
10.00	0.2247	0.2122	0.0295	0.0648	0.9503	0.8977
30.00	0.2280	0.2164	0.0376	0.0623	0.9317	0.8841
50.00	0.2345	0.2215	0.0322	0.0698	0.9364	0.8845
70.00	0.2436	0.2271	0.0200	0.0873	0.9567	0.8919
80.00	0.2525	0.2303	0.0198	0.1134	0.9560	0.8722
90.00	0.2479	0.2103	0.0938	0.2004	0.8111	0.6883
95.00	0.2103	0.1890	0.1843	0.1452	0.6445	0.5793
MASS AVERAGED	0.2357	0.2188	0.0447	0.0905	0.9125	0.8470

*** SECOND STAGE ***

PHH	HEAD RISE COEFFICIENT ROTOR	HEAD RISE COEFFICIENT STAGE	LOSS COEFFICIENT ROTOR	LOSS COEFFICIENT STATOR	EFFICIENCY ROTOR	EFFICIENCY STAGE
5.00	0.2412	0.1854	0.1240	0.2885	0.8506	0.6537
10.00	0.2157	0.1844	0.0706	0.1699	0.8834	0.7552
30.00	0.2192	0.1987	0.0491	0.1105	0.9084	0.8235
50.00	0.2236	0.2082	0.0359	0.0811	0.9258	0.8624
70.00	0.2297	0.2100	0.0383	0.1010	0.9171	0.8385
80.00	0.2372	0.2080	0.0405	0.1439	0.9134	0.8010
90.00	0.2412	0.2113	0.0544	0.1632	0.8875	0.7777
95.00	0.2265	0.2145	0.1494	0.0839	0.7204	0.6821
MASS AVERAGED	0.2258	0.2041	0.0505	0.1157	0.8998	0.8134

*** OVERALL ***

PHH	HEAD RISE COEFFICIENT	EFFICIENCY
5.00	0.3767	0.7139
10.00	0.3966	0.8253
30.00	0.4151	0.8540
50.00	0.4298	0.8736
70.00	0.4372	0.8654
80.00	0.4383	0.8369
90.00	0.4217	0.7303
95.00	0.4035	0.6298
MASS AVERAGED	0.4229	0.8304

Table 11.8 Circumferential-mean performance parameters for the baseline 2 compressor build ($\phi = 0.500$).

*** FIRST STAGE ***

	HEAD RISE ---COEFFICIENT----		LOSS ---COEFFICIENT----		----EFFICIENCY----	
PHH	ROTOR	STAGE	ROTOR	STATOR	ROTOR	STAGE
5.00	0.2286	0.1887	0.0398	0.2010	0.9367	0.7733
10.00	0.2247	0.2099	0.0295	0.0768	0.9503	0.8878
30.00	0.2280	0.2158	0.0376	0.0654	0.9317	0.8818
50.00	0.2345	0.2205	0.0322	0.0755	0.9364	0.8803
70.00	0.2436	0.2277	0.0200	0.0843	0.9567	0.8941
80.00	0.2525	0.2285	0.0198	0.1226	0.9560	0.8653
90.00	0.2479	0.2133	0.0938	0.1847	0.8111	0.6979
95.00	0.2103	0.1935	0.1843	0.1145	0.6445	0.5931
MASS AVERAGED						
	0.2357	0.2185	0.0447	0.0920	0.9125	0.8459

*** SECOND STAGE ***

	HEAD RISE ---COEFFICIENT----		LOSS ---COEFFICIENT----		----EFFICIENCY----	
PHH	ROTOR	STAGE	ROTOR	STATOR	ROTOR	STAGE
5.00	0.2465	0.2041	0.1172	0.2158	0.8612	0.7130
10.00	0.2199	0.1957	0.0638	0.1300	0.8959	0.7972
30.00	0.2207	0.1992	0.0472	0.1155	0.9122	0.8232
50.00	0.2254	0.2091	0.0334	0.0856	0.9313	0.8642
70.00	0.2297	0.2109	0.0389	0.0961	0.9158	0.8409
80.00	0.2391	0.2092	0.0378	0.1475	0.9196	0.8045
90.00	0.2431	0.2113	0.0572	0.1693	0.8827	0.7673
95.00	0.2235	0.2112	0.1559	0.0846	0.7073	0.6686
MASS AVERAGED						
	0.2273	0.2060	0.0492	0.1132	0.9026	0.8178

*** OVERALL ***

PHH	HEAD RISE COEFFICIENT	EFFICIENCY
5.00	0.3929	0.7408
10.00	0.4056	0.8417
30.00	0.4150	0.8527
50.00	0.4296	0.8724
70.00	0.4386	0.8677
80.00	0.4377	0.8352
90.00	0.4246	0.7308
95.00	0.4048	0.6302
MASS AVERAGED		
0.0	0.4245	0.8320

Table 11.9 Circumferential-mean performance parameters for the modified 1 compressor build (ϕ = 0.500).

*** FIRST STAGE ***

	HEAD RISE ---COEFFICIENT----		LOSS ---COEFFICIENT----		----EFFICIENCY----	
PHH	ROTOR	STAGE	ROTOR	STATOR	ROTOR	STAGE
5.00	0.2267	0.1930	0.0503	0.1717	0.9232	0.7861
10.00	0.2242	0.2066	0.0281	0.0925	0.9540	0.8789
30.00	0.2280	0.2087	0.0312	0.1040	0.9431	0.8634
50.00	0.2334	0.2136	0.0247	0.1078	0.9500	0.8693
70.00	0.2423	0.2281	0.0239	0.0759	0.9479	0.8923
80.00	0.2500	0.2314	0.0146	0.0972	0.9671	0.8949
90.00	0.2473	0.2164	0.0854	0.1658	0.8242	0.7214
95.00	0.2093	0.1939	0.1756	0.1064	0.6540	0.6059
MASS AVERAGED						
	0.2349	0.2158	0.0403	0.1031	0.9202	0.8455

*** SECOND STAGE ***

	HEAD RISE ---COEFFICIENT----		LOSS ---COEFFICIENT----		----EFFICIENCY----	
PHH	ROTOR	STAGE	ROTOR	STATOR	ROTOR	STAGE
5.00	0.2391	0.1947	0.1426	0.2304	0.8272	0.6734
10.00	0.2209	0.2022	0.0569	0.1017	0.9068	0.8301
30.00	0.2247	0.2064	0.0442	0.0996	0.9208	0.8461
50.00	0.2302	0.2129	0.0373	0.0927	0.9273	0.8574
70.00	0.2282	0.2127	0.0394	0.0805	0.9141	0.8517
80.00	0.2356	0.2126	0.0347	0.1143	0.9237	0.8337
90.00	0.2377	0.2151	0.0591	0.1227	0.8751	0.7917
95.00	0.2243	0.2153	0.1439	0.0623	0.7245	0.6953
MASS AVERAGED						
	0.2282	0.2106	0.0480	0.0949	0.9058	0.8356

*** OVERALL ***

PHH	HEAD RISE COEFFICIENT	EFFICIENCY
5.00	0.3877	0.7252
10.00	0.4088	0.8541
30.00	0.4152	0.8547
50.00	0.4265	0.8633
70.00	0.4407	0.8722
80.00	0.4440	0.8645
90.00	0.4315	0.7548
95.00	0.4092	0.6499
MASS AVERAGED		
0.0	0.4264	0.8406

Table 11.10 Circumferential-mean performance parameters for the modified 2 compressor build ($\phi = 0.500$).

*** FIRST STAGE ***

	HEAD RISE ---COEFFICIENT----		LOSS ---COEFFICIENT----		----EFFICIENCY----	
PHH	ROTOR	STAGE	ROTOR	STATOR	ROTOR	STAGE
5.00	0.2267	0.1931	0.0503	0.1713	0.9232	0.7864
10.00	0.2242	0.2065	0.0281	0.0927	0.9540	0.8787
30.00	0.2280	0.2095	0.0312	0.0998	0.9431	0.8666
50.00	0.2334	0.2140	0.0247	0.1059	0.9500	0.8707
70.00	0.2423	0.2275	0.0239	0.0788	0.9479	0.8902
80.00	0.2500	0.2302	0.0146	0.1031	0.9671	0.8905
90.00	0.2473	0.2185	0.0854	0.1546	0.8242	0.7283
95.00	0.2093	0.1951	0.1756	0.0982	0.6540	0.6097
MASS AVERAGED						
	0.2349	0.2161	0.0403	0.1016	0.9202	0.8466

*** SECOND STAGE ***

	HEAD RISE ---COEFFICIENT----		LOSS ---COEFFICIENT----		----EFFICIENCY----	
PHH	ROTOR	STAGE	ROTOR	STATOR	ROTOR	STAGE
5.00	0.2449	0.2104	0.1483	0.1741	0.8230	0.7070
10.00	0.2240	0.2049	0.0664	0.1028	0.8931	0.8170
30.00	0.2254	0.2056	0.0435	0.1078	0.9214	0.8406
50.00	0.2312	0.2127	0.0248	0.0987	0.9504	0.8742
70.00	0.2298	0.2129	0.0259	0.0869	0.9422	0.8730
80.00	0.2391	0.2142	0.0229	0.1229	0.9492	0.8501
90.00	0.2359	0.2142	0.0517	0.1175	0.8879	0.8062
95.00	0.2208	0.2149	0.1347	0.0415	0.7332	0.7135
MASS AVERAGED						
	0.2294	0.2107	0.0408	0.1000	0.9188	0.8439

*** OVERALL ***

PHH	HEAD RISE COEFFICIENT	EFFICIENCY
5.00	0.4035	0.7429
10.00	0.4114	0.8468
30.00	0.4151	0.8535
50.00	0.4266	0.8725
70.00	0.4405	0.8818
80.00	0.4444	0.8706
90.00	0.4327	0.7649
95.00	0.4100	0.6600
MASS AVERAGED		
0.0	0.4268	0.8452

END

FILMED

DTIC